NTNU – Trondheim
Norwegian University of
Science and Technology

Simulating Underbalanced Drilling

Development of a GUI flow simulator to
evaluate UBD operations for aerated fluids
and foams

Rune Sørflaten Leirkjær

Petroleum Geoscience and Engineering
Submission date: June 2014
Supervisor: John-Morten Godhavn, IPT

Norwegian University of Science and Technology
Department of Petroleum Engineering and Applied Geophysics

ACKNOWLEDGEMENT

This is an M.Sc thesis written for the Department of Petroleum Engineering and Applied Geophysics at the Norwegian University of Science and Technology (NTNU). The thesis was written as a completion of my graduate degree at NTNU in drilling technology, during my tenth and last semester at the university.

I would first of all like to thank John-Morten Godhavn, Adjunct Professor/Professor II, at the Department of Petroleum Engineering and Applied Geophysics, who has been my supervisor during the process. He has given me guidance, provided feedback on my work, and helped me contact professionals within the petroleum industry.

Personal correspondence with Martin Culen, General Manager, at Blade Energy Partners proved to be very helpful for me in writing this thesis. I would extend my sincere gratitude to him for clarifying information for me and for providing great explanations for questions I have had.

I would also like to thank Johan Eck-Olsen, Drilling Supervisor Offshore, Statoil ASA, for allowing me to republish content from *"IADC RIGPASS for Statoil: Underbalanced Drilling Operations"* and Torbjørn Pedersen, PhD Candidate, Department of Petroleum Engineering and Applied Geophysics for providing me with relevant background information and providing feedback on my programming.

Lastly I would like to send a special thank-you to all of those who have contributed towards me having five great years at the university both socially and academically.

Trondheim, 09.06.14 Rune Leirkjær

ABSTRACT

As more oil fields mature, new methods are required to be able to drill additional wells without damaging the reservoir and to limit pressure related drilling problems. This can in most cases be solved by drilling underbalanced, intentionally lowering the pressure below the reservoir pressure, allowing the well to flow. Systems available to drill underbalanced include; air, gas, mist, stable foam, foam with back-pressure, aerated mud and oils.

The thesis focuses mainly on foam drilling and drilling with aerated systems. Both systems are pneumatic drilling fluids, this means they are a mixture of a liquid- and a gas phase. The main difference between foam and aerated systems is how the fluid structure is built up.

When drilling with aerated fluids, no emulsifier or stabilization agent is added to the fluid, so the gas phase will normally travel faster than the liquid phase due to gravitational forces. Foams are added foaming agents so that the fluid system remains stable by trapping the gas bubbles inside a liquid film, making the fluid act as normal one-phase flow. The thesis explains the theory behind, usage, design and operational procedures for these fluid systems.

In this master thesis an advanced fluid simulator was developed in MATLAB to simulate drilling with these fluids, and to design operational limits in the planning phase. The finished program is presented in a graphical interface which easily allows the user to run even complex simulations regarding; well path, reservoir model, tubular- and fluid design.

For the two-phase flow modeling eight different empirical pressure correlations were implemented in the simulator. The first two-phase flow model described in the literature on flow modeling, was developed by Poettmann & Carpenter, and is one of the simplest models available. This model was included in two versions. Besides this model, two other models are included from each of the three main categories; neither slippage nor flow regimes considered, only slippage considered, and; both slippage and flow regimes considered. The models that consider both slippage and flow regimes, such as Beggs & Brill, are complex models which require much computational force. However these models will often produce very reliable results.

For foam modeling, six different empirical viscosity models were implemented. Einstein was the first to describe foam rheology mathematically, and his model is the simplest model included in the simulator. Some of the simpler models included in the simulator produces output with much uncertainty, however more complex models such as Sanghani produce more trustworthy results.

Multiple simulations were run for foam and aerated system utilizing these models with a large range of varying inputs. The results from simulations proved to provide reliable outputs, with deviations well within the expected range.

SAMMENDRAG

Etter hvert som flere oljefeld blir modne kreves nye metoder for videre boring av nye brønner uten å forårsake reservoarskade og begrense trykk realterte problemer under boring. Dette kan i de fleste tilfeller løses ved underbalansert boring, der bunnhullstyrkket med hensikt senkes under reservoartrykket, slik at brønnen kan strømme. Systemer tilgjengelig for å bore underbalansert inkluderer; luft, gass, dugg, stabilt skum, trykkpåført skum, gasluftet væske og olje.

Avhandlingen fokuserer hovedsakelig på boring med skum med gasluftet væske. Begge systemene er pneumatiske borevæsker, noe som betyr at de er en blanding av en væske- og en gassfase, den viktigste forskjellen mellom systmer med skum og gasluftet væske er hvordan fluidstrukturen er oppbygd.

I boring med gasluftet væske er ingen emulgeringsmiddel eller stabiliseringsmiddel tilsatt til fluiden, slik at gassfasen normalt vil bevege seg raskere enn væskefasen på grunn av tyngdekraften. Skum blir derimot tilsatt kjemikalier, slik at fluidsystemet forblir stabilt ved å fange gassboblene inne i en væskefilm. Dette gjør at fluiden oppfører seg som en normal enfasestrømning. Avhandlingen forklarer teorien bak, bruk av, design av og operasjonelle prosedyrer for disse fluidsystemene.

I denne masteroppgaven er en avansert fluidsimulator utviklet i MATLAB for å kunne simulere boring med disse fluidsystemene, samt sette operative grenser i planleggingsfasen. Det ferdige programmet er presentert i et grafisk grensesnitt som enkelt lar brukeren kjøre komplekse simuleringer på varierende brønnbane, reservoarmodell, foringsrør-, borestreng-, og fluid design.

For modellering av tofasestrømning ble åtte ulike empiriske trykk korrelasjoner implementert i simulatoren. Den første tofasestrømningsmodell, som er beskrevet i litteraturen på strømningsmodellering, ble utviklet av Poettmann og Carpenter og er en av de enkleste modellene tilgjengelig. Denne modellen ble inkludert i to versjoner. Sett bort fra denne modellen er to modeller inkludert fra hver av de tre hovedkategoriene; verken faseglidning eller strømningsregimer vurdert, bare faseglidning vurdert, og; både faseglidning og strømningsregimer vurdert. Modellene som vurderer både faseglidning og strømningsregimer som Beggs og Brill, er komplekse modeller som krever mye beregningskraft, men disse vil ofte gi svært pålitelige resultater.

For modellering av skum ble seks ulike empiriske viskositetmodeller implementert. Einstein var den første til å beskrive skumreologi matematisk og hans modell er den enkleste inkludert i simulatoren. Noen av de enklere modellene som inngår i simulatoren produserer data med stor usikkerhet, mer komplekse modeller, slik som Sanghani, gir mer pålitelige resultater.

Flere simuleringer ble kjørt for skumsystem og gasluftet-væskesystem ved hjelp av disse modellene ved bruk av et stort spekter av ulike inngangsparametre. Resultatene fra simuleringene viste seg å gi pålitelige verdier, med avvik innenfor det forventede området.

NOMENCLATURE

A	area	[sqft]
API	API gravity	[degrees]
B	formation volume factor	[scf/stb, bbl/stb]
c	coefficient, compressibility	[-],[1/psi]
C	coefficient, concentration	[-],[-]
d	diameter	[ft]
E_k	acceleartion component	[-]
f	friction factor, liquid fraction	[-],[-]
F	ratio factor	[-]
g	gravitiational constant	[32.2 ft/s^2]
h	height	[ft]
H	holdup	[-]
J	productivity index	[stb/d-psi]
k	permeability	[mD]
K	pseudo-plastic parameter	[lbf-s^(n-2)/ft]
L	length, regime-boundary parameter	[ft],[-]
M	molacular weight, mass flow rate	[-],[lbm/sec]
MD	measured depth	[ft]
n	pseudo-plastic parameter	[-]
N	number	[-]
p	pressure	[psia]
q	rate	[cuft/sec]
r	radius	[ft]
R_p	rate of penetration	[ft/hr]
R_s	solution gas oil ratio	[scf/stb]
S	skin, slip ratio	[-],[-]
T	temperature	[degrees F]
v	velocity	[ft/sec]
V	realtive volumetric rate	[cuft/stb]
Z	gas compressibility factor	[-]

ε	roughness	[ft]
γ	specific density/gravity	[s.g.]
Γ	gas quality	[-]
λ	no-slip holdup	[-]
ϕ	inclination	[degrees]
ρ	density	[lbm/cuft]
σ	interfacial tension	[dyne/ cm]
τ_y	yield stress	[lbm/ft^2]
ψ	correlation angle	[degrees]
θ	azimuth	[degrees]

SUBSCRIPTS

$0, 1, 2, ...$	index
b	bubble point
bit	drill bit
c	choke
d	discharge
dyn	dynamic
e	effective
f, F	foam
FR	freude
g	gas
h	hydraulic
i	inner, index
k	index, adjusted mixture
l	liquid
m	mixture
max	maximum
min	minimum
n	no-slip
o	outer, oil
P	plastic
pc	pseudo-critical
pr	pseudo-reduced
r	reservoir
Re	reynolds
rel	realtive
req	required
sc	standard conditions
sl	settling
t	total
tp	two-phase
tr	terminal
sl	settling
w	water
wf	well flowing (bottom hole)

TABLE OF CONTENTS

LIST OF FIGURES

LIST OF TABLES

1 INTRODUCTION

Many oil fields around the world are moving into to the mature phase and are starting to get depleted. Depleted reservoirs are often challenging to drill, with many occurring situations such as lost circulation, drill pipe sticking and reservoir damage. To be able to better limit these problems a specialized drilling technique, known as underbalanced drilling (UBD); has become an essential principle in oil well drilling during the last century.

Underbalanced drilling consists of keeping the bottom-hole pressure (BHP) intentionally below the reservoir pressure, allowing the well to produce fluid while drilling. To be able to properly execute an UBD operation safely, an extensive planning phase is required. Designing an UBD operation requires many factors to be considered, including equipment design and operational procedures, which require complex flow modeling.

The author's main task was to develop an UBD simulator for aerated fluid systems and foam systems, which could be easily used for a range of well-known two-phase pressure correlations and foam rheology models. The motivation behind selecting this task was to continue working with, and further improve, a MATLAB model earlier constructed by the author on the subject. The inspiration to continue developing this model was to create an easy-to-use graphical interface, which can hopefully be understood and used by anyone interested in flow modeling.

The improvements made focus more on steady-state solutions with reservoir influx than the previous model developed. The improved model is able to handle a large range of input parameters including well design, reservoir model and drilling fluid system. The author of this thesis especially focuses on how the simulator now can be used in setting operational limits for an UBD operation.

In addition to the programming and simulations, this thesis further discusses basic principles in UBD operations including, but not limited to; equipment, fluid design, benefits and challenges.

The thesis is divided into three main subjects; aerated fluid systems, foam systems and program understanding. The three subjects are presented within the following chapters:

- Chapter 2 gives an introduction to drilling a well underbalanced, including subjects regarding pressure control, fluid design and equipment.
- Chapter 3 explains the theory behind phase properties and two-phase flow, including fluid properties like density and viscosity, and two-phase terms such as slippage and superficial velocity.
- Chapter 4 is about aerated systems, explaining subjects such as usage of the fluid system and two-phase pressure calculations.
- Chapter 5 is about foam systems and contains information about the basics in foam drilling, foam rheology models, pressure calculation and other related subjects.
- Chapter 6 uses the information from the previous chapters to explain how operational limits are set in UBD operations and how they are affected during drilling.
- Chapter 7 explains how the UBD simulator was developed and the theory behind how each calculation step that is involved when running the simulations.
- Chapter 8 gives an introduction to how the simulator functions, including defining inputs and running simulations.
- Chapter 9 discusses some of the simulation results and includes a comparative study of the different models included in the simulator.

2 INTRODUCTION TO UNDERBALANCED DRILLING

The following chapter includes some basics about underbalanced drilling (UBD) including topics such as pressure control, general advantages and disadvantages, fluid systems and basic equipment for an UBD operation.

2.1 DEFINITION AND PRESSURE CONTROL

An underbalanced operation is when an oil well is either under construction or intervened with. Simultaneously, the pressure down hole is kept below the formation pressure. The operation is designed to allow the formation fluid to flow to the surface. The International Association of Drilling Contractors (IADC) defines underbalanced drilling (UBD) as:

"A drilling activity employing appropriate equipment and controls where the pressure exerted in the wellbore is intentionally less than the pore pressure in any part of the exposed formations with the intention of bringing formation fluids to the surface."

$$P_{\text{Res}} > BHP = P_{hyd} + P_{fric} + P_{acc} + P_{surf} \tag{1.1}$$

To be able to keep the bottom-hole pressure below the reservoir pressure the parameters such as flow/pump rates, fluid densities (and contribution) and applied surface pressure have to be controlled.

Changing the surface pressure is the simplest, quickest and most predictable way of adjusting the pressure down hole. This is shown in Figure 1. The hydrostatic pressure is affected by the choice of drilling fluid, the fluid design, the encountered formation fluid and the cuttings in the well (Rehm, 2012).

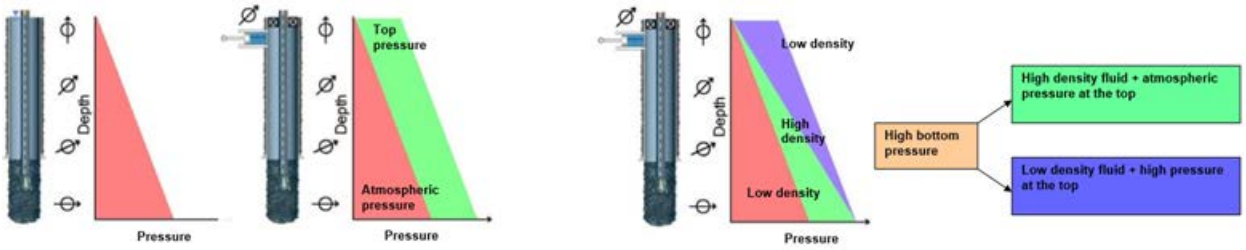

FIGURE 1 - PRESSURE CONTROL IN STATIC CONDITIONS (ECK-OLSEN, 2003).

The friction contribution is largely impacted by the flow rate in each well segment. The flow rate can be adjusted by changing the injection rates. Acceleration pressure is often neglected in calculations. However, where the geometry of the well changes the acceleration effect can be noticed by the change in fluid velocity.

To be able to predict the actual BHP, a hydraulic model must be applied for the relevant conditions in the well (Rehm, 2012). In this project a UBD simulator was written in MATLAB to estimate these hydraulic changes and corresponding pressures for an underbalanced operation.

2.2 WHY SELECT UBD?

Initially the main reason operators chose the UBD technique in oil well drilling was to reduce drilling related problems. As the managed pressure drilling (MPD) technique improved, UBD is more often replaced by MPD to improve pressure related issues. Today UBD is more often used where it is desired to reduce formation damage (Rehm, 2012).

More recently UBD has become a more attractive method to evaluate the reservoir while drilling and thereby improving the overall efficiency of each well (Rehm, 2012).

Drilling (pressure) related problems include:

- Narrow mud weight window
- Problems eliminated when underbalanced:
    - Lost Circulation
        - Mud expensive
    - Differential sticking
        - Reduced NPT
    - Increased ROP
    - Increased bit life

Enhances the production:

- Reduced formation damage
    - Less skin due to influx of drilling fluid
    - Earlier and better production
- Well stimulation

Evaluate the reservoir while drilling:

- Reveals hidden production zones
    - Reservoir flow measurements during drilling

Despite these advantages it is not preferable for most operators to choose to drill underbalanced in all feasible wells. Due to extra required planning, equipment, rig space and crew training. Alternatives to using UBD for pressure related drilling challenges, the use of additives like Wellbore Strengthening Material (WSM) or Lost Circulation Material (LCM) can be added to the fluid system. In addition, drilling with casing/tubing or expandable tubular may also be utilized in the system. These new technologies have proven to be effective towards solving these pressure related challenges(Rehm, 2012).

Typical candidate wells for UBD are wells where lost circulation and/or differential sticking are expected. Examples of these are wells with:

- Depleted reservoirs
- Under pressured formations
- Fragile formations (to mud invasion)
- Producing formations with little reservoir data

2.3 DRILLING FLUIDS

The drilling fluid is in drilling operations normally the first barrier against a well control incident. The fluid density with the corresponding hydrostatic pressure, keeps the wellbore stable if correctly designed.

For UBD it is important to balance this density so that the BHP is kept below the pore pressures and above the wellbore collapse pressure at all times, also during tripping and connections. Both the static wellbore pressure and the ECD (equivalent circulating density) should be considered during drilling. When the pump is regulated and/or shut off, the annular velocities change, this causes ECD changes due to frictional pressure (Rehm, 2012).

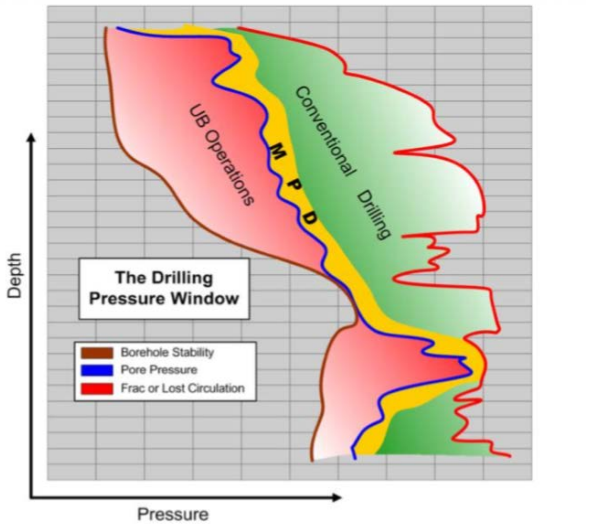

FIGURE 2 - DRILLING PRESSURE WINDOW (ECK-OLSEN, 2003)

While drilling underbalanced, appropriate fluid systems consists of the following compositions listed below according to increasing BHP they can provide (Eck-Olsen, 2003):

- Air/Gas (nitrogen, natural gas, exhaust etc.)
- Mist (<2.5% liquid content)
- Foam (55-97% gas)
- Gasified Liquid, aerated fluid
- Liquid

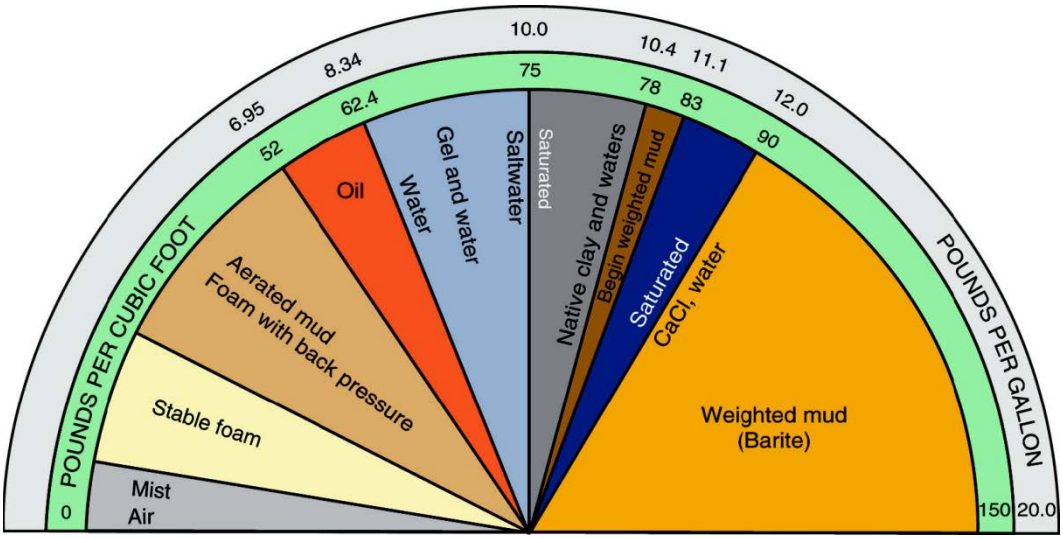

FIGURE 3 - TYPICAL FLUID DENSITIES ACCORDING TO FLUID SYSTEMS IN DRILLING

Choice of drilling fluid is also dependent on the desired flow and reservoir fluid- and matrix compatibility (Rehm, 2012).

The UBD simulator developed in this thesis includes a gasified liquid system, which requires two-phase modeling and a foam system which are modeled upon one-phase principles.

2.4 Injection Methods for UBD Fluids

The most appropriate fluid injection method for a UBD operation depends on the fluid and well design. Each technique has its own purpose, advantages and disadvantages. Some of the available injection methods are (Rehm, 2012):

- Two phase injection (aerated liquid)
  - Drill string (standpipe) injection
  - Annular injection
    - Parasite string
    - Parasite casing
    - Micro-Annulus (no drilling fluid through drill-string)
  - Dual Well System
- Pumped Conventionally
  - Flow drilling (single-phase, liquid)
  - Foam drilling (generated at surface, treated as single-phase)
  - Compression down-hole (air/gas)
- Compression and injection
  - Single-phase (gas/air)
  - Two-phase (droplets of liquid added to gas stream)

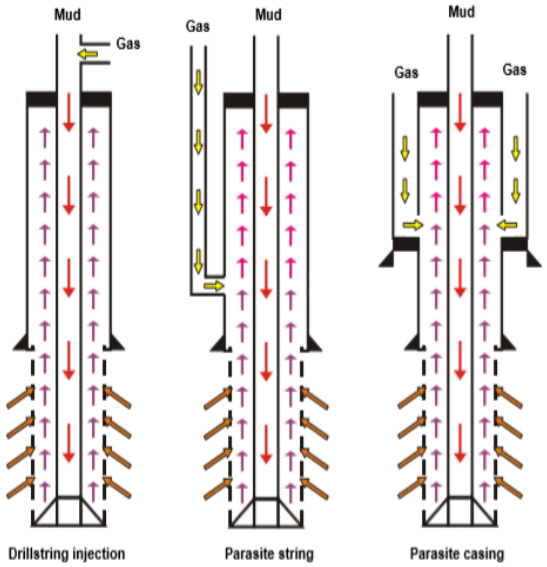

FIGURE 4 – INJECTION TECHNIQUES FOR AERATED LIQUID (ECK-OLSEN, 2003)

When using an aerated (gas/liquid mixture) mud system, the two phases can be mixed either at the surface (drill-string injection) or down-hole (parasite casing/string), as shown in Figure 4. In aerated simulation the UBD simulator assumes that the drill-string injection method is used as it is a commonly used practice and easier to model.

2.5 Equipment Used in an UBD Operation

All UBD operations include a rotating control device (RCD), drill pipe non return valves (NRV), a choke and manifold system, a separator- and flare system, surface valves and piping systems.

Figure 5 shows the nescessary well barrirers for a conventional drilling operation and a UBD operartion (NORSOK, 2004). Primary barriers are colored blue and secondary red. In both cases the secondary barriers are the same; casing cement, casing, wellhead, high pressure riser and BOP. In the conventional case the drilling fluid is considered the primary well barrirer. However, this is not true for the UBD case. In UBD the fluid column cannot be relied upon to control the well. Instead NPVs and a RCD must be installed as a part of the primary barriers. In addition, the drill string itself and the secondary barriers (now common) from convential drilling are considered primary barriers in UBD operations(NORSOK, 2004).

RDC is a well control device. It is installed on top of the blowout preventer (BOP), which allows the flow path to be closed. It is designed to divert returned flow (gas/liquid/solids) safely to a separation system. It provides a seal around the drill string and allows the pipe to rotate at the same time (Rehm, 2012).

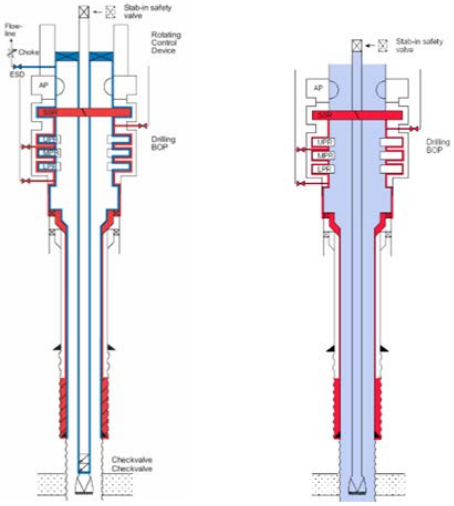

FIGURE 5 - WELL BARRIERS FOR UBD (LEFT) AND CONVENTIONAL DRILLING (RIGHT)

Drill pipe NRVs are valves placed inside the string to prevent back-flow while making connections. It prevents upwards gas flow inside the drill string and acts as a barrier. It also improves efficiency in bleeding of pressure(Rehm, 2012).

The choke and manifold system can be regulated to restrict the flow from the wellhead to the flow lines and separation equipment. Regulating the choke opening controls the pressure drop across it and the corresponding backpressure of in the annulus. When the choke is closed, the flow is prevented from flowing. In turn, the surface

pressure increases and the BHP will be further affected. Regulating the choke is the most common way of controlling the BHP in a well(Rehm, 2012).

When a well is drilled underbalanced, the return flow consists of: drilling fluid, produced fluid and cuttings. The separator systems for UBD operations must therefore be capable of separating the returned flow into four phases: heavy liquid (mud and water), light liquids (oil and condensate), gas and solids/cuttings(Eck-Olsen, 2003).

The returned gas must be discharged into the atmosphere (nitrogen and air only), treated and re-injected into the well, sent to a production facility or flared in a flaring system(Rehm, 2012).

In addition to this equipment, the UBD setup might also include: air compressors and boosters, nitrogen generators, mud treating equipment, down-hole casing NRVs, systems for gas detection and analysis, systems for constant circulation, special chemical injection equipment and/or other special instruments (Rehm, 2012).

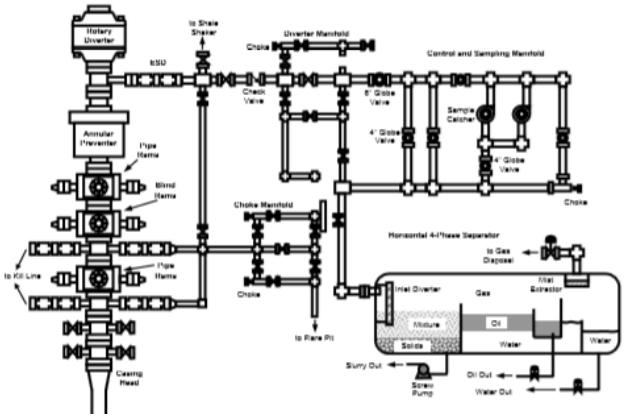

FIGURE 6 - TYPICAL SETUP OF UBD EQUIPMENT(ECK-OLSEN, 2003)

3 FLUID PROPERTIES THEORY

When designing an UBD simulator for two-phase flow many fluid properties and velocities are required to estimate relevant parameters like pressure drops.

The following chapter focuses on the relevant fluid properties included in multiphase flow modeling and the necessary mixing rules. These properties are further used in the subsequent chapters when explaining how the UBD models are implemented.

As multiphase properties are difficult to model and no good three-phase equations are available, two-phase equations are instead implemented. A mixture of oil, gas and water are assumed to be modeled as a two-phase, gas and liquid flow. Therefore all properties of the oil and water have to be combined into an averaged liquid component.

Single phase equations are neither implemented nor explained in this thesis (with the exception of foam rheology) as the authors work was mainly based upon two-phase modeling for UBD operations, making this theory irrelevant to the thesis.

3.1 FORMATION VOLUME FACTOR

Formation volume factor, FVF, is a factor of how a given volume at specific pressure and temperature conditions (in-situ) change at surface pressure and temperature (standard conditions). The general expression can be defined as:

$$FVF_i = \frac{V_i(p,T)}{V_{i,sc}} \tag{3.1}$$

As the FVF is the ratio of a specific volume to standard volume this factor can be used to convert volumes from reservoir conditions to surface conditions and vice versa.

3.1.1 GAS FVF

The gas formation volume in scf/stb is given by:

$$B_g = \frac{p_{sc}}{p}\frac{T}{T_{sc}}z = \frac{14.7}{p}\frac{T+459.67}{519.67}z \tag{3.2}$$

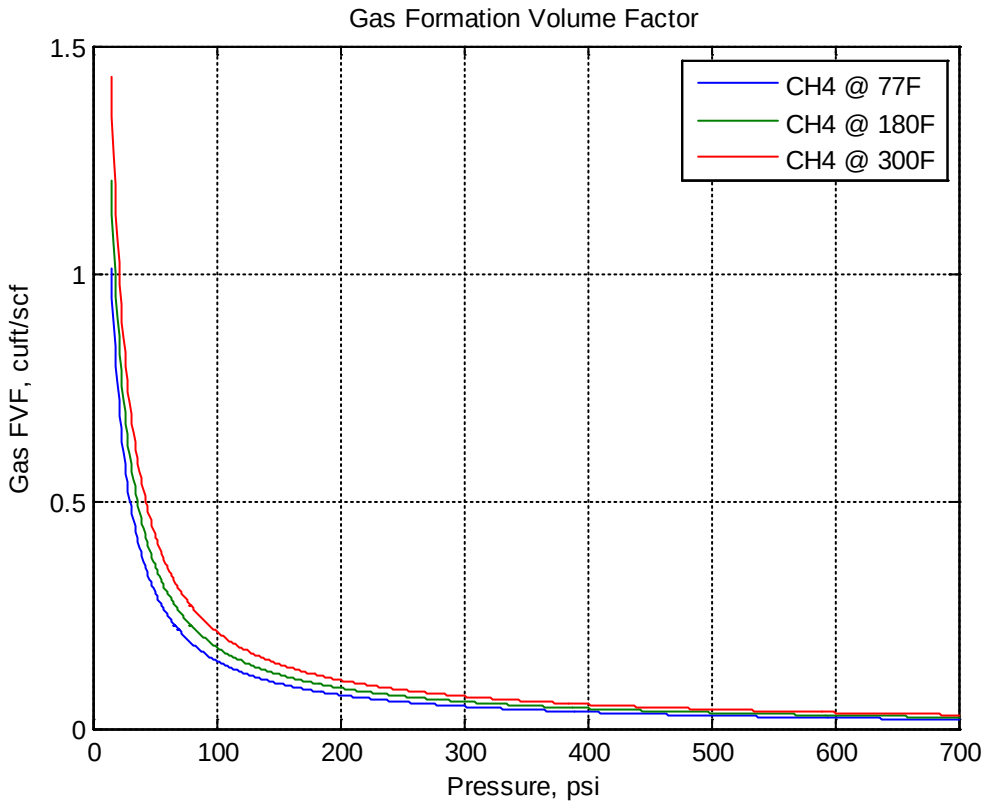

FIGURE 7 - FVF FOR METHANE AT LOWER PRESSURES

As pressures increases the formation volume factor for gas approaches zero and the temperature becomes less significant.

3.1.2 OIL FVF

The FVF is the ratio of volume of oil at in-situ conditions to the surface conditions. Below the bubble point it is given by:

$$B_o = 0.972 + 0.000147 F^{1.175} \tag{3.3}$$

$$F = R_s \left(\frac{\gamma_g}{\gamma_o} \right)^{0.5} + 1.25T \tag{3.4}$$

Above the bubble point the following relationship is valid:

$$B_o' = B_o \exp\left(c_o \left(p_b - p \right) \right) \tag{3.5}$$

Where the oil compressibility, c_o, can be expressed by Elsharkawys correlation:

$$c_o = \frac{-27321 + 33.784 R_s' + 238.81 T}{10^6 p} \tag{3.6}$$

The oil formation volume factor value is influenced by the gas in the solution (ratio and gas gravity).

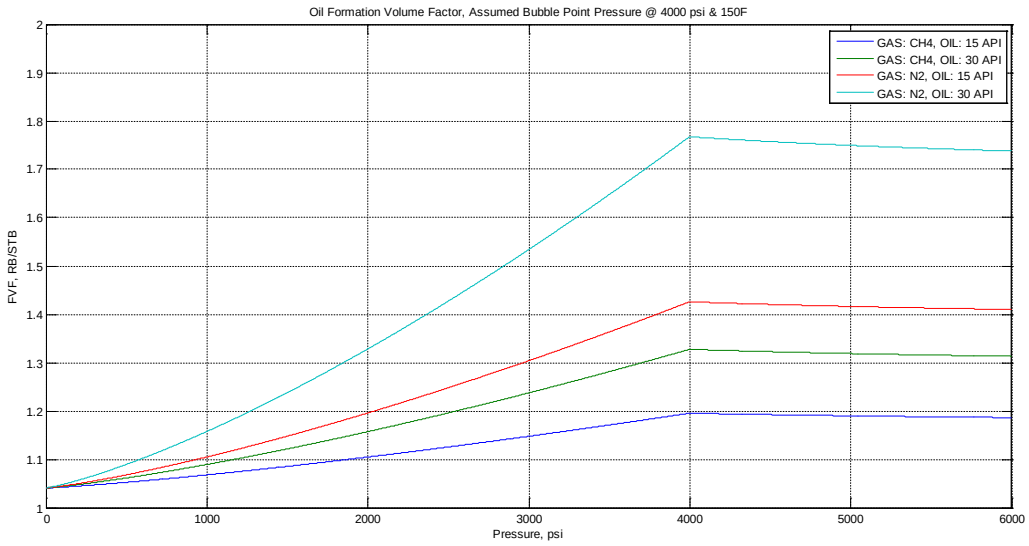

FIGURE 8 - OIL FVF FOR DIFFERENT OIL AND GAS MIXTURES, BUBBLE POINT AT 4,000 PSI

3.1.3 WATER FVF

The McCain correlation is used to determine the water formation volume factor (McCain, 1990).

$$B_w = \left(1+\Delta V_{wp}\right)\left(1+\Delta V_{wT}\right) \tag{3.7}$$

$$\Delta V_{wp} = -1.0001\times10^{-2} + 1.33391\times10^{-4}T + 5.50654\times10^{-7}T^2 \tag{3.8}$$

$$\Delta V_{wT} = -1.95301\times10^{-9}\,pT - 1.72834\times10^{-13}\,p^2T - 3.58922\times10^{-7}\,p - 2.25341\times10^{-10}\,p^2 \tag{3.9}$$

The correlation is not valid for pressures from 5,000 psi and above.

Figure 9 and Figure 10 shows that the water formation volume factor is relatively stable towards pressure and temperature change. Water FVF is often close to 1.0 RB/STB as these two contributions works against each other. Normally an increase in pressure will also cause temperature to rise.

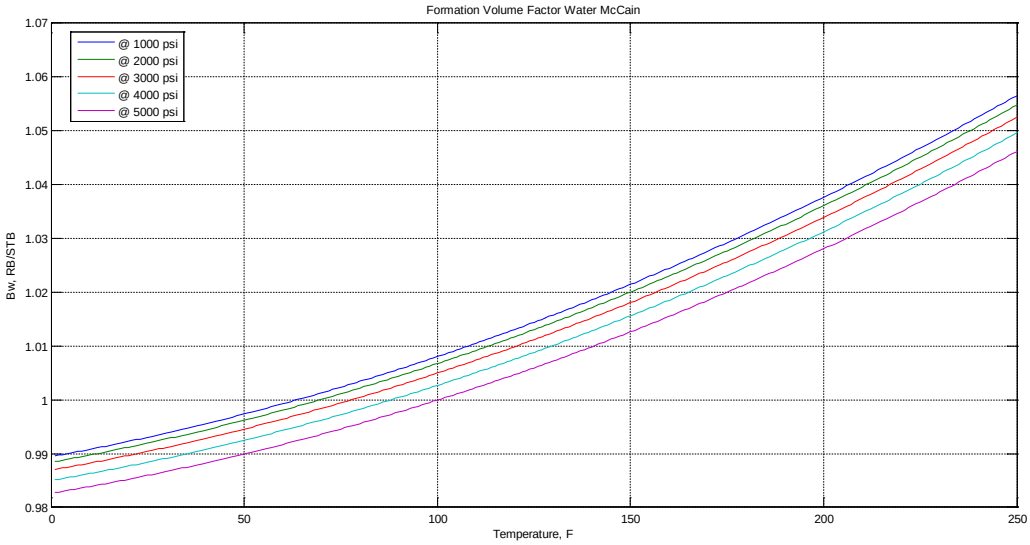

FIGURE 9 - WATER FVF WITH VARYING TEMPERATURE

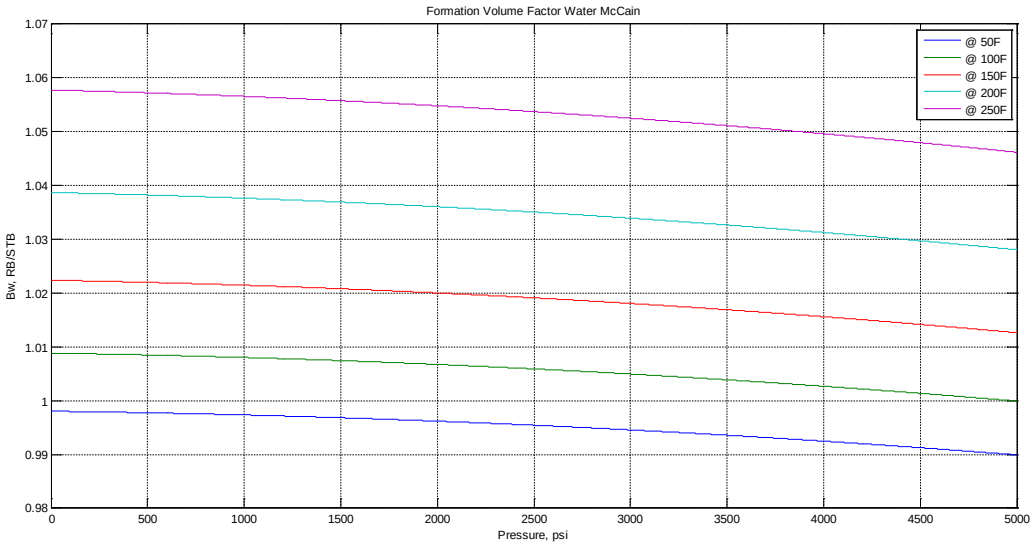

FIGURE 10 - WATER FVF WITH VARYING PRESSURE

3.2 DENSITY

The density of a phase influences both the kinetic and potential energy change which is used to find the total energy change and corresponding pressure drop. It can be very difficult to determine the density of a two-phase mixture due to the gravitational separation and slippage between liquid and gas, so several models have been

developed by petroleum and fluid mechanic experts to estimate these values. In this section the most commonly used and relevant expressions are listed.

The density of a phase is dependent upon pressure and temperature among other factors. For each phase the density can be found by dividing the density at standard conditions by the formation volume factor for the relevant conditions. The specific gravity of liquid and gas is set to 1.0, as represented in water and air respectively. Therefore a numerical constant must be included in the expressions to represent these values in lbm/cuft.

The general equation can therefore be expressed as:

$$\rho_i = \frac{\left(\frac{\rho}{\gamma}\right)_{i,ref} \gamma_i}{B_i} \tag{3.10}$$

3.2.1 Gas Density

The density of the gas phase can be found directly from the general expression if the gas-FVF and specific gravity is known. UBD simulator uses either a predefined list of gases or a user-inputted specific gravity in the calculation. These predefined gases are listed in Table 1.

TABLE 1 - GAS SPECIFIC DENSITIES

Gas	Air	NH3	CO2	CH4	N2	O2	C3H8	SO2	Custom
γ_g	1.0000	0.5900	1.5189	0.5537	0.9669	1.1044	1.5219	2.264	User-Input

As the density of air is 0.0764 lbm/cuft the expression for gas density becomes:

$$\rho_g = \frac{0.0764\gamma_g}{B_g} \tag{3.11}$$

If instead the molecular weight of a gas was known the specific density could be found by dividing the molecular weight by the molecular weight of air; 28.97.

$$\gamma_g = \frac{M_g}{28.97} \tag{3.12}$$

3.2.2 Oil Density

The density of oil is often presented in degrees API, which is a measurement of the inversed specific density at standard conditions. It can be converted by using the following equation:

$$\gamma_o = \frac{141.5}{^{o}API + 131.5} \tag{3.13}$$

Most oils have API densities greater than ten which makes them lighter than water and hence float on top of a water phase. Extra heavy oils are classified with gravities below 10 API and will sink in a contact with a water

phase. The best oils in regards to selling prices are within the range of 40-45 degrees API and are classified as light oils. Medium and heavy crudes are found in the ranges of 22.3-31.1 degrees API and 31.1-10 degrees API (Petroleum.co.uk, 2014).

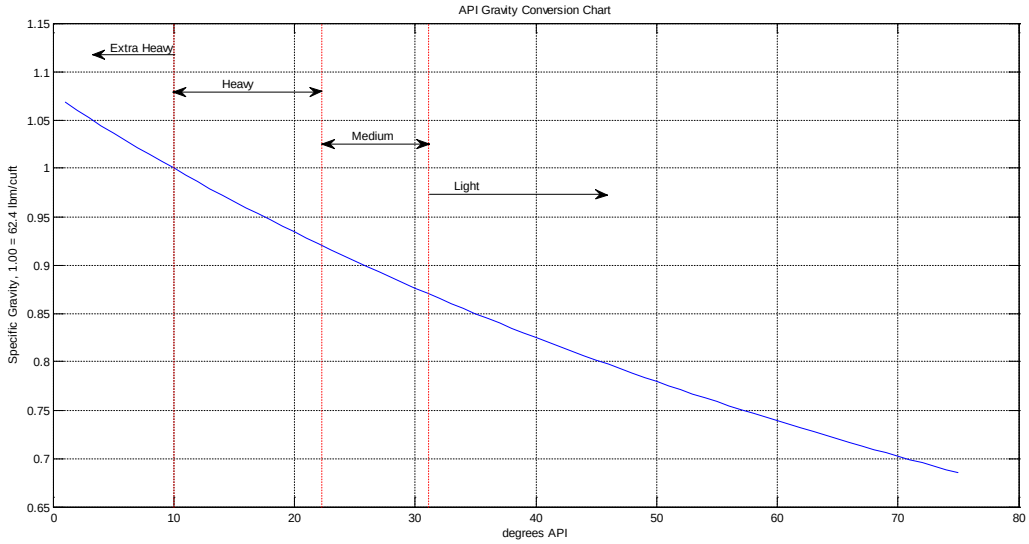

FIGURE 11 - API GRAVITY TO SPECIFIC GRAVITY CHART

The oil density is calculated according to the general equation. However, the value has to be adjusted for gas in the solution. The factor of 62.4 included in the expression below is the density of water in lbm/cuft. The conversion factor of the gas in the solution is divided by 5.615 to convert barrels into cuft.

$$\rho_o = \frac{62.4\gamma_o + \frac{0.0764 R_s}{5.615}}{B_o} \tag{3.14}$$

It is worth noticing that the oil density will have a slight increase above the bubble point as the gas is more compressed and the FVF term will be reduced.

3.2.3 WATER DENSITY

In two-phase modeling where water is present the gas phase is assumed not to be solvable in the water phase. This assumption is based on the fact that effect is very small compared to the effect from the solution gas oil ratio. However, this is not a valid assumption in all cases, and the simulator should therefore be used with care when water is present.

$$\rho_w = \frac{62.4\gamma_w}{B_w} \tag{3.15}$$

3.2.4 Mixture Densities

The liquid density used in multiphase modeling is the combined water and oil density weighted upon flow fractions. This density assumes the effect of slippage between the water and oil phase is negligible and is given as:

$$\rho_l = f_o \rho_o + f_w \rho_w \tag{3.16}$$

Slip density is an average density weighted from holdup fractions. This density is used in correlations which consider slippage and is the most commonly used in two-phase modeling. It is given by:

$$\rho_s = \rho_l H_l + \rho_g H_g \tag{3.17}$$

No-slip density is an average density weighted from flow rate fractions and is used in correlations which eliminate the effect from slippage. It is given by the following expression:

$$\rho_n = \rho_l \lambda_l + \rho_g \lambda_g \tag{3.18}$$

A third mixture density is expressed in a more complex way. It is used to calculate the friction factor and Reynolds number in some correlations. These correlations are however not included in the simulator developed and the value is only presented in a table as a reference. It is given by:

$$\rho_k = \frac{\rho_l \lambda_l^{\,2}}{H_l} + \frac{\rho_g \lambda_g^{\,2}}{H_g} \tag{3.19}$$

3.3 Standard and Actual Flow Rates

The standard flow rates are values which represents the true volume each phase would take up at standard conditions when it flows through a given area at a set time period, while the actual flow rates are adjusted for pressure and temperature variations.

The UBD simulator developed uses inputted gas liquid ratio (GLR) and water cut (WC) compared to a known total liquid flow rate to determine the actual flow of gas, oil and water in the system.

The liquid flow rate (oil and water combined) is given in bbl/day.

3.3.1 Gas Flow Rates

GLR is a measurement of the gas volumetric flow rate relative to the liquid volumetric flow rate at standard conditions. As the GLR is given in scf/day the unit for standard gas flow rate becomes scf/day when expressed as:

$$q_{g,sc} = q_{l,sc} \times GLR \tag{3.20}$$

The actual gas flow rate in a segment is found by adjusting the flow for gas in solution and is then divided by a factor of 86400 to convert the time frame from per day to per second.

$$q_g = \frac{q_{o,sc}\left(GOR - R_s\right)B_g}{24 \times 3600} \tag{3.21}$$

As the expression above shows the gas is only assumed to be solvable in the oil phase. The gas not in solution is the difference between the total gas phase volume at standard conditions or gas oil ratio (GOR) and the gas in solution at the current conditions. This assumption is made to avoid complex and unpredictable EOS-calculations. For systems with high WC this can become a problem and cause more uncertainty in the simulation results.

3.3.2 Oil Flow Rates

The standard oil flow rate is simply found in bbl/day (WC is a fraction) by the following expression:

$$q_{o,sc} = q_{l,sc} \times (1 - WC) \tag{3.22}$$

The actual flow is further converted to true flow rate by the expression below. The coefficient of 6.49E-5 is added to convert the flow rate from bbl/day to cuft/sec for further calculations.

$$q_o = 6.49 \times 10^{-5} \times q_{o,\mathrm{sc}} B_o \tag{3.23}$$

3.3.3 Water Flow Rates

The standard water flow rate is also presented in bbl/day by the remaining liquid fraction:

$$q_{w,sc} = q_{l,sc} \times WC \tag{3.24}$$

As with oil the water can be converted to an actual volume in cuft/sec by:

$$q_w = 6.49 \times 10^{-5} \times q_{w,\mathrm{sc}} B_w \tag{3.25}$$

3.3.4 Mixture Flow Rates

The combined actual flow rates, for liquid total flow and overall total flow respectively, (also in cuft/sec) required for further calculations then becomes:

$$q_l = q_o + q_w \tag{3.26}$$

$$q_t = q_l + q_g \tag{3.27}$$

The last two equations are also valid for flows at standard conditions.

3.4 Flow Ratios

In this section are some of the ratios used in other parts of this thesis described further.

3.4.1 Water Oil Ratio

The water oil ratio (WOR) is a dimensionless parameter which describes the fractional volume of water compared to the volume of oil. It is given as:

$$WOR = \frac{q_{w,sc}}{q_{o,sc}} \tag{3.28}$$

3.4.2 Gas Oil Ratio

The gas oil ratio (GOR) is a measurement of how much gas volume is present at standard conditions compared to the relevant oil volume. This number can be given in many different units, however in the simulator only scf/STB is used.

$$GOR = \frac{q_{g,sc}}{q_{o,sc}} \tag{3.29}$$

3.4.3 No-Slip Liquid Holdup

No-slip liquid holdup is the fraction of a pipe volume occupied by liquid phase in a given pipe segment if no-slip is present. This is the case if both phases have the same velocity and the value is given by the ratio of the in-situ liquid flow to in-situ total flow rate. The no-slip gas holdup is the vice versa case, or simply the no-liquid faction.

$$\lambda_l = \frac{q_l}{q_t} \tag{3.30}$$

$$\lambda_g = 1 - \lambda_l \tag{3.31}$$

3.4.4 Liquid Holdup

The liquid hold-up is an important value used in two-phase modeling to properly determine properties like mixture densities, velocities and viscosities. Liquid holdup is defined as the fraction of a pipe volume occupied by liquid phase in a given pipe segment. The gas filled fraction is usually referred to as gas holdup. For an entire segment is filled with gas the liquid hold-up is zero and the gas holdup is one.

$$H_l = \frac{V_{\text{liquid in segment}}}{V_{\text{segment}}} \tag{3.32}$$

The liquid holdup can be estimated through a variety of empirical correlations depending on which two-phase flow model one wishes to apply in the simulation. This is further explained in chapter 4.

The gas liquid hold up, often referred to as the void-fraction, is the non-liquid fraction of this number, simply given as.

$$H_g = 1 - H_l \tag{3.33}$$

3.4.5 Liquid Fractions

Liquid fractions can be calculated for water and oil at the in-situ conditions relative to total liquid volume flow rate. These are two other useful ratios for further calculations and are given for oil and water respectively as:

$$f_o = \frac{q_o}{q_l} \tag{3.34}$$

$$f_w = 1 - f_o \tag{3.35}$$

These fractions are often referred to as water-in-liquid ratio (WLR) and oil-in-liquid ratio (OLR).

3.5 Relative Volumetric Flow

In some cases it might be useful to know how much each phase expands in volume relative to each other. The relative volumetric flow is a measurement of the volume each phase take up in in-situ conditions which is present from the volume which corresponds from one barrel of oil at standard conditions. Volumetric flow rates below are given in cuft/stb.

The relative volumetric rates are found by multiplying the phase FVF with the volume fraction of the phase relative to oil volume:

$$V_i = B_i \left(\frac{V_i}{V_o} \right) \tag{3.36}$$

3.5.1 Gas Relative Volume

The relative volumetric flow of gas is found by multiplying the FVF of gas with the free gas from one stock-stank-barrel oil. This expression gives the answer directly in the correct units:

$$V_g = B_g \left(GOR - R_s \right) \tag{3.37}$$

3.5.2 Oil Relative Volume

As oil is the reference phase, the relative volume of the phase is found simply by adding the gas in solution to the oil volume. The initial oil volume is found by multiplying the FVF of with 5.615 to get the correct units; gas in solution is given directly from the FVF and solution GOR.

$$V_o = 5.615 B_o + B_g R_s \tag{3.38}$$

3.5.3 Water Relative Volume

As with oil, water requires the same conversion factor to get the answer in the correct units. The expression is then multiplied with the dimensionless WOR and FVF of water to get the water fraction equal to one barrel of oil.

$$V_w = 5.615 B_w \times WOR \tag{3.39}$$

3.5.4 Mixture Volumes

The mixture volumes are simply found by adding the terms together. The mixing rules for liquid- and total relative volumetric flow rates are found respectively by:

$$V_l = V_o + V_w \tag{3.40}$$

$$V_t = V_l + V_g \tag{3.41}$$

3.6 Mass Flow Rate

Mass flow rate is a measurement for how much of each fluid phase which crosses through a cross-sectional area is in a given time period.

The mass flow rates are given in lbm/sec, respectively for gas- oil- and water as:

$$M_g = q_g \rho_g \tag{3.42}$$

$$M_o = q_o \rho_o \tag{3.43}$$

$$M_w = q_w \rho_w \tag{3.44}$$

The normal mixing rules still apply in this case:

$$M_l = M_o + M_w \tag{3.45}$$

$$M_t = M_l + M_g \tag{3.46}$$

It is worth noticing that the total mass flow rate remains constant through all pressure and temperature conditions.

3.7 Velocities and Slippage

Slip is used to describe the flow conditions in the segment when the two-phases have different velocities. Velocities are used to calculate the friction factor term which is proportional to the pressure loss due to frictional forces and further used to estimate the slip in each segment. All of the velocities in this section are given in the unit ft/sec.

3.7.1 Superficial Velocity

The superficial velocity of a phase is the velocity it would have if it was the only phase flowing through the relevant flow area. It is found by dividing the in-situ flow rate with the area cross section that the flow passes through. The following expressions are used for liquid and gas superficial velocity respectively:

$$v_{sl} = \frac{q_l}{A} \tag{3.47}$$

$$v_{sg} = \frac{q_g}{A} \tag{3.48}$$

3.7.2 Mixture Velocity

Mixture velocity is the sum of the superficial velocities for liquid and gas. Mixture velocity can also be referred to as two phase velocity. It is calculated as:

$$v_m = v_{sl} + v_{sg} \tag{3.49}$$

3.7.3 Actual Velocity

The actual velocity is a velocity term which has been adjusted for holdup and therefore can give a representation of how fast each phase will rise inside the segment. The actual velocity is found by dividing the superficial velocity by the holdup for each phase. As holdup is a dimensionless parameter and a fraction the actual velocity will have the same unit as superficial velocity and have a higher value. The actual velocities for liquid and gas respectively are given by:

$$v_l = \frac{v_{sl}}{H_l} \tag{3.50}$$

$$v_g = \frac{v_{sg}}{H_g} \tag{3.51}$$

3.7.4 Slippage With Relevant Terms

Slippage is a measurement of how easily gas bubbles in a two-phase mixture can surpass the liquid phase. Slippage is dependent on factors such as densities, velocities, flow area, and flow pattern among others. As the two phases have different densities, the light gas phase will flow easier than the heavy liquid phase, due to buoyancy and will cause bubbles to rise faster in a non-horizontal section (Takács, 2005).

Slippage can be expressed in several ways, one of which is through slip velocity. Slip velocity is the actual velocity difference between the gas and liquid phase. The value of the slip velocity of how much faster the gas phase rises than the liquid phase through a given segment is therefore.

$$v_s = v_g - v_l \tag{3.52}$$

Slip ratio is a dimensionless ratio of gas velocity to liquid velocity:

$$S = \frac{v_g}{v_l} \tag{3.53}$$

3.8 Viscosity

Viscosities are used to determine dimensionless numbers further used in the calculation of the friction factor and liquid holdup. It is an advantage to estimate the viscosities through laboratory measurements. However many empirical correlations already exist. These correlations are used in the UBD simulator and are based upon temperatures, pressures and densities.

In this section are first some well-known industry standards to find the gas-, oil- and water viscosity presented. Second, some mixing rules are explained. All viscosities in this section are given in centipoise, cp.

3.8.1 Gas Viscosity

Gas viscosity is given by the Lee-Gonzalez model:

$$\mu_g = A \times 10^{-4} \exp\left(B \left(\frac{\rho_g}{62.37} \right)^C \right) \tag{3.54}$$

$$C = 2.447 - 0.2224B \tag{3.55}$$

$$B = 3.448 + 0.01009 M_g + \frac{986.4}{T + 459.67} \tag{3.56}$$

$$A = (9.379 + 0.01607 M_g)(T + 459.67)^{1.5/(209.2+19.26M_g+(T+459.67))} \tag{3.57}$$

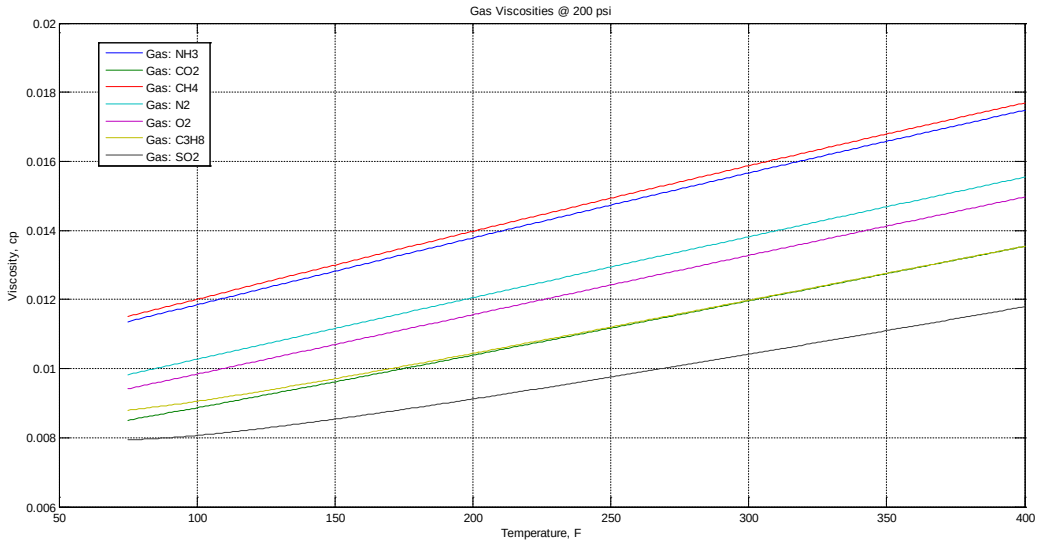

FIGURE 12 - GAS VISCOSITY FOR DIFFERENT GASES AT 200 PSI

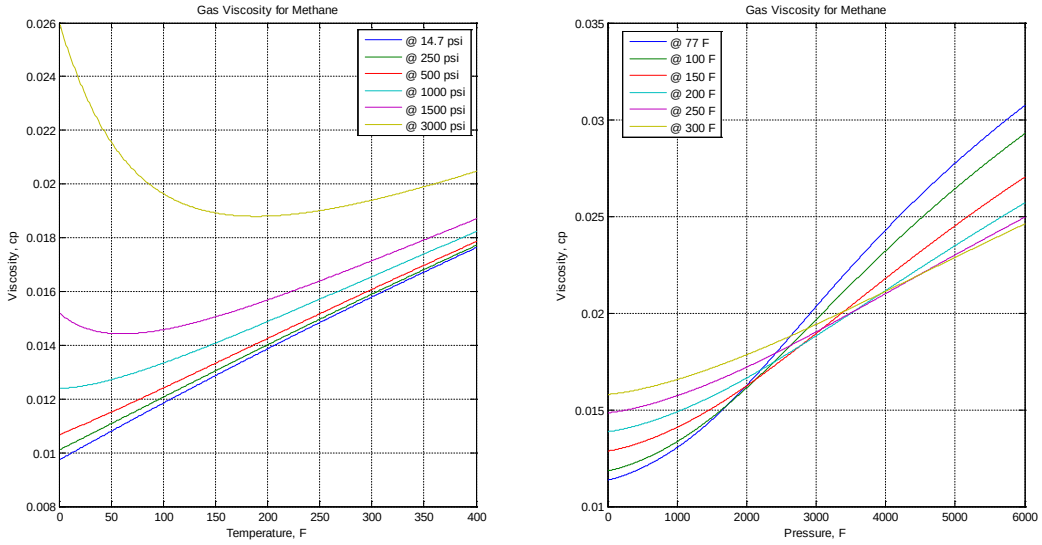

FIGURE 13 - VISCOSITY FOR METHANE AT A RANGE OF PRESSURES AND TEMPERATURES

3.8.2 OIL VISCOSITY

The viscosity of the saturated oil is based on Beggs and Robinsons model for dead oil (Whitson & Brulé, 2000).

$$\mu_{O,p<p_b} = A\left(10^x - 1\right)^B \tag{3.58}$$

$$x = T^{-1.163}\exp(6.9824 - 0.04658API) \tag{3.59}$$

$$A = 10.715\left(R_s + 100\right)^{-0.515} \tag{3.60}$$

$$B = 5.44\left(R_s + 100\right)^{-0.338} \tag{3.61}$$

If the relevant pressure is above the bubble point pressure the Vasquez and Beggs correlation is further used to find the true viscosity (Whitson & Brulé, 2000):

$$\mu_{O,p>p_b} = \mu_{O,p<p_b}\left(\frac{p}{p_b}\right)^m \tag{3.62}$$

$$m = 2.6p^{1.187}\exp\left(-11.513 - \left(8.98\times10^{-5}\right)p\right) \tag{3.63}$$

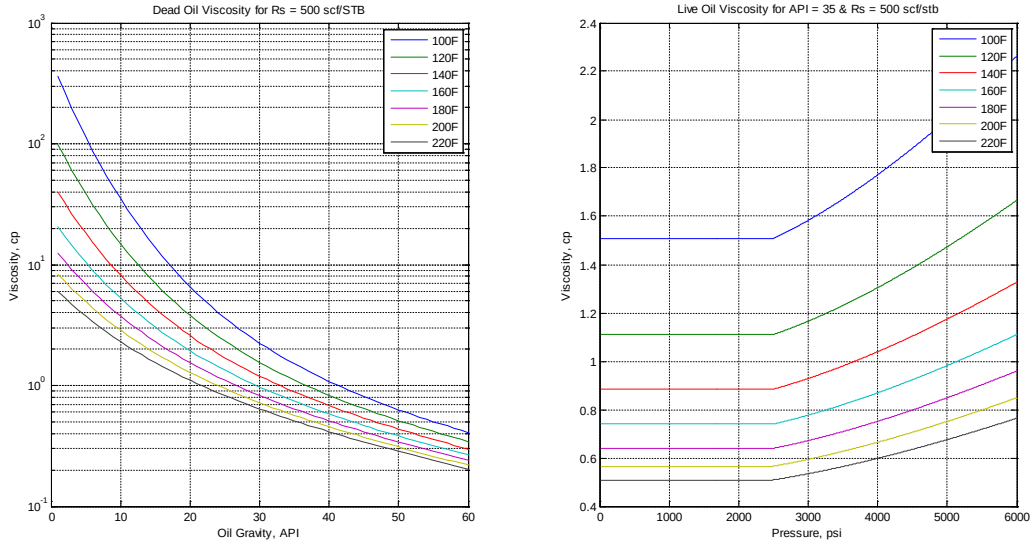

FIGURE 14 - DEAD AND LIVE OIL VISCOSITY FOR A THEORETICAL MIXTURE. BUBBLE POINT PRESSURE SET AT 2,500 PSI.

Figure 14 shows how 35 API oil would act if the solution gas oil ratio remained constant at 500 scf/stb. This is only a theoretical case. In a real situation the solution gas oil ratios, bubble point-pressures would also vary according to pressure and temperature and cause the oil viscosity to follow a completely different profile. An example is show in Figure 15. Here the oil properties are adjusted for the changing condition, the simulation then shows clearly that the viscosity is highly dependent upon both the conditions and the bubble-point pressures value. In

this specific case, oil with API gravity of 35 is assumed to be in solution with methane, the GOR at surface conditions is set to 500 scf/stb, giving bubble point ranging between 2301 psi and 2967 psi for the same temperature range as above.

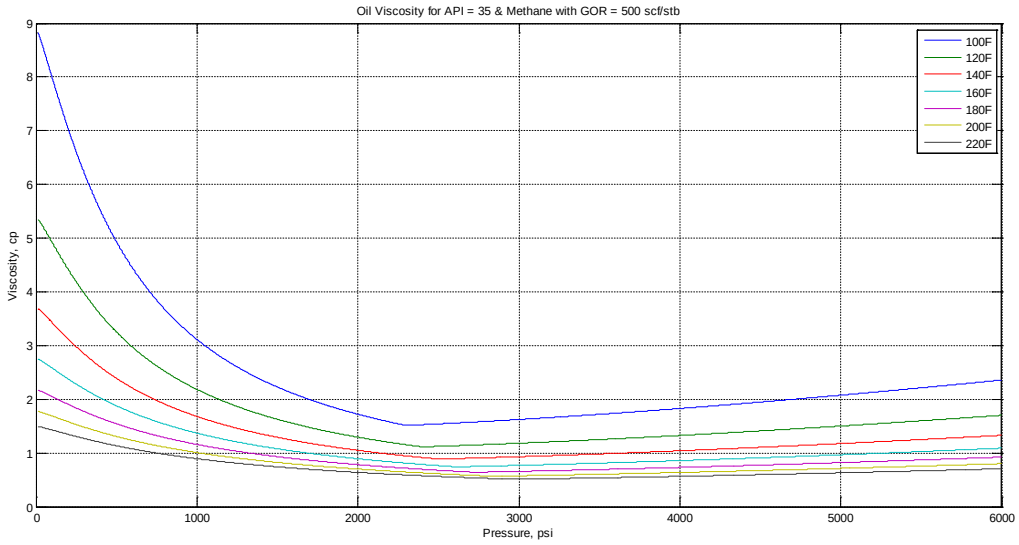

FIGURE 15 - OIL VISCOSITY 35 API OIL WITH METHANE AND GOR OF 500 SCF/STB

3.8.3 WATER VISCOSITY

Water viscosity is calculated according to a simple model described in "Two-phase flow in pipes" (Brill & Beggs, 1978). This model assumes only temperature influences the water viscosity and given as:

$$\mu_w = \exp\left(1.003 - 1.479\times10^{-2}T + 1.982\times10^{-5}T^2\right) \tag{3.64}$$

As Figure 16 shows the water viscosity declines relatively stable in the range from 1 cp to 0.25 cp for most relevant simulation temperatures.

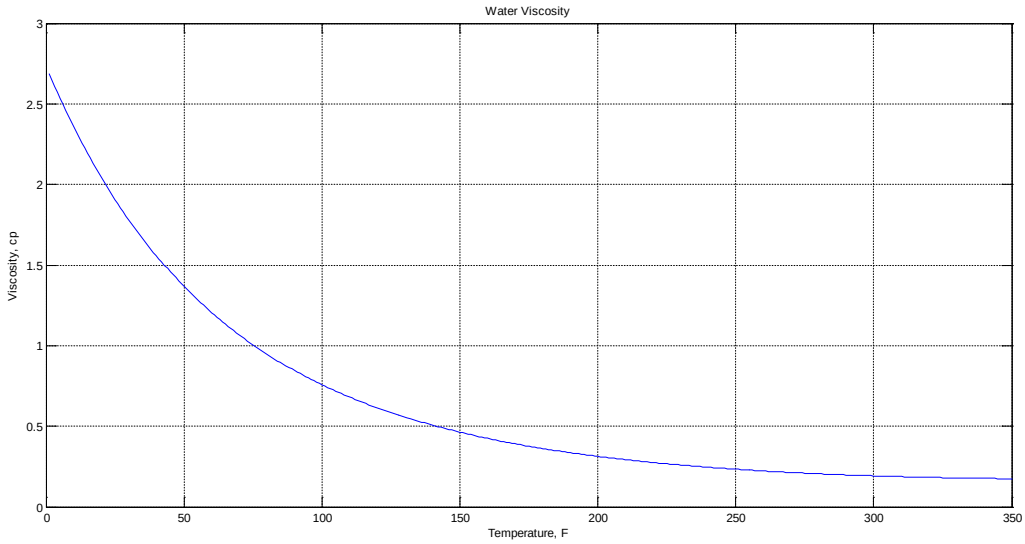

FIGURE 16 - WATER VISCOSITY AT DIFFERENT TEMPERATURES

3.8.4 LIQUID VISCOSITY

Liquid viscosity uses a mixing rule similar to the liquid density where the viscosities for oil and water are weighted upon flow fractions. This assumes the liquid mixture does not form an emulsion; however it is used through all calculations in the UBD simulator. The fluid phase viscosity for further calculations is given by the following mixing rule:

$$\mu_l = f_o \mu_o + f_w \mu_w \tag{3.65}$$

3.8.5 NO-SLIP VISCOSITY

For a situation where slippage is not considered the overall viscosity becomes:

$$\mu_n = \lambda_l \mu_l + \lambda_g \mu_g \tag{3.66}$$

3.8.6 SLIP VISCOSITY

When slippage is considered to be relevant multiple expressions exist to estimate the viscosity, the viscosity is normally calculated by adjusting the gas and liquid value with the power of the corresponding phase and adding these two terms together:

$$\mu_s = \mu_l^{H_l} + \mu_g^{H_g} \tag{3.67}$$

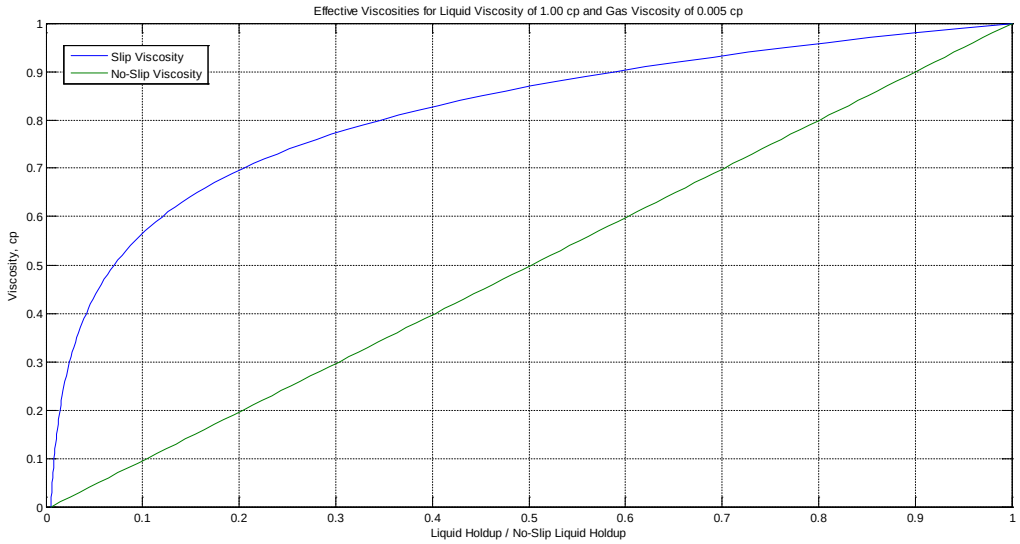

FIGURE 17 - PROFILE OF SLIP AND NO-SLIP VISCOSITY

3.9 INTERFACIAL TENSION

Interfacial tension is a measurement of the surface tension between two phases which keeps them from mixing. The interfacial tension in two-phase flow is rather small and insignificant for pressure drop. However, it is an important factor in pressure correlation which does consider slippage. In the UBD simulator it is determined empirically by factors such as density, temperature and pressure.

The mixing rule for oil-gas and water-gas interfacial tension is based upon the flow fractions, as with density and viscosity. Liquid interfacial tension is calculated by:

$$\sigma_l = f_o\sigma_o + f_w\sigma_w \tag{3.68}$$

3.9.1 OIL-GAS IFT

The dead oil interfacial tension used in the UBD model is given by the following equations presented by Baker and Swerdloff (Baker, 1956):

$$\sigma_{68} = 39 - 0.2571API \quad , \quad T \le 68°F \tag{3.69}$$

$$\sigma_{100} = 37.5 - 0.2571API \quad , \quad T \ge 100°F \tag{3.70}$$

$$\sigma_T = \sigma_{68} - \frac{(T-68)(\sigma_{68} - \sigma_{100})}{32} \quad , \quad 68°F < T < 100°F \tag{3.71}$$

The actual interfacial tension is further given by:

$$\sigma = \sigma_{68/T/100} \exp\left(-8.6306 \times 10^{-4}\, p\right) \tag{3.72}$$

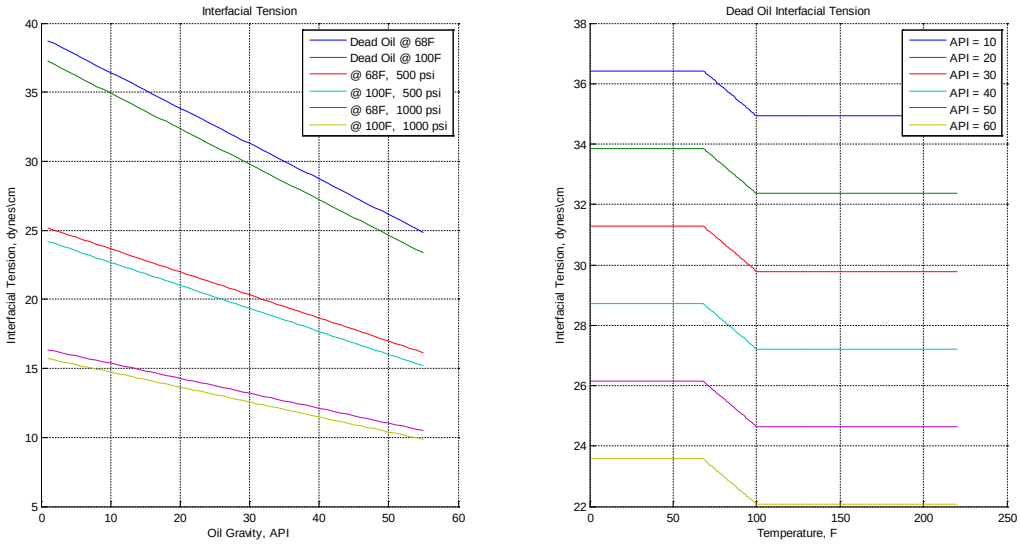

FIGURE 18 - INTERFACIAL TENSION BETWEEN OIL AND GAS

3.9.2 WATER-GAS IFT

A numerical estimate for water-gas interfacial tension based upon Hough's Correlation was used in the model when water is present (Hough, Rzasa, & Wood). The following values are used outside the valid temperature interval and to calculate values in between:

$$\sigma_{74} = 75 - 1.108\,\mathrm{p}^{0.349} \quad , \quad T \le 74°F \tag{3.73}$$

$$\sigma_{280} = 53 - 1.1048\,\mathrm{p}^{0.637} \quad , \quad T \ge 280°F \tag{3.74}$$

Between these temperatures linear interpolation is used:

$$\sigma_T = \sigma_{74} - \frac{(T - \sigma_{74})(\sigma_{74} - \sigma_{280})}{206} \quad , \quad 74°F < T < 280°F \tag{3.75}$$

This correlation is good enough for most simulations in UBD. However, it is not true that the interfacial tension remains constant with increasing temperatures exceeding 280 F. In fact, a temperature increase from 300 F to 400 F has shown to decrease the IFT for all gas compositions and pressures in laboratory experiments (Rushing, Newsham, Van Fraassen, Mehta, & Moore).

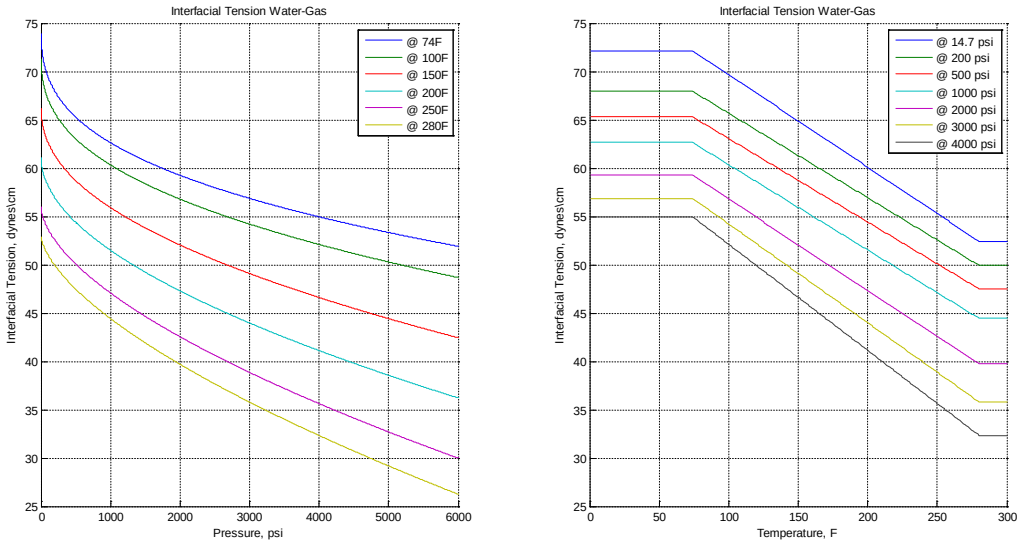

FIGURE 19 - INTERFACIAL TENSION BETWEEN WATER AND GAS

3.10 Bubble Point Pressure

The UBD model uses Standings correlation for California crude oils to calculate the bubble point pressure of the oil (Whitson & Brulé, 2000).

$$p_b = 18.2\left(A - 1.4\right) \tag{3.76}$$

$$A = \left(\frac{R_s}{\gamma_g}\right)^{0.83} 10^{0.00091T - 0.0125API} \tag{3.77}$$

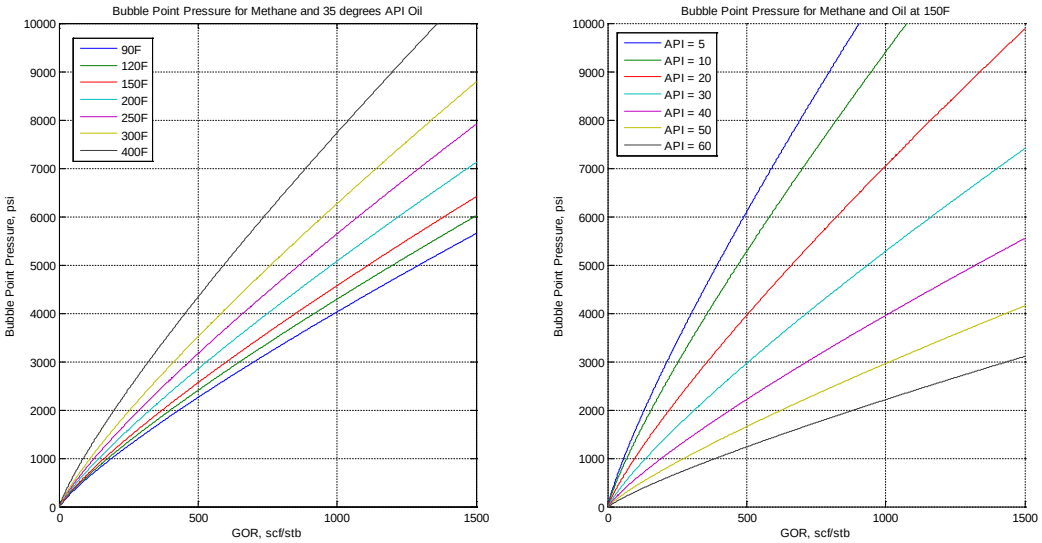

FIGURE 20 - BUBBLE POINT PRESSURES FROM STANDINGS CORRELATION

3.11 Gas Compressibility Factor

The compressibility factor, Z, represents the ratio of a real gas actual volume at a given temperature and a given pressure compared to the ideal volume for the same gas at the same conditions (Whitson & Brulé, 2000).

At low pressures and high temperatures the compressibility factor is close to 1.0. Therefore, the gas appears to be ideal at these conditions. With increasing pressure the compressibility factor will first decrease towards a minimum below 1.0. Afterwards it again increases, with pressure, towards values above 1.0. This is shown in the Standing-Katz diagram in Figure 22.

3.11.1 Pseudo-Reduced Properties

Before a compressibility factor algorithm can be applied to the estimated Z-value the pseudo-reduced properties of the gas have to be known. Pseudo-reduced properties are dimensionless and found by dividing the true pressure and temperature with the corresponding pseudo-critical properties.

Pseudo-critical values are presented in the table below for a range of gases included in the UBD model:

TABLE 2 - PSEUDO-CRITICAL PROPERTIES USED IN THE SIMULATOR

Gas	Air	NH3	CO2	CH4	N2	O2	C3H8	SO2	Custom
T_{pc} (°R)	238.68	729.90	547.56	342.90	227.16	278.10	665.64	775.44	Sutton
p_{pc} (psi)	546.79	1635.60	1070.46	666.42	492.99	731.24	616.25	1143.18	Sutton

As the pseudo-reduced temperatures looked up in Table 2 are given in Rankine; 459.67 additional degrees have to be added to convert the value from Fahrenheit to the correct unit. The dimensionless pseudo-reduced temperature is then given by:

$$T_{pr} = \frac{T + 459.67}{T_{pc}} \tag{3.78}$$

Both inputted pressure and pseudo-critical values found in the same table are given in psi, so the pseudo-critical pressure can be found directly. The pseudo-reduced pressure is calculated by:

$$p_{pr} = \frac{p}{p_{pc}} \tag{3.79}$$

3.11.2 SUTTONS CORRELATION

When the type of gas is either unknown or a mixture of two different gases; e.g. from reservoir influx, is Suttons correlation used by the simulator. Sutton's correlation uses only the known specific gas density to estimate the pseudo-critical properties and is designed to work on hydrocarbons.

The pseudo-critical temperature is found from the following expression and is given in Rankine:

$$T_{pc} = 169.2 + 349.5\gamma_g - 74.0\gamma_g{}^2 \tag{3.80}$$

The pseudo-critical pressure is given by:

$$p_{pc} = 756.8 - 131.07\gamma_g - 3.6\gamma_g{}^2 \tag{3.81}$$

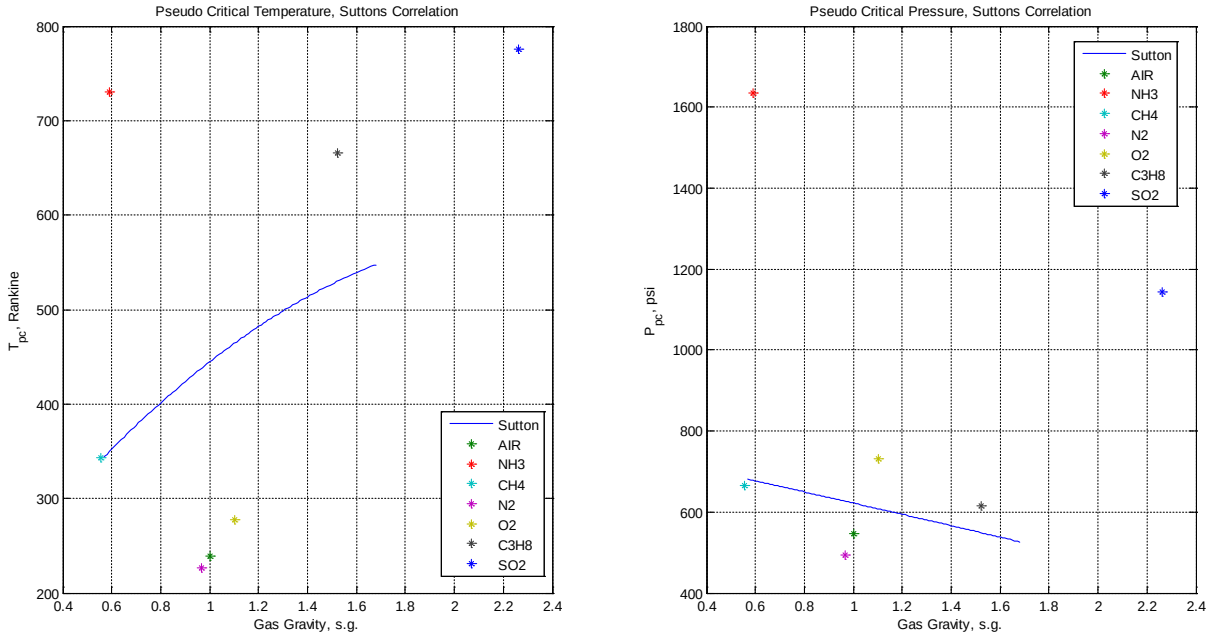

FIGURE 21 - SUTTONS CORREALTION WITH KNOWN GASES

3.11.3 DAK-EOS ALGORITHM

The UBD simulator uses the DAK-EOS to calculate the gas compressibility factor. This Equation of State was especially developed to estimate Z-factors and is relatively accurate for most gases (Dranchuk, 1975):

$$Z = 1 + c_1\rho_{pr} + c_2{\rho_{pr}}^2 - c_3{\rho_{pr}}^5 + c_4 \tag{3.82}$$

To evaluate this expression the terms below must also be calculated:

$$\rho_{pr} = \frac{0.27\,p_{pr}}{ZT_{pr}} \tag{3.83}$$

$$c_1 = A_1 + \frac{A_2}{T_{pr}} + \frac{A_3}{{T_{pr}}^3} + \frac{A_4}{{T_{pr}}^4} + \frac{A_5}{{T_{pr}}^5} \tag{3.84}$$

$$c_2 = A_6 + \frac{A_7}{T_{pr}} + \frac{A_8}{{T_{pr}}^2} \tag{3.85}$$

$$c_3 = A_9\left(\frac{A_7}{T_{pr}} + \frac{A_8}{{T_{pr}}^2}\right) \tag{3.86}$$

$$c_4 = A_{10}\left(1 + A_{11}{\rho_{pr}}^2\right)\left(\frac{{\rho_{pr}}^2}{{T_{pr}}^3}\right)\exp\left(-\frac{A_{11}}{{\rho_{pr}}^2}\right) \tag{3.87}$$

Where:

$$\begin{aligned} A_1 &= 0.3265 \\ A_2 &= -1.07 \\ A_3 &= -0.5339 \\ A_4 &= 0.01569 \\ A_5 &= -0.05165 \\ A_6 &= 0.5475 \\ A_7 &= -0.7361 \\ A_8 &= 0.1844 \\ A_9 &= 0.1056 \\ A_{10} &= 0.6134 \\ A_{11} &= 0.721 \end{aligned} \tag{3.88}$$

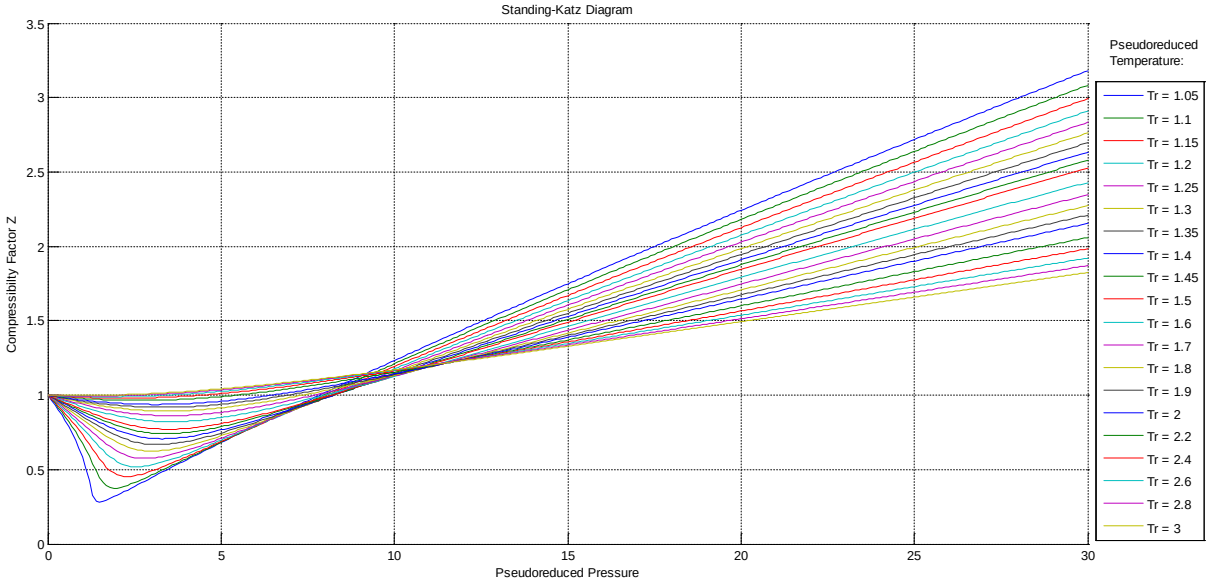

FIGURE 22 - STANDING KATZ DIAGRAM DEVELOPED IN MATLAB FROM DAK-EOS ALGORITHM

Figure 23 shows how the compressibility factor is affected for two different gases. Nitrogen gas is less influenced by the same actual pressure and temperature change as methane would be. The reason for this difference is due to the varying pseudo-critical properties of the gases.

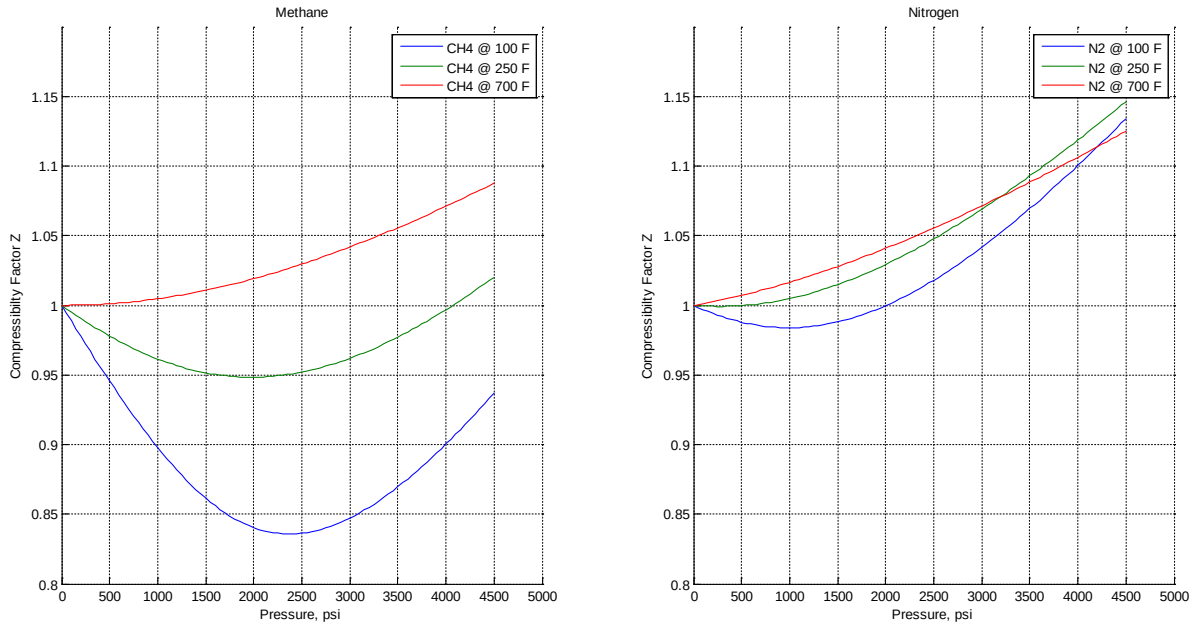

FIGURE 23 - GRAPHICAL REPRESENTATION OF THE COMPRESSIBILITY FACTOR OF METHANE AND NITROGEN GAS

4 Drilling With Aerated Fluids

4.1 Introduction To Aerated Drilling

An aerated drilling fluid is defined as: “a mixture of gas in a liquid drilling fluid without any special emulsifier or stabilizing agent” (Rehm, 2012). An aerated fluid system is the most flexible fluid system among the UBD candidate fluids, and has several advantages over the other systems.

The application of using aerated systems for drilling was described in the U.S in 1866. The first company to apply this technique was Imperial Oil Company in 1932 when the firm drilled an oil well in the Atlas Mountains; Persia.

A wide range of liquids can be used together with gas; normally nitrogen, air or natural gas, to achieve the required down-hole conditions. Although aerated fluid systems have many advantages over conventional methods, there are new challenges present in the design of the fluid gas-liquid mixture and operational procedures. The two main challenges in aerated fluid systems are to keep the two phases from breaking apart and for the fluid mixture to remain stable.

4.1.1 Advantages of Aerated Systems

Aerated fluid systems were originally used in oil well drilling to eliminate the NPT from LC. Later, other advantages like elimination of differential sticking and increased ROP were discovered.

As the aerated fluid system is very flexible in choice of base liquid, this fluid system allows sensitive formation types to be easily handled in UBD operations. The fluid makes it easy to control the BHP, especially in friction-dominated flow regimes, as the fluid will act more or less as a single-phase fluid in this regime.

An important advantage of aerated systems is that the chip hold-down pressure is eliminated, which results in much better hole cleaning and drill rate, when using roller cone bits. Aerated systems are therefore often an obvious choice in formations with very low ROP as this also helps reducing WOB, extends the overall bit life and tripping time.

4.1.2 Disadvantages of Aerated Systems

Due to the increased equipment, space and staff cost, aerated fluid systems are usually more expensive to operate than conventional fluid systems.

The aerated fluid system is generally an unstable system where the liquid and gas phase is naturally separated by gravitational forces. When the gas in the fluid rises in the wellbore, the liquid phase drops down and forms a fluid column. These gravitational forces repeat themselves in cycles as when gas escapes through the choke and the fluid column moves towards the surface compressing the gas below again, causing pressure surges. This can cause several problems, including wellbore instability and formation damage. It should therefore be controlled by adjusting the choke and possible alter the fluid viscosity if it is too excessive.

Other disadvantages due to the large presence of gas in the drilling fluid are the inability to use MWD tools while drilling, increased torque, drag and vibration with high friction pressures and more corrosion. When using an aerated system there is also an increased explosion hazard.

4.1.3 Design Parameters

The rate of liquid flow is normally the first factor to consider when designing the drilling parameters. This is due to the influence liquid rate has on the overall hole-cleaning and drilling motor operation. If the hole-cleaning is insufficient cuttings will build up in the fluid mixture and cause more pressure related problems like surging and stuck pipe. Hole-cleaning is especially important in horizontal sections of the well.

The first design criterion for the drilling fluid is therefore to select a liquid volume which would give an annular velocity sufficient for proper hole-cleaning. A rule of thumb in the industry is to select a liquid flow rate which would provide annular velocity of approximately 120 ft/min. The UBD simulator uses an annular mixture velocity of 120 ft/min to check for proper holes cleaning. Another rule of thumb is to design for a minimum annular velocity of two times the cuttings settling velocity.

Gas is added to the mixture until the fluid system acquires the proper conditions. The rate of gas injection can range from almost nothing to a severely large amount as long as the liquid stays in the continuous phase. A normal design factor would be to add gas so that the fluid mixture remains stable in the friction-dominated regime where the mixture will act more as a liquid only system.

Though Rehm et.al and many other papers on the subject states that an UBD operation should be operated using friction dominated regime this is not necessarily the answer to each operation. The engineered fluid design might not be possible when performing the operation. In general operating in the friction dominated region is desirable, but not a governing design or operational constraint. Factors such as reservoir deliverability, well geometry and surface equipment are among many factors that influence whether the well is to be drilled in the hydrostatic or friction dominated regime. The well might not produce as much gas as expected or the gas lift itself might be insufficient to reach the friction dominated regime (Culen, 2014).

Rehm et.al states that the maximum gas-quality at the surface should be limited to an amount where cuttings can still be transported and we avoid pressure surges. This maximum gas quality is approximately 80% for aerated systems. Exceeding this limit causes gas to become the continuous phase and the pressure related problems mentioned above to occur (Rehm, 2012).

Setting this limit at exactly at 80% is somehow an uncertain design factor as many conflicting explanations exist. According to Culen; this is not necessarily true for two phase systems due to the nature of liquid hold up. He explains that when the gas rises in the annulus, in multiphase flow systems, the gas phase volume will in most cases exceed this value of 80%. This is according to Culen very much expected, as gas becomes the dominant phase near the surface. This does not further compromise hole-cleaning as the annular velocity is still very high in these sections of the well and provides proper cuttings transport (Culen, 2014).

The annular backpressure can be adjusted to alter the fluid properties, keep a smooth pressure regime and contribute as a regulator for the BHP. The surface backpressure is usually estimated to be in the range of 100 psi and is from there adjusted (after simulations) to keep the flow stable within the operational limits.

4.2 Pressure Correlations

The pressure drop over a length increment in two-phase flow is composed of three different pressure contribution terms; hydrostatic, friction and acceleration pressure. The general equation for pressure drop over a pipe segment is given by:

$$\frac{dp}{dL} = \frac{g}{g_c}\rho_s \sin\phi + \frac{f\rho_f v_m^{\ 2}}{2g_c d} + \frac{\rho v_m dv_m}{g_c dL} \tag{4.1}$$

This can be rewritten as:

$$\frac{dp}{dL} = \left(\frac{dp}{dL}\right)_{el} + \left(\frac{dp}{dL}\right)_{f} + \left(\frac{dp}{dL}\right)_{acc} \tag{4.2}$$

and further simplified and converted into a pressure gradient (psi/ft):

$$\frac{dp}{dL} = \frac{\left(\frac{dp}{dL}\right)_{el} + \left(\frac{dp}{dL}\right)_{f}}{144(1-\mathrm{E}_k)} \tag{4.3}$$

The hydrostatic term is usually the one that is dominant for non-horizontal sections and the main contributor towards the final BHP. The hydrostatic pressure change is found by calculating the (slip) density and multiplying it with the respective inclination.

$$\left(\frac{dp}{dL}\right)_{el} = \rho_s \sin\phi \tag{4.4}$$

Frictional pressure is more important in highly inclined segments and for cases where the flow rates are high. Frictional pressure contribution in two-phase flow is complex to estimate, and several available correlations exist.

$$\left(\frac{dp}{dL}\right)_{f} = \frac{f_{tp}\rho_n^{\ 2} v_m^{\ 2}}{2gd\rho_s} \tag{4.5}$$

The contribution from acceleration is usually not noticeable and can often be set to zero. This contribution is only worth including for high flow rates that occur in segments with geometries which causes the flow velocity to become very large.

$$E_k = \frac{\rho_s v_m v_{sg}}{144gp} \tag{4.6}$$

Correlations to predict these three pressure contributions have been classified by Beggs & Brill into three different categories; a, b and c.

This thesis includes two well-known empirical correlations for each of the tree categories, not counting the original Poettmann & Carpenter correlation which is also implemented as a reference. The models included in the UBD simulator were chosen based upon the fact that they were reasonably easily implemented into a MATLAB program.

4.2.1 CATEGORY A

"Category A" correlations were among the first two phase flow correlations to be developed and are therefore fairly simple. The correlations placed in "Category A" have in common that they do not consider either flow regimes or slip. The effective friction factor in the flow is the only parameter which separates these "Category A" correlations from each other making this subgroup the easiest to estimate and often understand as it resembles one phase liquid flow. Using charts and a simple calculator pressure drops can be estimated without too much effort. However, these results are not expected to be as accurate as the other available correlations. Well known correlations within this category include Poettmann & Carpenter, Baxendell & Thomas and Fancher & Brown.

To calculate the friction factor for correlations within this category the following procedure is followed:

First the dynamic viscosity for the fluid flow is calculated in lbm/ft-sec as given by:

$$\mu_{dyn} = \rho_n v_m d_h \tag{4.7}$$

Next a correlation is chosen and the value of the two-phase friction factor is read from the relevant graph.

$$f_{tp} = f_{tp}\left(\mu_{dyn}\right) \tag{4.8}$$

4.2.1.1 POETTMANN & CARPENTER

The Poettmann & Carpenter method was the first model developed to estimate pressure gradients in two-phase wells, and was used for a long time period. The model is based on field data from 349 producing wells with production ranging up to 500 stb/d and GLR of 1500 scf/stb through tubing sizes between 2.375" and 3.5". Poettmann and Carpenter assumed that the acceleration was included in the friction factor, and therefore ignores the acceleration term. The model is based upon two data points and is designed to work on coarser grids. (Beggs, 1991).

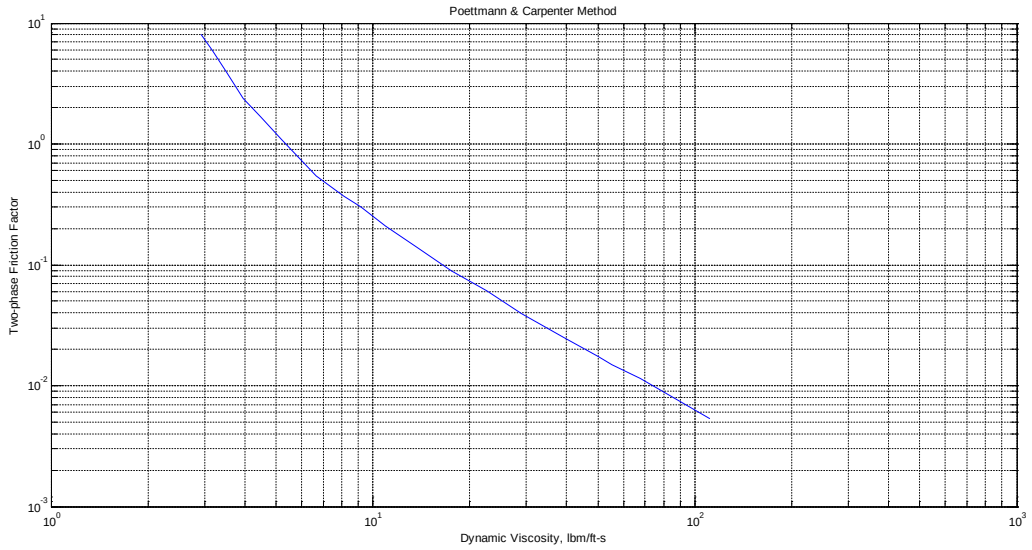

FIGURE 24 - TWO-PHASE FRICTION FACTOR FROM POETTMANN & CARPENTER

A simplified version of Poettmann & Carpenter Model is also included in the UBD simulator where the friction factor is simply found by the following expression:

$$f_{tp} = 4 \times 10^{1.444 - 2.5\log_{10}\left(\mu_{dyn}\right)} \tag{4.9}$$

4.2.1.2 BAXENDELL & THOMAS

Baxendell and Thomas improved upon the Poettmann and Carpenters model by increasing the range of production rates and pipe sizes. They did field experiments on a 10,500 feet well through 2.875" and 3.5" production tubing. The production rates ranged from 176 to 5082 bbl/day with GLRs stable around 730 scf/bbl. Pressures was measured in intervals of 500 and 1,000 ft. They also showed that the model was valid for annular flow when tests between 2.875" tubing and 7" casing proved good results (Baxendell & Thomas).

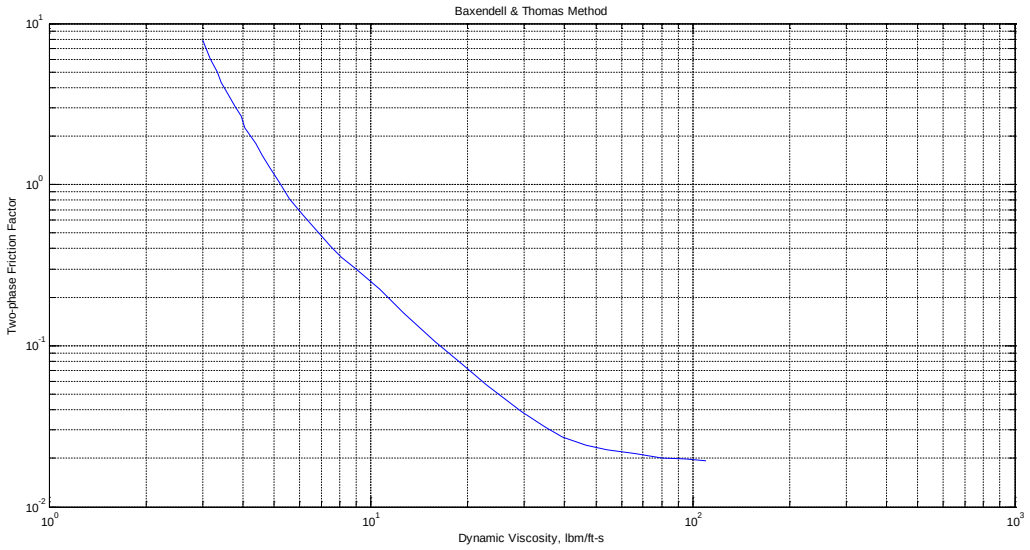

FIGURE 25 - TWO-PHASE FRICTION FACTOR FROM BAXENDELL & THOMAS

4.2.1.3 FANCHER & BROWN

Fancher and Brown also proposed an improvement of the original model by improving the model to better represent a variety of GLRs. The proposed model was based on production tests from an 8000 ft long well with 2.375" production tubing. Production rate varied between 75 and 938 bbl/day; with GLRs varying from 105 to 9433 scf/bbl. The results showed that the Poettmann and Carpenters model was not valid for higher and lower GLRs so a new relationship for the friction factor was developed for three different GLR ranges (Fancher & Brown).

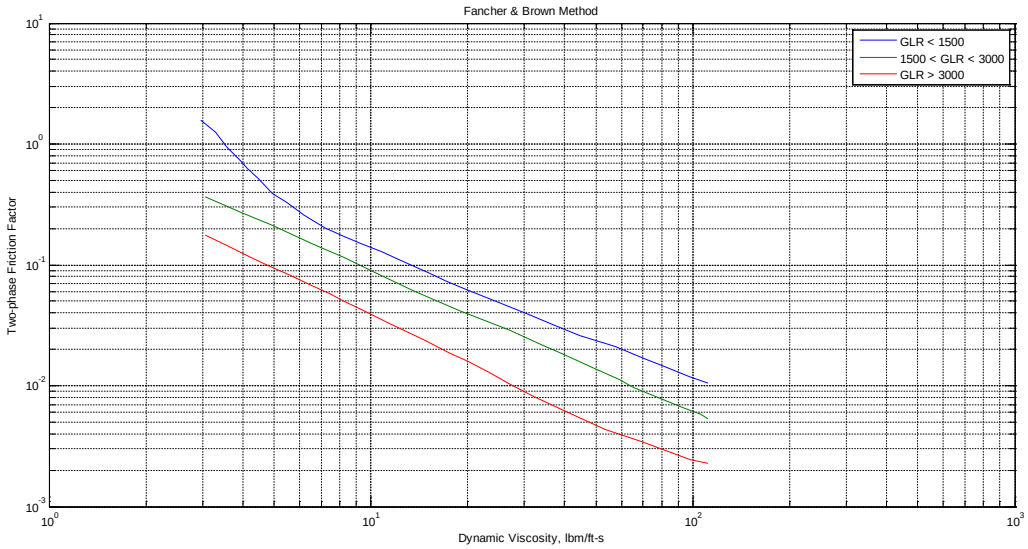

FIGURE 26 - TWO-PHASE FRICTION FACTORS FROM FANCHER & BROWN

4.2.2 CATEGORY B

"Category B" correlations do as "Category A" correlations not consider flow regimes. However slip is now considered. As this category allows gas and liquid to have different velocities in a single pipe segment; the correlations within also include estimation of liquid hold-up in addition to friction factor for the flow. The most recognized "Category B" correlation is Hagedorn & Brown. Grays correlation (used with high-gas content) is also mentioned in this paper and included in the simulator.

When the liquid holdup is known further calculations can be done and then the friction factor can be found by utilizing, for example the Haalands equation, as described in section A.1.2. Note: Gray's correlation uses a modified roughness parameter.

4.2.2.1 HAGEDORN & BROWN

Hagedorn and Brown developed their model based upon data from a 1,500 feet experimental well. A large variety of different liquid flow rates, GLRs and liquid viscosities were used in the testing. Tubing sizes which fluid was flowed through were 1.0" and 1.25" and 1.5" (Bai & Bai, 2005). They did not measure the liquid hold-up directly but instead calculated it to match the experimental data from the well (Brill & Beggs, 1978).

The correlation uses the following dimensionless numbers to determine the liquid holdup:

$$N_{lv} = 1.938 \times v_{sl} \left(\frac{\rho_l}{\sigma_l} \right)^{\frac{1}{4}} \tag{4.10}$$

$$N_{gv} = 1.938 \times v_{sg} \left(\frac{\rho_l}{\sigma_l} \right)^{\frac{1}{4}} \tag{4.11}$$

$$N_d = 120.872 \times d_h \left(\frac{\rho_l}{\sigma_l} \right)^{\frac{1}{2}} \tag{4.12}$$

$$N_l = 0.15726 \times \mu_l \left(\frac{1}{\rho_l \sigma_l^{\,3}} \right)^{\frac{1}{4}} \tag{4.13}$$

From these numbers the liquid holdup is found from reading values from the graphs in the following section:

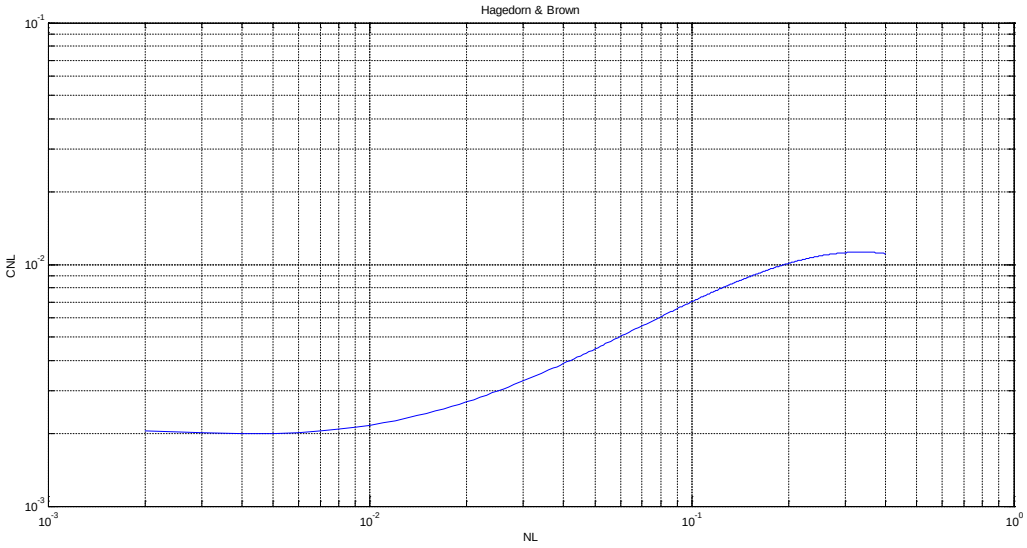

FIGURE 27 - FLOW PARAMETER CNL FROM HAGEDORN & BROWN

Or calculated by:

$$C_{NL} = 10^{-2.69851+0.1584095\times(\log_{10}(N_l)+3)-0.5509976\times(\log_{10}(N_l)+3)^2+0.5478492\times(\log_{10}(N_l)+3)^3-0.1219458\times(\log_{10}(N_l)+3)^4} \tag{4.14}$$

Before the next graphs are read CA and CB has to be determined:

$$C_A = \frac{N_{lv}}{N_{gv}^{\,0.575}} \left(\frac{p}{14.7} \right)^{0.1} \frac{C_{NL}}{N_d} \tag{4.15}$$

$$C_B = N_{gv} \frac{N_l^{\,0.38}}{N_d^{\,2.14}} > 0.012 \tag{4.16}$$

Liquid hold up can now be found in these graphs:

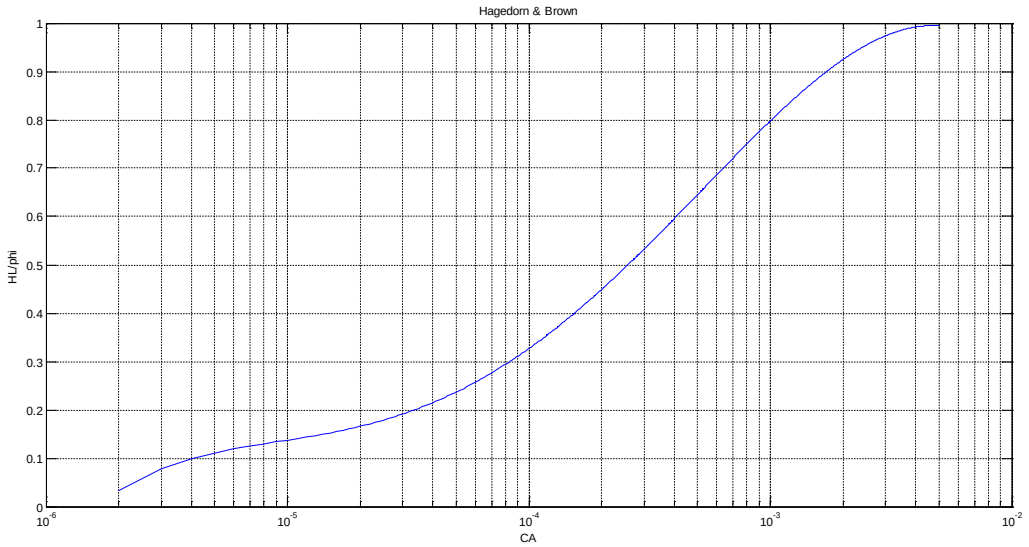

FIGURE 28 - LIQUID HOLDUP PARAMETER 1 FROM HAGEDORN & BROWN

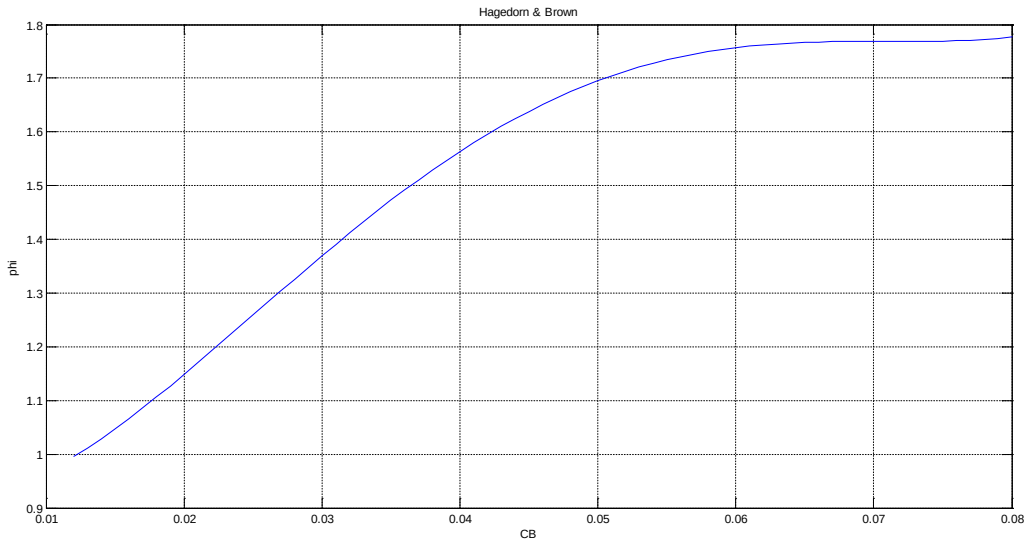

FIGURE 29 - LIQUID HOLDUP PARAMETER 2 FROM HAGEDORN & BROWN

or directly by these corresponding equations:

$$\frac{H_l}{\phi} = -0.1030658 + 0.617774 \times (\log_{10}(C_A) + 6) - 0.632946 \times (\log_{10}(C_A) + 6)^2 + 0.29598 \times (\log_{10}(C_A) + 6)^3 - 0.0401 \times (\log_{10}(C_A) + 6)^4 \quad (4.17)$$

$$\phi = 0.9116257 - 4.821756 \times C_B + 1.232250 \times 10^3 \times {C_B}^2 \\ -2.225358 \times 10^4 \times {C_B}^3 + 1.161743 \times 10^5 \times {C_B}^4 \tag{4.18}$$

$$H_l = \frac{H_l}{\phi}\phi \tag{4.19}$$

4.2.2.2 GRAYS CORRELATION

Gray developed a model valid for tubing sizes up to 3.5" where the mixture velocity does not exceed 50 ft/sec. The model is designed for production of gas wells and should therefore not be used in wells were the liquid fraction is high (> 50 bbl/MMscf) (Gray, 1974). However, studies have however shown that the model still provides very good results outside these limits when the fluid mixture is similar to what one would see when producing from a wet gas or condensate system (Bellarby, 2009). The model applies the following equations:

$$N_1 = \frac{{\rho_n}^2 {v_m}^4}{0.00220462 g \sigma_l \left(\rho_l - \rho_g\right)} \tag{4.20}$$

$$N_2 = \frac{g {d_h}^2 \left(\rho_l - \rho_g\right)}{0.00220462 \sigma_l} \tag{4.21}$$

$$N_3 = 0.0814\left(1 - 0.0554 \times \ln\left(1 + \frac{730 R_v}{R_v + 1}\right)\right) \tag{4.22}$$

$$R_v = \frac{v_{sl}}{v_{sg}} \tag{4.23}$$

$$f_1 = -2.314\left(N_1\left(1 + \frac{205}{N_2}\right)\right)^{N_3} \tag{4.24}$$

$$H_l = 1 - \left(1 - \lambda_l\right)\left(1 - \exp\left(f_1\right)\right) \tag{4.25}$$

$$\varepsilon_0 = \frac{28.5 \times 0.00220462 \sigma_l}{\rho_n {v_m}^2} \tag{4.26}$$

$$\varepsilon_e = \varepsilon_0, \quad \varepsilon_e \geq 2.77 \times 10^{-5}, \quad R_v \geq 0.007, \tag{4.27}$$

$$\varepsilon_e = \varepsilon + R_v \frac{(\varepsilon_0 - \varepsilon)}{0.007}, \qquad \varepsilon_e \geq 2.77 \times 10^{-5}, \qquad R_v < 0.007, \tag{4.28}$$

4.2.3 CATEGORY C

The last and most advanced category of correlations "Category C" are further improved upon "Category B" correlations as these also considers different flow regimes. This causes the entire process of estimating the liquid hold-up and friction factor to be much more complex as these values are calculated differently depending on which flow regime is present. "Category C" correlations must therefore also include ways of determining the flow regime, often presented in a flow map. Well known "Category C" correlations include Duns and Ros, Orkiszewski and Beggs & Brill among others.

4.2.3.1 DUNS & ROS

The Duns and Ros model was developed through an extensive large scale laboratory test over a period of four years. 20,000 data points were collected for a large variety of input parameters. With two more years of additional testing and model evaluation a reliable correlation was constructed and became an industry standard for pressure prediction in two-phase flow modeling (Duns & Ros).

This correlation considers both slippage and flow regimes and are therefore often a preferred correlation to use in more complex simulations. The model is however based upon vertical wells, and should be used with care in highly inclined wells. It requires the dimensionless flow parameters used from Hagedorn & Brown to first be calculated as they are used to set the flow regime boundaries.

Two parameters which influence these boundaries are given by:

$$L_s = 50 + 36 N_{lv} \tag{4.29}$$

$$L_m = 75 + 84 N_{lv}^{\,0.75} \tag{4.30}$$

This correlation uses multiple graphical interpolations to determine all parameters required in each pressure calculation. As interpolation is somehow slow to execute in MATLAB, this specific correlation can be time consuming to run compared to other available options. The initial interpolation is performed to find the limits of another flow regime boundary.

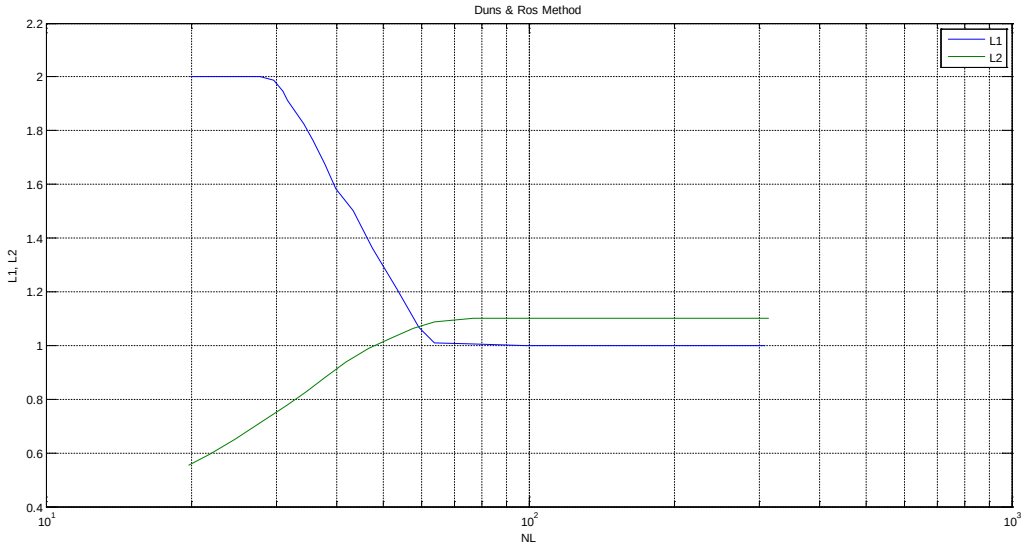

FIGURE 30 - BOUNDARY PARAMETERS FROM DUNS & ROS

The flow is considered to be bubble flow if:

$$0 \le N_{lv} \le L_1 + L_2 N_{lv} \tag{4.31}$$

$$F_3' = \mathrm{F}_3 - \frac{F_4}{N_d} \tag{4.32}$$

$$S = \left(F_1 + F_2\right) N_{lv} + F_3' \left(\frac{N_{gv}}{1 + N_{lv}} \right)^2 \tag{4.33}$$

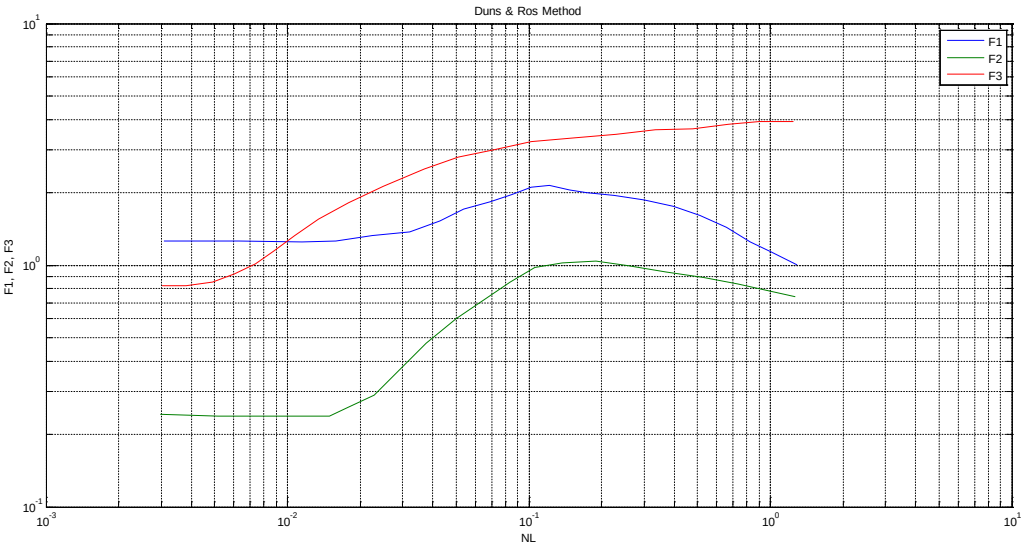

FIGURE 31 - FLOW PARAMETERS FROM DUNS & ROS

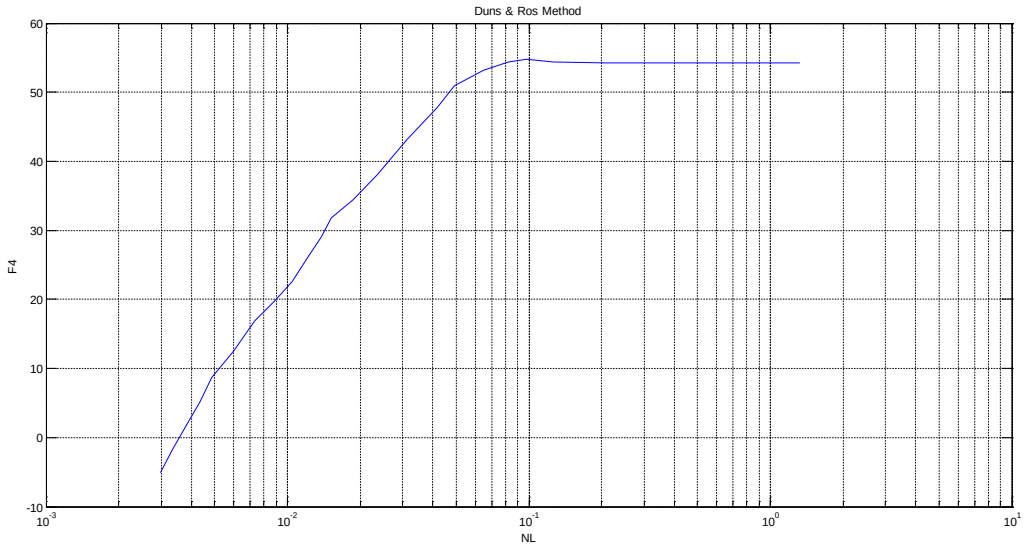

FIGURE 32 - FLOW PARAMETERS FROM DUNS & ROS

The flow is considered to be slug flow if:

$$L_1 + L_2 N_{lv} \le N_{gv} \le L_s \tag{4.34}$$

$$F_6' = 0.029\,\mathrm{N}_d + F_6 \tag{4.35}$$

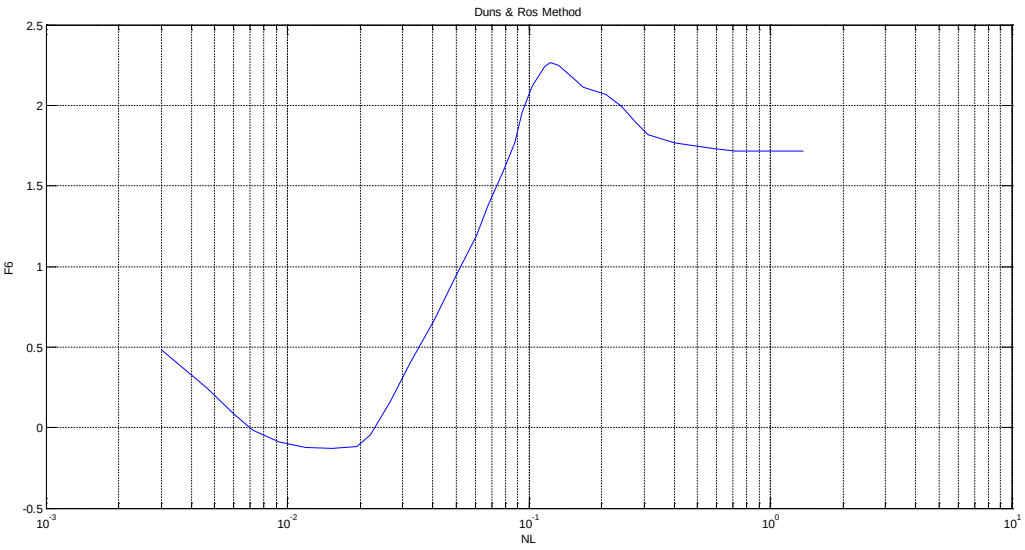

FIGURE 33 - FLOW PARAMETER FROM DUNS & ROS

$$S = \left(1 + F_5\right)\frac{N_{gv}^{\,0.982} F_6'}{\left(1 + F_7 N_{lv}\right)^2} \tag{4.36}$$

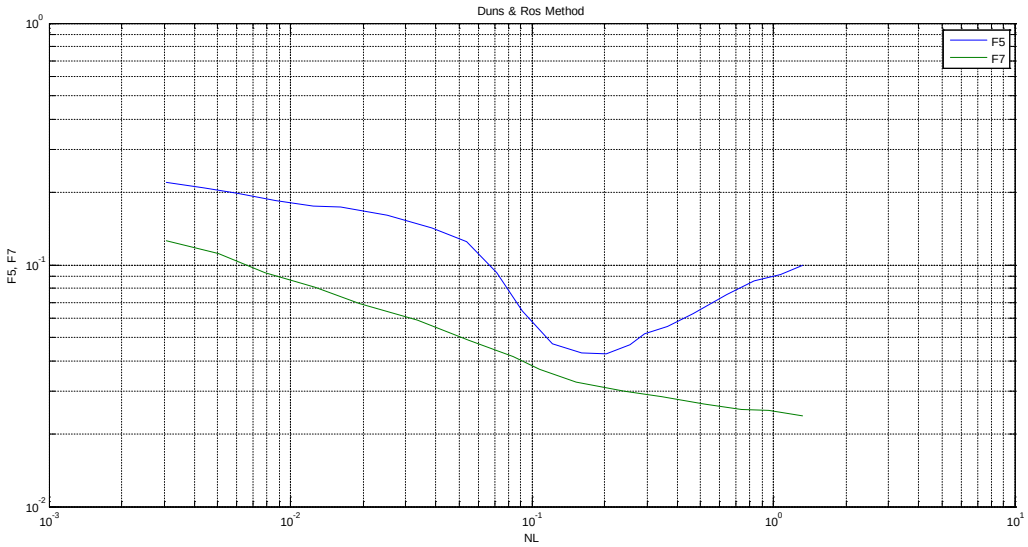

FIGURE 34 - FLOW PARAMETERS FROM DUNS & ROS

The flow is considered to be mist flow if:

$$L_m < N_{gv} \tag{4.37}$$

$$H_l = \lambda_l \tag{4.38}$$

$$N_{We} = \frac{\rho_G v_{sg}{}^2 \varepsilon}{\sigma_l} \tag{4.39}$$

$$N_{\mu} = \frac{\mu_l{}^2}{\rho_l \sigma_l \varepsilon} \tag{4.40}$$

$$\varepsilon = 0.0749 \frac{\sigma_l}{\rho_g v_{sg}{}^2 d_h} \quad , \quad N_{We} N_{\mu} \le 0.005 \tag{4.41}$$

$$\varepsilon = 0.3713 \frac{\sigma_l}{\rho_g v_{sg}{}^2} \left(N_{We} N_{\mu} \right)^{0.302} \quad , \quad N_{We} N_{\mu} > 0.005 \tag{4.42}$$

$$N_{\mathrm{Re},g} = \frac{\rho_g v_{sg} d_h}{\mu_g} \tag{4.43}$$

$$f = 4 \times \left(\left(\frac{1}{\left(4 \log_{10} \left(0.27 \frac{\varepsilon}{d_h} \right) \right)} \right)^2 + 0.067 \left(\frac{\varepsilon}{d_h} \right)^{1.73} \right) \quad , \quad \frac{\varepsilon}{d_h} > 0.05 \tag{4.44}$$

For values below 0.05 are the friction factor found by applying Haaland's equation.

$$\left(\frac{dp}{dL}\right)_{fric} = \frac{f\rho_g v_{sg}^{\ 2}}{2gd_h} \tag{4.45}$$

The flow is considered to be transitional if:

$$L_s < N_{gv} < L_m \tag{4.46}$$

$$A = \frac{L_m - N_{gv}}{L_m - L_s} \tag{4.47}$$

$$H_l = AH_{l,slug} + (1-A)\lambda_l \tag{4.48}$$

$$\left(\frac{dp}{dL}\right)_{fric} = A\left(\frac{dp}{dL}\right)_{fric,slug} + (1-\mathrm{A})\left(\frac{dp}{dL}\right)^{*}_{fric,mist} \tag{4.49}$$

* The friction contribution from mist flow is slightly modified as the calculations are made with the following substitution:

$$\rho_g{}' = \rho_g \frac{N_{gv}}{L_m} \tag{4.50}$$

The slip parameter is then used to calculate the slip velocity and corresponding liquid hold-up.

$$v_s = \frac{S}{1.938}\left(\frac{\sigma_l}{\rho_l}\right)^{1/4} \tag{4.51}$$

$$H_l = \frac{v_s - v_m + \sqrt{(v_m - v_s)^2 + 4v_s v_{sl}}}{2v_s} \tag{4.52}$$

Note: In mist flow the liquid hold up is assumed to be equal to the no-slip liquid holdup.

For bubble/slug flow the following equations are used:

$$N_{\mathrm{Re,l}} 1488\frac{\rho_l v_{sl} d_h}{\mu_l} \tag{4.53}$$

$$f_3 = 1 + f_1\sqrt{\frac{v_{sg}}{50v_{sl}}} \tag{4.54}$$

The friction factor, f1 can either be found in the Moody diagram or by using a relevant correlation. The simulator applies Haaland's equation as explained in section A.1.2.

Friction factor f2 is found in graphically in Figure 35 and is dependent on:

$$f_2 = f_2\left(f_1 \frac{v_{sg}}{v_{sl}} N_d^{2/3} \right)$$

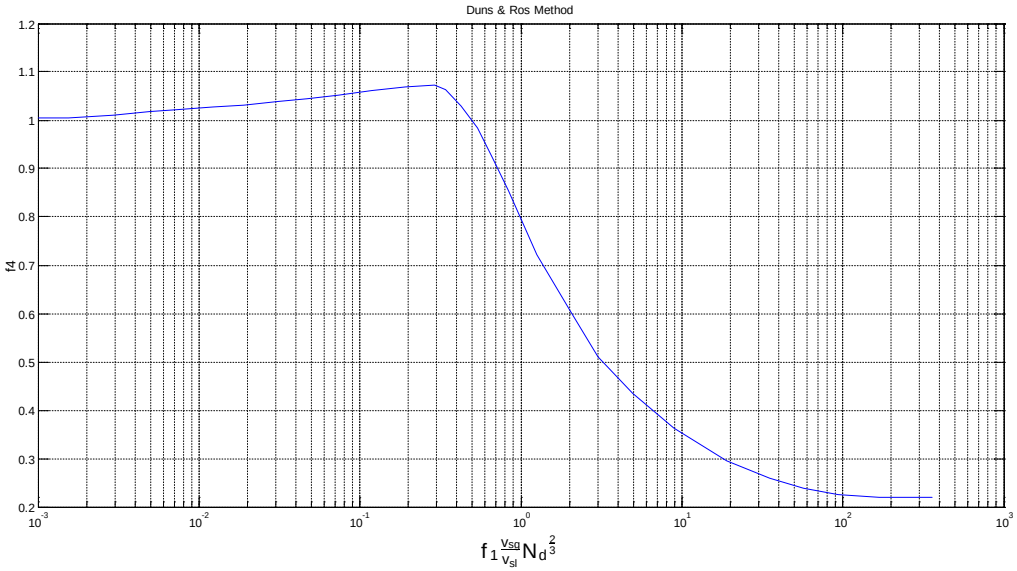

FIGURE 35 - DUNS & ROS, F4 PARAMETER

The combined and final friction factor is then given by:

$$f_m = f_1 \frac{f_2}{f_3} \tag{4.55}$$

$$\left(\frac{dp}{dL} \right)_{fric} = \frac{f_m \rho_l v_{sl} v_m}{2 g d_h} \tag{4.56}$$

The flow map used in Duns and Ros' correlation varies with the dimensionless parameter Nd. Below are two examples of how the flow regime boundaries shift with varying pipe diameter.

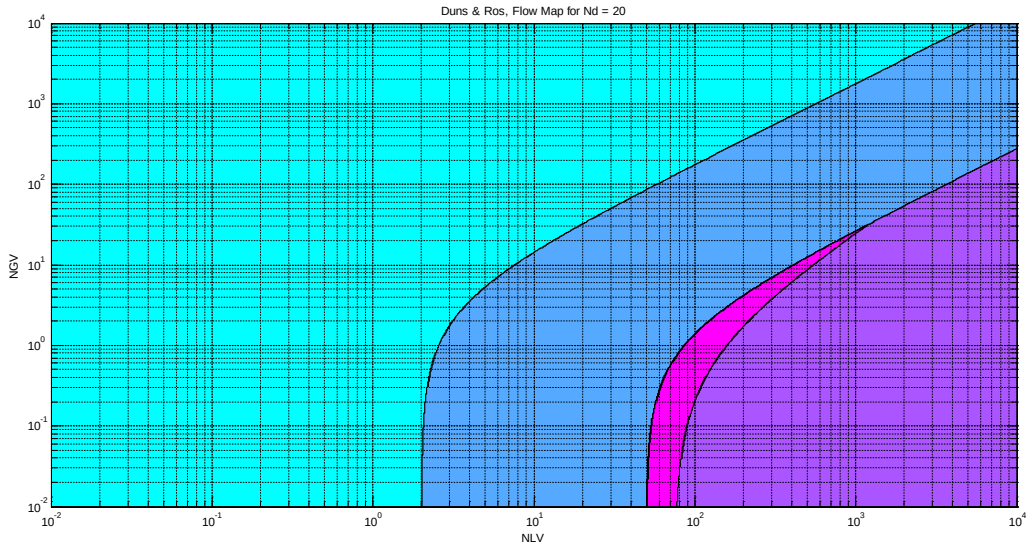

FIGURE 36 - DUNS & ROS FLOWMAP IN A SMALL DIAMETER SECTION FLOWMAP (LIGHT BLUE SLUG. PINK TRANSITION, DARK MIST, PURPLE BUBBLE)

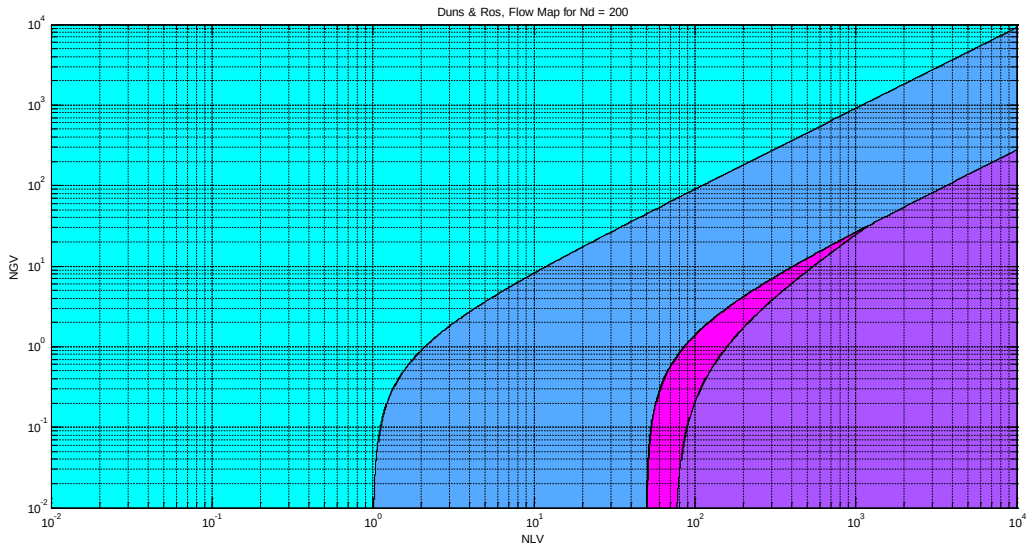

FIGURE 37 - DUNS & ROS FLOWMAP IN A LARGE DIAMETER SECTION FLOWMAP (LIGHT BLUE SLUG. PINK TRANSITION, DARK MIST, PURPLE BUBBLE)

4.2.3.2 BEGGS & BRILL

The Beggs & Brill model was developed in a laboratory to estimate pressure drops through a variety of pipe inclinations, including both up- and downhill flow. This correlation allows for more advanced well paths and an overall more complex flow than the other models earlier described in this chapter. The liquid hold-up was measured for air and water flowing through pipes at 1.0" and 1.5" and a model was constructed on 584 data points. The tests were performed with liquid flow rates ranging from 0-30 gpm and gas rates ranging from 0-300 Mscf/day (Brill & Beggs, 1978).

$$N_{FR} = \frac{v_m^{\ 2}}{g d_h} \tag{4.57}$$

The first step to find the pressure drop while using the Beggs-Brill correlation to determine the flow regime in the interval given by the following parameters:

$$L_1 = 316\lambda_l^{\,0.302} \tag{4.58}$$

$$L_2 = 0.0009252\lambda_l^{\,-2.4684} \tag{4.59}$$

$$L_3 = 0.1\lambda_l^{\,-1.4516} \tag{4.60}$$

$$L_4 = 0.5\lambda_l^{\,-6.738} \tag{4.61}$$

These parameters are further used to examine what type of flow that is present inside the pipe. The flow patterns are divided into three main types; segregated, intermittent and distributed(Brill & Beggs, 1978).

In a horizontal pipe the flow can be stratified, wavy or centric to be considered segregated. The flow regime is assumed to be segregated if:

$$\lambda_L < 0.01 \text{ and } \mathrm{N_{FR}} < \mathrm{L_1} \tag{4.62}$$

or:

$$\lambda_L \geq 0.01 \text{ and } \mathrm{N_{FR}} < \mathrm{L_2} \tag{4.63}$$

Plug and slug flows are examples of an intermittent flow regime. This flow regime is recognized when:

$$0.01 \leq \lambda_L < 0.4 \text{ and } \mathrm{L_3} < \mathrm{N_{FR}} \leq \mathrm{L_1} \tag{4.64}$$

or:

$$\lambda_L \geq 0.4 \text{ and } \mathrm{L_3} < \mathrm{N_{FR}} \leq \mathrm{L_4} \tag{4.65}$$

Distributed flow is when the flow is more homogenous and consists of smaller bubbles or as a mist. The flow is considered distributed if:

$$\lambda_L < 0.4 \text{ and } \mathrm{N_{FR}} \geq \mathrm{L_1} \tag{4.66}$$

or:

$$\lambda_L \geq 0.4 \text{ and } \mathrm{N_{FR}} > \mathrm{L_4} \tag{4.67}$$

In addition, the flow is considered transient if it falls between being segregated and intermittent. The flow is therefore considered to be transient if:

$$\lambda_L \geq 0.01 \text{ and } \mathrm{L}_2 \leq \mathrm{N}_{\mathrm{FR}} \leq \mathrm{L}_3 \tag{4.68}$$

After the flow pattern has been determined, the next step is to find the liquid hold-up for the relevant regime given by:

$$H_{l,0} = \frac{a\lambda_l^{\,b}}{N_{FR}^{\,c}} \tag{4.69}$$

Where:

TABLE 3 - BEGGS & BRILL FLOW REGIME COEFFICIENTS

	Segregated	Intermittent	Distributed
a	0.98	0.845	1.065
b	0.4846	0.5351	0.5824
c	0.0868	0.0173	0.0609

If the flow regime is transient an interpolation between segregated flow and intermittent flow is used. The interpolation is given by:

$$H_{l,transient} = \frac{L_3 - N_{FR}}{L_3 - L_2} H_{l,segregated} + \left(1 - \frac{L_3 - N_{FR}}{L_3 - L_2}\right) H_{l,\text{intermittent}} \tag{4.70}$$

Next, the liquid hold up has to be adjusted for non-horizontal flow. The actual liquid hold-up is therefore given by:

$$\mathrm{H}_l = \psi H_{l,0} \tag{4.71}$$

Where:

$$\psi = 1 + C\left(\sin(1.8\phi) - \frac{\sin^3(1.8\phi)}{3}\right) \tag{4.72}$$

and:

$$C = (1-\lambda_l)\ln\left(\mathrm{d}'\lambda_l^{\,e}\,\mathrm{N}_{lv}^{\,f}\,\mathrm{N}_{FR}^{\,g}\right) \tag{4.73}$$

The required coefficients are given as follows:

TABLE 4 - BEGGS & BRILL FLOW INCLINED FLOW COEFFICIENTS

	Segregated Uphill	Intermittent Uphill	All patterns downhill
d'	0.011	2.96	4.70
e	-3.768	0.305	-0.3692
f	3.539	-0.4473	0.1244
g	-1.614	0.1244	-0.5056

No adjustment is needed for the distributed flow downhill and the coefficient, C, is set to zero.

The total pressure drop is affected by gravity, friction and acceleration. First, the hydrostatic (gravitational) term is calculated. The pressure gradient from gravity is found by:

$$\left(\frac{dp}{dL}\right)_g = \rho_s \sin\phi \tag{4.74}$$

Second, the frictional pressure is calculated by:

$$\left(\frac{dp}{dL}\right)_f = f_{tp}\rho_n \frac{v_m^{\,2}}{2gd_h} \tag{4.75}$$

To evaluate this expression, the friction factor has to be calculated. This requires the Reynolds number for a no-slip case and the corresponding friction factor to be found. Then it is adjusted for slippage using the liquid hold-up and the following equations:

$$N_{\mathrm{Re},n} = 1488\frac{\rho_n v_m d_h}{\mu_l\lambda_l + \mu_g\left(1-\lambda_l\right)} \tag{4.76}$$

$$f_n = \frac{1}{\left(2\log_{10}\left(\frac{N_{\mathrm{Re},n}}{4.5223\log_{10}\left(N_{\mathrm{Re},n}\right)-3.8215}\right)\right)^2} \tag{4.77}$$

$$y = \frac{\lambda_l}{H_l^{\,2}}, \qquad y_1 = \ln(y) \tag{4.78}$$

$$S = \ln\left(2.2y-1.2\right), \qquad \mathrm{y} \in \langle 1,1.2\rangle \tag{4.79}$$

$$S = \frac{y_1}{-0.0523+3.182y_1-0.8725y_1^{\,2}+0.01853y_1^{\,4}}, \qquad \mathrm{y} \notin \langle 1,1.2\rangle \tag{4.80}$$

$$f_{tp} = f_n e^S \tag{4.81}$$

After the friction gradient has been calculated, the acceleration term of the pressure gradient is estimated by:

$$E_k = \rho_s v_m \frac{v_{sg}}{144gp} \tag{4.82}$$

Lastly, the total pressure drop over the interval can be calculated:

$$\frac{dp}{dL} = \frac{\left(\frac{dp}{dL}\right)_g + \left(\frac{dp}{dL}\right)_f}{144\left(1-E_k\right)} \tag{4.83}$$

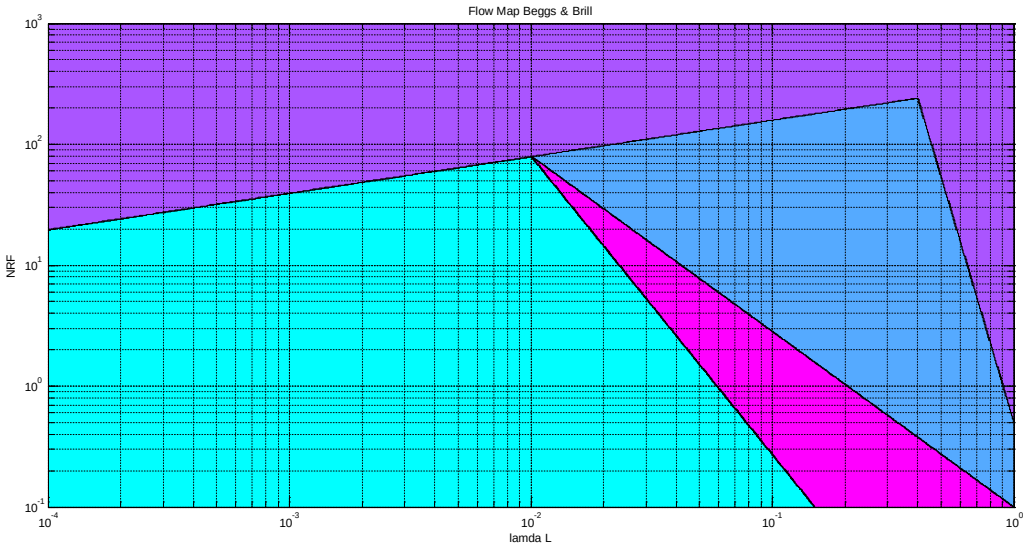

FIGURE 38 - BEGGS & BRILL FLOWMAP (LIGHT BLUE SEGREGATED. PINK TRANSITION, DARK BLUE INTERMITTENT, PURPLE DISTRIBUTED)

4.2.4 Choosing the Appropriate Model

Choosing the correct model in two-phase modeling is important as some of the models are not designed to be valid in most cases. A general guideline given by the author of this thesis is to simulate using a model which does consider both slippage and flow regimes when accuracy is more important than speed.

Much research is available in predicting which model that will fit most cases. Aggour et.al. showed through data from 414 (high flow rate and large tubular) wells in the Middle East that Beggs & Brill provided best simulation results among many other recognized simulation routines. For water cuts above 80% the Hagedorn & Brown model provided best results (Aggour & Al-Yousef).

4.3 Flow Patterns

For multiphase flow in a pipe, the flow can behave in different ways. For flow modelling it is important to know the flow regime in each segment to get an accurate result. The flow regime can be defined as (NFOGM/Tekna, 2014):

"The physical geometry exhibited by a multiphase flow in a conduit; for example, in two-phase oil/water, free water occupying the bottom of the conduit with oil or oil/water mixture flowing above."

The flow regime determines how the liquid hold up is calculated and further influences the frictional pressure drop in the well. The flow regime pattern is influnced by the following factors:

- Gas/liquid velocity
- Inclination angle
- Fluid properties

The flow patterns in the well can be controlled through choke adjustments as this causes the gas to expand/compress and increase/decrease the gas velocity in the segments altering the flow patterns.

Generally, different flow patterns are observed between horizontal and vertical pipes. This is implemented into the model through Beggs & Brills correlation. The other correlations implemented always assume the flow is vertical and calculates the flow regime and friction thereafter. For annular flow the same flow patterns appears as with pipe flow. However, the hydraulic diameter has to be adjusted for annular flow.

Many models are developed to predict these properties in two-phase flow, the research on multiphase flow are however not as thorough. It is therfore recommended to run the developed UBD model with 0% water cut for a more accurate result. For cases where water is present the model averages the fluid properties of water and oil present to determine the mixture liquid properties and further uses the two-phase corrolations available.

As gas is added to a fluid mixture, the flow pattern will change gradually from a homogenous liquid flow to a gas mist. For very high gas rates the gas becomes the continuous phase present where the liquid in the segment only occurs as dispersed droplets, known as mist flow. Between these two boundaries many flow patterns can be present in the relevant pipe segment. Several different classifications exists, however, this section explains each pattern between one phase liquid and mist flow based on Griffith (1984).

4.3.1 Vertical Flow Regimes

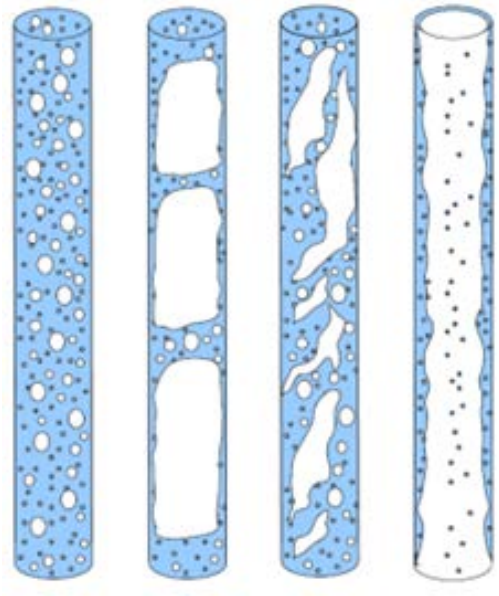

FIGURE 39 - VERTICAL FLOW REGIMES (LEFT TO RIGHT: BUBBLE-, SLUG-, CHURN- AND ANNULAR FLOW)

4.3.1.1 Bubble flow

At low gas injection rates discrete gas bubbles are present in an overall continuous liquid phase. The bubbles will usually be located in the center of the pipe and move upwards in a spiral.

4.3.1.2 Slug Flow

When the gas rate increases larger bubbles start to form as bubbles merge. Normally Taylor bubbles, large bullet-shaped bubbles, will fill the entire cross-sectional area, followed by a gap with liquid between each Taylor-bubble. The bubbles will surpass the liquid phase causing the liquid to come in contact with the next bubble when it arrives. This flow is referred to as slug flow.

4.3.1.3 Churn Flow

When the gas rate further increases the slug flow starts to break up causing deformed Taylor-bubbles and oscillating movement in the flow.

4.3.1.4 Annular Flow

For high gas rates the gas will keep centralized in the well as a stream separated from the liquid. There are still liquid drops present in the stream. However, these normally flow closer to the wall.

4.3.2 Horizontal Flow Regimes

4.3.2.1 Dispersed bubble flow

For very low gas rates the gas will flow as dispersed bubbles in the liquid phase. The bubbles present will normally flow closer to the upper wall due to gravity effects.

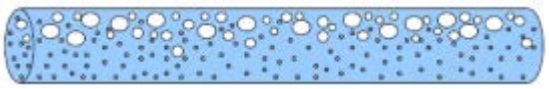

FIGURE 40 - DISPERSERD BUBBLE FLOW

4.3.2.2 Stratified smooth flow

As the gas rate increases the gas and liquid phase will start to separate and flow in different stratified streams. The gas will be located above the liquid phase due to gravity effects. As long as the gas rates do not increase more, the flow distribution will stay smooth.

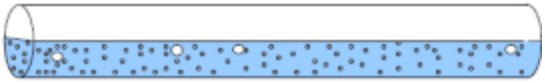

FIGURE 41 - STRATIFIED SMOOTH FLOW

4.3.2.3 Stratified wavy flow

If the gas rate further increases the flow will become more turbulent. From stratified smooth flow, the flow will develop wave patterns and be referred to as stratified wavy flow.

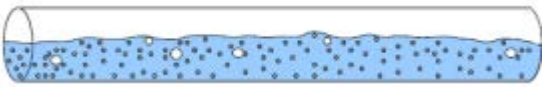

FIGURE 42 - STRATIFIED WAVY FLOW

4.3.2.4 Slug Flow

For even higher gas rates more turbulence will cause higher “waves” until the liquid phase reaches the upper wall of the pipe. This causes the gas phase to appear in discontinued sections followed by liquid slugs in the pipe and is called slug flow.

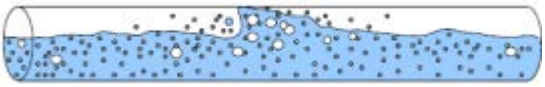

FIGURE 43 - SLUG FLOW

4.3.2.5 ANNULAR FLOW

For high gas rates the gas will move almost as a single phase in the gravity center of the pipe separated from the liquid. Liquid droplets are still present in the stream. However, these normally flow closer to the wall, where again, most are located at the lower wall due to gravity.

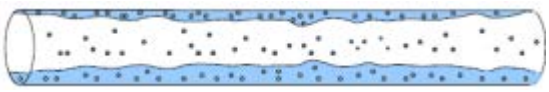

FIGURE 44 - ANNULAR FLOW

5 Drilling With Foam Systems

This chapter describes the basics in foam drilling. Why foam is a good option in UBD including advantages and possible challenges. Multiple foam pressure calculations are described in detail and further information on how to set the operational limits in foam drilling is also included.

5.1 Introduction to Foam Drilling

Foam can have many different definitions, one of which is that the foam is; "an agglomeration of bubbles surrounded by a thin liquid film" (Rehm, 2012). A foam system can be compared to an inverted mist, as liquid is the continuous phase instead of gas.

Foam drilling was first introduced in a testing facility in Nevada; USA in the 60's and was later adapted by the petroleum industry in work-overs by Chevron Oil Company.

Choosing foam as a drilling- (and workover-) fluid has proven to have many advantages when performing underbalanced operations. A foam system has a relatively low density compared to other underbalanced options while still having a high lifting capacity for cuttings even at low flow rates. For a well at 10,000 ft. the hydrostatic pressure can be reduced in half compared to using a standard water column while still keeping the system stable for underbalanced operations. For a shallow well the same factor is a reduction in hydrostatic pressure of five.

The liquid phase in a foam system is normally (drinking) water; however oil can also be used. More complex base fluid types, e.g. brines will drastically increase the operational cost. The simulator allows the liquid phase to be anything as the pressure calculations are only dependent on the density of the liquid phase itself among other factors not influenced by the base liquid. The normal gas to use is air, nitrogen or natural gas. The gas chosen is based upon the same principles as with an aerated fluid mixture. More gas types have however been implemented into the simulator to examine the properties of how other gases would act in a theoretical case.

Foam systems are overall very stable as long as the operational limits are within the limits of the chosen emulsifier. The assessment of the emulsifier (or foaming agent) is to form a coating around each gas bubble in the system so that the bubbles do not merge into larger bubbles and the liquid continuous phase breaks up. A correct emulsifier should allow the foam system to be flexible for changes in the fluid properties. Most foam systems are temperature stable up to 200F. The structure will not absorb too much heat from its surroundings and break down unless they it is exposed for a longer time period e.g. during longer trips. In general, the foam system is more stable when pressurized. This may lead to problems as the structure often breaks up in low pressure areas like the flow lines and pits if not designed to do otherwise, e.g. recyclable foam systems.

5.1.1 Advantages of Foam Systems

Selecting foam as a fluid system has many advantages over other fluid systems. The most important ones are mentioned below.

Lost circulation is reduced in low pressure zones where this normally is an issue. The gas bubbles in the foam will expand and act as a seal towards extensive fluid loss. This also causes minimal formation damage when drilling through under-pressured formation zones.

Foam systems are very stable, even at low densities. As the foam system acts as a mud system (opposed to an air system), it will not have pressure surges when stable. The stable foam system will also not collapse when the compressors are stopped which is a problem with mist.

Possible to reach lower ECDs than with aerated fluid systems. To minimize the hydrostatic pressure in foam drilling it is best to keep the gas amount higher than in the equivalent aerated system.

Foam systems have the highest lifting capacity of any fluid systems, as the slip velocity of the system is very low. This provides great hole-cleaning (especially in horizontal sections), easy clean-up and very high drilling rates. Foam systems are therefore an obvious choice for power drilling and drilling in highly inclined wells.

Other important advantages are the elimination of differential sticking and reduced corrosion on down-hole equipment and tubular.

5.1.2 Disadvantages of Foam Systems

The major disadvantages of choosing a foam system are related to the cost of the equipment, high temperatures and foam breakdown due to longer time periods and contamination.

The cost of choosing a foam system is as with aerated fluids, mostly dependent of equipment cost for gas compression. Another large disadvantage comes from chemicals such as foaming agents, stabilizers and corrosive inhibitors, which are major contributors to cost when the temperature is high or the liquid phase is either and oil or impure water.

5.1.3 Design Parameters

The lower liquid injection rate during foam drilling is dependent on the hole size and generally increases proportionally to the flow area, as shown in Figure 45. The upper limit for the liquid injection rate is controlled by the required down-hole and motor conditions.

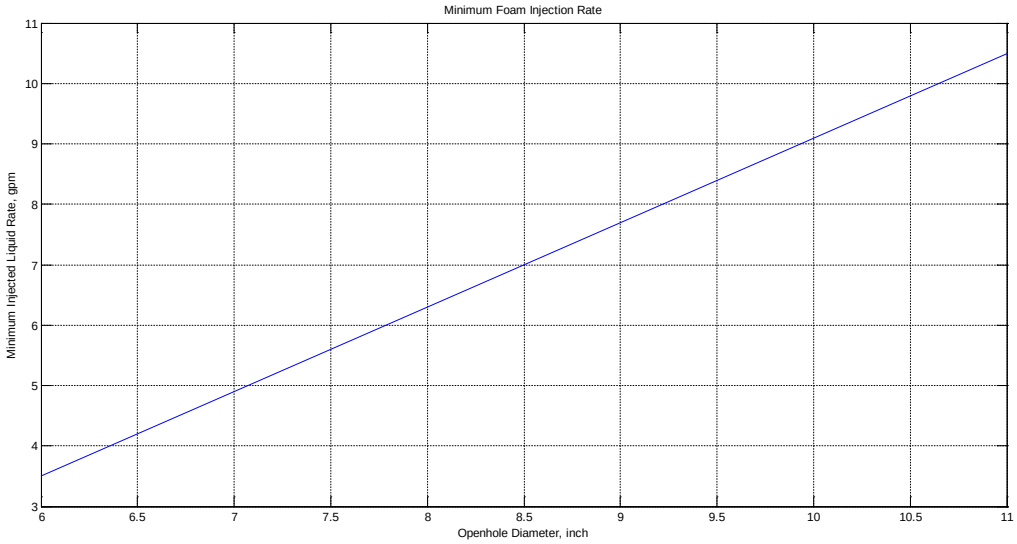

FIGURE 45 - MINIMUM LIQUID INJECTION RATE FOAM

A normal industry standard for gas injection in foam is to choose a ratio between 50/1 and 500/1. 50/1 is equivalent to 50 scf of gas to every cuft (or 7.48 gallons) of liquid. These values will ensure gas qualities ranging from 52-90% down-hole and provide great lifting capacity; this is further explained in section 5.2 and 5.5.

The most efficient way to alter the BHP in foam drilling is to change the annular surface pressure by adjusting the choke opening. This method is a quick fix and should be applied for minor changes as the foam compression is slow reacting. The required time for foam to stabilize can easily be up to one hour after a major change in surface pressure, giving a large lag time in the recorded pressure response. It is also important to keep the surface pressure above 100 psi so that the foam structure will not break down in the upper part of the annulus. When it is necessary to make larger adjustments or make a permanent adjustment to the BHP the correct response would be to either change the injection rate or GLR and circulate the entire well. This major lag time underlines the importance of having a proper UBD envelope available to ensure that the driller executes the correct response in controlling the pressure and gas quality down-hole.

5.2 Foam Quality

The quality of foam is the percentage volume of gas to total volume at predefined conditions.

The normal foam quality should never exceed 85-90%, and slightly higher for some waters where the limit is set to around 90-98%. Gas qualities above this limit may cause the liquid continuous phase to break up; further leading pressure surges and insufficient lifting capacity for the cuttings as gas becomes the continuous phase. The lifting capacity of the foam also has a lower limit around 40-52% as the system starts degrading.

Foam qualities are sometimes described with the terms: wet foam, dry foam, stiff foam and stable foam. Wet foam is foam with a high percentage of water. This foam type will easily break and should sometimes be added more foaming agents to keep stable. Dry foam is the case where a high amount of foaming agents is included in stream to keep the system stable with a low water percentage. The terms stiff foam and stable foam are used respectively for foams with and without polymer and bentonite added.

A foam system will usually act as a plug flow. However, as the pressure increases, and the gas quality is reduced the flow will increasingly act more as a Bingham-plastic fluid.

5.3 Pressure Gradient in Foam

For foam systems are pressure calculations done as with ordinary liquid one-phase systems. The pressure gradient expressed as:

$$\frac{dp}{dL} = \rho_f \left[\sin\phi + \frac{f v_f}{2 g d_h} \right] \tag{5.1}$$

This gradient has both gravitational and frictional pressure contributions.

The gravitational pressure contribution is simply found by taking a weighted average of the gas and liquid according to the gas quality (fraction) and adjust for inclination.

$$\rho_f = \Gamma\rho_g + (1-\Gamma)\rho_l \tag{5.2}$$

Where the gas gravity is given by:

$$\rho_g = 2.7\frac{\gamma_g p}{T} \tag{5.3}$$

The GLR at maximum foam quality (assumed at surface) has to be determined before further calculations can be done. It is given by:

$$GLR = \frac{\Gamma_{\max}}{1-\Gamma_{\max}}\left[\frac{1}{7.48}+\frac{5.615q_f}{60q_l}\right] \tag{5.4}$$

When the GLR is known the foam quality at in-situ conditions can be found for each segment:

$$\Gamma = \frac{\frac{p_s T}{pT_s}GLR}{\frac{p_s T}{pT_s}GLR+\frac{1}{7.48}+\frac{5.615q_f}{60q_l}} \tag{5.5}$$

The foam velocity is found by dividing the total flow rate by the cross-sectional area:

$$v_f = \frac{\frac{p_s T}{pT_s}GLR+\frac{1}{7.48}+\frac{5.615q_f}{60q_l}}{A}\left(\frac{144}{60}q_l\right) \tag{5.6}$$

When the viscosity has been found from one of the selected foam viscosity models, presented in section 5.4, the Reynolds number for the flow can be found by using the following equation:

$$N_{\mathrm{Re}} = \frac{\overline{v}_f d_h \overline{\rho}_f}{\mu_e} \tag{5.7}$$

The averaged values in this expression are the mean of the inflow and outflow properties in each segment. The friction factor in foam friction should according to Rehm et.al be evaluated using the relationships presented in Table 5 and further described in chapter 0 (Rehm, 2012).

TABLE 5 - FRICTION FACTORS FOR FOAM SYSTEMS

Reynolds Number	Friction Factor
NRe<2000	Laminar
2000<NRe<4000	McAdams
NRe>4000	Haaland

5.4 Foam Viscosity Models

Several models have been developed to determine the foam viscosity with varying foam quality. In this section, six different models are presented. Note that some of the figures in this section use logarithmic scales.

Einstein, Hatschek and Mitchell related the foam viscosity directly to the gas fraction (the gas quality) in the system. These viscosities are used directly in conventional liquid pressure drop equations.

Reidenbach and Sanghani used experimental data to find the power law parameters for the foam system based upon gas quality. Power law models have proven to give good results for actual well conditions and are therefore recommended practices. The parameters are then used to calculate the viscosities through the following equations:

For annular flow:

$$\mu_{Annulus} = K\left(\frac{2n+1}{3n}\right)^{n}\left(\frac{12v_F}{d_h}\right)^{n-1} \tag{5.8}$$

For pipe flow:

$$\mu_{Pipe} = K\left(\frac{3n+1}{4n}\right)^{n}\left(\frac{8v_F}{d_h}\right)^{n-1} \tag{5.9}$$

These viscosities are then used in further calculations as already explained in section 5.3.

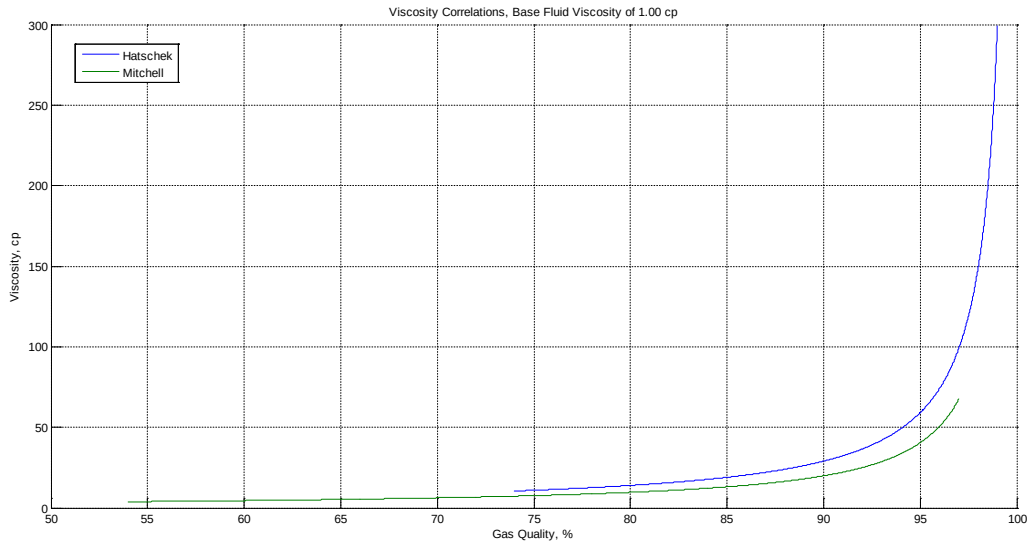

FIGURE 46 - FOAM VISCOSITY COMPARISMENT HIGHER QUALITIES

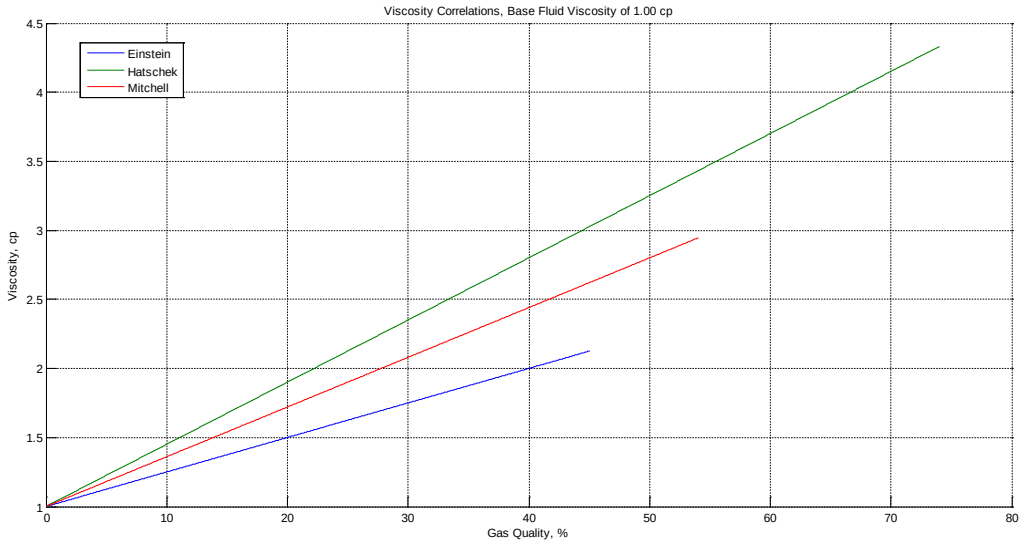

FIGURE 47 - FOAM VISCOSITY COMPARISMENT LOWER QUALITIES

5.4.1 EINSTEIN

Einstein was the first to mathematically explain foam rheology. He proposed the following model:

$$\mu_F = \mu_l \left(1 + 2.5\Gamma\right) \tag{5.10}$$

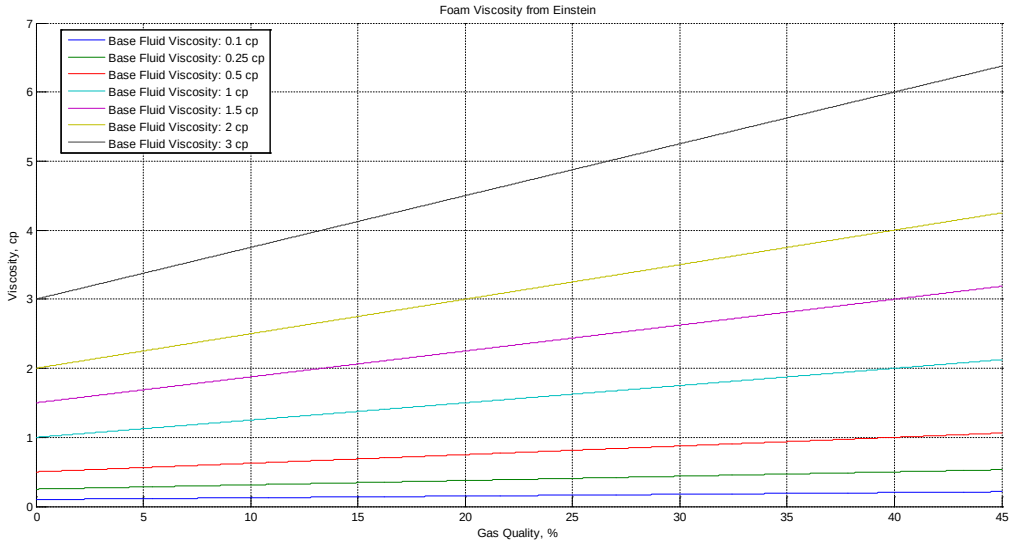

FIGURE 48 - EINSTEIN FOAM VISCOSITY MODEL

5.4.2 HATSCHEK

Hatschek developed a model similar to Einstein. It is valid for foam qualities ranging from 0% to 99%. For foam quality up to 74% the following relationship may be used:

$$\mu_F = \mu_l \left(1 + 4.5\Gamma\right) \tag{5.11}$$

Above 74% Hatschek found that the foam viscosity could be expressed as:

$$\mu_F = \mu_l \left(\frac{1}{1-\Gamma^{1/3}} \right) \tag{5.12}$$

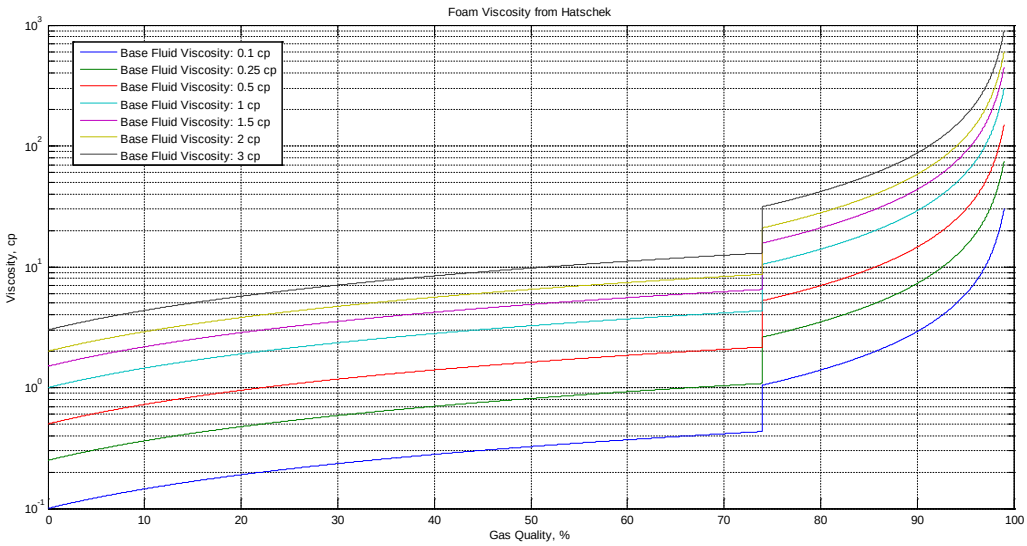

FIGURE 49 - HATSCHEK FOAM VISCOSITY MODEL

5.4.3 MITCHELL

Another similar model was presented by Mitchell and is valid for foam qualities up to 97%. Below 54% the following expression gives the foam viscosity:

$$\mu_F = \mu_l \left(1+3.6\Gamma\right) \tag{5.13}$$

Between 54% and 97% the viscosity is found by:

$$\mu_F = \mu_l \left(\frac{1}{1-\Gamma^{0.49}} \right) \tag{5.14}$$

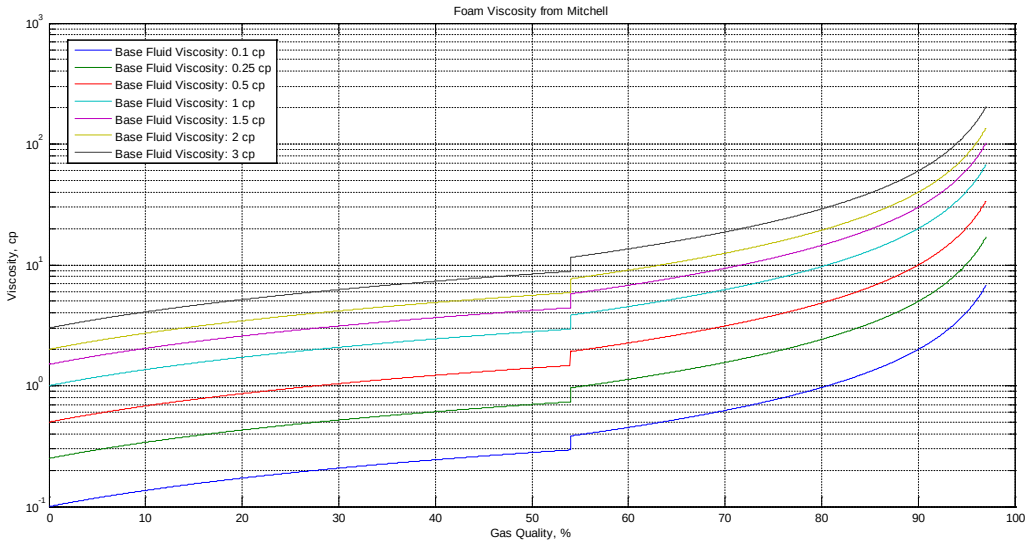

FIGURE 50 - MITCHELL FOAM VISCOSITY MODEL

5.4.4 BLAUER

Blauer proposed that foam can behave as a Bingham-Plastic fluid and that the viscosity therefore can be expressed as:

$$\mu_e = \mu_P + \frac{32.2 \times \tau_y d_h}{6 v_f} \tag{5.15}$$

5.4.5 REIDENBACH

Reidenbach proposed that foam quality could be fitted to the power law model using the following parameters:

$$K = 0.0813 \left[\frac{1-\Gamma}{\Gamma} \right]^{-1.591} \tag{5.16}$$

$$n = 0.8242 \left[\frac{1-\Gamma}{\Gamma} \right]^{0.5164} \tag{5.17}$$

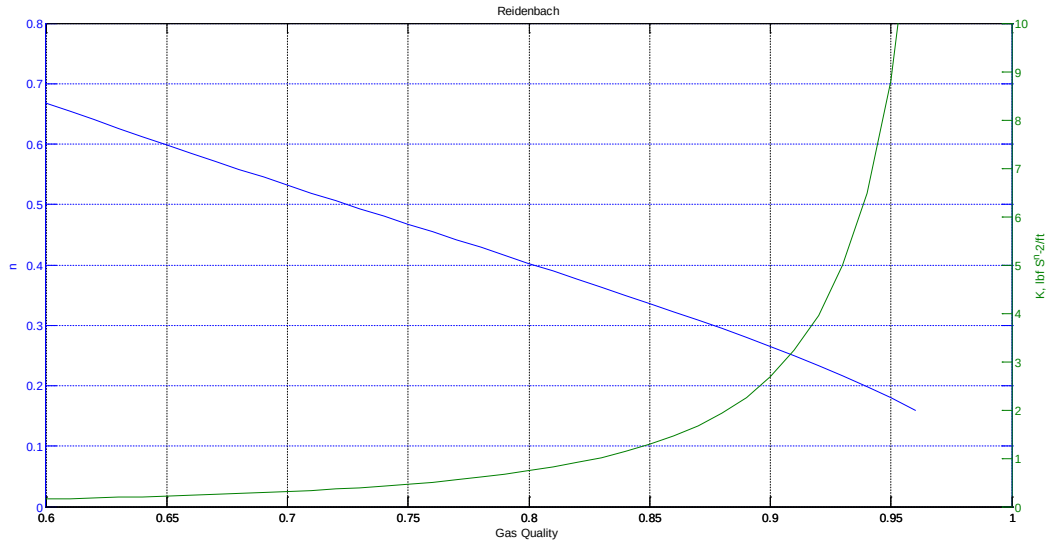

FIGURE 51 - REIDENBACH FOAM POWER LAW PARAMETERS

5.4.6 SANGHANI

Sanghani developed another model to relate the power law parameters to gas quality:

$$n = 0.095932 + 2.3654\Gamma - 10.467\Gamma^2 + 12.955\Gamma^3 + 14.467\Gamma^4 - 39.673\Gamma^5 + 20.625\Gamma^6 \quad (5.18)$$

$$K = -0.15626 + 56.147\Gamma - 312.77\Gamma^2 + 576.65\Gamma^3 + 63.960\Gamma^4 - 960.46\Gamma^5 - 154.68\Gamma^6 + 1670.2\Gamma^7 - 937.88\Gamma^8 \quad (5.19)$$

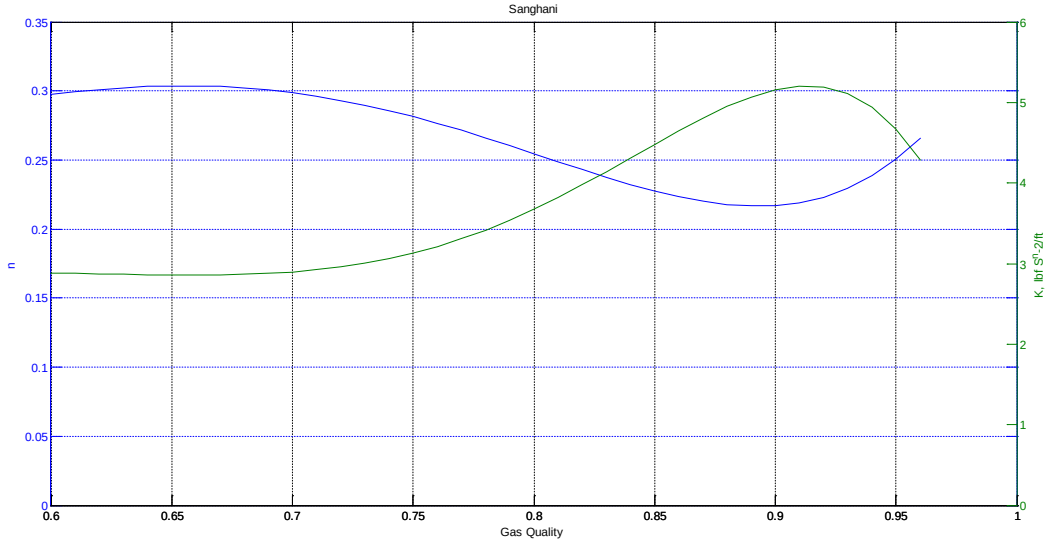

FIGURE 52 – SANGHANI FOAM POWER LAW PARAMETERS

5.4.7 Choosing the Appropriate Model

Choosing the correct model in foam modeling can be difficult. The models can produce a large percentage deviational output depending on the inputted values. In general, it would be advised to use either Sanghani or Reidenbach as neither of these correlations require addition viscosities or yield point to be inputted. Rehm et.al uses Sanghani in the IADC textbook "Underbalanced Drilling" for pressure calculations (Rehm, 2012). Several other textbooks on foam rheology also specifically mentions this viscosity model (William C. Lyons, 2009). A general guideline given by the author of this thesis is to simulate using either only Sanghani or taking an average of the two power-law models; Sanghani and Reidenbach. Einsteins correlation especially should not be used for complex simulations as the validity of this correlation is rather limited.

Limited research is available in predicting which model that will fit most cases. One study from the University of Tulsa states that model prediction of the friction loss in foam could range from as little as 2% to 250% in horizontal pipes. The study concluded that there was really no "best" model available in predicting pressure losses in most experiments (Ozbayoglu, Kuru, Miska, & Takach).

5.5 Hole Cleaning During Foam Drilling

To ensure proper hole cleaning the foam velocity must exceed the required velocity to keep the foam system stable and keep cuttings suspended in the system. According to Culen stability in a foam system is a term used to describe the phase makeup of the fluid. He explains that a stable foam system traps the cuttings inside its fluid matrix while retaining its structure. This allows foam velocities to have great lifting capacity for cuttings at very low circulation rates. The problem related to hole cleaning in foam systems, as already mentioned in section 5.2, first occurs when the gas quality exceeds 85%, and causes cuttings to possible drop out of the stream. This will occur as the foam structure will start to break down at these gas qualities, as gas becomes the dominant phase and foam stability is lost (Culen, 2014).

The velocity to keep the cuttings suspended are dependent on the drilling rate, bit size, cuttings concentration, -size and –density, among other factors dependent on the fluid properties. This required velocity is given by:

$$v_{req} = v_{sl} + v_{tr} \tag{5.20}$$

The first contribution towards the required velocity is the settling velocity of the cuttings. It is controlled by the drag force acting on the cuttings when they are accelerating. This is calculated by:

$$v_{sl} = 1.56 \frac{d_s \left(\rho_s - \rho_f\right)^{0.667}}{\rho_f{}^{0.333} \mu_e{}^{0.333}} \tag{5.21}$$

The second velocity contribution is the terminal velocity of the cuttings, which is reached when they have stopped accelerating and have reached a constant velocity. This can be calculated as:

$$v_{tr} = \frac{\pi d_{bit}{}^2}{4 C_s A} \frac{R_p}{3600} \tag{5.22}$$

6 OPERATIONAL LIMITS IN UBD

In underbalanced operations the annular pressure profile is strongly influenced by the frictional pressure contribution compared to conventional drilling. As the frictional pressure is influenced by many factors and can see rapid changes, it can be difficult to set the operational limits for achieving the required down-hole conditions. Due to this complexity, it is necessary to develop an operational envelope with gas/liquid flow rates and surface pressures.

An operational drilling envelope usually shows the calculated BHP or ECD for different liquid and gas circulation rates. The fluid design should stay within limits set by the estimated reservoir pressure, motor limitations, drilling cost, cuttings transport, fluid compatibility, wellbore stability and friction dominated flow regime.

The lower limit for liquid injection rate in a drilling envelope is decided by hole-cleaning and the upper limit is to maintain a friction dominated regime. The drilling motor (and auxiliary equipment) limits the total flow rate in both an upper and lower manner.

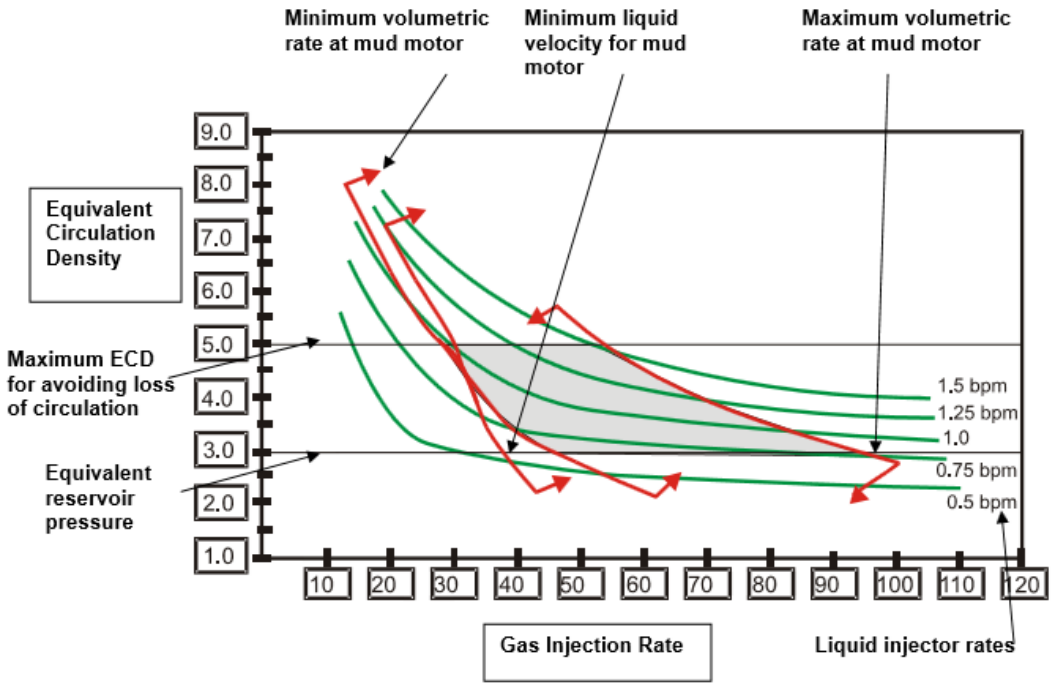

FIGURE 53 - SETTING OPERATIONAL LIMITS TO CONSTRUCT AN UBD ENVELOPE

To design the operating envelope in UBD a graph with pressure versus gas injection rate is normally plotted, where hydrostatic-, frictional- and bottom-hole pressures are calculated for different x-values of gas injection and presented on the y-axis for a specific liquid rate. The graph will show that as the gas rate increases, the hydrostatic contribution towards BHP will be reduced while the corresponding frictional pressure contribution increases. The flow is referred to as friction dominated where a reduction in hydrostatic pressure is less than the frictional increase for a given increase in gas volume.

The friction dominated flow can easily be seen on the BHP graph, as the combined frictional and hydrostatic pressure will increase with increasing flow rate. If the total pressure is decreasing, with an increased gas flow is the

flow referred to as hydrostatic dominated. The hydrostatically dominated part of the flow normally has a fast decline for total BHP for increasing gas flow; while the friction dominated flow has a more flat profile. This process is repeated for three-four more liquid flow rates until a good range of relevant drilling rates are included. The liquid injection rates chosen should all be able to provide sufficient hole-cleaning. It is also worth noticing that friction dominated flow does not imply that the pressure contribution from friction exceeds the hydrostatic contribution.

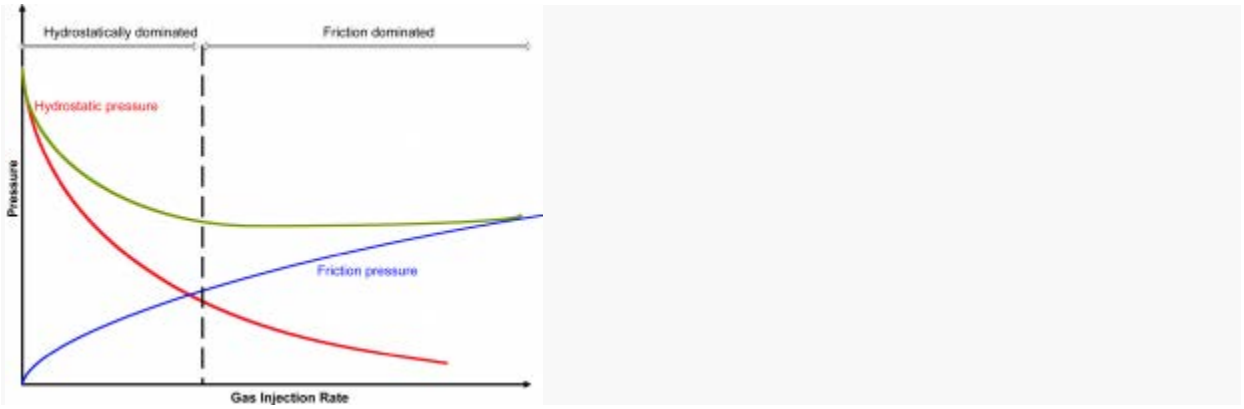

FIGURE 54 - FRICTION DOMINATED REGIME BOUNDARY

The next stage in developing the operational envelope is to set the target pressure limits. For an underbalanced operation one would normally design for an upper BHP of 250 psi below the estimated reservoir pressure while circulating. There should also be a lower pressure limit as the wellbore can collapse if the pressure drawdown exceeds the formation strength.

The last limits to include in the operational envelope are the maximum and minimum fluid flow rates. These limits are set by the down-hole drilling motor. These lines will not be straight as the total flow is a sum of the gas and liquid flow. If the overall flow rate is too low, the motor will not be provide enough torque to keep the bit moving. In contrast, if the flow rate is too high, the motor can be damaged.

With a properly designed operational envelope available it is easy for the driller to understand two-phase flow properly and make the right decisions. For any circulating rates the driller can look at the slope of the BHP curve to plan his next action. To avoid problems related to instability, slugging and pressure spikes the driller can also use the curve to easier keep the flow friction dominated just by identifying a positive slope of the curve and keep the parameters within this area.

It is important for the driller to understand the hydraulics of two-phase flow while drilling as further gas injection can both increase and decrease the pressure down-hole depending on whether the flow is friction- or hydrostatically dominated. A decision to increase the gas flow can therefore be very unfavorable if the driller thinks the flow is hydrostatically dominated (associated with one-phase flow) and he/she wishes to lower the BHP further, as this will cause both pressure in the well to act in an opposite manner and at the same time increase the overall cost of the drilling process related to gas usage.

One analogy explaining the two different flow regimes can be to think of the annular fluid as a coiled spring. In the hydrostatically dominated flow the fluid will act as a loose spring where surface pressure change propagates downwards in transient waves, causes slugging and requires some time before the BHP again stabilizes. The fluid

response might be very unpredictable, therefore making it difficult for the choke operator to provide the correct response. Friction dominated flow acts more as a tightly coiled spring, causing the pressure changes to faster propagate down-hole and quicker reaching a steady state situation again. This makes the choke response much more intuitive and therefore easier to control (Culen, 2014).

An operating envelope should not be considered to be a representation of the true pressure response of the hydraulics down-hole, but instead act as a guideline for how the pressure will be influenced by changing the injection rates. It is also recommended to develop several different operational envelopes with varying input parameters for a better understanding.

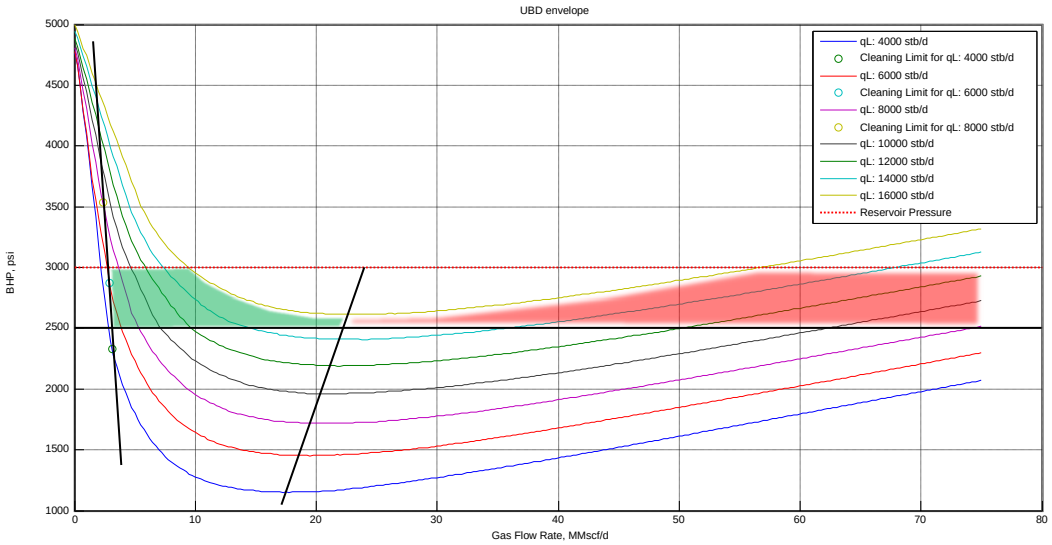

FIGURE 55 – UBD ENVELOPE FOR "WELL 1" (FROM APPENDIX B) PRODUCED BY THE SIMULATOR USING BEGGS & BRILL

Figure 55 shows how an UBD envelope might look if example well 1 would be circulated at 12,500 ft. (lower casing shoe). It is here assumed that the valid range of BHP is within 2500 and 3000 psi, with liquid injection rates from 4,000 up to 16,000 stb/d and gas injection rate up to 75 MMscf/day. In this figure the flow hydrostatical is dominated when shaded in green and friction dominated is shaded red to better explain how to understand the envelopes which are produced by the simulator.

If one would like to continue drilling to a TD of 13,000 ft. the UBD envelope would change. Assuming a reservoir zone is located between 12,900 and 13,000 ft. influx will be encountered when the BHP is less than the reservoir pressure. For the UBD envelope in Figure 56 is the reservoir first set to be impermeable so no influx is encountered. In the UBD envelope presented in Figure 57 is the zone is set to have a permeability of 50mD and 2000 ft. of effective drainage radius. Reservoir fluid in this example is set to 45 API oil with 10% WC (1.1 s.g.) and methane with an GLR of 750 scf/stb. The two figures show that when reservoir fluid and injected fluid are mixed the calculated BHPs will shift depending on the new fluid properties, and the operational limits for further drilling will change.

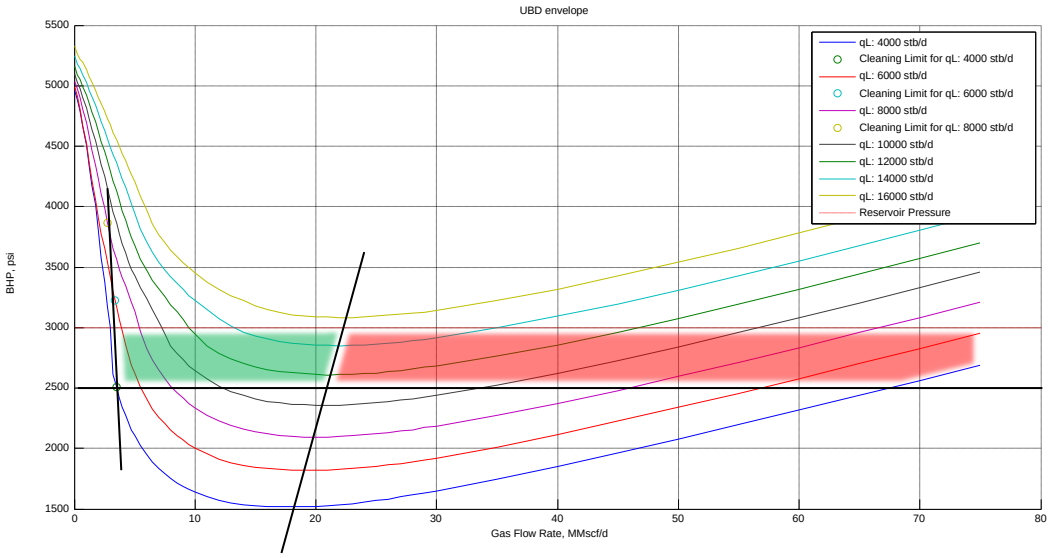

FIGURE 56 - UBD ENVELOPE NON-PERMEABLE ZONE

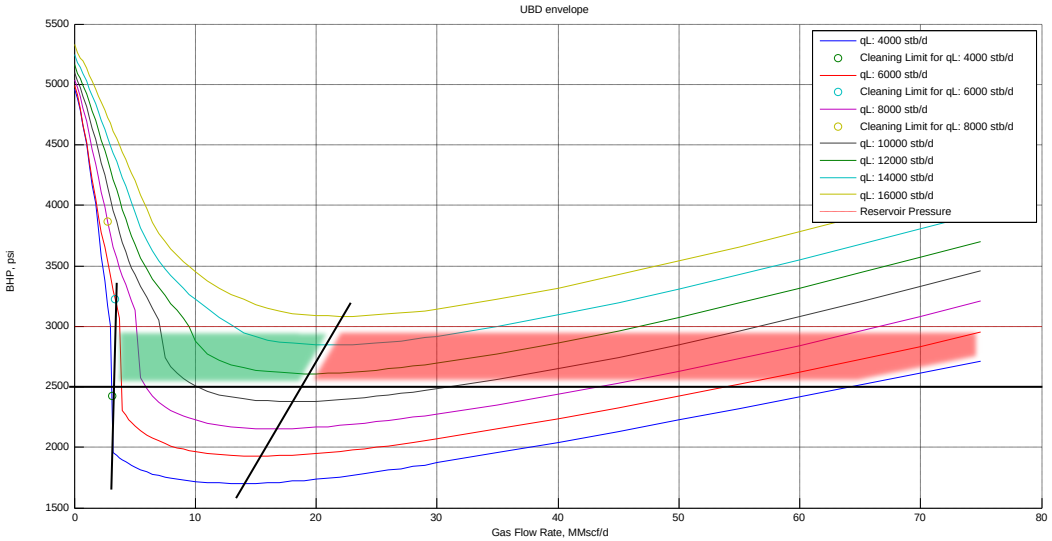

FIGURE 57 - UBD ENVELOPE PERMEABLE ZONE

7 DEVELOPMENT AND THEORY OF THE SIMULATOR

The UBD simulator constructed as a part of this thesis was based upon a simpler non-graphic MATLAB program developed by the author as a drilling specialization project (Leirkjær, 2013). The code was further extensively tweaked, extended and improved in order to provide a large range of simulation cases in a relatively simple GUI.

The original code written in MATLAB was mainly based on the dissertation given by Carlos Perez-Tellez and only included aerated fluids using the Beggs & Brill correlation. In Perez-Tellez's paper, "Improved Bottom-hole Pressure Control for Underbalanced Drilling Operations", Perez-Tellez provided the necessary "process of thought" to develop a UBD simulator and described how he constructed his own model in FORTRAN90 (Perez-Tellez, 2003).

The original source code from Perez-Tellez was not available for the author of this thesis, so all coding have been done from a variety of public pseudo-codes, relevant SPE papers and petroleum engineering textbooks. Most of which was presented in the text-books "Production Optimization: Using NODAL Analysis" (Beggs, 1991) and "Two-phase flow in pipe" (Brill & Beggs, 1978).

The current UBD simulator implements many of the basic principles described in Perez-Tellez's dissertation and these text-books. However, the algorithm had to be changed in multiple ways to be able to efficiently implement it into a MATLAB GUI. The finished simulator has roughly 7,500-15,000 lines of MATLAB code to properly function.

This chapter further explains how the UBD simulator operates and how it was constructed.

7.1 INTRODUCTION TO GUI PROGRAMMING IN MATLAB

The author of this thesis had no prior experience creating a GUI program. The programming of the GUI was first started as a text-only code where all the buttons and tables were programmed in code. This process turned out to be very time-consuming as the program became more complex. When around 5-10% of the finished GUI was completed, the author decided to start from scratch using MATLAB's own GUI programming interface. This simplified the work substantially. However, the programming still required extensive effort to complete.

MATLABs GUI programming tool, later referred to as GUIDE, is developed by MathWorks Inc. as a tool for less experienced programmers to develop simple programs, and for the more experienced to develop a larger scale GUI.

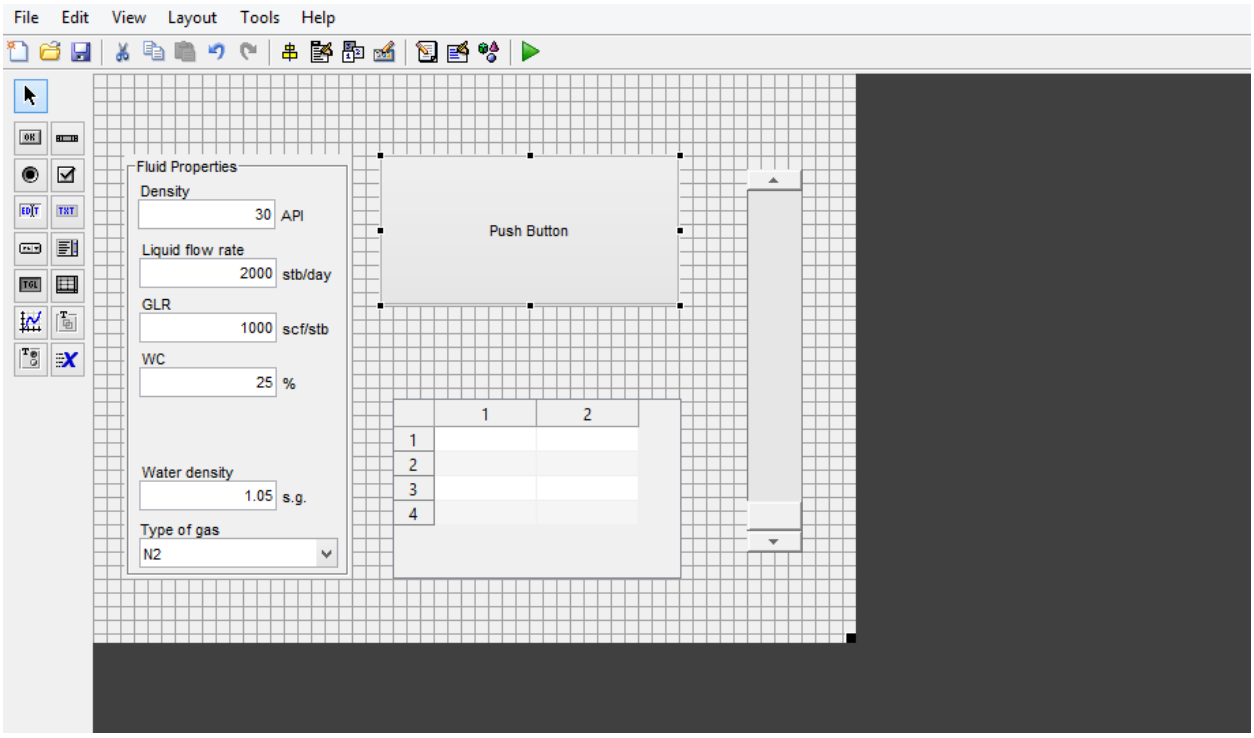

FIGURE 58 - EXAMPLE OF THE GUIDE INTERFACE IN MATLAB

GUIDE generates a script containing code to show and operate the dragged and dropped components in a GUI program. It is worth noticing that GUIDE does not have the capability of automatically assigning certain callback done in the GUI with a function. For instance one would not be able to simply add a button to the GUI and choose from a list what you would like this button to do, e.g. plot something in a predefined field. An example code for how a button can be set to perform an operation is showed in the figure below:

```
4142
4143      % --- Executes on button press in pushbutton54.
4144    function pushbutton54_Callback(hObject, eventdata, handles)
4145    % hObject    handle to pushbutton54 (see GCBO)
4146    % eventdata  reserved - to be defined in a future version of MATLAB
4147    % handles    structure with handles and user data (see GUIDATA)
4148 -  [cdata,map] = imread('NTNUlogo.png');
4149 -  h=msgbox({'Program developed by Rune Leirkjær as a part of master thesis in drilling engineering.' ...
4150          ' ' 'Copyright: Rune S. Leirkjær, 2014' 'rune@leirkjaer.com'},...
4151              'About','custom',cdata,map);
4152
4153
```

FIGURE 59 - EXAMPLE CODE TO PRODUCE A DIALOG BOX IN MATLAB

A mouse-click at the corresponding pushbutton will create a dial box with the following outcome:

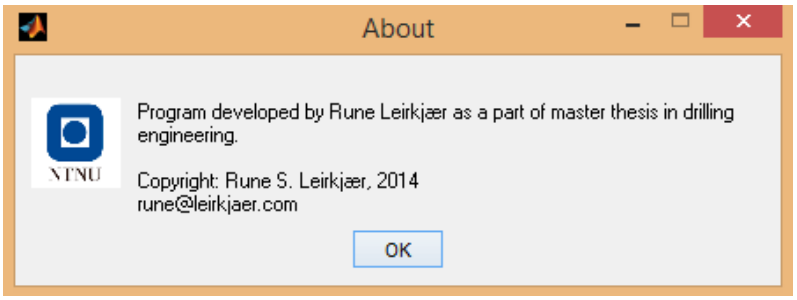

FIGURE 60 - DIALOG BOX CREATED WITH MATLAB

This example shows some of the simplest actions performed in the finished program. Every callback has to be programmed with normal MATLAB code, so a large amount of coding is still required to develop a GUI program when using GUIDE. The main advantage of choosing to use GUIDE; is the ability to easier control the appearance of the GUI itself and make changes to it later on.

A disadvantage of using GUIDE is that the program does not have the ability to store variables inside the workspace as with normal MATLAB codes. Instead, each callback must be programmed to collect the information physically written into text-boxes and tables by the user, translate it to the correct variable type and then further use it to in the correct function. As the programmer never has a workspace available when collecting variables the code itself will often be challenging to understand for a person not involved in development of program. In addition to this GUIDE creates a large amount of "dummy-functions" which might not have a purpose for the finished program itself and are therefore never called.

7.2 Model Description

7.2.1 Correlations / Functions

The UBD simulator uses a range of correlations as described in chapter 3 through 5. These correlations are summarized in the table below.

TABLE 6 - CORREALTIONS USED IN THE UBD SIMULATOR

Variable	Correlation
Oil Compressibility	Elsharkawys
Water FVF	McCain
Gas Viscosity	Lee-Gonzalez
Oil Viscosity	Beggs-Robinson (DO) Vasquez-Beggs (LO)
Water Viscosity	Brill-Beggs
Gas-Oil IFT	Baker-Swerdloff
Water-Gas IFT	Hough

Bubble Point Pressure	Standing (California Crude)
Gas Compressibility Factor	DAK-EOS
Pseudo-Critical Properties	Table (common gasses) Sutton (custom gasses)
Aerated Fluids Pressure Gradient - Category A	Poettmann-Carpenter (original and simplified model) Baxendell-Thomas Fancher-Brown
Aerated Fluids Pressure Gradient - Category B	Hagedorn-Brown Gray
Aerated Fluids Pressure Gradient - Category C	Duns-Ros Beggs-Brill
Friction Factor	Haaland Coolbrook-White
Foam Fluids Viscosity	Einstein Hatschek Mitchell Blauer Reidenbach Sanghani

7.2.2 Iteration Process

The iteration process used in the UBD simulator is rather complex and requires a fast computer to run properly. Generalized flow charts are included in Appendix D as a reference.

The iterative process through the wellbore starts at the top of the annular section, and continues downwards for each segment. The segments or grid points are taken from the predefined survey inputted by the user. Each segment has known input parameters of pressure and temperature found from the last interval. For the first section, the value is either inputted by the user or guessed by the simulator.

When the inflow conditions in a given segment is known the simulator first guesses a pressure drop/increase across the section. This value can be set to anything except zero and is not controllable by the user to avoid errors. The pressure at the end of the section is then found by adding the guessed pressure drop/increase to the inflow pressure. The two pressures and temperatures at the inflow and outflow are next averaged to find the in-situ conditions for the section used in further calculations.

The UBD simulator then calculates all the necessary fluid properties at these conditions and calls the function corresponding to the selected correlation selected for the simulation. The UBD simulator then uses the output from this function to estimate a pressure gradient and finds the calculated pressure drop over the segment. The pressure drop guessed from the simulator is then compared to the calculated pressure drop and the deviation is found. The deviation between the guessed value and the calculated one is further used to make a new guess.

Unless the deviation is below a set limit, this iterative process will continue until the results converge so that the calculated pressure equals the guessed pressure. When this state is reached all the relevant average fluid properties (based upon simulation type), pressure gradients, and outflow properties are saved. The simulator then moves to the next segment and uses the pressure found in the last segment as the new input and repeats the entire process.

In cases where a set BHP is to be acquired the pressure at the top of the annular is first guessed. The iteration process is then continued downwards throughout the annular sections until the BHP is found for this surface pressure. Next a new surface pressure is guessed based on the deviation between the inputted BHP and the calculated BHP and the process is repeated until the grid calculation converges towards zero deviation.

When the BHP is found and is below the reservoir pressure, the influx is calculated (if selected to be relevant) and the new fluid mixture-properties are found. Influx is not considered if the bit has not drilled into the pay-zone selected by the user, or if the zone is set to be impermeable. The entire process must then be repeated until the influx is balanced and also this iterative process converges. As the UBD simulator is design on the purpose of simulating underbalanced situations it does not consider fluid loss to the reservoir.

When the bottom-hole conditions calculated satisfy the relevant simulation type, will the simulator first calculate, or collect the predefined value, for the pressure drop across the bit. This value is then subtracted from the BHP to find the pressure just above the bit before the iterative process continues up through the drill-string until the surface again is reached.

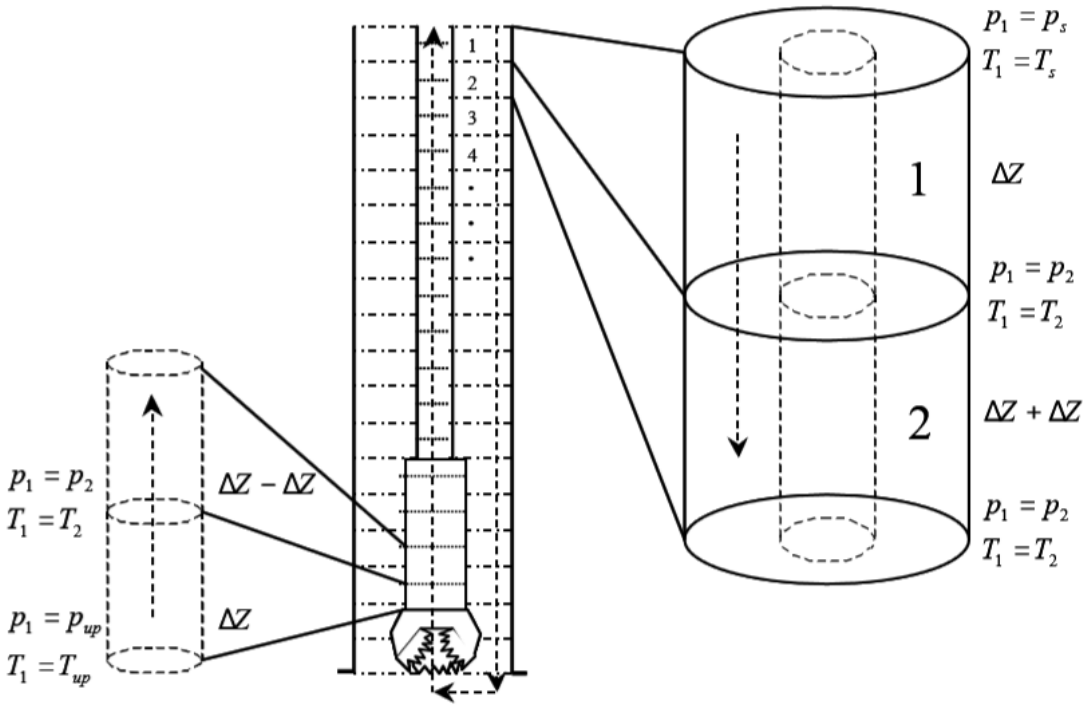

FIGURE 61 - ITERATIVE WELLBORE CALCULATION

8 USAGE OF THE SIMULATOR

The program written requires a large amount of available computer memory due to the number of iterations for each time step. Therefore it is recommended to run the simulation with either fewer depth intervals and/or time steps if the code demonstrates to be time consuming.

In this chapter are the procedures presented to perform a variety of simulations on 12,500 feet deep well with an S-shaped (almost slant) trajectory. Information about this well, “example well 1” can be found in section B.2 in the appendix.

8.1 INPUT SURVEY DATA

Inputting survey data is done in the “Input Survey” section marked in blue on Figure 62. Inputting the survey data into the model is done the following way:

1. Select the survey input section marked in blue
2. Clear all data currently in the table:
    a. Input the number of survey points which is to be defined in the text box marked in red on Figure 62.
    b. Press the “Clear button”
3. In the green section enter the survey data available.
    a. Data entered must start with 0,0,0 and have increasing depth
    b. No rows (below the first row) can contain “dummy-data” (depth set to zero) and should be deleted

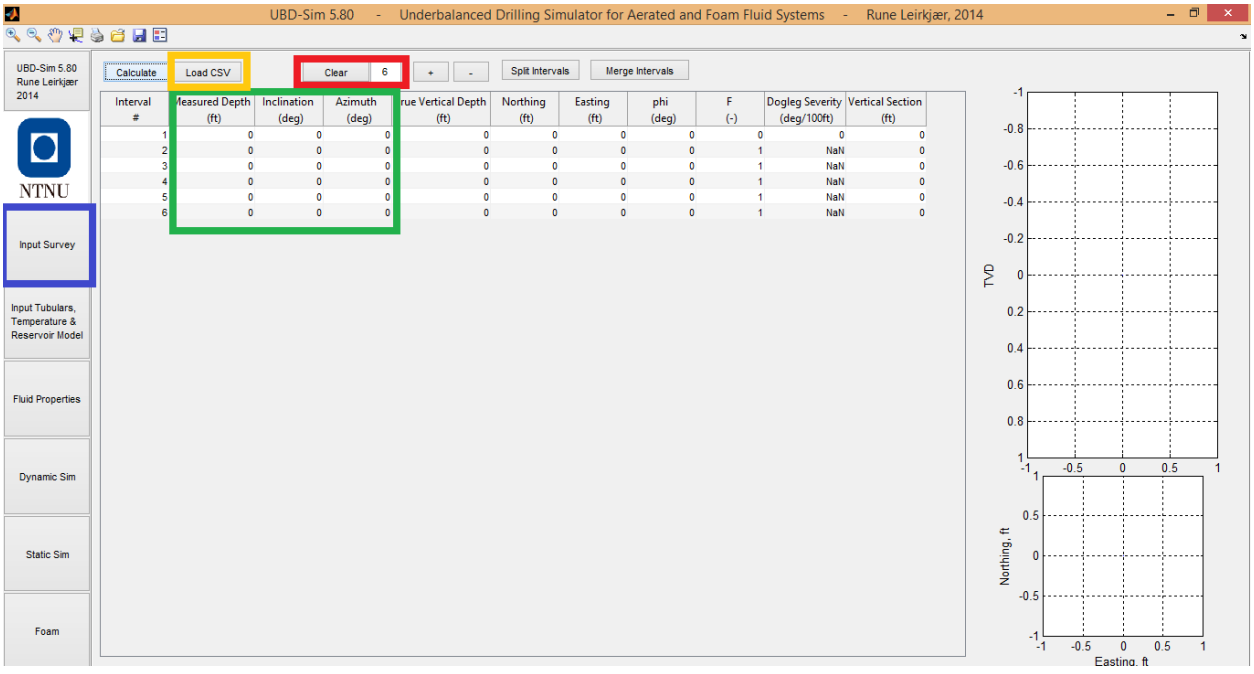

FIGURE 62 - CLEARING SURVEY DATA

Survey data can also be loaded from a predefined ".csv-file". This is done by pressing the button marked in yellow in the same figure. The "csv-file" must be present in the same directory as the MATLAB program is located.

When the values are defined the "Calculate" button (marked yellow on Figure 63) should be pressed to evaluate the well path.

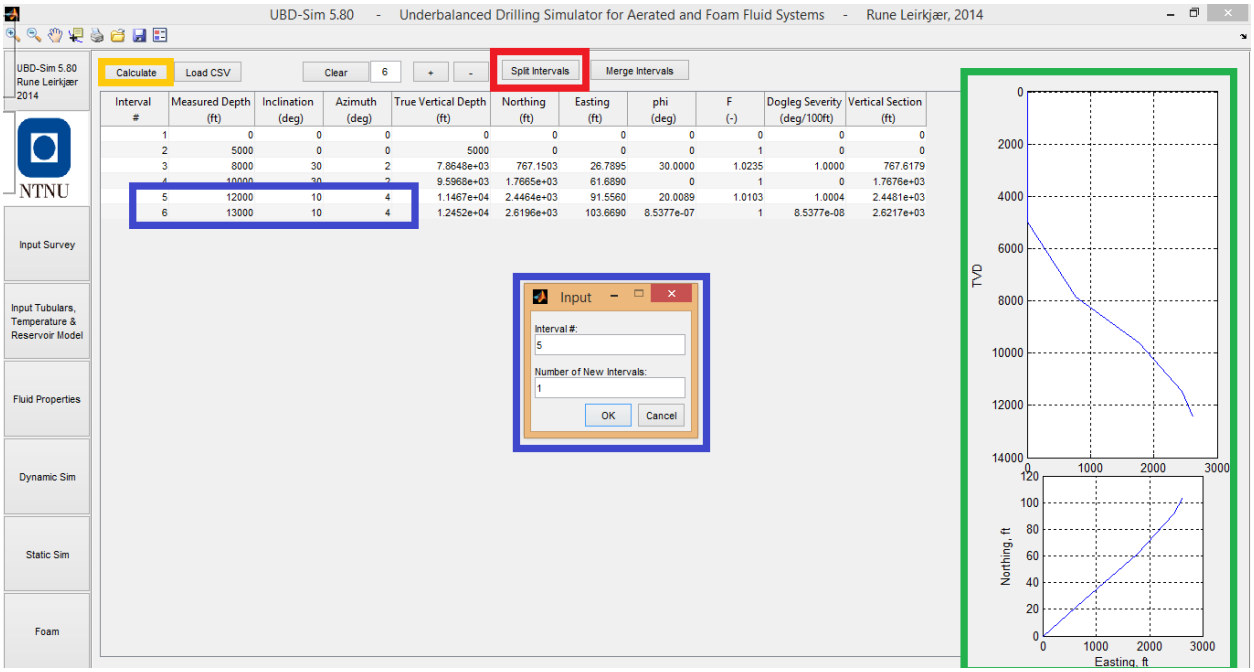

FIGURE 63 - SURVEY DATA INTERVAL SPLITTING

This causes to current survey data to be evaluated and plotted in the green section on Figure 63. As the figure shows this grid is not exactly good for simulation purposes. The simulator is designed to handle any grid. However, it is generally preferred to have grid points with equal distance. In this example we would like to use segments of 500 feet. To be able to easily split coarser grids into a better grid size a split function has been implemented into the simulator. To split an interval the "Split Intervals" button (marked in red on Figure 63) should be pressed and a dialog box (marked in blue) will appear. It is preferable to start splitting in the lower section of the survey points as interval numbers are renumbered as splitting occurs.

The process of splitting this grid into 500 feet sections can be done the following way:

1. Split interval 5 into 1 new interval
2. Split interval 4 into 3 new intervals
3. Split interval 3 into 3 new intervals
4. Split interval 2 into 5 new intervals
5. Split interval 1 into 9 new intervals
6. Re-evaluate survey data using "Calculate "-button

In Figure 64 are the survey data produced by the program marked in yellow. As the figure shows the segments must be split into nine, five, three, three and one interval to get 500 feet spacing.

If necessary, specific segments can also be deleted through the “Merge Interval” function marked in red on Figure 64.

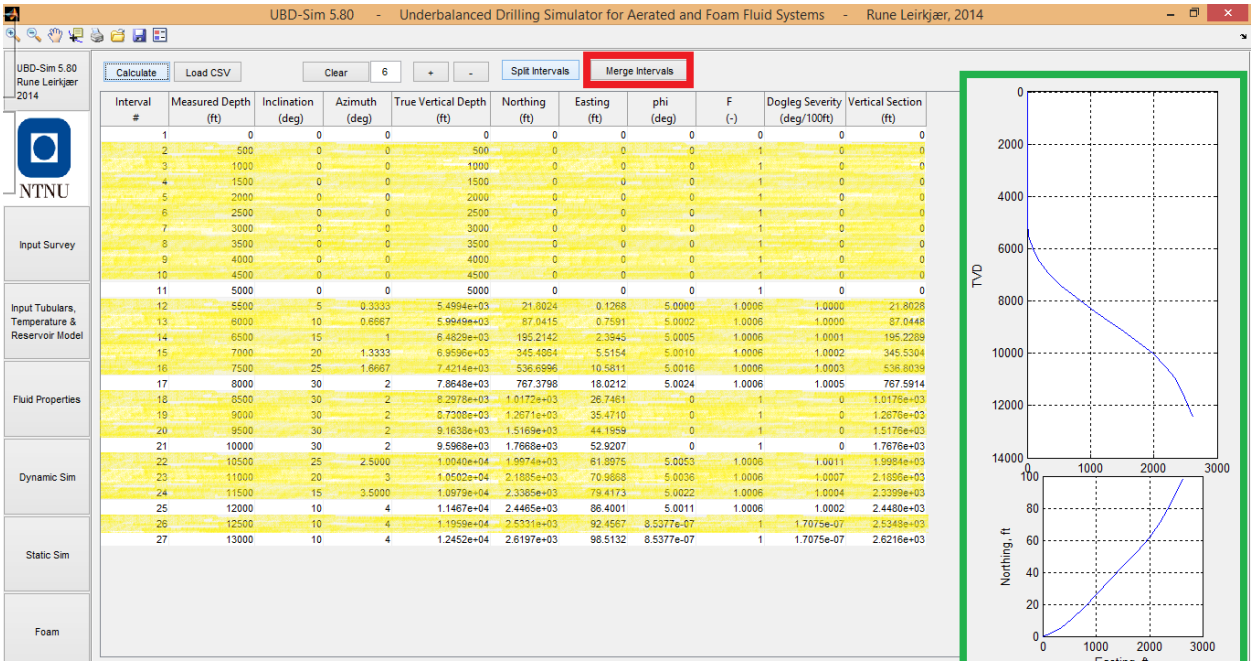

Interval #	Measured Depth (ft)	Inclination (deg)	Azimuth (deg)	True Vertical Depth (ft)	Northing (ft)	Easting (ft)	phi (deg)	F (-)	Dogleg Severity (deg/100ft)	Vertical Section (ft)
1	0	0	0	0	0	0	0	0	0	0
2	500	0	0	500	0	0	0	1	0	0
3	1000	0	0	1000	0	0	0	1	0	0
4	1500	0	0	1500	0	0	0	1	0	0
5	2000	0	0	2000	0	0	0	1	0	0
6	2500	0	0	2500	0	0	0	1	0	0
7	3000	0	0	3000	0	0	0	1	0	0
8	3500	0	0	3500	0	0	0	1	0	0
9	4000	0	0	4000	0	0	0	1	0	0
10	4500	0	0	4500	0	0	0	1	0	0
11	5000	0	0	5000	0	0	0	1	0	0
12	5500	5	0.3333	5.4994e+03	21.8024	0.1268	5.0000	1.0006	1.0000	21.8028
13	6000	10	0.6667	5.9949e+03	87.0415	0.7591	5.0002	1.0006	1.0000	87.0448
14	6500	15	1	6.4829e+03	195.2142	2.3945	5.0005	1.0006	1.0001	195.2289
15	7000	20	1.3333	6.9596e+03	345.4864	5.5154	5.0010	1.0006	1.0002	345.5304
16	7500	25	1.6667	7.4214e+03	536.6996	10.5811	5.0016	1.0006	1.0003	536.8039
17	8000	30	2	7.8648e+03	767.3798	18.0212	5.0024	1.0006	1.0005	767.5914
18	8500	30	2	8.2978e+03	1.0172e+03	26.7461	0	1	0	1.0176e+03
19	9000	30	2	8.7308e+03	1.2671e+03	35.4710	0	1	0	1.2676e+03
20	9500	30	2	9.1638e+03	1.5169e+03	44.1959	0	1	0	1.5176e+03
21	10000	30	2	9.5968e+03	1.7668e+03	52.9207	0	1	0	1.7676e+03
22	10500	25	2.5000	1.0040e+04	1.9974e+03	61.8975	5.0053	1.0006	1.0011	1.9984e+03
23	11000	20	3	1.0502e+04	2.1886e+03	70.9868	5.0036	1.0006	1.0007	2.1898e+03
24	11500	15	3.5000	1.0979e+04	2.3365e+03	79.4173	5.0022	1.0006	1.0004	2.3399e+03
25	12000	10	4	1.1467e+04	2.4465e+03	86.4001	5.0011	1.0006	1.0002	2.4480e+03
26	12500	10	4	1.1959e+04	2.5331e+03	92.4567	8.5377e-07	1	1.7075e-07	2.5348e+03
27	13000	10	4	1.2452e+04	2.6197e+03	98.5132	8.5377e-07	1	1.7075e-07	2.6216e+03

FIGURE 64 - INTERPOLATED SURVEY DATA AND MERGE FUNCTION

After the grid have been adjusted to 27 survey points instead of six as before, the well profile (shown in green on Figure 64) is now much smoother and simulation results will become more accurate.

8.2 Input Tubular, Temperature and Reservoir Data

When the UBD simulator is opened the last saved simulation is shown:

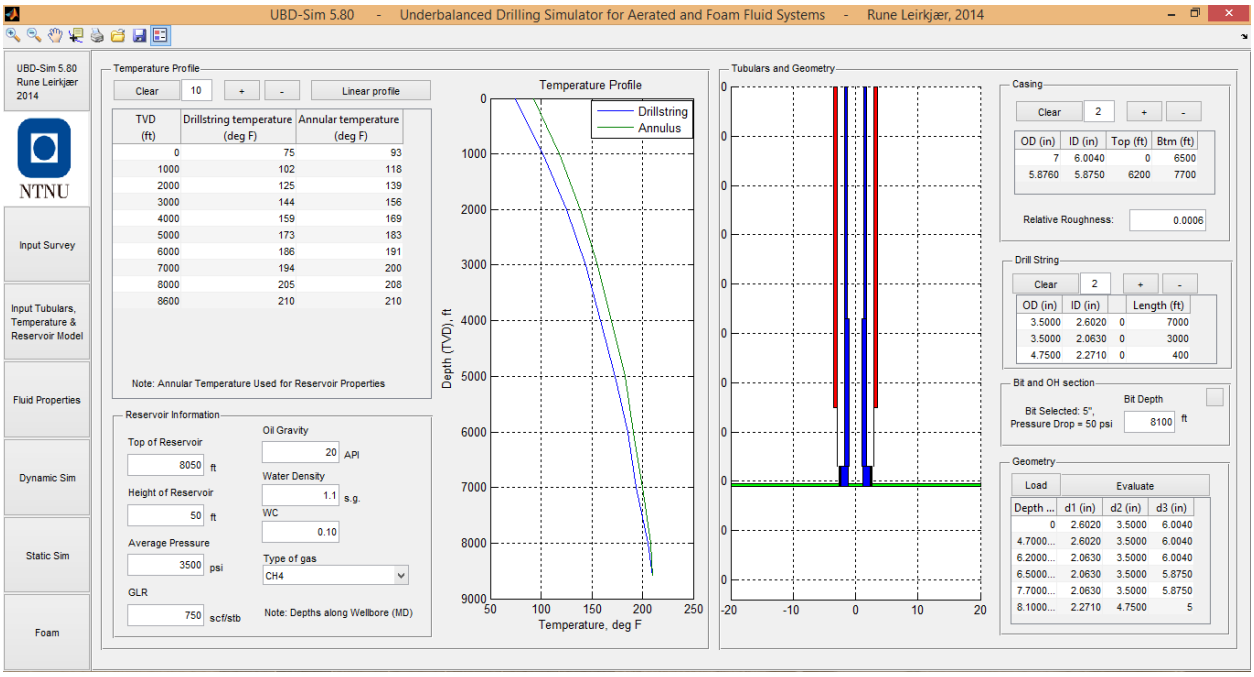

FIGURE 65 - INPUT SECTION TWO, BEFORE INITIATION

Supposed we want to simulate drilling on the well presented in the wellbore schematics shown in Figure 87. To input this tubular data the following steps have to be followed:

We want to reset the entire figure first before inputting the simulation data. This is done in a few simple steps:

1. Clear temperature profile
2. Clear casing data
3. Clear drill string data

This is done by pressing the clear button in each of the respectively panels. Next to each clear button there is a text-input box. This should be set to the number of data-points we would like to use in each category. As we have two times eight temperature points, five casing strings and two types of drill pipes, these values are set to 8, 5 and 2, before each clear-button is pressed. These sections are marked in red on Figure 66. Next, the new data should be inputted into the corresponding tables shown in yellow on Figure 66, this is further explained below.

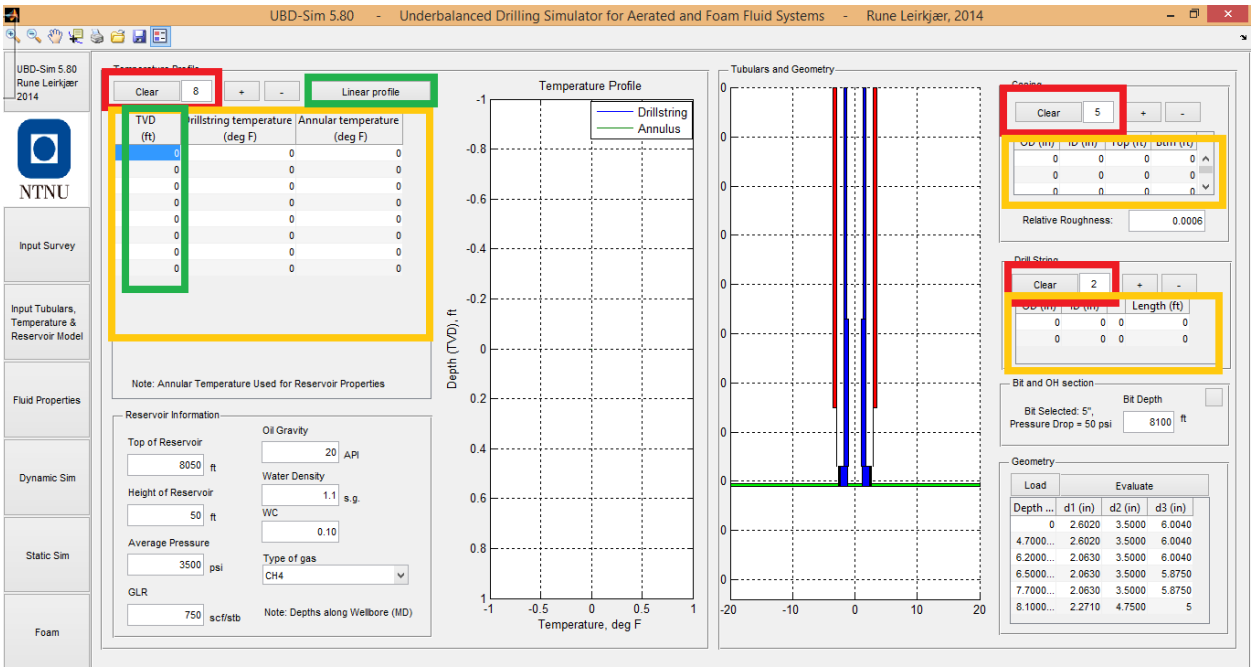

FIGURE 66 - INPUT TUBULAR SECTION, RESETTING DATA

When entering the temperature data, the first column, indicating depth (marked in green on Figure 66) should always start with 0 and be increasing towards a depth larger or equal to the simulation depth. To apply a linear temperature data the “linear-profile” button (marked in green on Figure 67) should be pressed and a dialog box will appear where temperature data should be entered as shown in Figure 67.

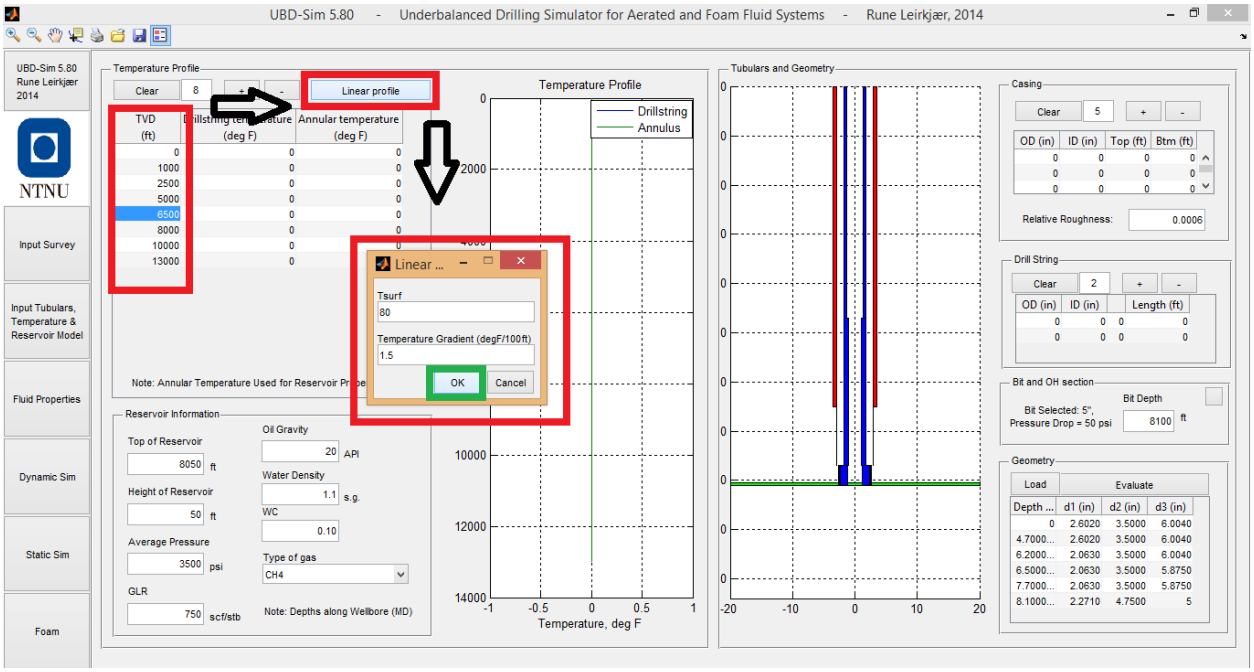

FIGURE 67 - SETTING A LINEAR TEMPERATURE PROFILE

Figure 67 shows the correct order of action to apply a linear temperature profile. First, the relevant depths are entered. Next, the button for linear profile is pressed, where the gradient and surface temperature are entered. Linear profiles are automatically applied to both the drill pipe and annular segments so the annular temperature has to be manually entered into the area marked in green on Figure 68.

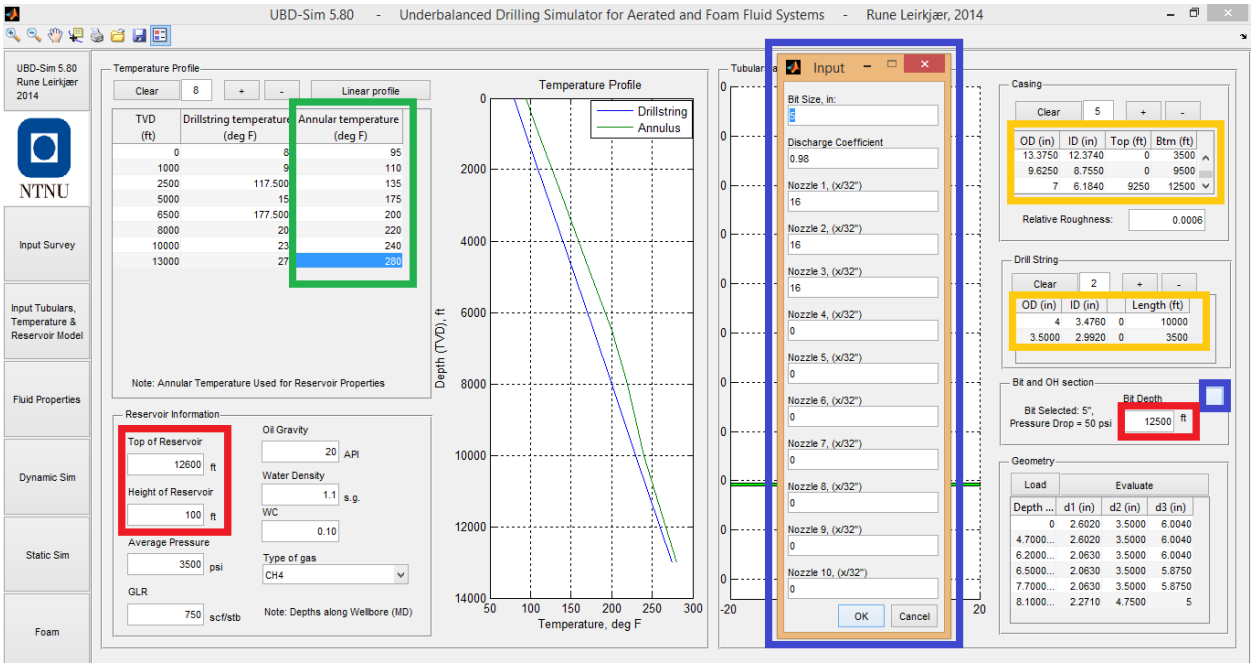

FIGURE 68 - ADDITIONAL INPUTS

The tubular information should be entered into the fields marked in yellow on Figure 68. The casing string list must always start with the largest string first and be decreasing in size. For casing strings, the outer diameter, inner diameter, top and bottom depth of each string are entered into the first, second, third and fourth column respectively. The drill string list starts with the topmost string first and every drill string segment is added on the bottom of the string defined in the row above it. Each string should be defined with outer diameter, inner diameter and length in column one, two and four (row three is not editable and are used simply for programming purposes).

The (top of) reservoir depth and length are then set in the section marked in red on Figure 68. The depth of the reservoir must always be below the cased of sections to avoid errors during simulations.

The bit depth is inputted into the text box also marked in red on the same figure, while the bit size and pressure drop model are inputted by pressing the small button next to the depth marked in blue. When setting the bit size and pressure drop; a question dialog will appear asking for which model pressure drop model is to be applied. Two models are available; a simple model and a complex model. The simple model assumes the pressure drop is known and asks for the bit size and pressure to be inputted. The complex model input is shown in the figure and is also marked in blue. As shown in the figure, this model requires the bit size, discharge coefficient and (up to ten) nozzle sizes to be defined. In this example we would want to simulate drilling using a 5” bit with 3x16 (1/32”). The discharge coefficient is set to 0.98 as this is the standard recommended by API.

The bit depth must be set after the drill string is defined and should never exceed the total length of the drill string to avoid errors. The depth of the bit is also what is referred to as the TD in simulations and this is where BHP is assumed to be.

The reservoir zone should always be set below the cased off area, or else the UBD simulator will still believe the zone is intersection and inflow may be encountered. At this point we would not like to drill into the reservoir, so the bit depth is set to 12,500 feet, and the case is evaluated by pressing the button highlighted in Figure 69.

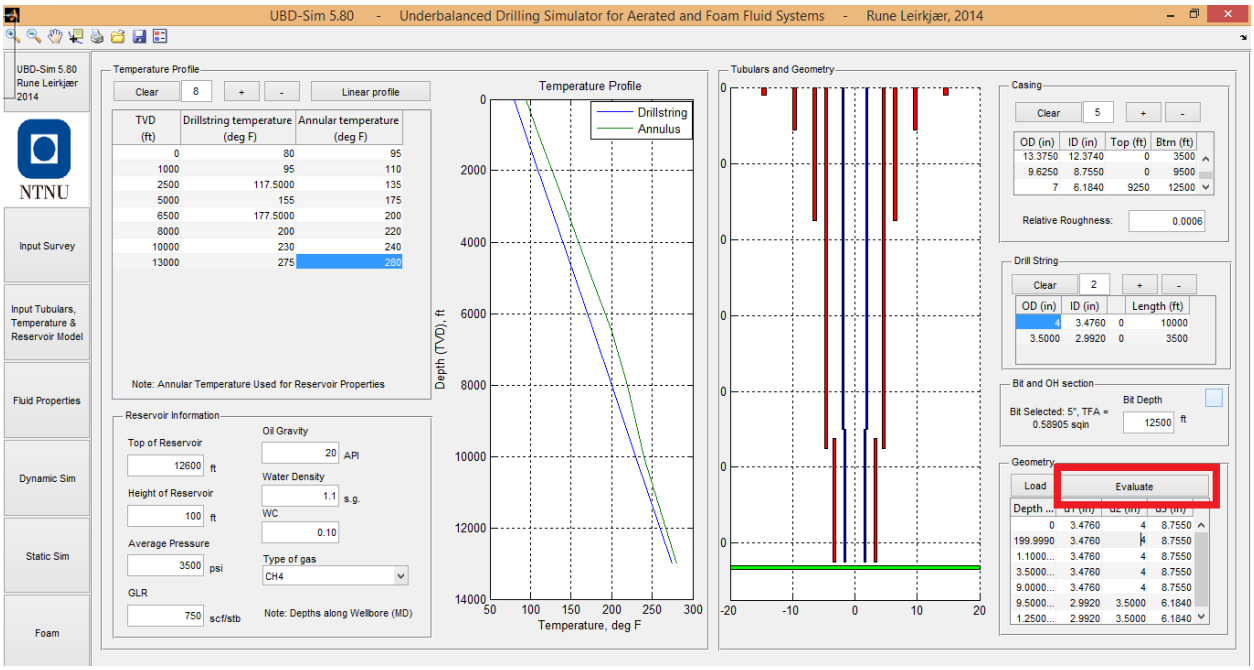

FIGURE 69 - EVALUATING THE INPUTTED DATA

This will cause the wellbore schematics to update and check if the bit intersected the reservoir. As the bit in this example is above the top of the reservoir no further actions are required and simulations are now possible to run if the survey and fluid data is defined.

If a reservoir would have been intersected a question dialog would have appeared when the “Evaluate” button would be pressed. This dialog is marked green on Figure 70. When a selection is made, a new dialog will appear if either “Known Reservoir Properties” or “Known Maximum Flowrate” is selected. These dialogs are shown on Figure 71. The maximum flow rate is then calculated and outputted in a new dialog shown in the same figure.

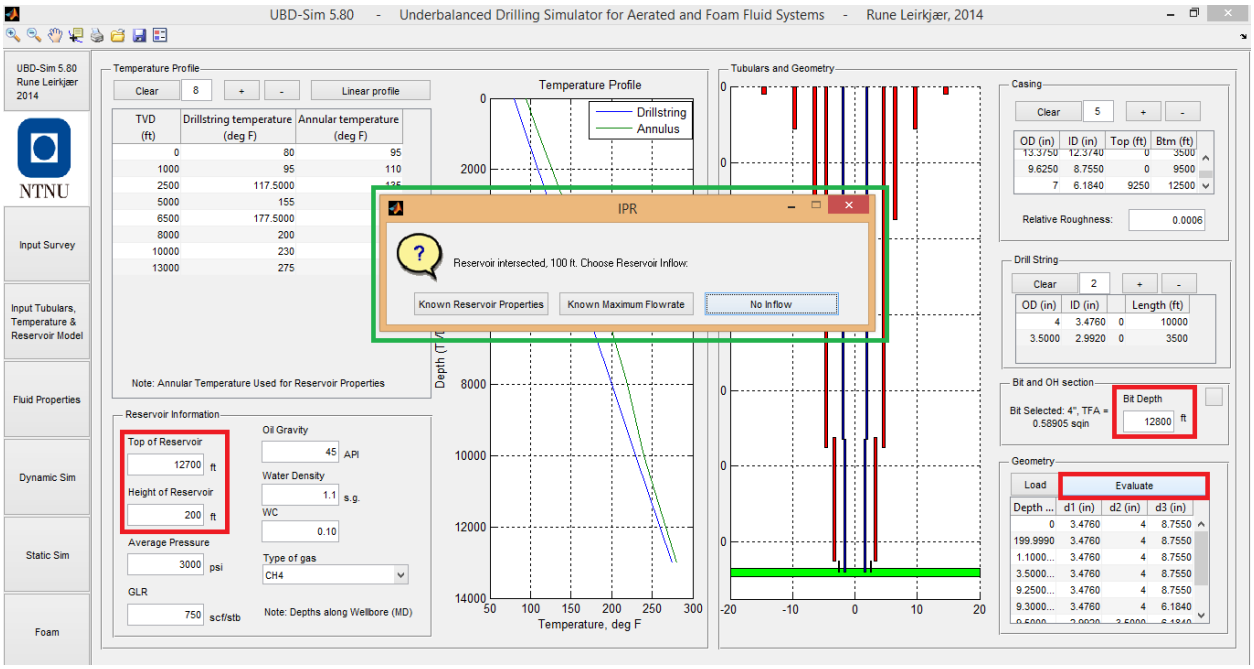

FIGURE 70 - SELECTION OF IPR MODEL (RED FIELDS SHOWS HOW INTERSECTED PAYZONE IS CALCULATED)

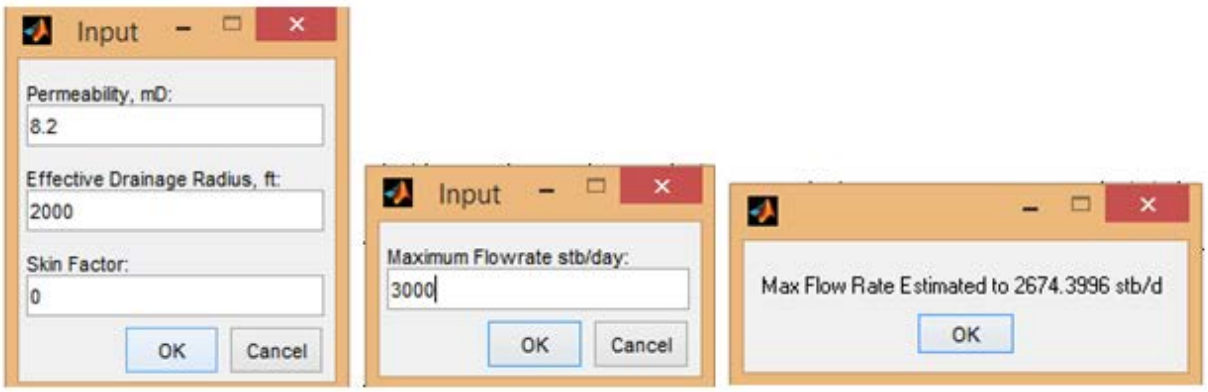

FIGURE 71 - INPUT AND OUTPUT DIALOGS RESERVOIR MODELS

8.3 Input Aerated Fluid Properties

When performing simulations with aerated fluid the injected fluid properties are inputted in the section marked in blue on Figure 72.

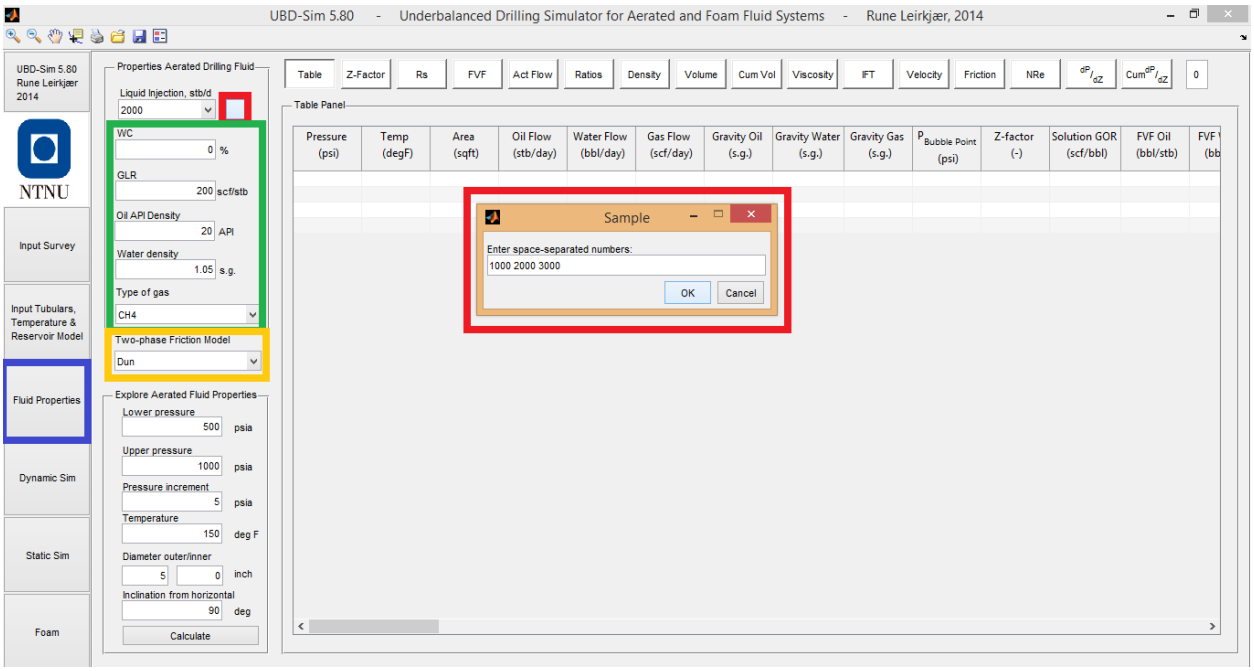

FIGURE 72 - INPUT AERATED FLUID PROPERTIES

To set the liquid rates used in the simulation the small button (marked red on Figure 72) must be pressed to open the input dialog (also marked red). In this section, the liquid flow rates are written into the text box separated by a space, as shown in the same figure. Other fluid properties are written into the respectively text box or selected in the drop-box, all marked by the green section on this figure. The two-phase correlation used in aerated simulations is chosen from the drop-box marked in yellow on the same figure.

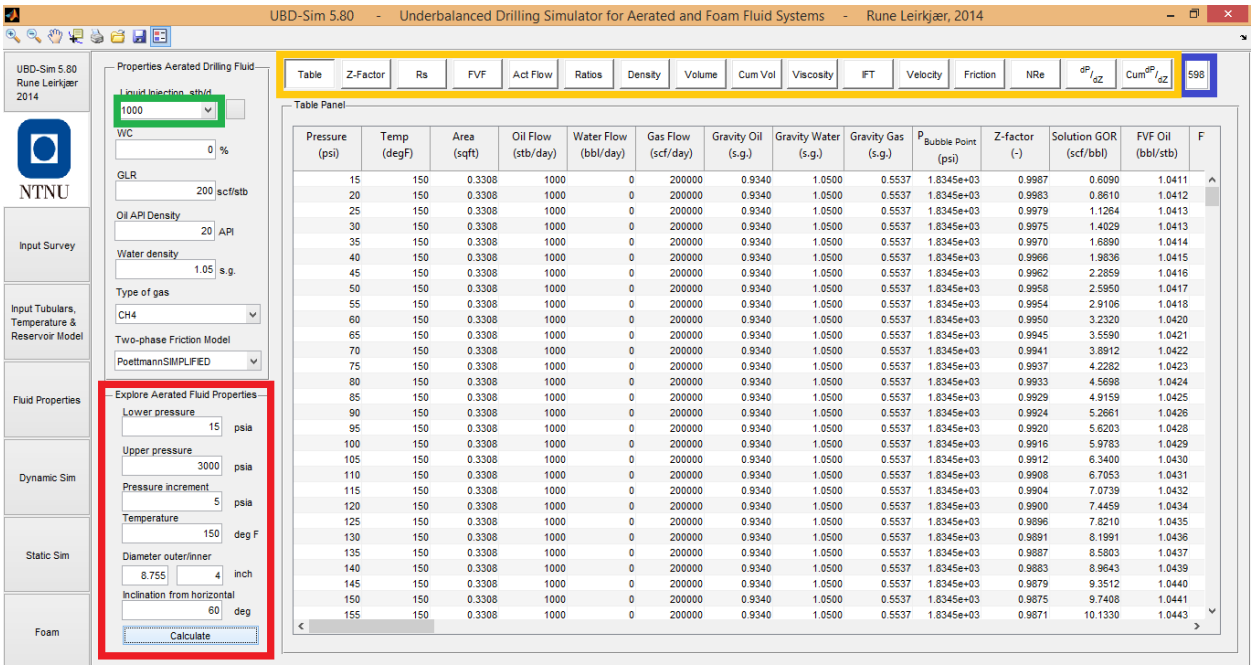

FIGURE 73 - EXAMINING FLUID PROPERTIES

To examine how the fluid properties and simulation parameters will perform for the selected fluid in different in-situ conditions the “Explore Aerated Fluid Properties” section (marked in red on Figure 73) can be used. In this example it is preferable to have more information about the fluid properties in the 2,000 feet slant annular section will be. The outer diameter in this section is the same as the ID of the casing string, or 8.755”, and the inner diameter is set to the OD of the drill string which is 4”. The inclination in this section (from the survey) is 30 degrees and is therefore set to 60 degrees from horizontal. The temperature we want to examine is here set to be 150 F. Pressures we want to examine in this case range from atmospheric pressure (15 psi) to 3,000 psi with an incremental value of 5 psi. Only one liquid rate can be examined so the one the user wants to test has to be chosen from the drop-down box marked in green on Figure 73.

Before the fluid properties are calculated for this section, it is preferable to clear the current (if any) values previously calculated. This is done by setting a zero in the line counter located in the top-most right corner, marked in blue on Figure 73. Afterwards the values can be calculated by pressing the “Calculate” button in the red section in the same figure. The calculation and plotting of these results might take some time depending on the computer the user is running the simulator on. When the wait-bar which appears after the simulation button are pressed is closed, can the calculated properties be viewed either in a tabular form (shown in figure) or plotted versus pressure. To switch between the table and plots the buttons marked in yellow at top of the same figure should be used.

8.4 Static Simulations Aerated Fluids

Static, or steady-state, simulations are simulations which are run for one time step only. These are found in the section marked in blue on Figure 75. Inputs and simulation properties must be entered in the sections previously described in this chapter.

Static simulations can be run in five different modes:

1. Static Simulation
2. UBD envelope
3. Pressure Contributions
4. Gas Qualities
5. Back-Pressure Envelope

Mode selection is done through the drop-down menu, marked in red, and run by pressing the “Simulate” button marked in green, both in Figure 75. All modes require the (annular) surface-pressure to be defined. This pressure is entered into the text-box, marked in yellow on the same figure, for mode one through four. The back-pressure envelope will open an input-dialog (shown in Figure 74) where the pressures to evaluate will be defined before the simulation is initiated.

Liquid rates simulated are collected from the liquid-rate drop box marked green in Figure 73. For the first mode, only the selected rate in the drop-box menu is used. In mode two through five all the rates are used in the simulation.

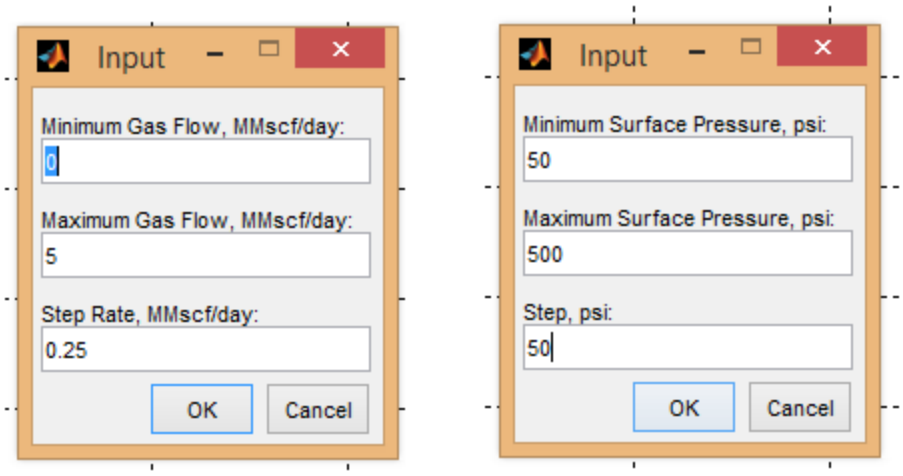

FIGURE 74 – INPUT DIALOG GAS RATE AND SURFACE PRESSURE

Gas rates are for mode two through four user-inputted through a dialog box (shown in Figure 74) which opens when the simulation is started. For mode one and five the GLR are collected from the text-box in the section marked green on Figure 72.

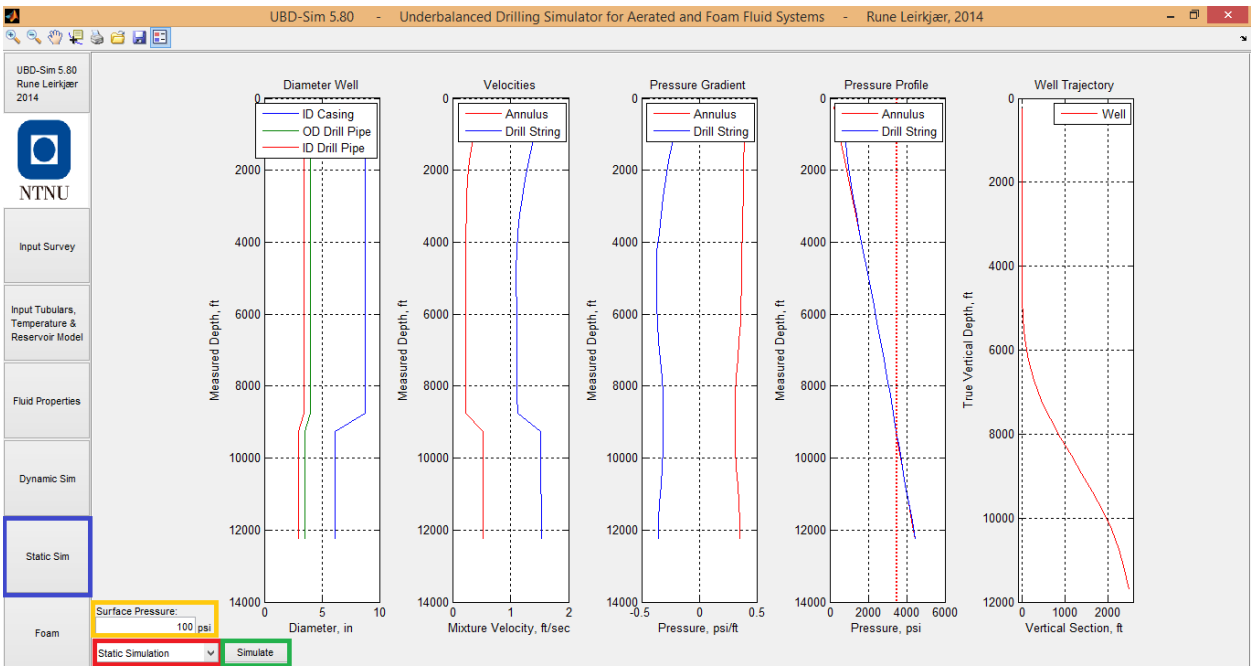

FIGURE 75 - STATIC SIMULATION SECTION

8.5 Dynamic Simulation Aerated Fluid

Dynamic simulations are multiple steady-state simulations run in a sequence. The first time step is the same as the result one would get if a static-simulation was run, and the following are based upon the fluid conditions present in

the wellbore and, additional influx, rising gas, rate changes and choke performance. The dynamic simulation for aerated fluids is included in the section marked blue on Figure 76.

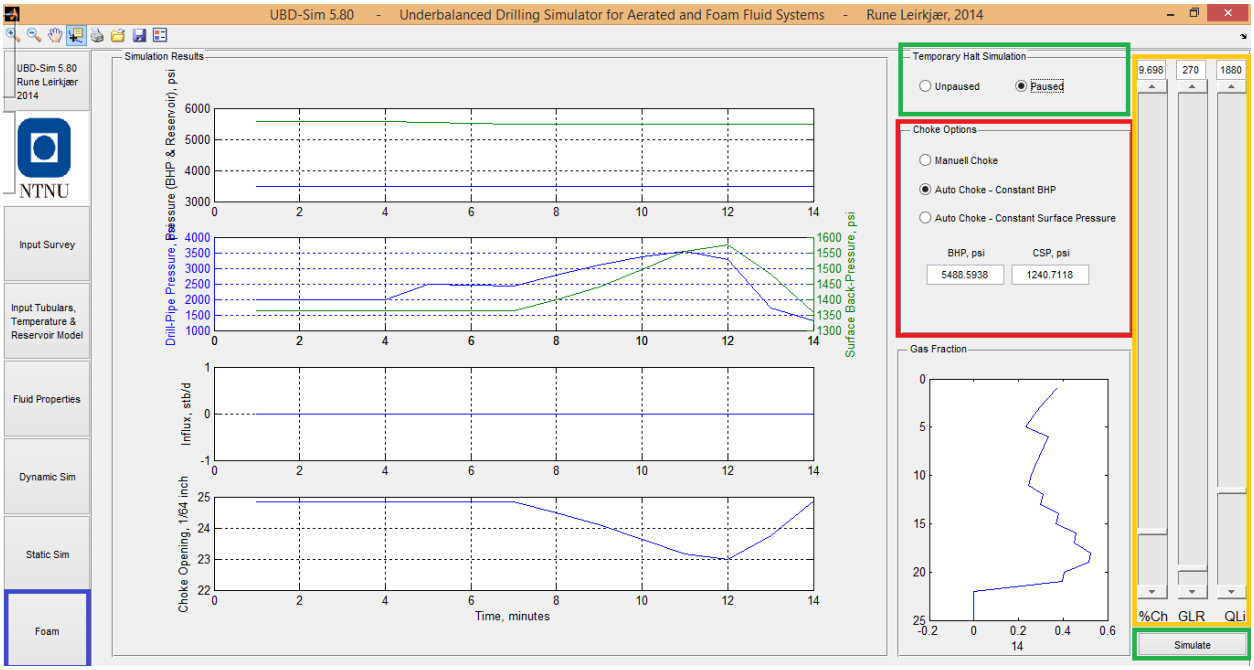

FIGURE 76 - DYNAMIC SIMULATION INPUT

The dynamic simulation uses fluid-property inputs from the “Fluid Properties” section with reservoir, temperature, geometry and well path information as previously described in this chapter. The simulation parameters which can be changed as the simulation is run in the dynamic simulation are the choke opening, gas-liquid ratio and liquid injection rate. These three parameters are regulated by either typing the required value into the corresponding text-box or adjusting the relevant slider. These sliders and text-boxes are marked in the yellow field on Figure 76, and from left to right are inputted as:

- Choke opening in percentage - 100% (maximum) choke opening assumed to be 4.00” (hard-coded)
- Injected GLR in scf/bbl – changeable between 0.01 and 10,000
- Liquid injection rate in bbl/day – changeable between 0.01 and 10,000

These values should all be set within a valid range of the UBD envelope before the simulation is initiated by pressing the “Simulate” button marked in green on Figure 76. The simulator will first start calculating when the simulation is set to “Un-paused” by pressing the radio-button marked in the red field in the same figure. The pause function is included to avoid iteration errors when major changes are done between time-steps, e.g. moving from manual to automatic choke-control.

Changes done to the choke-control are performed in three different ways depending on which choke-mode that is selected. The choke-mode is changed by setting the radio-buttons marked in the red section to the required mode. The choke is then either set manually by the user or automatic through an iteration process by the program to match the user-inputted design-parameters inputted in the text-boxes in the same section.

- Manual Choke – User controlled through the slider and/or text-box

- Auto w/constant BHP – Program controlled to match user-inputted value in BHP text-box
- Auto w/constant SBP – Program controlled to match user-inputted value in CSP text-box (surface back-pressure)

Due to limitations of the MATLAB GUI will the dynamic simulation run until it is stopped by the user itself by closing the wait bar which opens for each time-step. It is worth noticing that the dynamic simulator will write one file for each time-step to hold values for later simulation steps, this requires some memory by the computer the simulation is run on. On longer simulations this will also require some disk-space (approximately, 3.9 MB per 1,000 time-steps).

8.6 Static Simulations Foam Systems

In foam simulations are all the fluid properties and simulation mode selected in the same section (marked in blue on Figure 77).

Foam simulations can be run in the same five modes as with aerated fluids. Modes are selected from the drop-down box marked red in Figure 77. As simulations performed on foam systems do not consider the flow inside the drill-string all the liquid-rates in the drop-down box are included in the static-simulation mode. The gas rates, surface back-pressure and liquid rates are used for these modes as explained in section 8.4.

Fluid properties in foam simulations are limited to liquid injection rate, maximum gas quality, liquid density, type of gas and formation water; influx all of which are entered in the section marked in green on Figure 77. Liquid rates are as with aerated fluids entered via an input dialog activated by pressing the small button marked in blue on the same figure. Foam simulations use a more complex model than aerated fluid to check for proper hole-cleaning. This cuttings properties and ROP to calculate cleaning is inputted in the section marked in yellow on the figure.

Surface back-pressure is inputted in the text-box marked in red on Figure 78. Foam viscosity is calculated by the UBD simulator and required input is correlation selected in the drop box marked in blue in the same figure. Some of the correlations require additional inputs, if these correlations are selected more input fields will be showed in the blue section.

After all properties have been defined, the simulations are run by pressing the “Calculate” button, marked in green on Figure 78.

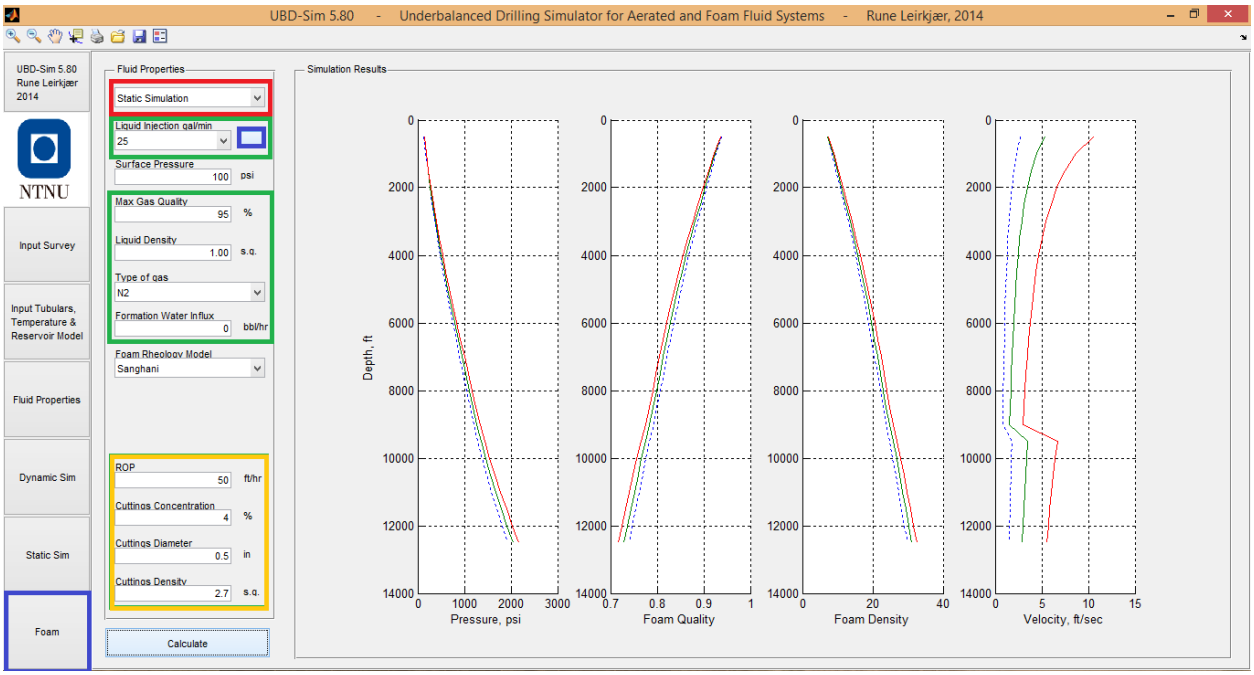

FIGURE 77 - INPUT FOAM SIMULATIONS

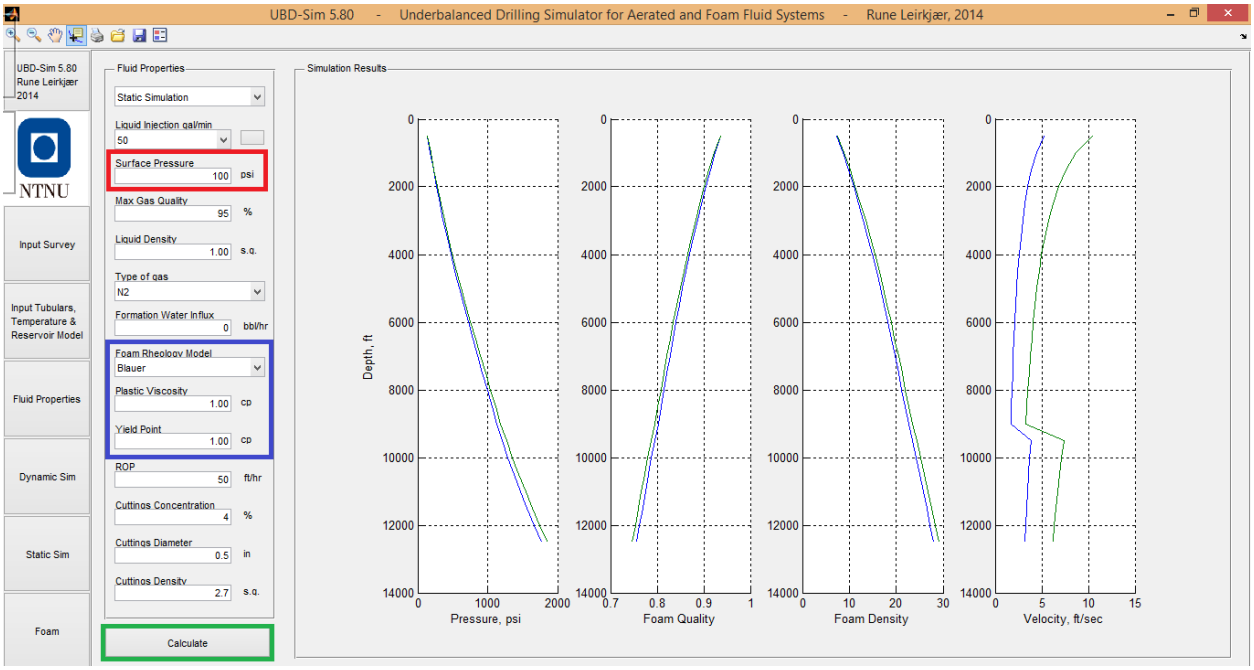

FIGURE 78 - FOAM RHEOLOGY MODEL SELECTION

9 Simulation Results

In this chapter, aerated fluid correlations and foam rheology models are compared for one vertical well. All the models have been compared and the deviation in the results has been discussed. Further simulations are included Appendix C, where multiple well geometries have tested using a large range of input parameter.

9.1 Correlation Comparison Aerated Fluids

A simple simulation was performed to compare the pressure correlations as described in chapter 4.

The simulation was performed on a vertical well with a depth of 8600 ft, no reservoir influx was expected. The well was circulated with 20 API oil at a rate of 4500 stb/day, injected with methane at 167.3 scf/stb and applied with a surface back pressure of 100 psi. In addition, the well simulated had the following temperature and tubular specifications:

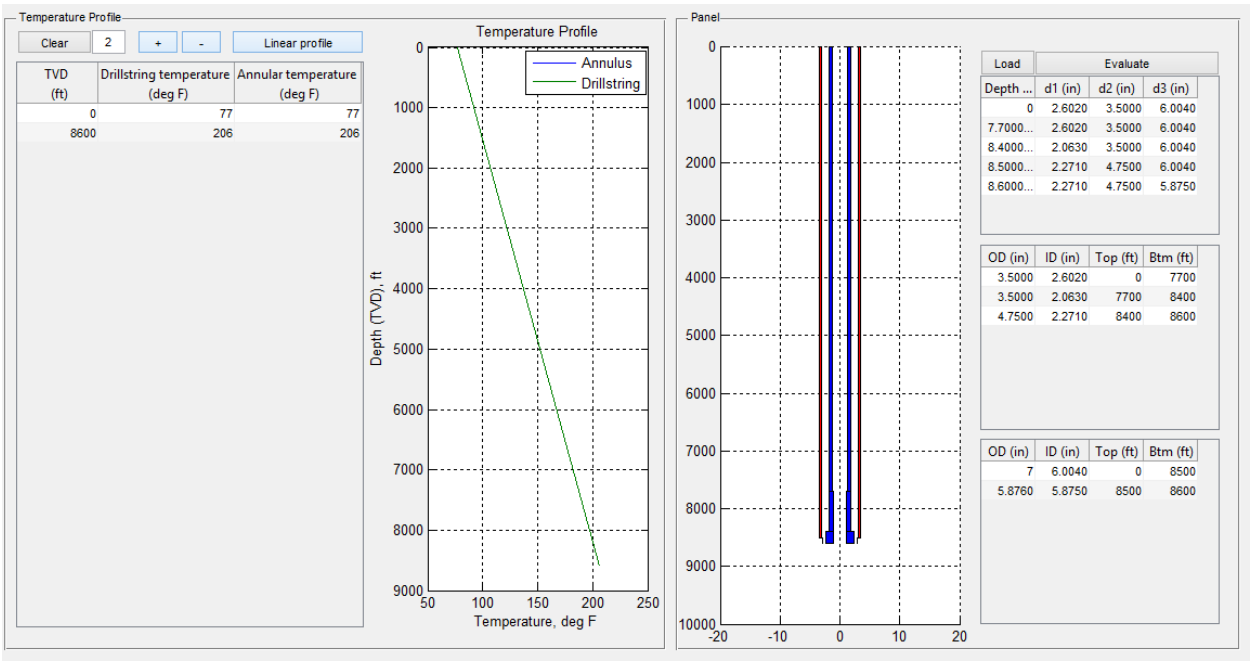

FIGURE 79 - SIMULATION INPUT SIMPLE WELL (SCREENSHOT FROM EARLIER VERSION OF THE SIMULATOR)

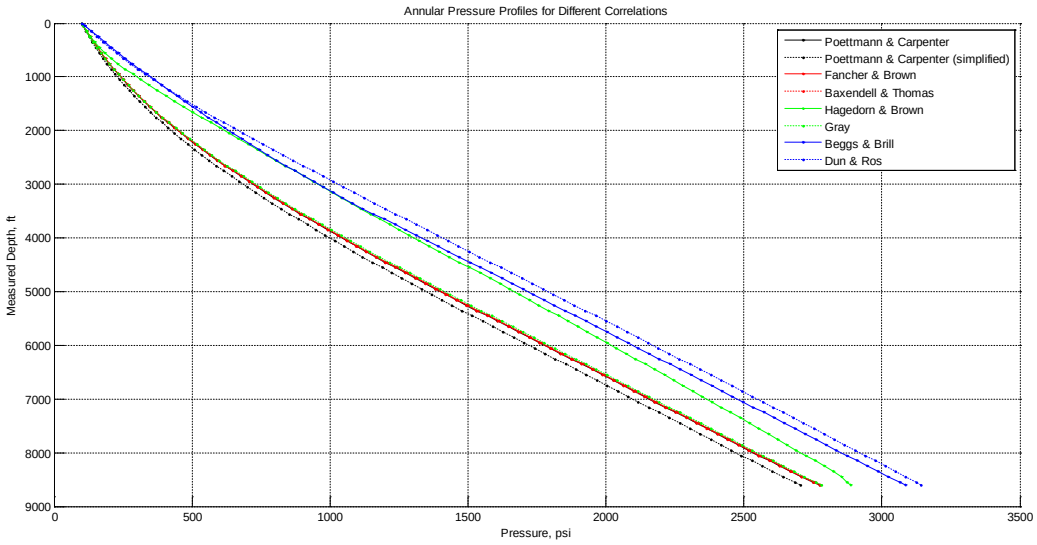

FIGURE 80 - COMPARISMENT OF THE AERATED PRESSURE CORRELATIONS FOR A SIMPLE VERTICAL WELL

Figure 80 show that the original pressure correlation, Poettmann & Carpenter Method along with the other no-slip "Category A" correlations predicts the lowest BHPs for this specific case. Poettmann & Carpenter was set as a reference for comparing the other correlations as it was a base for development of the others.

Most correlations predict pressures above the set reference throughout the profile of the well, with the exception of the Baxendell & Thomas, and simplified Poettmann & Carpenter Method, also including a general exception at some shallower depths.

The Baxendell & Thomas correlation produces almost identical values as the reference, Poettmann & Carpenter, with a maximum negative deviation of 0.03%. The simplified Poettmann & Capenter Method under predicts the pressures compared to the original version with approximately 3.75%.

The last "Category A" correlation, Fancher & Brown, predicts pressures 0.34% above the reference in this case. With the exception of the simplified model, the Fancher & Brown correlation differ the most from the reference. As the maximum deviation only reaches a maximum of 0.49%, these no-slip correlations can be said to produce very similar values.

TABLE 7 - PERCENTAGE DEVIATION FROM POETTMANN AND CARPENTER

	Median	Mean	Max	Min
Poettmann & Carpenter (simplified)	-3.76%	-3.75%	0.00%	-5.35%
Fancher & Brown	0.34%	0.34%	0.49%	0.00%
Baxendell & Thomas	-0.02%	-0.02%	0.00%	-0.03%
Hagedorn & Brown	17.85%	19.09%	37.73%	-0.61%
Gray	0.85%	0.73%	1.34%	-0.74%
Beggs & Brill	24.12%	25.61%	45.48%	0.00%
Dun & Ros	28.84%	29.90%	48.97%	0.00%

In “Category B” correlations which evaluate slip, but eliminate the effect of flow regimes, the values predicted tend to vary more. Values produced by Gray’s correlation more or less follow the reference values from Poettmann & Carpenter. As depth increases, the calculations performed using the Hagedorn & Brown model corresponds better with results from the “Category C” models. Both of these correlations predict pressures below the Poettmann & Carpenter reference in low pressure zones. Hagedorn & Brown overestimates the pressure (compared to the no-slip reference) with 19.09% on average with an extreme value of 37.73% in this case. These results are far from what is found by using Gray’s correlation, also in “Category B”, giving the same corresponding numbers of 0.73% and 1.34%.

Beggs & Brill’s together with Dun & Ros’ Correlation predicts the pressure profile in the well to be approximately 30% higher on average than what the original Poettmann & Carpenter Method yields. The maximum percentage deviation is found in shallower parts of the well as these two categories consider flow regimes and causes the pressure profile to have a slightly different shape. This maximum percentage deviation is calculated to be 45.48% and 48.97% for Beggs & Brill and Dun & Ros respectively.

9.2 Correlation Comparison Foams

The same well as described in section 9.1 was simulated using a foam system to compare the foam viscosity models discussed in chapter 5. The pressure profiles outputted from the program is presented in Figure 81.

The simulation was performed with no reservoir water influx. The well was circulated with 85% max gas quality, using nitrogen, with a foam rate of 50 gpm. Applied surface back pressure was set to 100 psi and base liquid density to 1.0 s.g.

For foam rheology models which required the base liquid viscosity to be known, the value was set to 1.0 cp. Plastic viscosity was assumed to have the same value in Blauers correlation, and the yield point was assumed to be 0.2 lbm/ft^2. These inputted values made the calculated outputs from Blauer match the output results from Sanghani with only a small deviation.

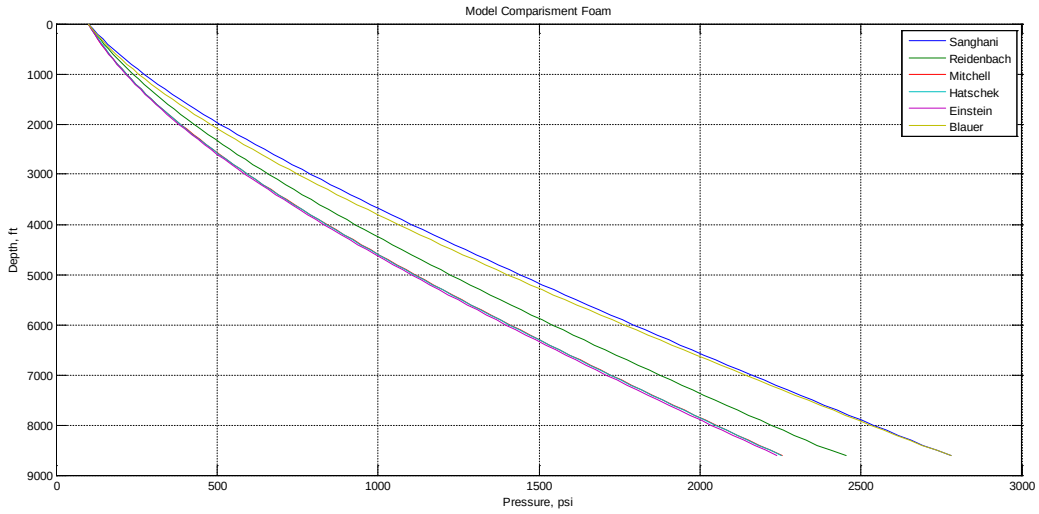

FIGURE 81 - COMPARISMENT OF THE FOAM PRESSURE CORRELATIONS FOR A SIMPLE VERTICAL WELL

Figure 81 shows that the viscosity models provide BHPs ranging from approximately 2,250 to 2,750 psi. For further calculation of percentage deviations Sanghani was selected as the reference model. Percentage deviations are presented in Table 8.

Sanghani produced overall higher pressure gradient estimates throughout all depths in the well bore, with a maximum deviation of 25.73%. This maximum deviation is from the Einstein correlation, which is not really expected to be valid for these gas qualities, and should generally be used with care in foam pressure calculations. Einsteins correlation provided overall the lowest pressures in all segments, with a deviation of 4.30% to Sanghani already at 100 ft.

The two power-law correlations, Sanghani and Reidenbach produced outputted pressures with an average segment deviation off 13.87%. This value seems to still be a good approximation when considering the relatively large variation in gas quality and corresponding pseudo-plastic parameters down-hole.

Einstein, Mitchell and Hatschek all produced relatively similar pressure gradients, which might be due to the estimated liquid base viscosity of 1.0 cp. The maximum deviations for these correlations were 25.73%, 24.72% and 24.87% respectively. A larger inputted base viscosity would easily bring these results much closer to the outputted values from Sanghani, however it is not necessarily a good option to manipulate results this way. Rehm et.al. specifically presents Sanghani viscosity model for use in calculations, and the model is overall mentioned as reliable. The author of this thesis therefore believes that these correlations would normally produce lower pressure estimates, than the for example Sanghani and Reidenbach, due to the limitations of the governing equations in these models.

An overall maximum pressure deviation for these six foam rheology models was approximately 25%, assuming the inputted values are realistic, is believed by the author to be very good results for this well.

TABLE 8 - PERCENTAGE DEVIATION FROM SANGHANI (EXLUDING SURFACE PRESSURE)

	Median	Mean	Max	Min
Reidenbach	14.37%	13.87%	16.49%	2.31%
Mitchell	21.87%	21.21%	24.72%	4.20%
Hatschek	21.92%	21.26%	24.87%	3.89%
Einstein	22.66%	21.99%	25.73%	4.30%
Blauer	3.13%	3.22%	6.21%	0.03%

10 Assumptions and Sources of Error

This chapter includes the assumptions made when writing the simulator and possible sources of error in the model. These are listed below.

Some assumptions had to be made to simplify the making of the simulator. In the current build of the program the following assumptions were made:

- Mixture gas properties from reservoir influx and injected gas will follow Suttons correlation if the two gas types are unequal.
- Mixture fluid properties from reservoir influx and drilling fluid are calculated upon volumetric flow fractions at standard conditions.
- Well geometry is assumed to remain constant during the simulations. ROP set does not influence the depth of the well and is only used to calculate well-cleaning.
- No drill string rotation, and 100% eccentricity is assumed.
- Water together with oil is assumed to make up the liquid flow in the well-bore, making two-phase equations valid.
- Reservoir temperature is assumed to be equal to the set annular temperature at the corresponding depth.
- Reservoir influx is assumed to come from radial drainage.
- All two-phase fluid correlations and foam rheology correlations are assumed to work in inclined sections.
- Joule-Thomas effect below the drill bit is ignored.
- BHPs are calculated at the depth of the bit. The bit itself is not assumed to have any length.
- The cleaning boundaries for foam are based on drag forces.
- The cleaning boundaries for aerated systems are based on a minimum annular mixture velocity of 120 ft/min.
- Cuttings concentration is assumed not to exceed 4.0%.
- Foam pressure calculations assume the ideal gas law is valid, and fluids act as power-law fluids.
- Pressures are given in absolute values.
- Gas in the system is only solvable in the oil phase.
- No lag time is assumed in pressure propagation.

Due to the complexity of the finished code there are some sources of error which might occur. These include:

- High WC can cause the models implemented in the problem to become invalid.
- Pressures below the atmospheric pressure will cause functions to fail and possible force the program into an infinite loop.
- Inputted reservoir can be produced through the casing if the bit depth is set below the reservoir depth inside a casing string.
- Incorrect input procedure, or undefined values, might cause problems when running simulations.
- In some rare cases, the inputted values will be outside the model range and cause MATLAB to crash without any warnings.

- MATLAB will often output calculated values as complex numbers, if these are used in an interpolating function will the program stop working. Much time has been spent to avoid this, and hopefully this has been fixed in most cases in the final build of the simulator.

11 CONCLUSION

When drilling underbalanced it is important to have a good understanding about the pressure down-hole. An underbalanced operation could be jeopardized if the bottom-hole pressure exceeds the formation pressure even if it is just for a few minutes. To be ready for such a situation, one should always plan an UBD situation extensively and use a UBD simulator to examine the effect of possible well hydraulics incidents.

The purpose of this thesis was to develop a UBD simulator in MATLAB which could be useful in calculating pressure drops, explore fluid properties and setting operational limits for aerated drilling fluids and foam systems. The work done was a continuation of the author's previous project on the subject, where extensive improvements were made.

There are many uncertainties in two-phase flow modeling and a large amount of available fluid correlations to choose from. This thesis implements a large variety of these correlations. From the simplest pressure correlations, such as Poettmann & Carpenter, to complex ones used in commercial UBD simulators, such as Beggs & Brill.

The main challenge in this thesis was without a doubt the extensive programming required for all the correlations and the graphical user phase. The final build of the simulator developed is able to handle a large range of input parameters. Outputted results have in most cases proven to be fairly reliable considering that the simulator is based upon empirical correlations.

The program allows the user to calculate anything from the pressure drop over a small pipe segment, to run advanced simulations to find the correct choke response when drilling underbalanced and while a large well kick is occurring.

The author of this thesis has good faith in the finished product, but still recommends against relying upon the results to the same degree as with a commercial simulator. Especially in regards to neglecting the effect of dispersed cuttings, pipe rotation and eccentricity which are important factors that to a large extent would affect the overall ECD in the well. The dynamic mode is heavily based upon the steady-state model. Therefore should output from this model be used more as general guideline, of what to expect from such a situation, other than the pressure response which one would actually see. It is also worth noticing that the model does not assume any lag time before a pressure response occurs when changing the choke. This lag time would in a real field situation normally be in the range of 1min/1000ft dependent on the fluid system.

12 ABBREVIATIONS

API	=	American Petroleum Institute
APL	=	Annular Pressure Drop
BHP	=	Bottom-hole Pressure
CBHP	=	Constant Bottom-hole Pressure
CSG	=	Casing
DAK-EOS	=	Dranchuk and Abou-Kassern Equation of State
DP	=	Drill Pipe
ECD	=	Equivalent Circulating Density
FVF	=	Formation Volume Factor
GLR/GOR	=	Gas Liquid/Oil Ratio
IADC	=	International Association of Drilling Contractors
LCM	=	Lost Circulation Material
MD	=	Measured Depth
MPD	=	Managed Pressure Drilling
NPT	=	Non-productive Time
NRV	=	Non Return Valve
RCD	=	Rotating Control Device
ROP	=	Rate of Penetration
TD	=	Total Depth
TVD	=	True Vertical Depth
UBD	=	Underbalanced Drilling
WC	=	Water Cut (fraction water)
WOR	=	Water-Oil Ratio
WSM	=	Wellbore Strengthening Material

13 REFERENCES

Aggour, M. A., & Al-Yousef, H. Y. Vertical Multiphase Flow Correlations for High Production Rates and Large Tubulars. doi: 10.2118/28465-PA

Bai, Y., & Bai, Q. (2005). *Subsea Pipelines and Risers*: Elsevier.

Baker, O. S., W. (1956). Calculating of Surface Tension. *Oil Gas J. (Dec 1955)*.

Baxendell, P. B., & Thomas, R. The Calculation of Pressure Gradients In High-Rate Flowing Wells. doi: 10.2118/2-PA

Beggs, H. D. (1991). *Production Optimization: Using NODAL Analysis*: OGCI Publications.

Bellarby, J. (2009). *Well Completion Design*: Elsevier Science.

Brill, J. P., & Beggs, H. D. (1978). *Two-phase flow in pipes*. [Tulsa].

Culen, M. (2014, 25.03.14). [Personal communication].

Dranchuk, D. M. A.-K., J.H. (1975). Calculation of Z Factors For Natural Gases Using Equations of State. *Journal of Canadian Petroleum Technology, Volume 14, Number 3*.

Duns, H., Jr., & Ros, N. C. J. *Vertical flow of gas and liquid mixtures in wells*.

Eck-Olsen, J. (2003). IADC RIGPASS for Statoil: Underbalanced Drilling Orientation.

Fancher, G. H., Jr., & Brown, K. E. Prediction of Pressure Gradients for Multiphase Flow in Tubing. doi: 10.2118/440-PA

Gilbert, W. E. (1954). Flowing and Gas-Lift Well Performanc. *Drill. & Prod. Prac*.

Gray, H. E. (1974). Vertical Flow Correlation in Gas Wells. *User manual for API 14B, Subsurface controlled safety valve sizing computer program, API*.

Hough, E. W., Rzasa, M. J., & Wood, B. B. Interfacial Tensions at Reservoir Pressures and Temperatures; Apparatus and the Water-Methane System. doi: 10.2118/951057-G

Leirkjær, R. S. (2013). Simulation of underbalanced drilling in MATLAB. *TPG4520 Drilling Specialization Project - Department of Petroleum Engineering and Applied Geophysics*.

McCain, W. D. (1990). *The properties of petroleum fluids*: Petroleum Pub. Co.

NFOGM/Tekna. (2014). Handbook of Multiphase Flow Metering. Retrieved 01.06.14, from http://www.haimo.com.cn/uploadfiles_1/File/20090801114552980.pdf

NORSOK. (2004). NORSOK STANDARD D-010: Well integrity in drilling and well operations. *Rev. 3*.

Ozbayoglu, M. E., Kuru, E., Miska, S., & Takach, N. A Comparative Study of Hydraulic Models for Foam Drilling. doi: 10.2118/02-06-05

Perez-Tellez, C. (2003). *Improved bottomhole pressure control for underbalanced drilling operations.* Universidad Nacional Autonoma de Mexico.

Petroleum.co.uk. (2014). API Gravity.

Rehm, B. (2012). *Underbalanced drilling: limits and extremes*. Houston, TX: Gulf Publishing Company.

Rushing, J. A., Newsham, K. E., Van Fraassen, K. C., Mehta, S. A., & Moore, G. R. *Laboratory Measurements of Gas-Water Interfacial Tension at HP/HT Reservoir Conditions*.

Takács, G. (2005). *Gas Lift Manual*: PennWell.

Whitson, C. H., & Brulé, M. R. (2000). *Phase behavior* (Vol. vol. 20). New York: SPE.

William C. Lyons, P. D. P. E. (2009). *Air and Gas Drilling Manual: Applications for Oil and Gas Recovery Wells and Geothermal Fluids Recovery Wells*: Elsevier Science.

APPENDIX A

This appendix includes additional expressions used to evaluate parameters in the simulator.

A.1 MINIMUM CURVATURE METHOD

The minimum curvature method has been used to calculate the well path from survey data:

$$\phi_k = \cos^{-1}\left(\cos\phi_0\cos\phi_1 + \sin\phi_0\sin\phi_1\cos\left(\theta_1-\theta_0\right)\right) \tag{5.23}$$

$$\mathrm{F} = \frac{2}{\phi_k}\frac{180}{\pi}\tan\frac{\phi_k}{2} \tag{5.24}$$

$$L = MD_1 - MD_0 \tag{5.25}$$

$$DLS = 100\frac{\phi_k}{L} \tag{5.26}$$

$$\Delta TVD = F\frac{L}{2}\left(\cos\phi_0 + \cos\phi_1\right) \tag{5.27}$$

$$\Delta N = F\frac{L}{2}\left(\sin\phi_0\cos\theta_0 + \sin\phi_1\cos\theta_1\right)$$

$$\Delta E = F\frac{L}{2}\left(\sin\phi_0\sin\theta_0 + \sin\phi_1\sin\theta_1\right) \tag{5.28}$$

A.2 GEOMETRY EQUATIONS

General geometric equations used through the report:

$$d_h = d_o - d_i \tag{5.29}$$

$$\varepsilon = \varepsilon_{rel} d_h \tag{5.30}$$

$$A = \frac{\pi}{4}\left(d_0{}^2 - d_i{}^2\right) \tag{5.31}$$

A.3 RESERVOIR INFLOW

Reservoir influx is calculated according to Vogel's IPR model. The maximum production index is given by:

$$J_{\max} = \frac{kh}{141.2B\mu_l\left(log\left(\frac{r_e}{r_w}\right) - 0.75 + S\right)} \tag{5.32}$$

The following expression is used when reservoir pressure is below the bubble point pressure:

$$q_{\max} = J_{\max} \frac{p_r}{1.8} \tag{5.33}$$

For pressures above the bubble point pressure is the next expression used:

$$q_{\max} = J_{\max} \left[\left(p_r - p_b \right) + \frac{p_b}{1.8} \right] \tag{5.34}$$

When the maximum flow rate is known, is the inflow calculated using the original Vogel's equation (Beggs, 1991):

$$q_l = q_{\max} \left[1 - 0.2 \left(\frac{p_{wf}}{p_r} \right) - 0.8 \left(\frac{p_{wf}}{p_r} \right)^2 \right] \tag{5.35}$$

A.4 Choke Performance

The well head flowing pressure is highly dependent on the choke opening. Choke openings are normally divided into 1/64 inches or in % of total opening. Choke designs vary, a normal maximum choke opening is in the range of 1-5 inches. For this simulator a maximum choke opening of 4" is used. This is hard-coded and should not be changed by the user to avoid invalid results.

The UBD model assumes that the choke can be regulated to any value. However, most chokes operate in intervals of 1/64 inch. The correlation used between the choke opening and choke pressure is given by Gilberts Choke Equation (Gilbert, 1954):

$$p_c = 3.86 \times 10^{-3} \times q_l \frac{GLR^{0.546}}{d_c^{\,1.89}} \tag{5.36}$$

A.5 Bit Pressure Drop

The pressure drop across the bit is given by the following equation:

$$p_{bit} = \frac{156 \rho_n \left(\frac{231}{12^3} \right) \left(60 \times q_t \frac{12^3}{231} \right)^2}{C_d{}^2 \left(N_1{}^2 + N_2{}^2 + \ldots + N_n{}^2 \right)^2} \tag{5.37}$$

The temperature, pressure and fluid properties at the bit must be determined as previously describe in the report before this expression can be evaluated. N1 through Ni are the jet sizes in the bit of 1/32 inch (Rehm, 2012). The

discharge coefficient is a constant value which is normally in the range between 0.8 and 1.03. The recommended value according to API is a discharge coefficient of 0.98.

A.6 Friction Factor Correlations

This subsection includes the friction factors used in the UBD simulator.

A.1.1 Colbrook-White

Rehm et.al recommends the use of the Colbrook-White equation. This equation is given as:

$$\frac{1}{\sqrt{f}} = -2\log_{10}\left(\frac{\varepsilon}{3.7d_h} + \frac{2.51}{N_{\mathrm{Re}}\sqrt{f}}\right) \tag{5.38}$$

As Colbrook-White requires an iterative procedure to be solved, which require additional data power was instead Haalands equation used in the simulator. Figure 82 and Figure 83 shows how the two correlations compare, the Moody chart using Coolbrok-White was very time-consuming to plot in MATLAB, for a fine grid, did the total calculation time exceed one hour.

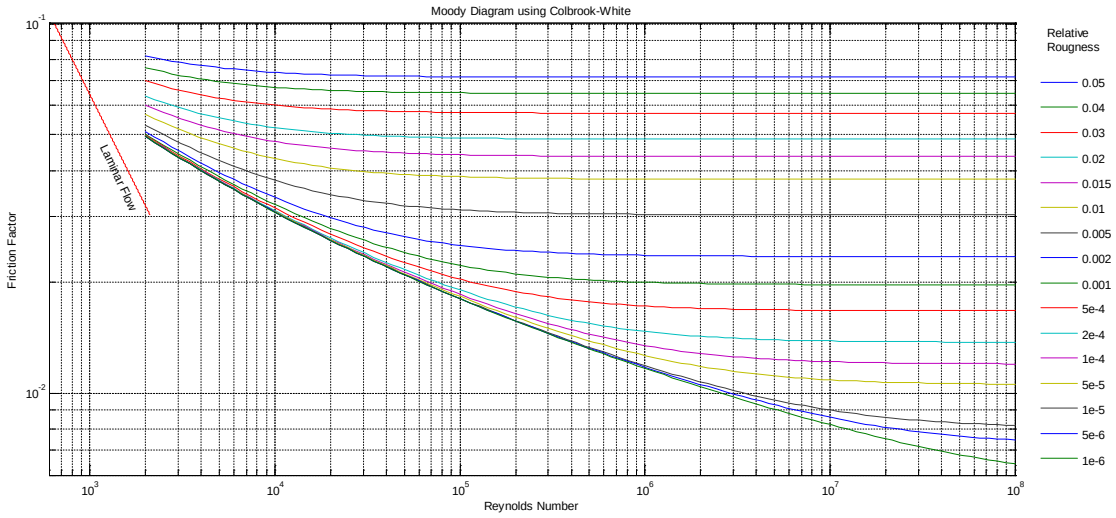

FIGURE 82 - MOODY DIAGRAM FROM COLBROOK-WHITE

A.1.2 Haaland

Haaland's equation for the friction factor proved to be at least 75 times faster to solve in MATLAB and was therefore implemented in all simulations. The expression for the friction factor can be solved directly by:

$$\frac{1}{\sqrt{f}} = -1.8\log_{10}\left[\left(\frac{\varepsilon}{3.7d_h}\right)^{1.11} + \frac{6.9}{\mathrm{N_{Re}}}\right] \tag{5.39}$$

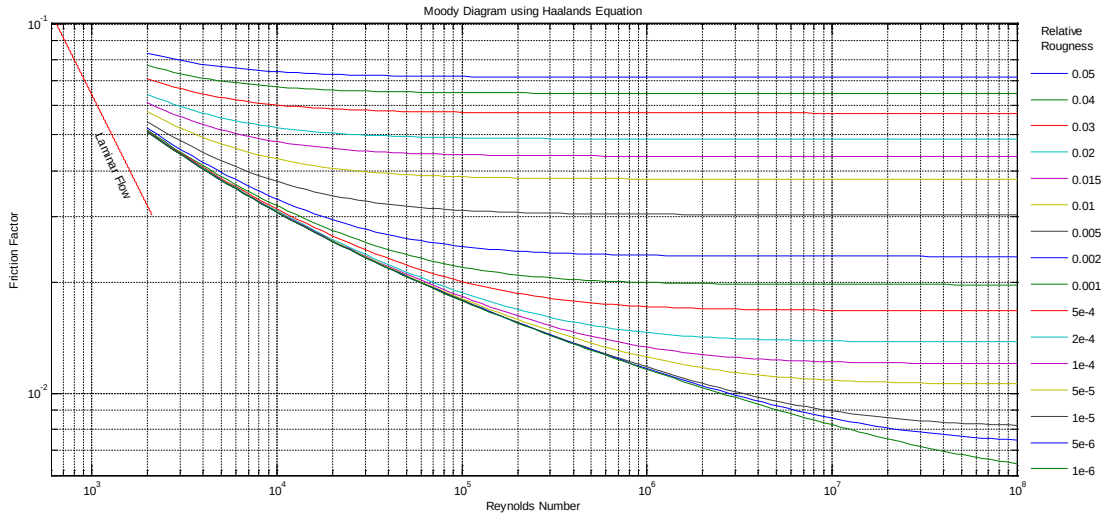

FIGURE 83 - MOODY DIAGRAM FROM HAALAND

A.1.3 LAMINAR FRICTION FACTOR

The laminar friction factor is used for foams with Reynolds number below 2000. Aerated systems are assumed to non-laminar and are calculated with Haalands equation.

$$f = \frac{64}{N_{\mathrm{Re}}} \tag{5.40}$$

A.1.4 MCADAMS FRICTION FACTOR

McAdams friction factor is generally valid for turbulent flow in smooth pipes, however Rehm et.al states that this should be used in the transition zone for foams. The equation is used for foams with Reynolds number between 2000 and 4000. Aerated systems are assumed to have turbulent flow and are calculated with Haalands equation.

$$f = 0.184\left(N_{\mathrm{Re}}\right)^{-0.2} \tag{5.41}$$

APPENDIX B

This appendix includes information about the wells simulated

B.1 GENERAL INFORMATION

Unless stated otherwise are the following reservoir properties used when influx are encountered in simulations.

TABLE 9 – DEFAULT RESERVOIR SIMULATION PARAMETERS

Default parameter	Value
Depth – TVD	12,400+-50 ft.
Pay Zone	100 ft.
Average Pressure	3000 psi
Oil Gravity	45 API
Gas	Methane
Water Density	1.05 s.g.
Water Cut	10 %
GLR	750 scf/stb
Permeability	8.2 mD
Drainage Radius	2000 ft.
Influx water (foam systems)	0

In simulations presented a liner temperature profile has been used for the drill-pipe temperature. The linear profile was set with a surface temperature off 80F with a gradient of 1.5F/100ft. In annular segments the data from Table 10 were used in simulations.

TABLE 10 – TEMPERATURE PROFILE ANNULAR SEGMENTS

Depth (ft)	0	1,000	2,500	5,000	6,500	8,000	10,000	13,000
Temperature (F)	95	110	135	175	200	220	240	280

The wells presented in the section below are simulated using 27 survey points with even spacing.

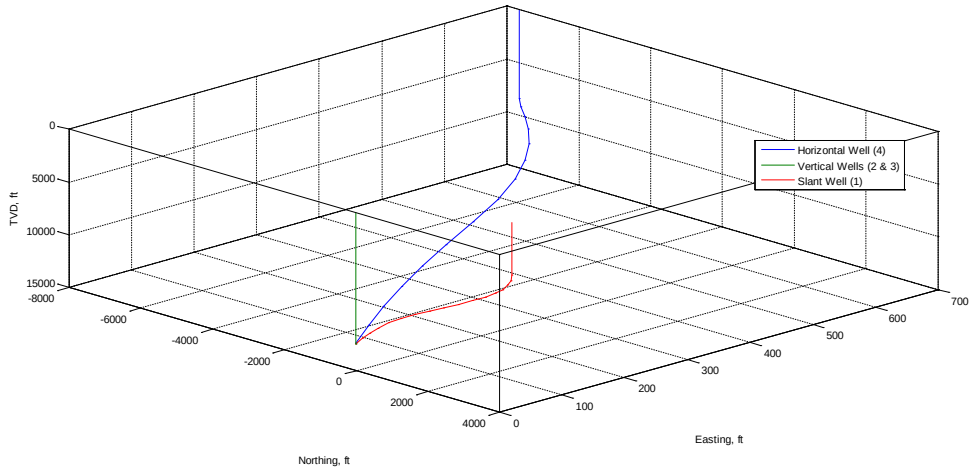

FIGURE 84 - WELL TRAJECTORIES SEEN FROM NORTH-WEST

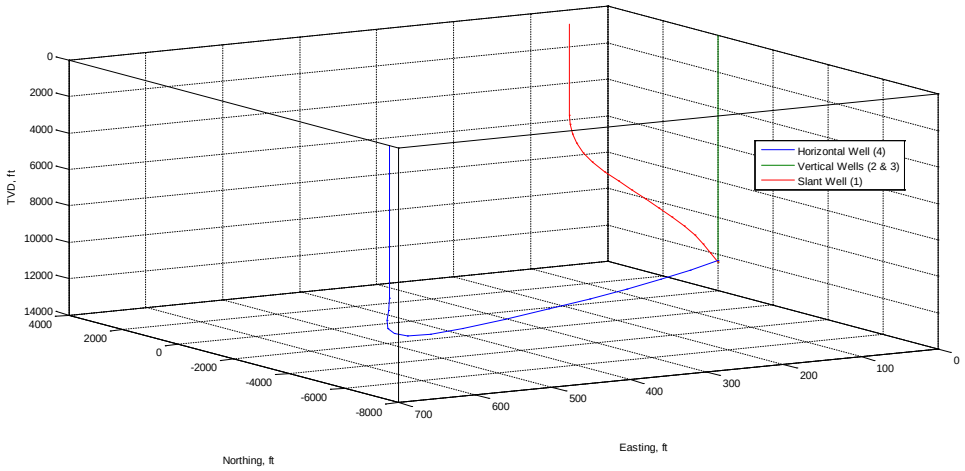

FIGURE 85 - WELL TRAJECTORIES SEEN FROM SOUTH-EAST

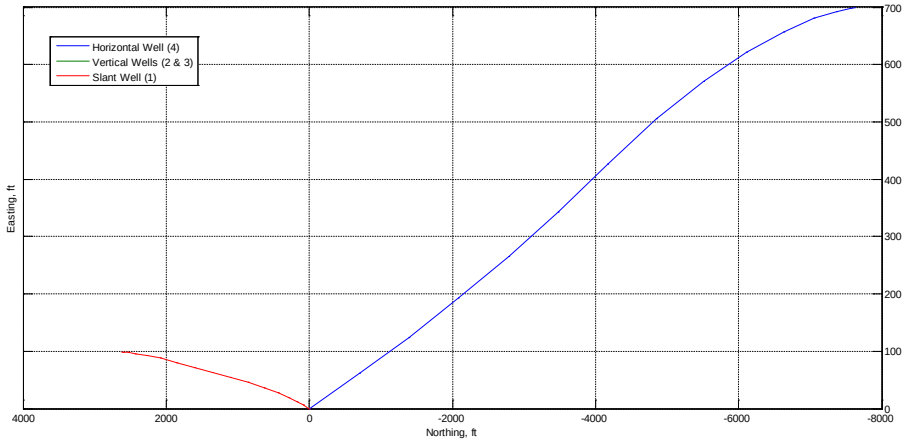

FIGURE 86 - WELL TRAJECTORIES HORIZONTAL SECTION

B.2 WELL 1

The set tubular for this well is shown in Figure 87. Further drilling will be performed with a 5" bit installed with 3x16 (1/32") jets. Drill pipe consists of >9,000 ft. of 4" 11.85 lbm/ft. and 3,500 ft of 3.5" 9.50 lbm/ft.

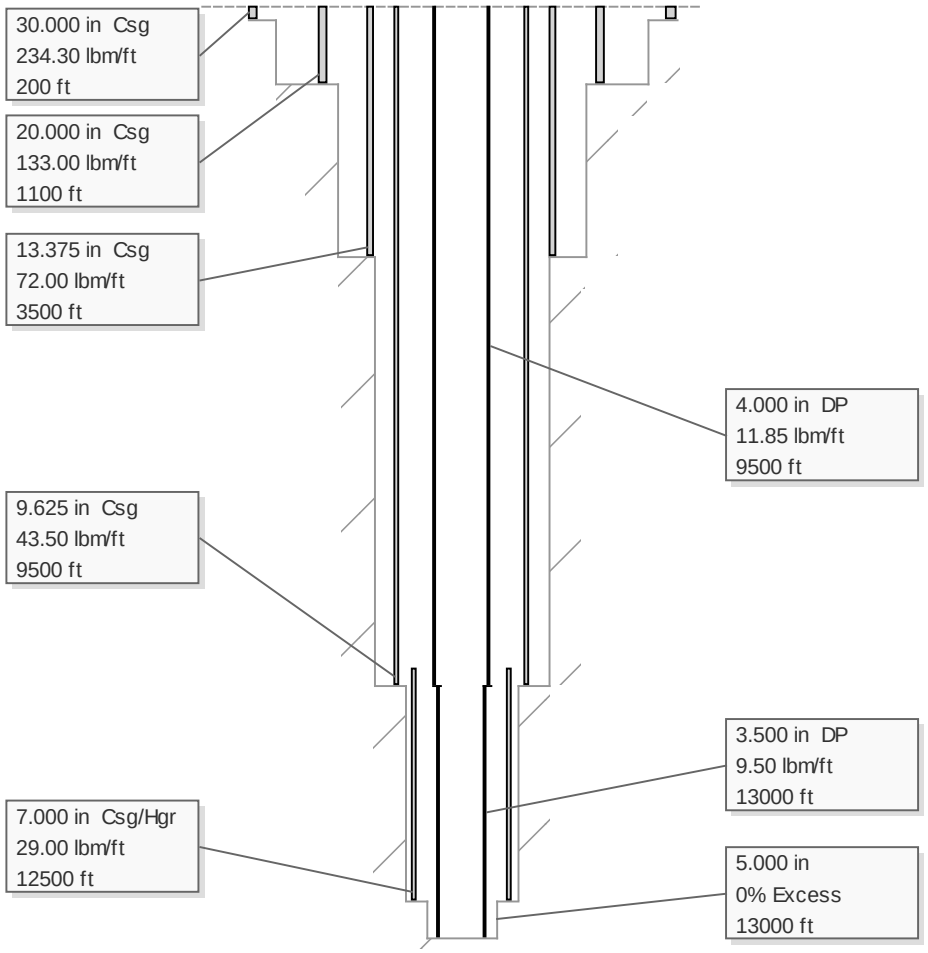

FIGURE 87 - TUBULAR FOR EXAMPLE WELL 1

This well has an S-shaped trajectory which is almost slant-formed. The well kicks off at 5,000 feet and builds angle with 1deg/100ft to 30 degrees inclination. This angle is the held for 2000 feet MD until the well drops angle down to 10 degrees with the same drop angle as in the build section. 10 degrees are then held until TD. The well in this example heads south and slightly towards west. This trajectory is presented with the survey data in Table 11.

TABLE 11 - SURVEY WELL 1

MD (feet)	Inclination (deg)	Azimuth (deg)
0	0	0
5000	0	0
8000	330	2
10000	330	2
12000	350	4
13000	350	4

B.3 WELL 2

The set tubular for this well is shown in Figure 88. Further drilling will be performed with a 7" bit installed with 3x16 (1/32") jets. Drill pipe consists of >8,952 ft. of 4" 11.85 lbm/ft. and 3,500 ft of 3.5" 9.50 lbm/ft.

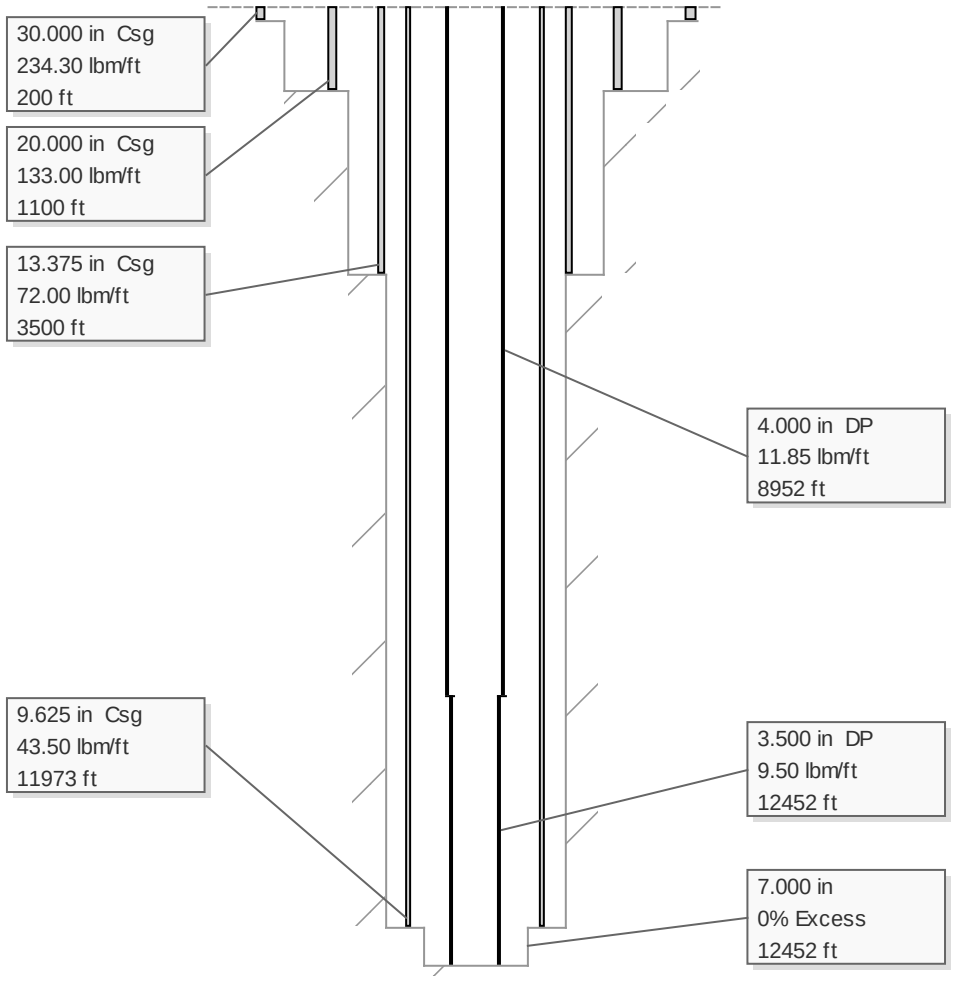

FIGURE 88 - TUBULAR FOR EXAMPLE WELL 2

This well is vertical, as shown in the survey data in Table 12.

TABLE 12 - SURVEY WELL 2

MD (feet)	Inclination (deg)	Azimuth (deg)
0	0	0
12452	0	0

B.4 WELL 3

The set tubular for this well is shown in Figure 89. Further drilling will be performed with a 5” bit (under-reamer) installed with 3x16 (1/32”) jets. Drill pipe consists of >12,452 ft. of 2.375” 6.65 lbm/ft.

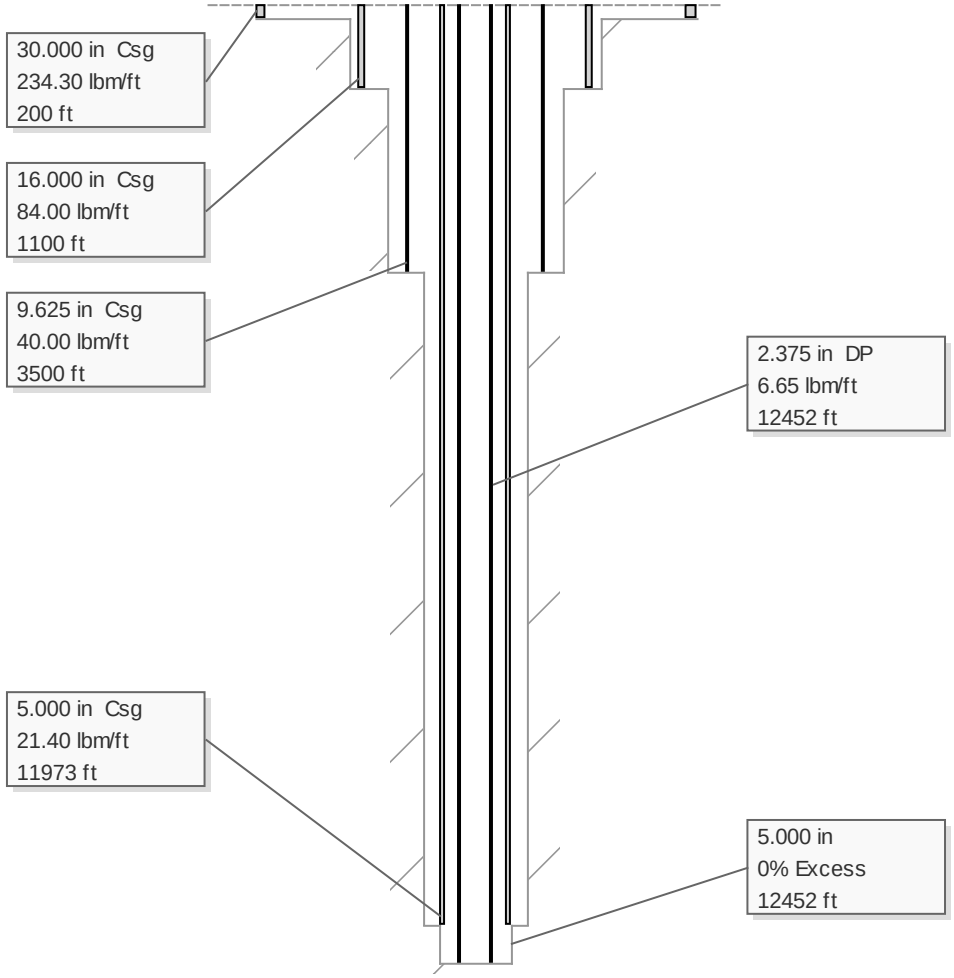

FIGURE 89 - TUBULAR FOR EXAMPLE WELL 3

This well is vertical, as shown in the survey data in Table 13.

TABLE 13 - SURVEY WELL 3

MD (feet)	Inclination (deg)	Azimuth (deg)
0	0	0
12452	0	0

B.5 WELL 4

The set tubular for this well is shown in Figure 90. Further drilling will be performed with a 5" bit installed with 3x16 (1/32") jets. Drill pipe consists of >9,200 ft. of 4" 11.85 lbm/ft. and 9,000 ft. of 3.5" 9.50 lbm/ft.

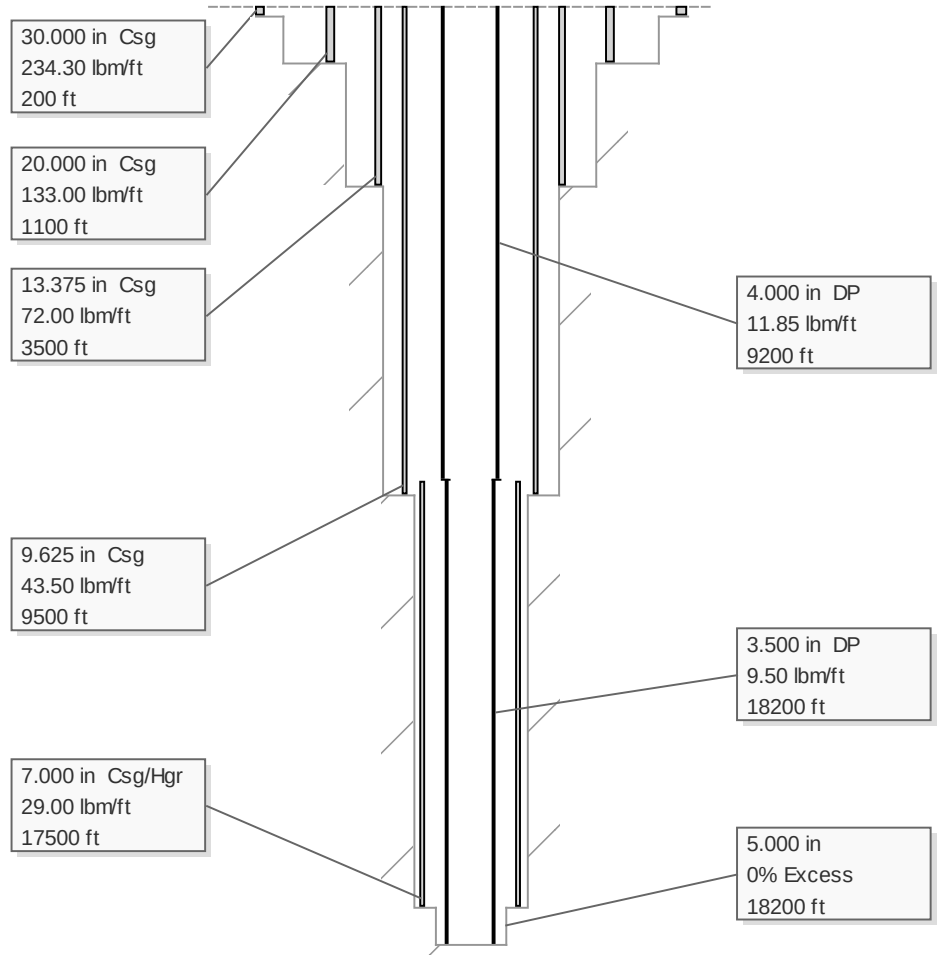

FIGURE 90 - TUBULAR FOR EXAMPLE WELL 4

This well is horizontal. The well kicks off at 8,400 feet and builds angle with over 5,000 ft. to 86 degrees inclination. The angle is further built to 87 degrees at 17,500 ft. and 90 degrees at 18,200 ft. reaching the vertical depth of 12,350 at TD of 18,200 ft. The well in this example heads north and slightly towards west. This trajectory is presented with the survey data in Table 14.

TABLE 14 - SURVEY WELL 4

MD (feet)	Inclination (deg)	Azimuth (deg)
0	0	0
8400	0	0
14000	86	352
17500	87	355
18200	90	355

APPENDIX C

This appendix includes simulation results for the wells defined in Appendix B. Drilling fluid used was pure 25 API oil mixed with methane for aerated systems, with 250 psi back-pressure applied. Beggs and Brill's model was used in the simulations. For foam systems the same back-pressure were used with 1.0 sg. liquid combined with nitrogen gas using Sanghani's model.

Each of the wells has first been simulated at the rates of; 4000, 6000, 8000, 10000, 12000, 14000 and 16000 stb/d for aerated systems with gas rates from 0 up to 75 MMscf/d. For foam systems were the liquid injection rates; 3, 5, 10, 20, 35, 50 and 75 gpm with for gas rates up to 300 scfpm. If these rates did not produce good operational envelopes the rates were adjusted until an UBD envelope was available.

For aerated systems one liquid rate was selected that produced a least on valid data-point in both the friction dominated and hydrostatic dominated flow regime for further simulation. The GLR at these liquid and gas rates were then manually calculated and the following simulations were performed:

- Back-pressure envelope at the hydrostatic dominated GLR constructed, using all liquid rates
- Back-pressure envelope at the friction dominated GLR constructed, using all liquid rates
- Gas quality evaluated for a range of gas rates, using selected liquid rate
- Pressure contributions evaluated for a range of gas rates, using selected liquid rate

For foam systems one valid data point in the hydrostatic dominated regime was selected and the following simulations performed:

- Back-pressure envelope at 95 % max surface gas quality, using all liquid rates
- Gas quality evaluated for a range of gas rates, using selected liquid rate
- Pressure contributions evaluated for a range of gas rates, using selected liquid rate

This makes a total of nine figures for each of the four base cases. In addition, sensitivity analyses were performed on the three selected rates for each of the wells. These results are presented in tabular form later in this appendix in section C.5. Further sensitivity analysis in the simulator (for aerated fluids) can be read in "Simulation of underbalanced drilling in MATLAB" (Leirkjær, 2013).

C.1 WELL 1

Standard rates for this well proved to provide good results and were therefore not adjusted.

The selected liquid rate in aerated simulations was set to 10,000 stb/d. This liquid rate provided hydrostatic dominated flow at a GLR of 800 scf/stb and frictional dominated flow at 4,500 scf/stb. Aerated simulation results are shown in Figure 91 through Figure 95.

The selected liquid rate in foam simulations was set 35 gpm. Foam simulation results are shown in Figure 96 through Figure 99.

C.1.1 AERATED

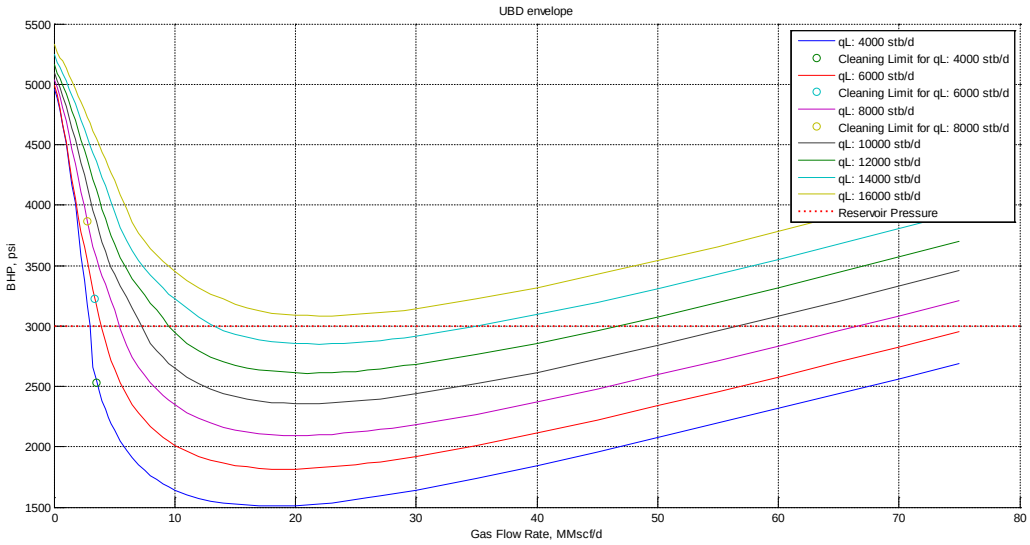

FIGURE 91 - UBD ENVELOPE FOR AERATED FLUID IN WELL 1 (STANDARD RATES)

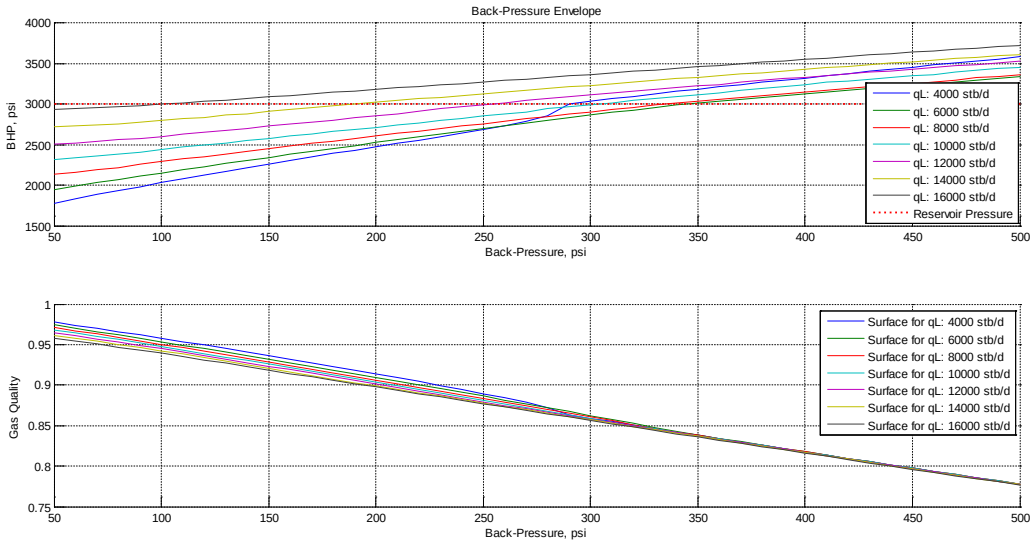

FIGURE 92 - BACK-PRESSURE ENVELOPE FOR AERATED FLUID AT GLR = 800 SCF/STB IN WELL 1

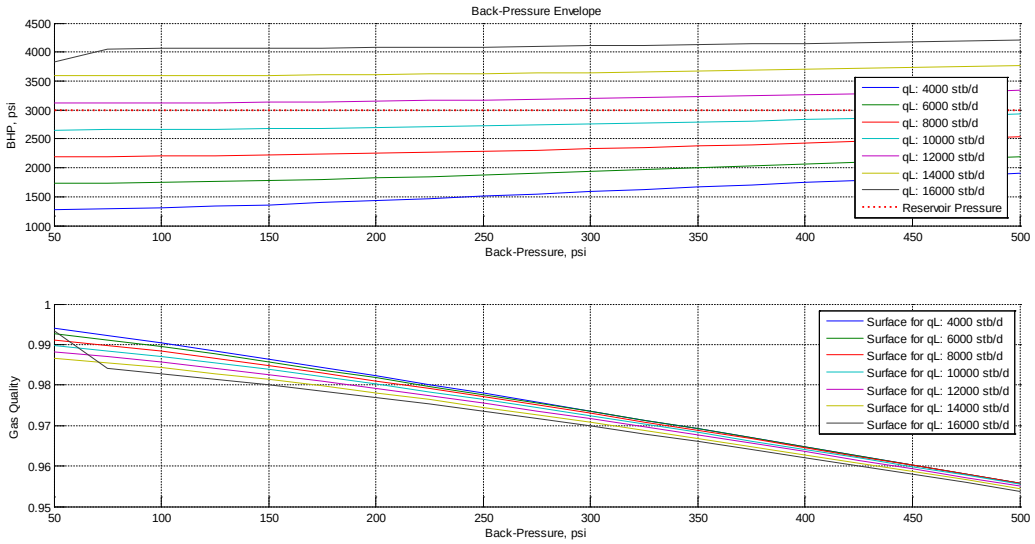

FIGURE 93 - BACK-PRESSURE ENVELOPE FOR AERATED FLUID AT GLR = 4,500 SCF/STB IN WELL 1

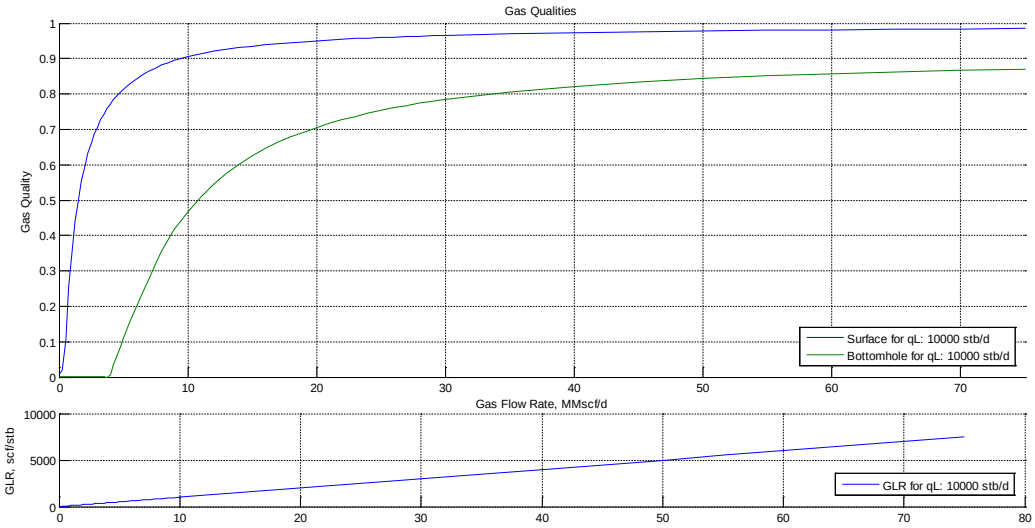

FIGURE 94 - GAS QUALITIES FOR AERATED FLUIDS AT 10,000 BBL/D IN WELL 1

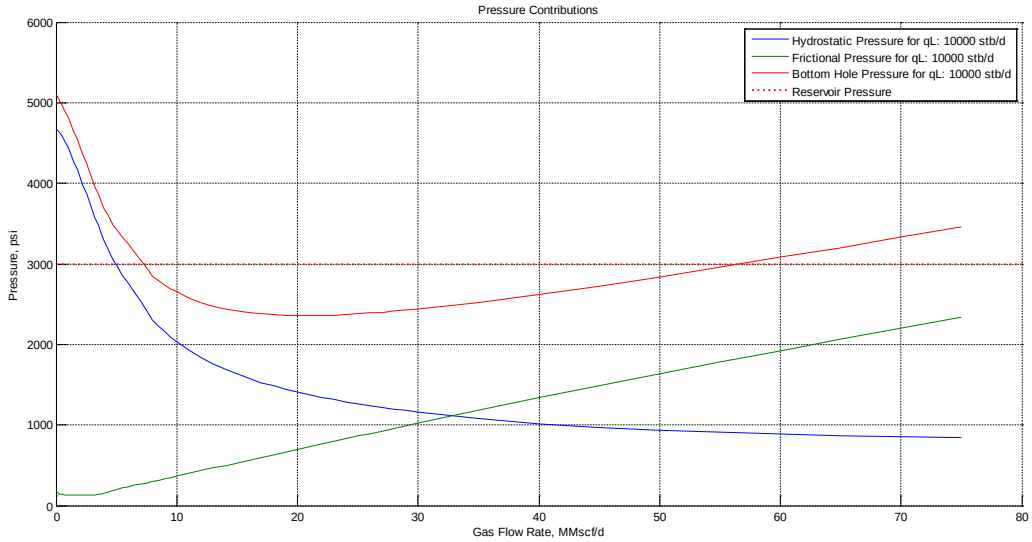

FIGURE 95 - PRESSURE CONTRIBUTIONS FOR AERATED FLUIDS AT 10,000 BBL/D IN WELL 1

C.1.2 FOAM

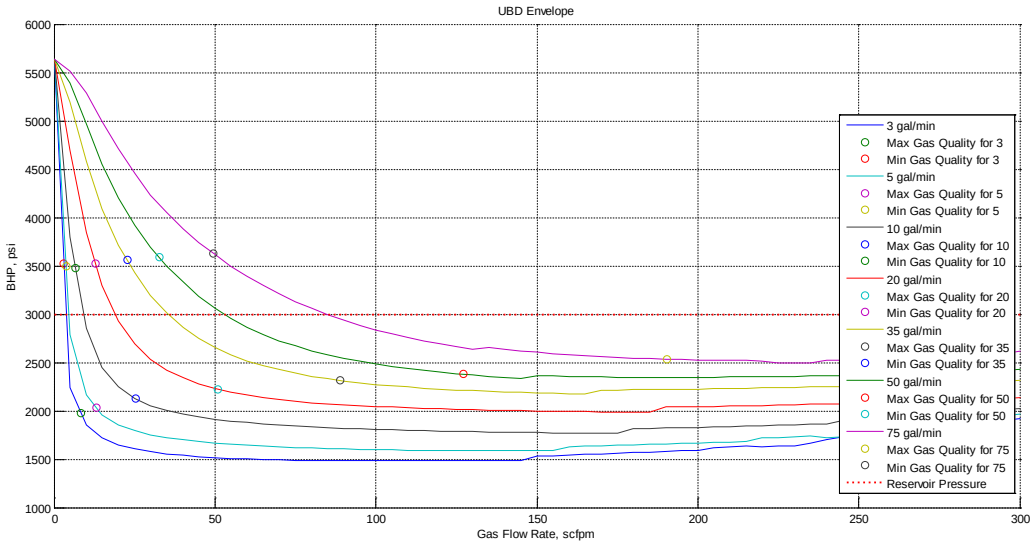

FIGURE 96 - UBD ENVELOPE FOR FOAM IN WELL 1 (STANDARD RATES)

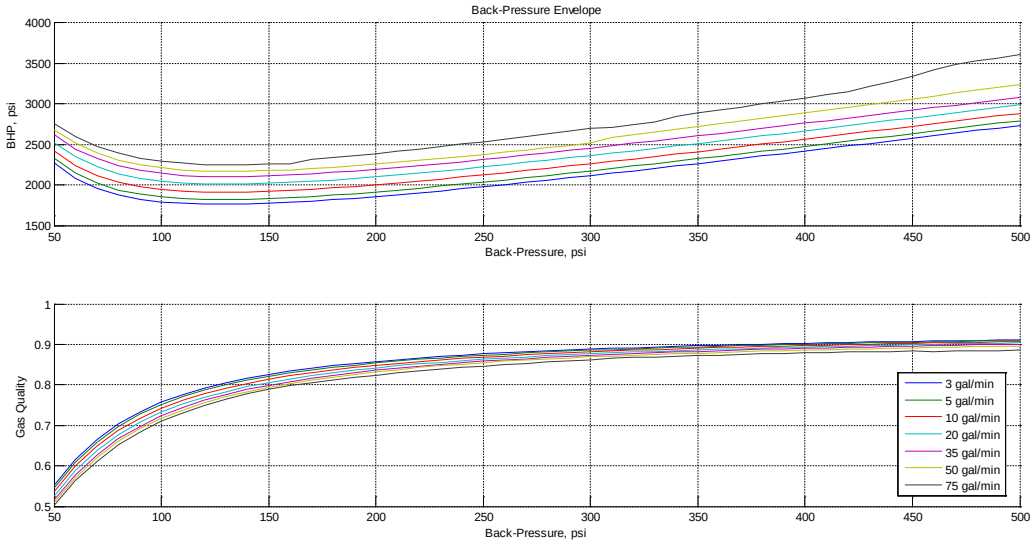

FIGURE 97 - BACK-PRESSURE ENVELOPE FOR FOAM AT 95% MAX GAS QUALITY IN WELL 1

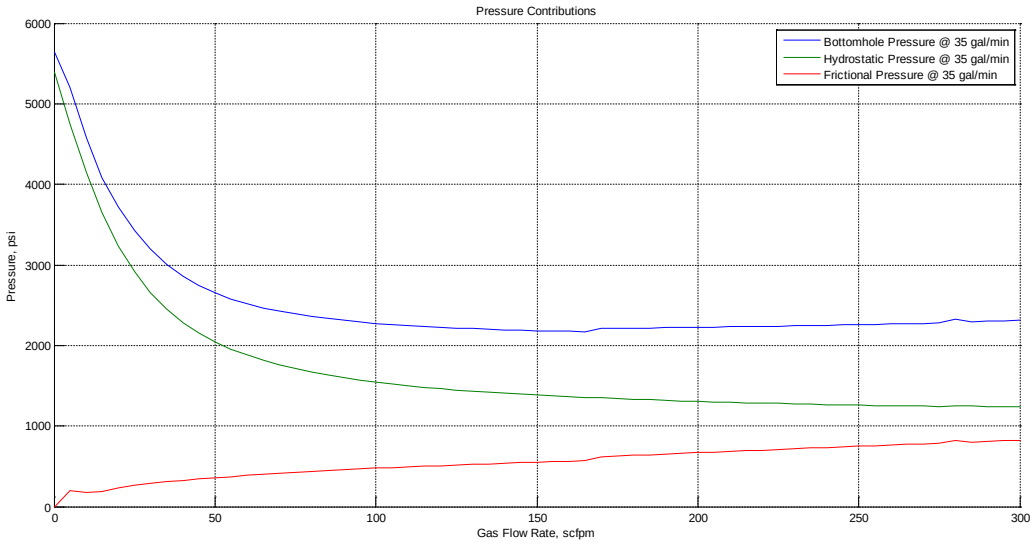

FIGURE 98 - PRESSURE CONTRIBUTIONS FOR FOAM AT 35 GPM IN WELL 1

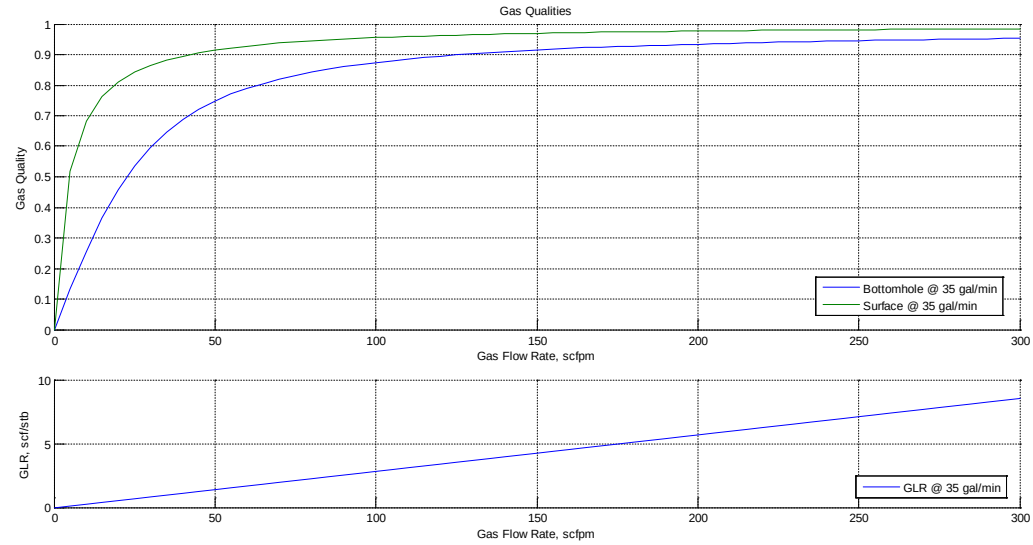

FIGURE 99 - GAS QUALITIES FOR FOAM AT 35 GPM IN WELL 1

C.2 WELL 2

Standard rates for this well provide too low BHP for aerated simulations (Figure 100), so the liquid rates were adjusted to; 14000, 16000, 18000, 20000, 22000, 24000 and 26000 stb/d. Foam rates provided good results and were not adjusted.

The selected liquid rate in aerated simulations was set to 20,000 stb/d. This liquid rate provided hydrostatic dominated flow at a GLR of 1,000 scf/stb and frictional dominated flow at 3,500 scf/stb. Aerated simulation results are shown in Figure 101 through Figure 105.

The selected liquid rate in foam simulations was set 35 gpm. Foam simulation results are shown in Figure 106 through Figure 109.

C.2.1 AERATED

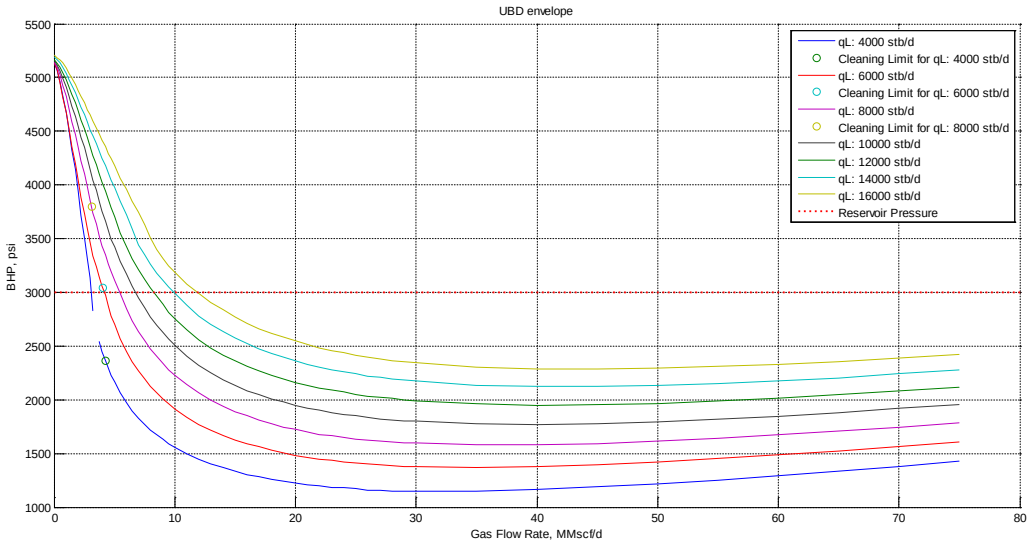

FIGURE 100 - UBD ENVELOPE FOR AERATED FLUID IN WELL 2 (STANDARD RATES)

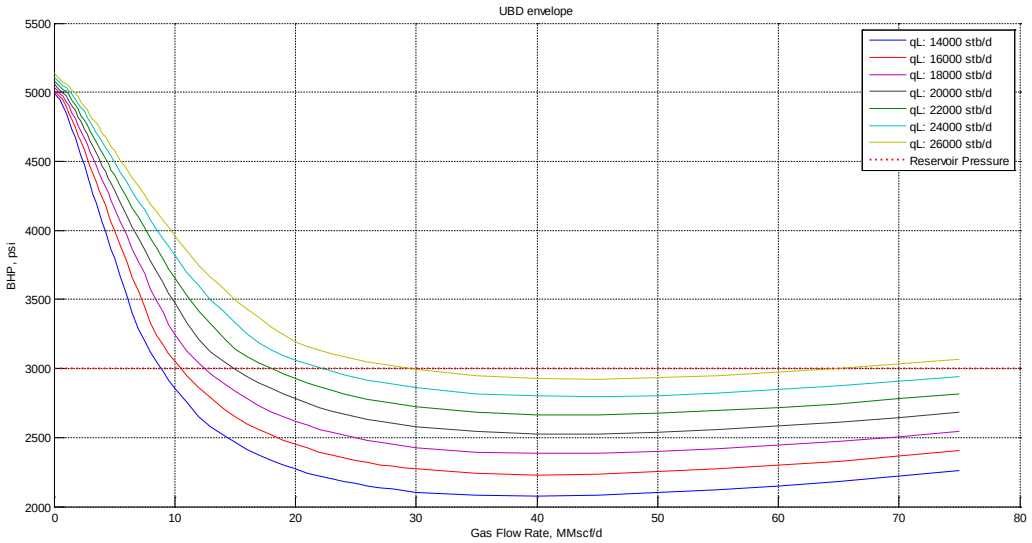

FIGURE 101 - UBD ENVELOPE FOR AERATED FLUID IN WELL 2 (ADJUSTED RATES)

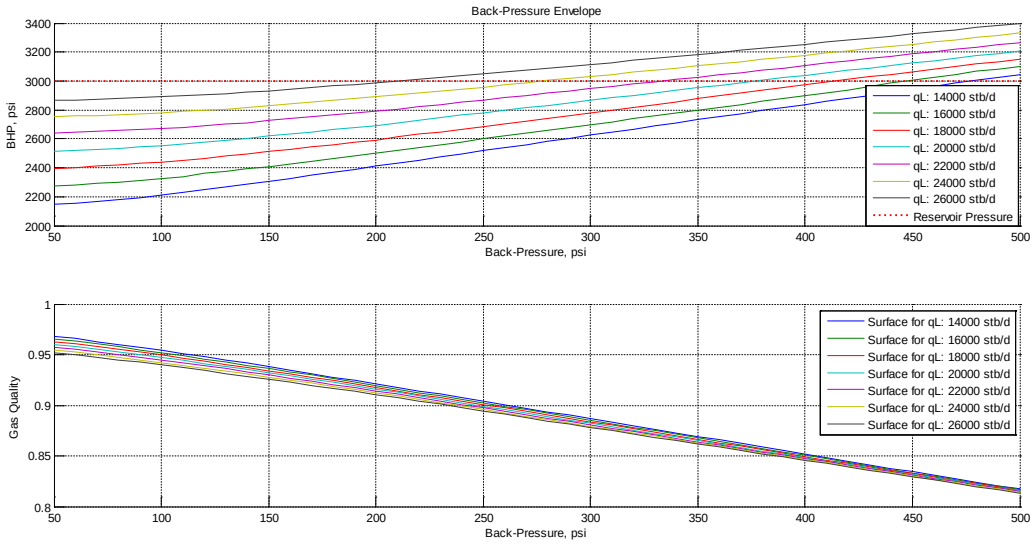

FIGURE 102 - BACK-PRESSURE ENVELOPE FOR AERATED FLUID AT GLR = 1,000 SCF/STB IN WELL 2

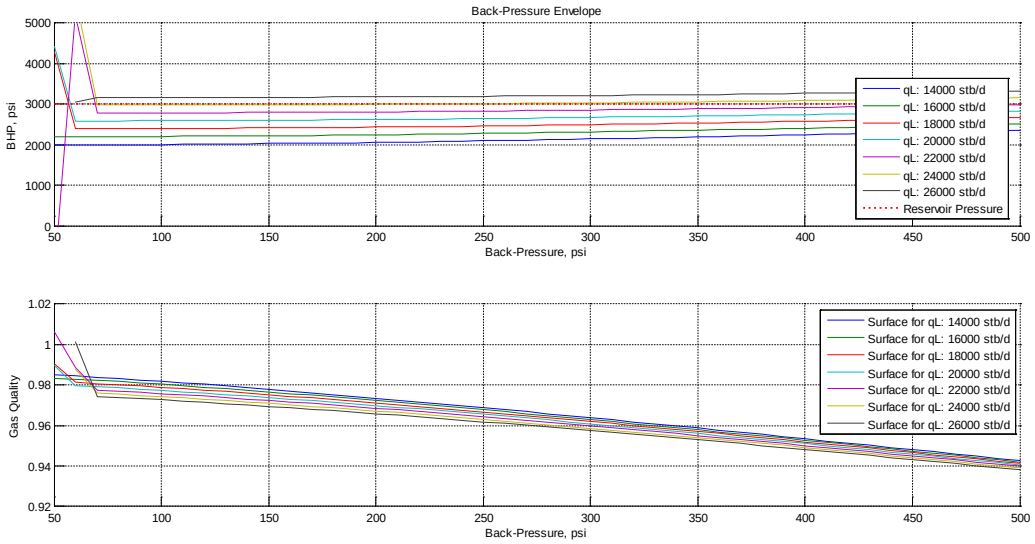

FIGURE 103 - BACK-PRESSURE ENVELOPE FOR AERATED FLUID AT GLR = 3,500 SCF/STB IN WELL 2

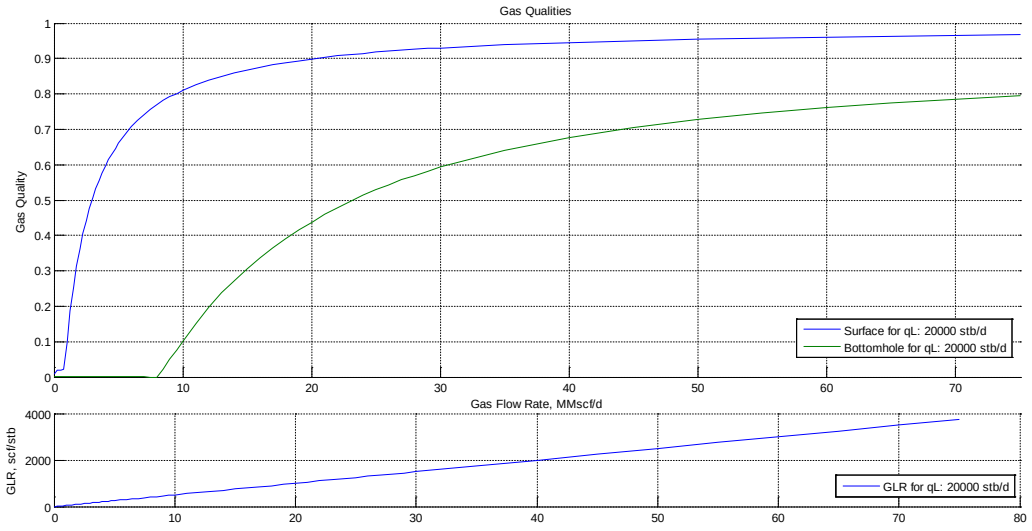

FIGURE 104 - GAS QUALITIES FOR AERATED FLUIDS AT 20,000 BBL/D IN WELL 2

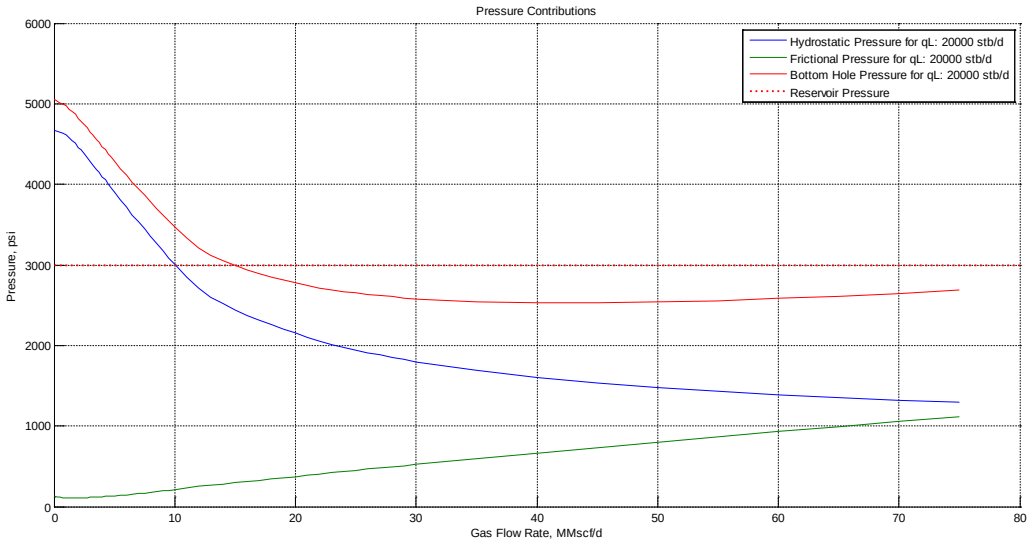

FIGURE 105 - PRESSURE CONTRIBUTIONS FOR AERATED FLUIDS AT 20,000 BBL/D IN WELL 2

C.2.2 FOAM

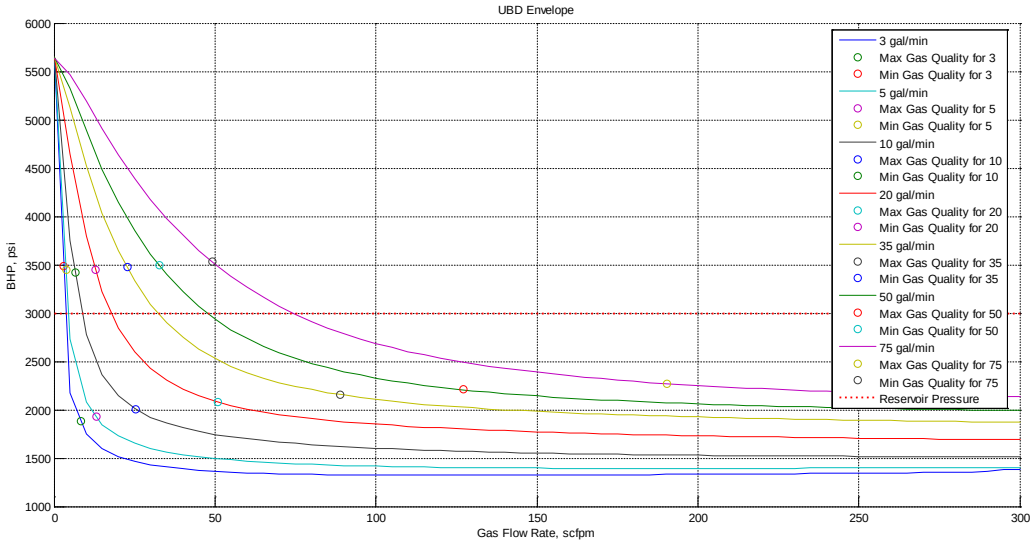

FIGURE 106 - UBD ENVELOPE FOR FOAM IN WELL 2 (STANDARD RATES)

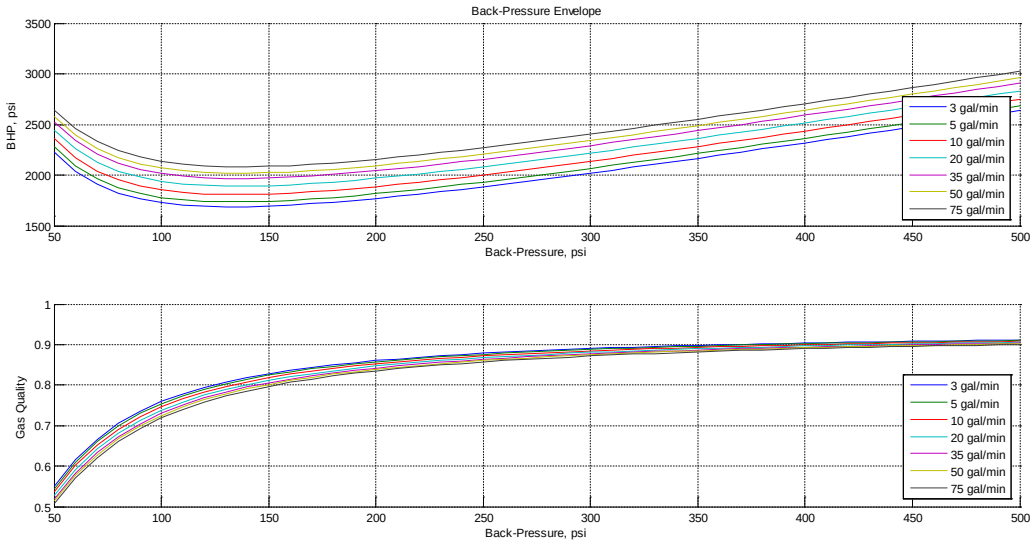

FIGURE 107 - BACK-PRESSURE ENVELOPE FOR FOAM AT 95% MAX GAS QUALITY IN WELL 2

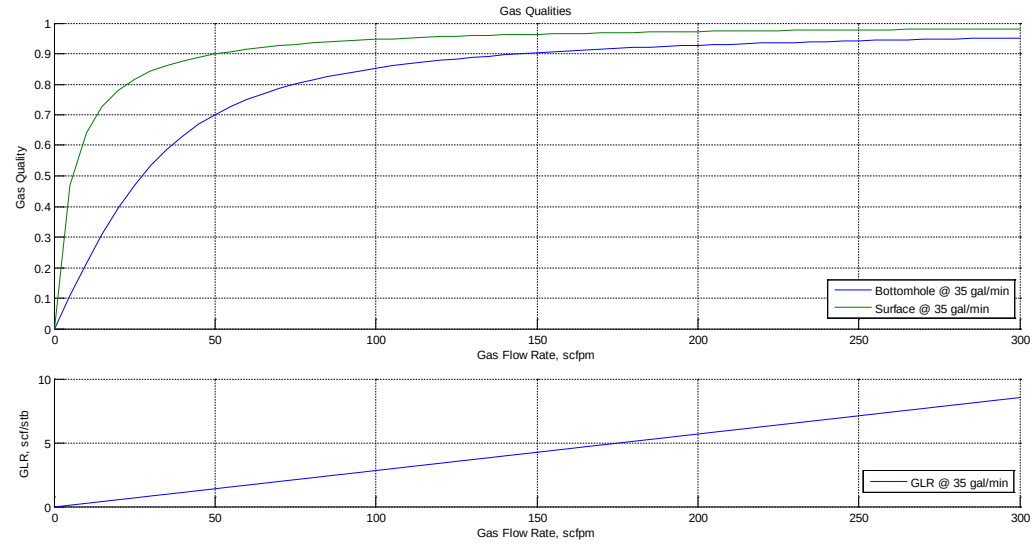

FIGURE 108 - GAS QUALITIES FOR FOAM AT 35 GPM IN WELL 2

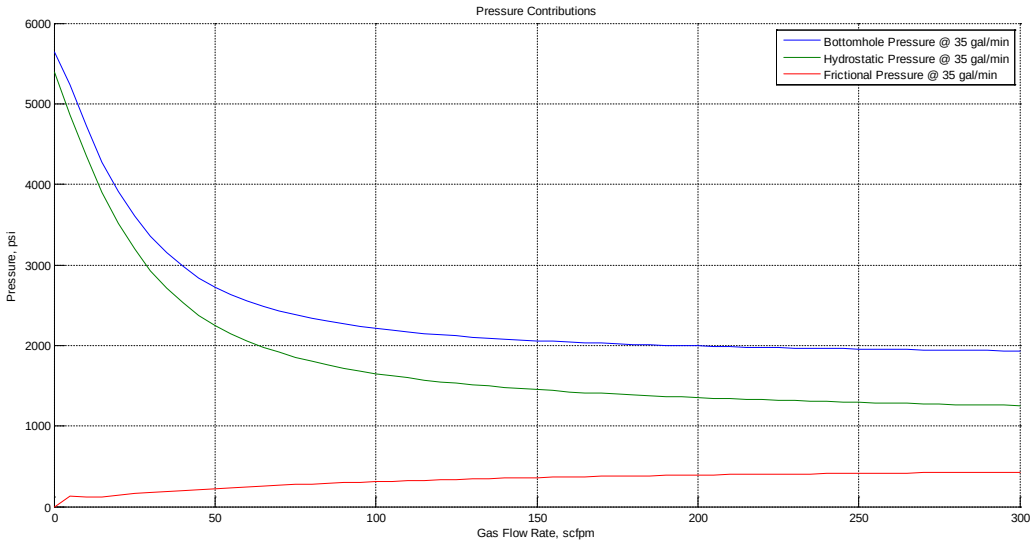

FIGURE 109 - PRESSURE CONTRIBUTIONS FOR FOAM AT 35 GPM IN WELL 2

C.3 WELL 3

Standard rates for this well provide too high BHP for aerated simulations (Figure 110), so the liquid rates were adjusted to; 700, 1000, 1300, 1600, 1900, 2200 and 2500 stb/d. Foam rates also provided too high pressures (Figure 116) and was adjusted to; 0.25, 0.50, 0.75, 1.00, 1.25, 1.50 and 1.75 gpm. These foam rates are very low and the drilling would most likely not be possible using a foam system. For simulation purposes is it still assume these rates are valid and provide proper hole-cleaning.

The selected liquid rate in aerated simulations was set to 1,600 stb/d. This liquid rate provided hydrostatic dominated flow at a GLR of 781.25 scf/stb and frictional dominated flow at 8,125 scf/stb. Aerated simulation results are shown in Figure 111 through Figure 115.

The selected liquid rate in foam simulations was set 1.00 gpm. Foam simulation results are shown in Figure 117 through Figure 120.

C.3.1 AERATED

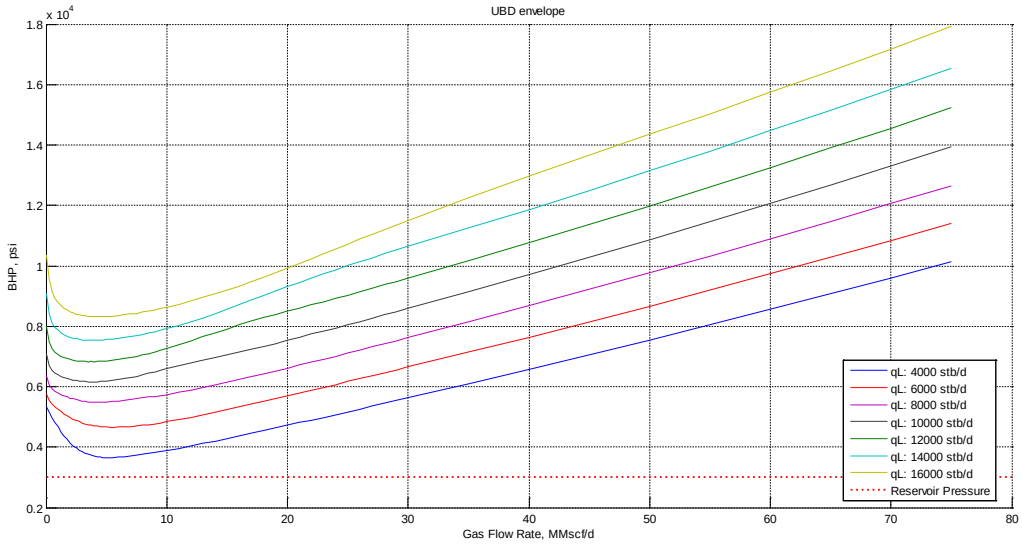

FIGURE 110 - UBD ENVELOPE FOR AERATED FLUID IN WELL 3 (STANDARD RATES)

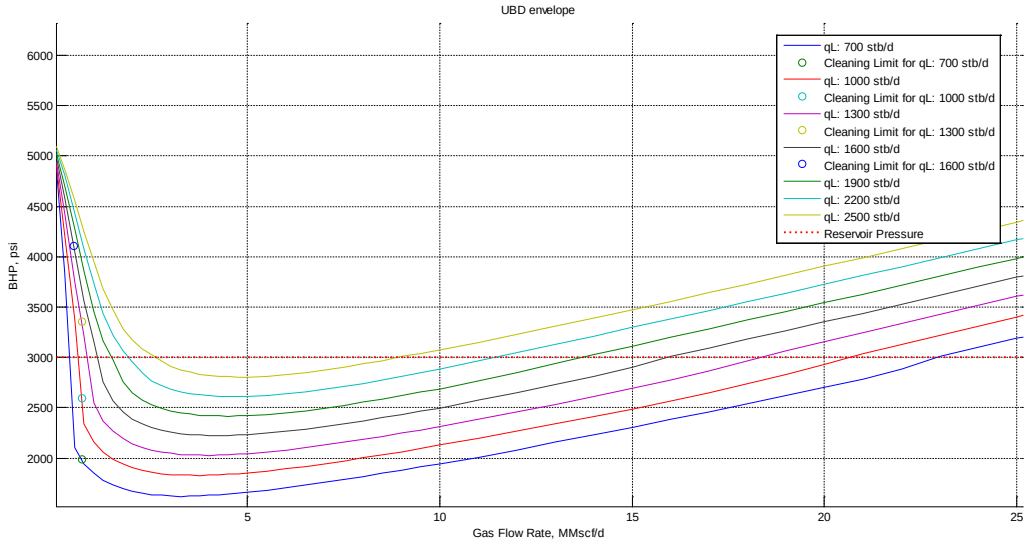

FIGURE 111 - UBD ENVELOPE FOR AERATED FLUID IN WELL 3 (ADJUSTED RATES)

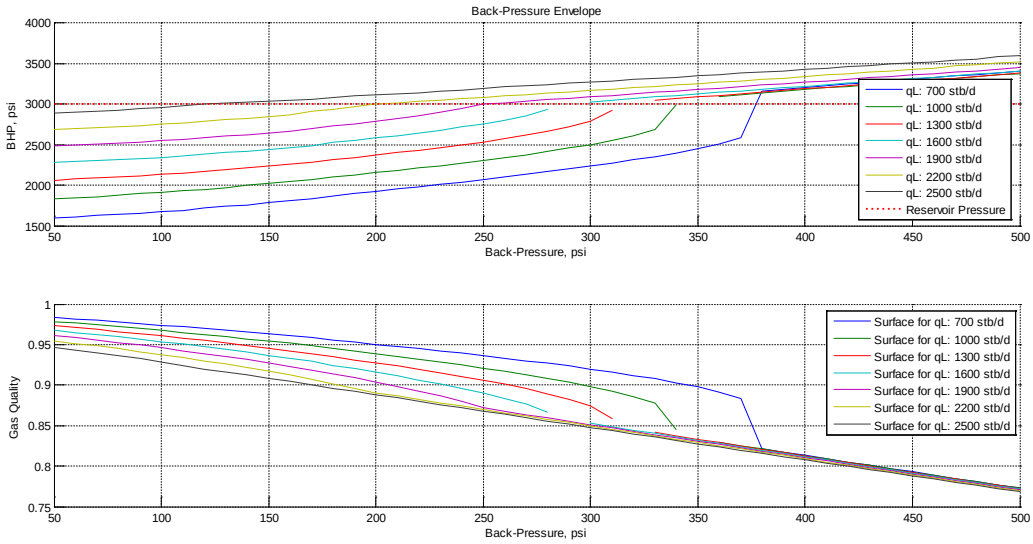

FIGURE 112 - BACK-PRESSURE ENVELOPE FOR AERATED FLUID AT GLR = 781.25 SCF/STB IN WELL 3

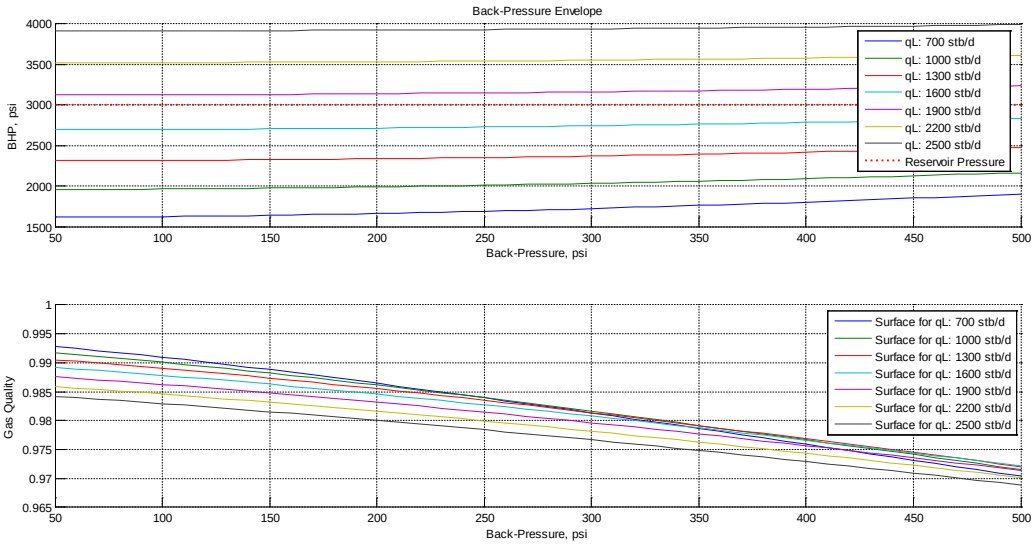

FIGURE 113 - BACK-PRESSURE ENVELOPE FOR AERATED FLUID AT GLR = 8,125 SCF/STB IN WELL 3

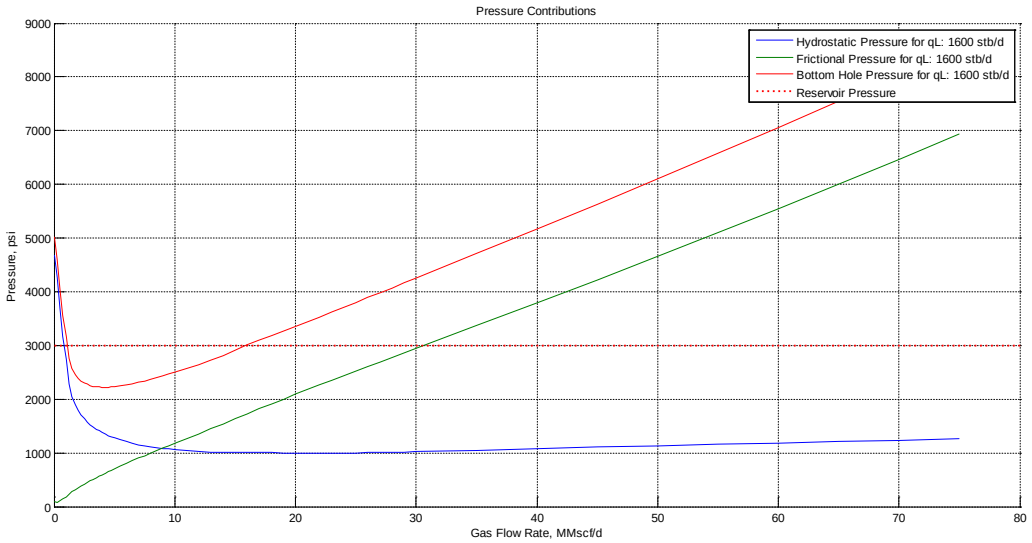

FIGURE 114 - PRESSURE CONTRIBUTIONS FOR AERATED FLUIDS AT 1,600 BBL/D IN WELL 3

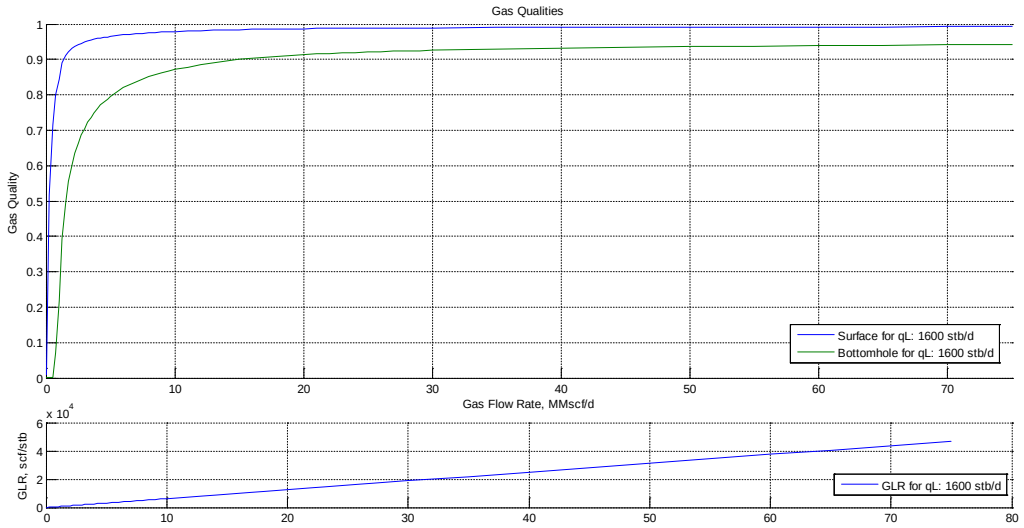

FIGURE 115 - GAS QUALITIES FOR AERATED FLUIDS AT 1,600 BBL/D IN WELL 3

C.3.2 FOAM

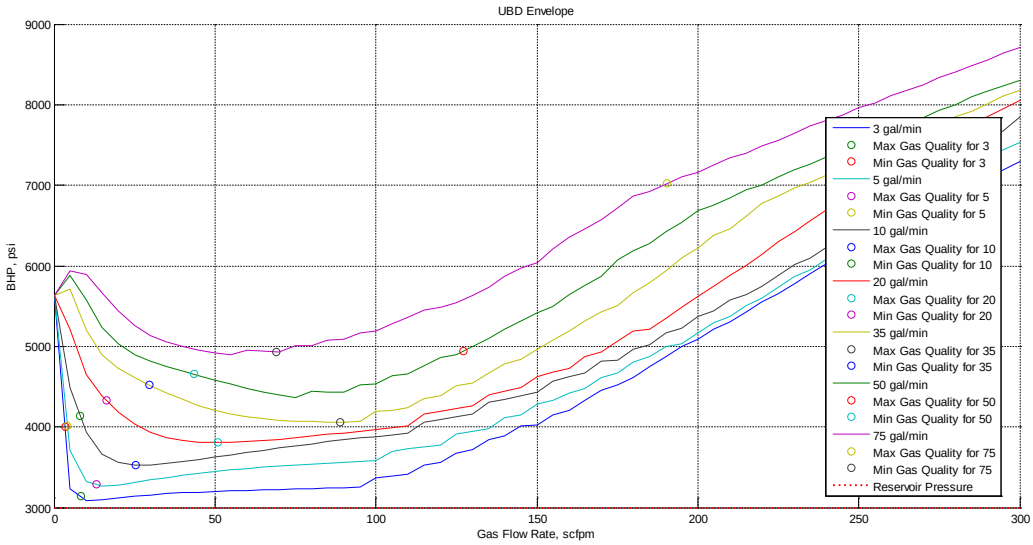

FIGURE 116 - UBD ENVELOPE FOR FOAM IN WELL 3 (STANDARD RATES)

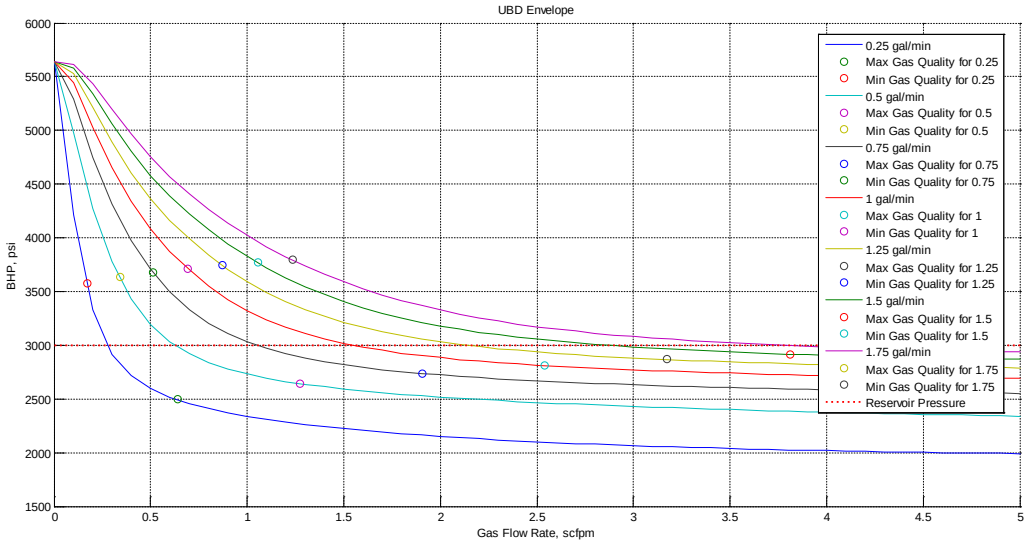

FIGURE 117 - UBD ENVELOPE FOR FOAM IN WELL 1 (ADJUSTED RATES)

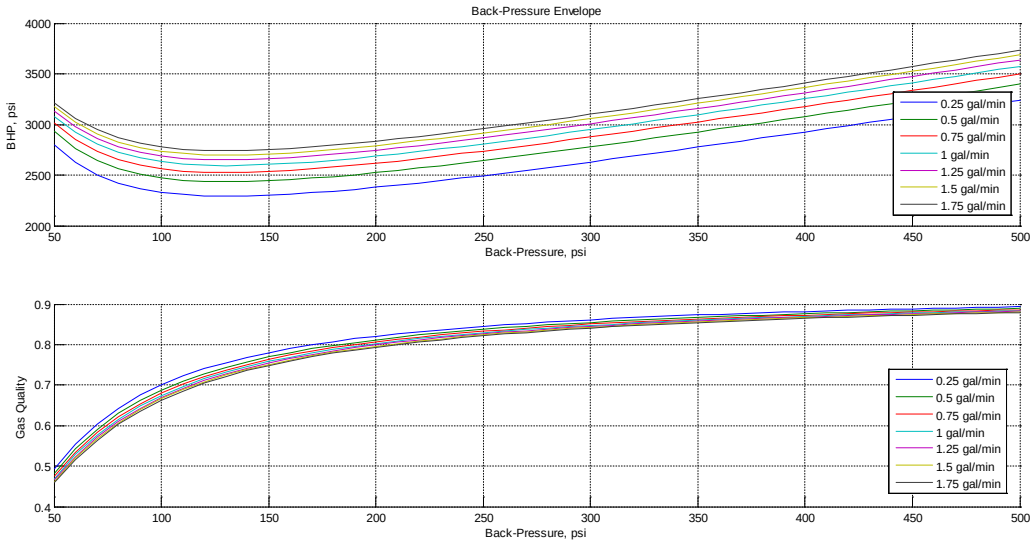

FIGURE 118 - BACK-PRESSURE ENVELOPE FOR FOAM AT 95% MAX GAS QUALITY IN WELL 3

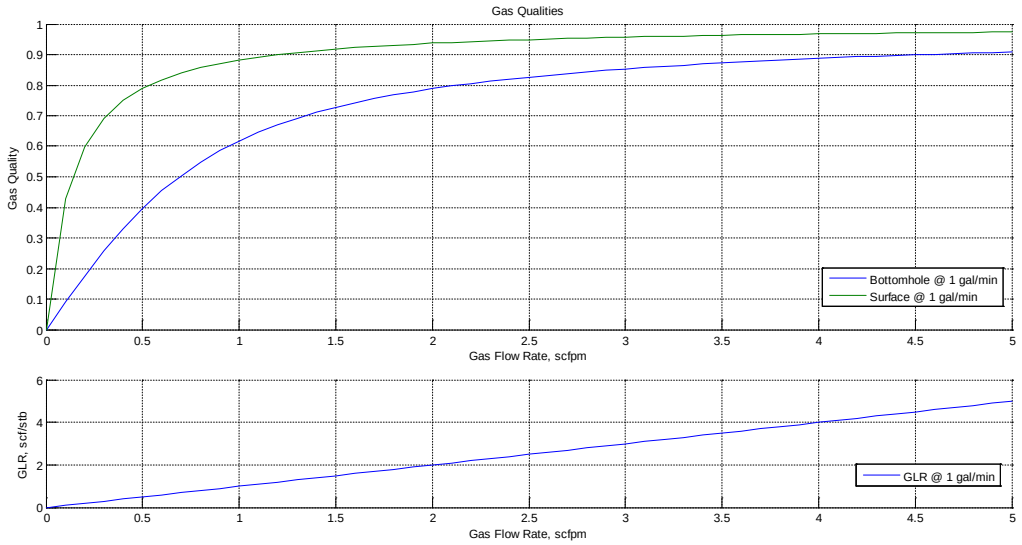

FIGURE 119 - GAS QUALITIES FOR FOAM AT 1.0 GPM IN WELL 3

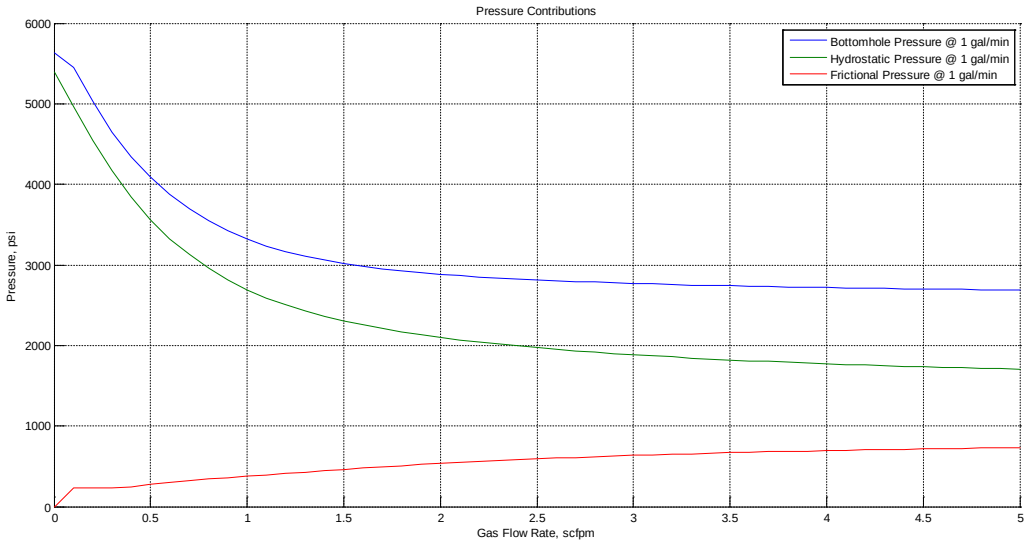

FIGURE 120 - PRESSURE CONTRIBUTIONS FOR FOAM AT 1.0 GPM IN WELL 3

C.4 WELL 4

Standard rates for this well proved to provide good results and were therefore not adjusted.

The selected liquid rate in aerated simulations was set to 8,000 stb/d. This liquid rate provided hydrostatic dominated flow at a GLR of 875 scf/stb and frictional dominated flow at 4,375 scf/stb. Aerated simulation results are shown in Figure 121 through Figure 125.

The selected liquid rate in foam simulations was set 35 gpm. Foam simulation results are shown in Figure 126 through Figure 129.

C.4.1 AERATED

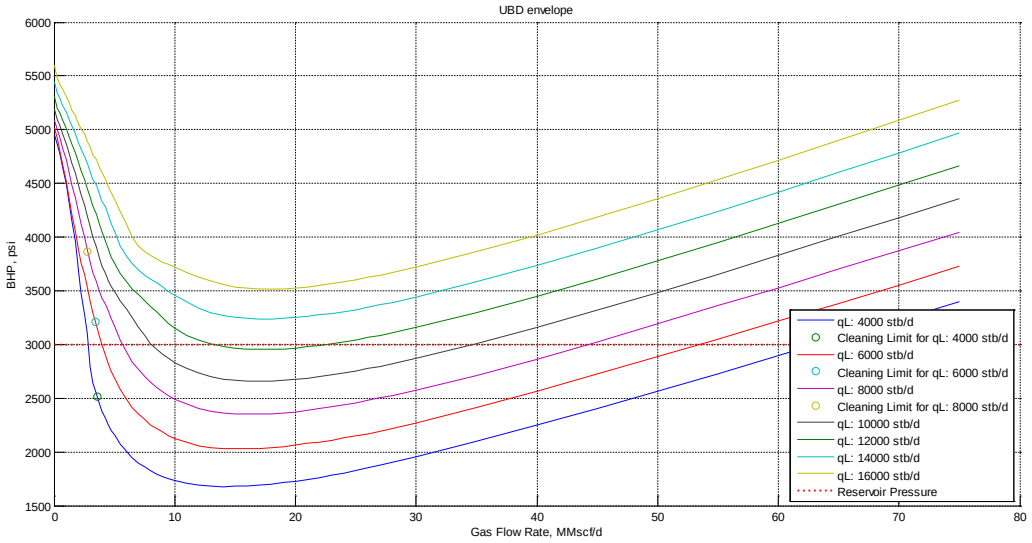

FIGURE 121 - UBD ENVELOPE FOR AERATED FLUID IN WELL 4 (STANDARD RATES)

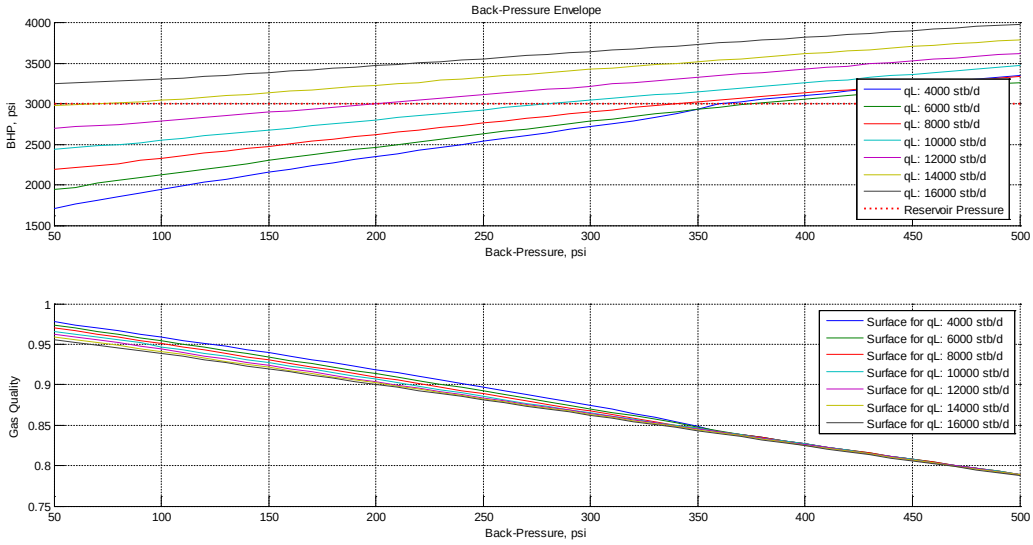

FIGURE 122 - BACK-PRESSURE ENVELOPE FOR AERATED FLUID AT GLR = 875 SCF/STB IN WELL 4

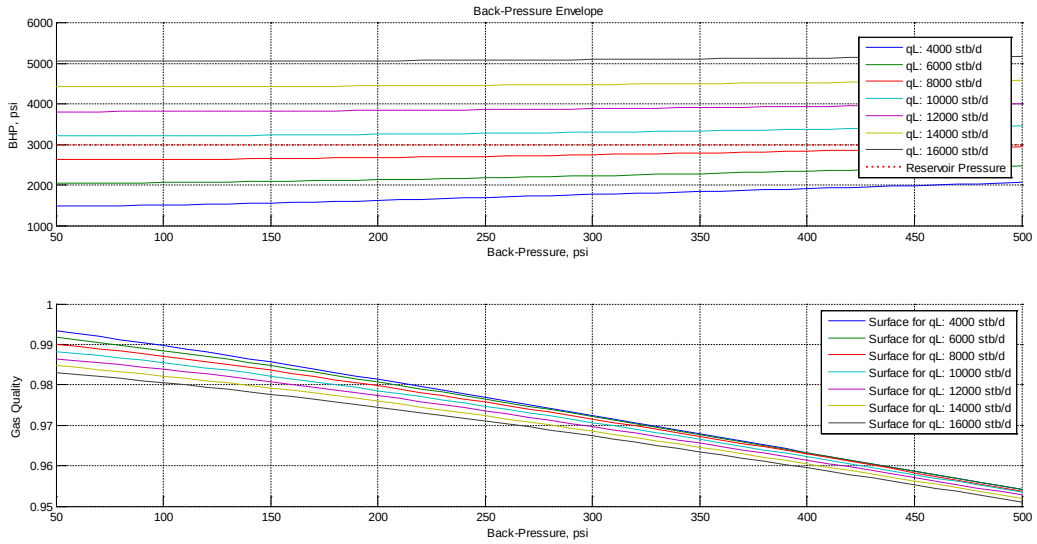

FIGURE 123 - BACK-PRESSURE ENVELOPE FOR AERATED FLUID AT GLR = 4,375 SCF/STB IN WELL 4

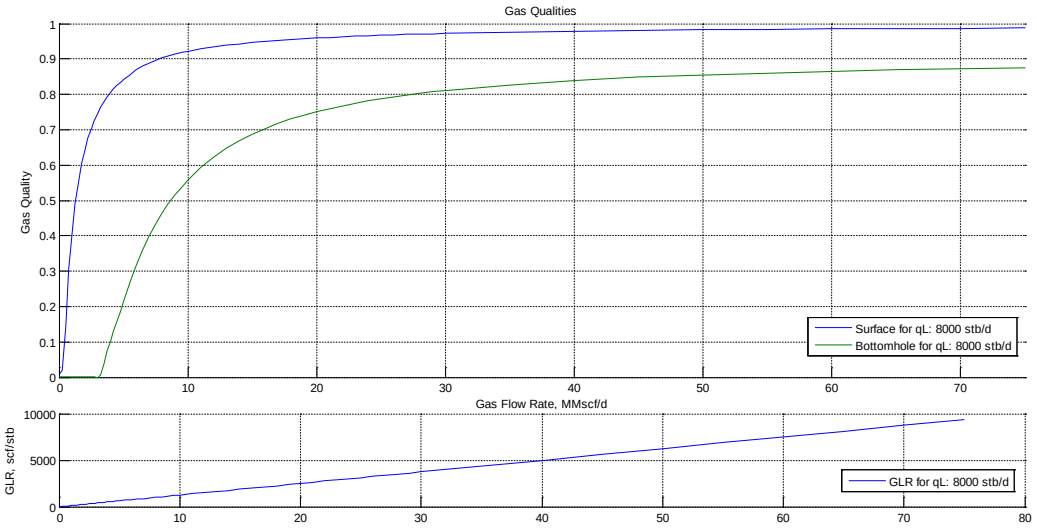

FIGURE 124 - GAS QUALITIES FOR AERATED FLUIDS AT 8,000 BBL/D IN WELL 4

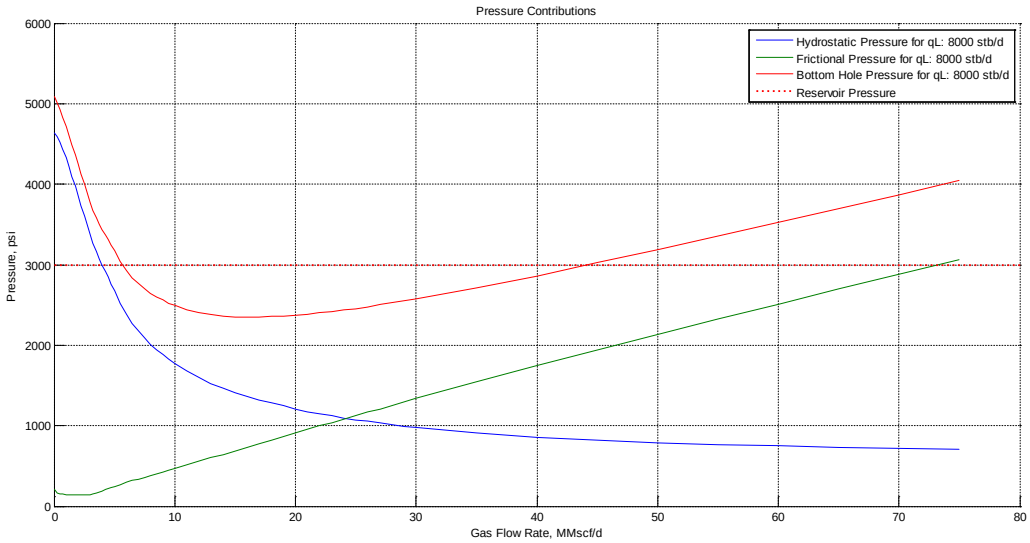

FIGURE 125 - PRESSURE CONTRIBUTIONS FOR AERATED FLUIDS AT 8,000 BBL/D IN WELL 4

C.4.2 FOAM

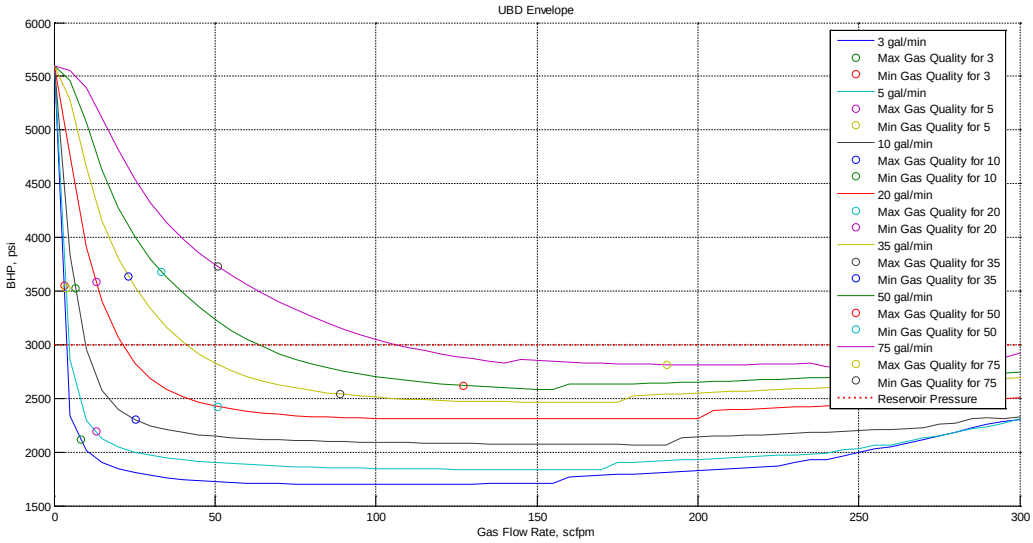

FIGURE 126 - UBD ENVELOPE FOR FOAM IN WELL 4 (STANDARD RATES)

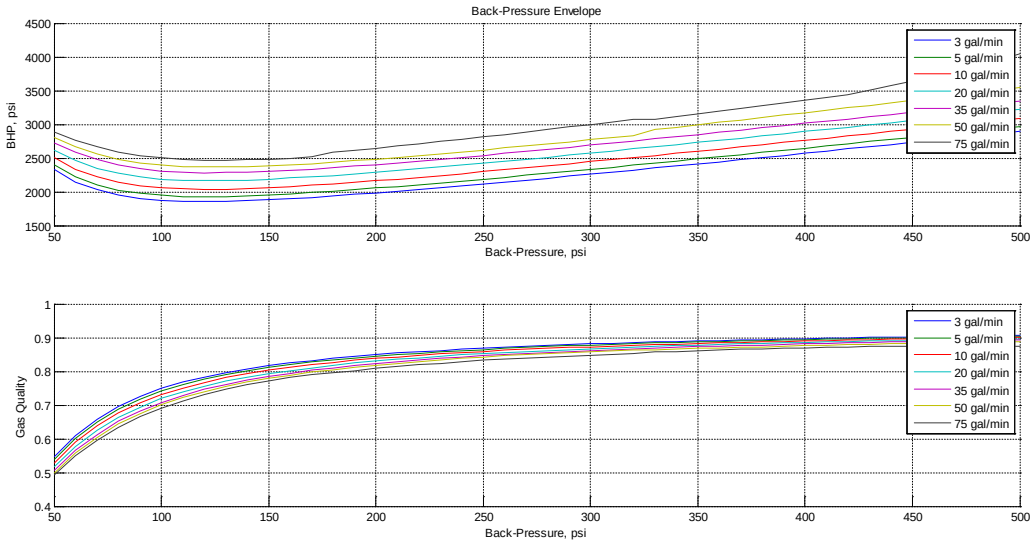

FIGURE 127 - BACK-PRESSURE ENVELOPE FOR FOAM AT 95% MAX GAS QUALITY IN WELL 4

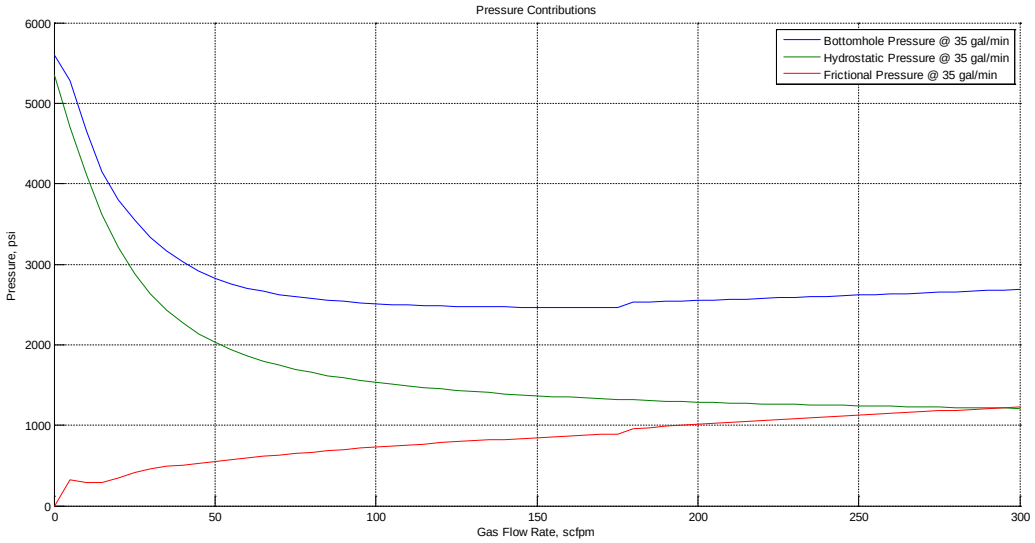

FIGURE 128 - PRESSURE CONTRIBUTIONS FOR FOAM AT 35 GPM IN WELL 4

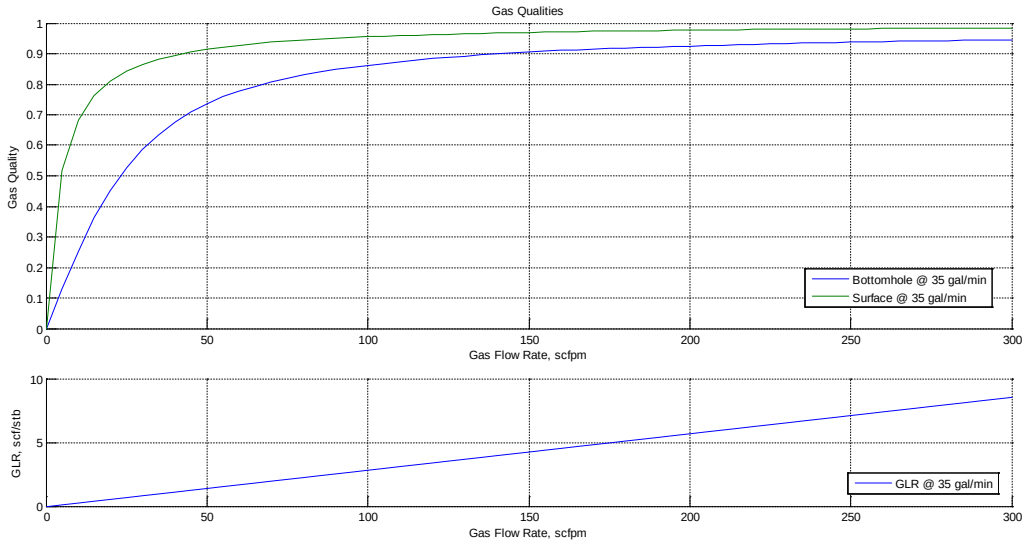

FIGURE 129 - GAS QUALITIES FOR FOAM AT 35 GPM IN WELL 4

C.5 COMBINED RESULTS

TABLE 15 - SENSITIVITY ANALYSIS FOAM

	Well 1 35 gpm	Well 2 35 gpm	Well 3 1.0 gpm	Well 4 35 gpm
Water Influx (bbl/hr)	BHP (psi)	BHP (psi)	BHP (psi)	BHP (psi)
0.00	2314.27	2140.08	2809.26	2539.49
5.00	2330.77	2153.10	3244.60	2560.42
10.00	2346.09	2165.18	3443.61	2579.88
20.00	2373.87	2187.07	3686.26	2615.19
40.00	2472.45	2224.12	3974.20	2736.08
80.00	2623.18	2281.51	5461.70	2883.71
160.00	3206.17	2375.58	9154.93	3819.51
320.00	4815.00	3289.46	15756.42	5827.15
Max Gas Quality	BHP (psi)	BHP (psi)	BHP (psi)	BHP (psi)
70%	4478.57	4420.70	4610.35	4549.23
75%	4170.58	4115.93	4338.44	4235.13
80%	3802.00	3732.12	4010.83	3882.09
85%	3352.22	3247.19	3609.88	3478.13

90%	2809.43	2680.49	3162.89	2972.86
95%	2314.27	2140.08	2809.26	2539.49
Liquid Density (s.g.)	BHP (psi)	BHP (psi)	BHP (psi)	BHP (psi)
0.70	2064.69	1882.61	2519.43	2301.74
0.80	2144.26	1964.79	2612.42	2377.39
0.90	2227.42	2050.58	2708.99	2456.60
1.00	2314.27	2140.08	2809.26	2539.49
1.10	2404.93	2233.42	2913.33	2626.17
1.20	2499.51	2330.71	3021.31	2716.76
Gas:	BHP (psi)	BHP (psi)	BHP (psi)	BHP (psi)
Nitrogen	2314.27	2140.08	2809.26	2539.49
Air	2378.80	2206.53	2883.40	2601.17

TABLE 16 - SENSITIVITY ANALYSIS FRICTION DOMINATED FLOW

Well:	**Well 1**	**Well 2**	**Well 3**	**Well 4**	**Well 1**	**Well 2**	**Well 3**	**Well 4**
Liquid Rate (bbl/d)	**10,000**	**20,000**	**1,600**	**8,000**	**10,000**	**20,000**	**1,600**	**8,000**
GLR (scf/bbl)	**4,500**	**3,500**	**8,125**	**4,375**	**4,500**	**3,500**	**8,125**	**4,375**
WC (%)	BHP (psi)	BHP (psi)	BHP (psi)	BHP (psi)	PDS (psi)	PDS (psi)	PDS (psi)	PDS (psi)
0	2723.91	2570	2728.11	2711	5709.24	13319.85	5511.58	5353.8
10	2728.7	2583.42	2726.95	2714.68	5691.81	13463.37	5488.7	5319.38
20	2732.08	2595.5	2726.23	2717.53	5677.28	13553.68	5458.63	5293.91
30	2733.76	2605.9	2723.53	2719.43	5658.81	13576.56	5424.44	5266.06
40	2733.35	2614.16	2715.65	2719.28	5635.88	13592.19	5389.6	5237.91
50	2730.68	2619.63	2708.35	2716.6	5608.05	13610.1	5345.7	5200.87
60	2725.51	2621.29	2699.36	2710.79	5574.62	13630.3	5301.56	5157.72
70	2713.35	2613.71	2686.43	2701.07	5533.76	13649.58	5250.22	5112.09
80	2698.09	2601.61	2678.19	2686.75	5485.52	13631.02	5187.59	5053.12
90	2677.11	2577.45	2675.33	2664.44	5427.91	13554.4	5123.52	4988.42
100	2667.4	2554.43	2681.02	2658.82	5363.34	13454.17	5051.06	4920.51
Oil Gravity (API)	BHP (psi)	BHP (psi)	BHP (psi)	BHP (psi)	PDS (psi)	PDS (psi)	PDS (psi)	PDS (psi)
5	3763.27	3864.55	4236.94	3680.08	7903.69	16663.54	8363.7	7403.36
10	3349.38	3330.48	3601.1	3297.44	6990.54	15336.74	7155.51	6572.07

15	3074.06	2991.51	3209.38	3039.93	6401.89	14481.41	6396.39	6023.32
20	2872.3	2744.41	2905.44	2850.36	5997.42	13861.01	5868	5636.56
25	2723.91	2570	2728.11	2711	5709.24	13319.85	5511.58	5353.8
30	2610.73	2435.49	2630.48	2606.01	5496.21	12801.75	5264.15	5136.11
35	2520.64	2329.45	2560.08	2518.09	5333.09	12312.37	5075.44	4963.63
40	2443.48	2236.57	2504.91	2446.92	5204.18	11858.23	4929.06	4824.64
45	2378.8	2161.45	2461.11	2385.23	5093.19	11399.14	4812.94	4708.59
50	2320.6	2091.96	2424.17	2329.59	4989.68	10945.25	4718.41	4602.5
55	2270.17	2034.68	2390.99	2281.17	4886.65	10516.19	4639.42	4505.92
60	2224.47	1983.6	2363.1	2237.15	4779.02	10210.8	4578.69	4397.81
65	2182.4	1937.52	2338.27	2196.49	4671.38	9997.55	4525.6	4281.33
70	2141.76	1895.53	2315.89	2158.37	4522.2	9774.48	4474.01	4161.93
Gas:	BHP (psi)	BHP (psi)	BHP (psi)	BHP (psi)	PDS (psi)	PDS (psi)	PDS (psi)	PDS (psi)
Nitrogen	3016.36	2934.79	3243.24	2959.68	7054.27	15727.13	6919.77	6513.73
Methane	2723.91	2570	2728.11	2711	5709.24	13319.85	5511.58	5353.8
Air	3041.65	2971.98	3286.31	2981.48	7043.41	15830.58	6896.4	6496.63
Drainage Radius (ft)	BHP (psi)	BHP (psi)	BHP (psi)	BHP (psi)	PDS (psi)	PDS (psi)	PDS (psi)	PDS (psi)
0	2723.11	2573.3	2751.24	2708.47	5709.01	13317.7	5520.51	5352.78
500	2724.43	2569.16	2729.42	2712.19	5709.39	13320.4	5512.08	5354.26
1000	2724.12	2569.62	2728.39	2711.49	5709.3	13320.1	5511.69	5354
1500	2723.99	2569.85	2728.16	2711.18	5709.26	13319.95	5511.6	5353.87
2000	2723.91	2570	2728.11	2711	5709.24	13319.85	5511.58	5353.8
2500	2723.86	2570.11	2728.12	2710.87	5709.22	13319.78	5511.59	5353.75
3000	2723.82	2570.19	2728.16	2710.77	5709.21	13319.73	5511.6	5353.71
3500	2723.79	2570.26	2728.21	2710.69	5709.2	13319.69	5511.62	5353.68
4000	2723.76	2570.31	2728.26	2710.63	5709.19	13319.65	5511.64	5353.65
4500	2723.74	2570.36	2728.31	2710.57	5709.19	13319.62	5511.66	5353.63
5000	2723.72	2570.4	2728.36	2710.53	5709.18	13319.59	5511.68	5353.61
Permeability (mD)	BHP (psi)	BHP (psi)	BHP (psi)	BHP (psi)	PDS (psi)	PDS (psi)	PDS (psi)	PDS (psi)
5	2723.42	2571.16	2730.83	2709.74	5709.1	13319.1	5512.65	5353.3
10	2724.28	2569.43	2728.89	2711.84	5709.34	13320.22	5511.88	5354.12
20	2727.35	2567.13	2748.35	2717.97	5710.22	13321.72	5519.39	5356.57
40	2737.32	2566.57	2797.44	2734.69	5713.12	13322.09	5538.59	5360.36
80	2761.81	2574.13	3078.69	2769.35	5720.31	13317.17	5650.54	5374.6
160	2810.12	2613.4	3621.88	2899.23	5735.12	13292.82	5900.74	5430.13
320	3140.66	2690.15	4733.18	3338.24	5854.57	13250.45	6515.43	5639.38

TABLE 17 - SENSITIVITY ANALYSIS HYDROSTATIC DOMINATED FLOW

Well:	Well 1	Well 2	Well 3	Well 4	Well 1	Well 2	Well 3	Well 4
Liquid Rate (bbl/d)	10,000	20,000	1,600	8,000	10,000	20,000	1,600	8,000
GLR (scf/bbl)	1,000	1,000	781.25	875	1,000	1,000	781.25	875
WC (%)	BHP (psi)	BHP (psi)	BHP (psi)	BHP (psi)	PDS (psi)	PDS (psi)	PDS (psi)	PDS (psi)
0	2851.4	2745.48	2758.53	2765.75	1662.95	4634.55	1231.27	1626.48
10	2910.06	2779.16	2899.15	2819.92	1679.8	4796.33	1262.06	1650.74
20	2966.34	2812.3	3033.98	2873.21	1696.76	4953.46	1295.96	1675.46
30	3017.82	2844.73	3080.38	2930.45	1711.26	5095.92	1299.06	1692.94
40	3063.15	2876.25	3125.05	2987.43	1721.78	5203.4	1299.84	1715.97
50	3109.96	2906.54	3168.16	3035.3	1731	5254.51	1297.78	1730.21
60	3155.61	2937.26	3209.66	3079.37	1737	5286.21	1295.42	1739.31
70	3199.54	2967.51	3249.15	3121.87	1736.86	5313.54	1288.1	1751.34
80	3241.28	2993.9	3285.76	3162.42	1732.04	5332.67	1273.53	1748.54
90	3279.69	3011.13	3317.24	3200.05	1724.36	5338.43	1250.26	1751.21
100	3310.17	3006.61	3334.47	3231.09	1691.5	5321.21	1199.9	1728.85
Oil Gravity (API)	BHP (psi)	BHP (psi)	BHP (psi)	BHP (psi)	PDS (psi)	PDS (psi)	PDS (psi)	PDS (psi)
5	3717.55	3925.02	4062.06	3599.33	3325.22	8010.62	2997.96	3101.37
10	3378.15	3421.65	3587.58	3287.1	2575.51	6744.41	2152.99	2451.09
15	3160.65	3123.11	3283.52	3081.46	2146.46	5865.17	1693.69	2073.8
20	3000.12	2909.01	3081.59	2909.56	1869.68	5192.5	1461.65	1817
25	2851.4	2745.48	2758.53	2765.75	1662.95	4634.55	1231.27	1626.48
30	2734.61	2618.32	2596.34	2651.88	1503.8	4142.5	1089.58	1485.53
35	2649.72	2515.02	2496.27	2558.02	1374.88	3685.41	989.45	1366.7
40	2580.76	2434.55	2422.05	2479.13	1260.07	3251.32	908.31	1253.93
45	2534.65	2367.83	2363.19	2412.3	1155.14	2869.81	838.89	1147.41
50	2497.82	2307.98	2314.86	2357.62	1043.27	2632.97	776.32	1039.24
55	2470.4	2259.29	2274.45	2327.51	928.13	2496.13	712.37	919.64
60	2439.25	2222.22	2240.31	2299.74	827	2364.74	647.54	806.43
65	2435.3	2204.64	2211.4	2291.27	751.01	2240.1	583.57	729.49
70	2458.96	2238.6	2186.99	2282.79	689.09	2177.33	527.32	663.86
Gas:	BHP (psi)	BHP (psi)	BHP (psi)	BHP (psi)	PDS (psi)	PDS (psi)	PDS (psi)	PDS (psi)
Nitrogen	3254.86	3086.09	3332.16	3158.31	1563.06	4335.07	1236.95	1555.78
Methane	2851.4	2745.48	2758.53	2765.75	1662.95	4634.55	1231.27	1626.48
Air	3280.26	3117.88	3373.44	3198.74	1531.55	4391.97	1223.23	1521.99

Drainage Radius (ft)	BHP (psi)	BHP (psi)	BHP (psi)	BHP (psi)	PDS (psi)	PDS (psi)	PDS (psi)	PDS (psi)
0	2871.91	2757.23	2932.34	2800.02	1671.24	4637.75	1283.97	1641.25
500	2844.12	2741.53	2666.07	2753.95	1660.02	4633.48	1202.77	1621.43
1000	2848.3	2743.79	2717.29	2760.71	1661.7	4634.09	1217.23	1624.32
1500	2850.22	2744.84	2742.64	2763.82	1662.47	4634.37	1225.82	1625.65
2000	2851.4	2745.48	2758.53	2765.75	1662.95	4634.55	1231.27	1626.48
2500	2852.23	2745.94	2769.73	2767.11	1663.28	4634.67	1235.19	1627.06
3000	2852.87	2746.29	2778.15	2768.15	1663.54	4634.77	1235.2	1627.5
3500	2853.37	2746.57	2784.81	2768.97	1663.74	4634.84	1237.5	1627.86
4000	2853.79	2746.8	2790.25	2769.66	1663.91	4634.91	1239.39	1628.15
4500	2854.14	2746.99	2794.81	2770.23	1664.05	4634.96	1240.97	1628.4
5000	2854.44	2747.16	2798.73	2770.73	1664.17	4635	1242.34	1628.61
Permeability (mD)	BHP (psi)	BHP (psi)	BHP (psi)	BHP (psi)	PDS (psi)	PDS (psi)	PDS (psi)	PDS (psi)
5	2859.99	2750.12	2862.95	2779.95	1666.41	4635.81	1262.02	1632.57
10	2846.21	2742.85	2687.73	2757.31	1660.86	4633.84	1209.96	1622.87
20	2811.98	2727.95	2475.32	2705.3	1647.15	4629.82	1149.34	1609.47
40	2717.21	2697.52	2485.8	2597.79	1610.01	4621.73	1152.52	1572.89
80	2556.72	2636.33	2461.42	2502.82	1550.6	4605.97	1147.2	1534.79
160	2530.05	2575.05	2465.67	2550.53	1541.15	4590.11	1146.43	1553.74
320	2517.18	2593.23	2510.73	2535.29	1536.64	4594.75	1160.16	1547.64

C.6 Simulation Results Aerated Correaltions

In this section are some simulation-results (BHP) for example well 1 presented for a range of various inputs.

TABLE 18 - BASE CASE PARAMETERS

Parameter	Value:
Oil Density:	25 API
Gas:	Methane
WC:	0 %
Segment length:	500 feet
Liquid Rates:	4,000 – 16,000 bbl/day (2,000 bbl/day spacing)
Gas Rates:	0 – 60 MMscf/day (varying spacing, 12 values)
Simulation Depth:	12,500 feet (inside casing)
Reservoir Inflow:	0

This base case was run in ten different variations:

- Original Case
- Injected oil API gravity changed to 8, 15 and 40
- Injected gas phase changed to air and nitrogen
- Water fraction in injected liquid phase changed to 10%, 25%, 50% and 75%.

These ten variations were simulated for all eight aerated fluid correlations producing a total of 80 UBD envelopes (presented in tabular forms in this appendix) each holding 84 data points for the BHP. Some of this data have further been used to produce a range of simulation. The 6,720 data points have also been used as a guide-line towards setting limits when performing simulations presented in other appendices. To limit the length of this thesis itself, only this base case is presented in a tabular form.

The simulation results presented in this appendix have been simulated using an Intel® Atom™ CPU Z2760 1.80GHz processor with 2.00GB of RAM available. Approximate time to perform all simulation presented in this appendix has been estimated between five and eight hours, including manual changing of input parameters.

The results shown in the following figures only include the BHP, at the simulation depth of 12,500 feet. The values have been color coded to give a graphical representation of how the BHP changes with various rates and correlations. The color coding can also be used to find the transition from hydrostatic to friction dominated pressure regimes.

Tables are read the following way:

- Liquid rates in bbl/d in the top row
- Gas rates in MMscf/d in the left column
- BHP values in psi in main tabular
- Correlations used in top-left corner using the following abbreviation:

TABLE 19 - AERATED FLUID CORRELATIONS ABBREVATION

PC-S	PC	BT	FB	H	G	D	BB
Simplified Poettmann & Carpenter	Poettmann & Carpenter	Baxendell & Thomas	Fancher & Brown	Hagedorn & Brown	Gray	Duns & Ros	Beggs & Brill

	PC-S							PC						
Qg\Ql	4000	6000	8000	10000	12000	14000	16000	4000	6000	8000	10000	12000	14000	16000
0.0	4757.906	4753.814	4751.375	4749.711	4748.483	4747.528	4746.759	4763.458	4768.989	4773.715	4777.755	4782.317	4786.773	4790.265
0.5	4409.784	4574.721	4641.187	4672.046	4691.1	4700.933	4704.893	4416.181	4590.787	4664.359	4700.9	4725.683	4740.777	4749.067
1.0	3748.56	4204.126	4402.533	4507.029	4569.146	NaN	4636.455	3756.565	4222.372	4427.471	4537.507	4605.008	4649.742	4681.622
3.0	1631.207	2363.442	2978.879	3433.727	3733.851	3939.516	4086.377	1663.122	2410.711	3030.479	3484.742	3785.265	3993.139	4142.578
5.0	1078.567	1456.783	1908.374	2349.181	2741.021	3075.689	3351.378	1139.903	1539.798	2001.278	2444.077	2830.779	3162.765	3434.66
10	824.7856	889.8245	1027.549	1211.973	1425.92	1655.362	1888.817	950.3368	1059.637	1212.146	1406.852	1623.126	1846.435	2077.863
15	790.6857	780.4798	823.445	901.4274	1005.04	1128.1	1265.728	980.0758	1017.261	1082.024	1172.84	1285.235	1408.343	1544.065
20	785.1572	747.7616	753.2697	786.6657	840.3888	909.9762	992.4008	1013.488	1031.745	1073.119	1120.888	1182.881	1260.771	1337.852
30	785.5353	731.9367	709.6712	707.918	720.9254	745.2963	786.5252	1129.702	1116.183	1124.68	1145.817	1168.867	1200.592	1245.052
40	784.9969	729.9582	699.2262	684.8383	682.2958	692.5084	726.3624	1205.978	1199.618	1202.396	1197.622	1216.039	1224.275	1289.865
50	782.2128	729.6897	696.6054	676.9839	667.2674	686.9492	713.9985	1295.341	1278.277	1265.423	1269.97	1262.806	1307.398	1368.595
60	778.0607	729.1465	696.1111	674.3815	676.8419	698.6615	722.6724	1362.242	1348.873	1334.573	1328.162	1341.181	1402.441	1458.422

	BT							FB						
Qg\Ql	4000	6000	8000	10000	12000	14000	16000	4000	6000	8000	10000	12000	14000	16000
0.0	4762.819	4768.91	4779.447	4796.753	4818.142	4842.822	4872.762	4760.057	4771.373	4782.003	4794.431	4806.347	4817.712	4828.922
0.5	4415.527	4590.879	4670.504	4720.667	4762.627	4798.349	4833.326	4412.322	4593.435	4673.169	4718.067	4750.228	4772.332	4788.33
1.0	3755.938	4222.623	4434.215	4558.289	4643.426	4709.218	4768.037	3750.596	4225.313	4437.047	4555.465	4630.4	4682.192	4721.732
3.0	1659.002	2412.677	3042.953	3514.531	3837.31	4069.139	4246.718	1643.022	2419.179	3049.226	3511.902	3821.335	4035.815	4191.268
5.0	1135.036	1545.769	2028.076	2497.486	2917.161	3278.355	3576.801	1120.154	1561.408	2038.743	2493.549	2892.563	3230.325	3503.177
10	944.4008	1081.146	1286.893	1540.103	1814.866	2098.829	2380.106	826.7411	970.47	1296.586	1517.177	1751.248	1990.037	2224.841
15	978.331	1061.905	1208.469	1381.278	1571.148	1777.868	1989.579	616.6562	914.3602	1005.229	1108.145	1462.763	1604.648	1755.881
20	1036.684	1124.004	1251.993	1398.856	1557.387	1728.096	1903.809	621.4719	667.4949	985.6334	1052.126	1126.24	1497.711	1599.7
30	1198.329	1304.155	1426.817	1556.27	1699.727	1843.669	1999.375	657.5656	682.9361	720.1433	1071.903	1113.921	1164.575	1228.572
40	1382.674	1501.576	1625.797	1760.117	1897.609	2038.855	2192.321	698.5169	727.0533	754.0273	785.4862	819.521	1204.082	1273.918
50	1578.258	1703.537	1833.618	1971.901	2108.258	2258.088	2410.115	754.7989	773.8606	797.0233	823.0072	853.7305	900.5329	949.3703
60	1776.073	1903.933	2045.886	2183.464	2330.286	2483.106	2635.843	803.2993	821.9626	844.823	869.5978	907.3861	953.391	1002.072

	H							G						
Qg\Ql	4000	6000	8000	10000	12000	14000	16000	4000	6000	8000	10000	12000	14000	16000
0.0	4541.456	4363.345	4254.647	4164.565	4152.881	4147.848	4154.267	4758.048	4777.762	4802.918	4833.181	4868.369	4908.342	4953.004
0.5	3769.771	4283.053	4426.587	4488.586	4514.529	4529.319	4535.059	4423.55	4594.962	4680.284	4736.243	4785.613	4830.213	4873.682
1.0	2240.567	3457.889	4006.824	4259.386	4376.237	4452.435	4498.714	3821.149	4246.802	4450.769	4574.034	4661.61	4732.205	4796.205
3.0	1527.656	1860.967	2189.236	2549.888	2979.365	3403.318	3764.132	1801.049	2540.829	3138.341	3578.425	3880.288	4099.823	4269.318
5.0	1367.096	1629.628	1880.602	2123.526	2364.303	2612.669	2898.024	1166.083	1643.817	2135.025	2589.685	2988.628	3332.179	3613.77
10	1225.39	1426.056	1622.418	1813.658	2000.089	2182.568	2362.15	828.4176	1049.474	1294.227	1557.767	1831.869	2107.792	2378.385
15	1178.868	1355.835	1531.354	1704.785	1875.709	2044.194	2210.555	805.1803	966.9708	1137.32	1317.612	1507.353	1704.81	1907.578
20	1163.766	1329.404	1494.258	1658.602	1821.938	1984.069	2145.035	844.1117	984.8588	1127.836	1275.148	1427.689	1585.562	1748.33
30	1175.494	1333.252	1489.111	1645.561	1802.488	1959.634	2116.867	971.2698	1096.689	1220.074	1343.334	1467.657	1593.772	1723.047
40	1217.919	1375.81	1529.751	1684.249	1839.744	1996.122	2153.249	1115.668	1235.163	1351.555	1466.389	1583.061	1709.327	1837.049
50	1280.756	1441.583	1596.46	1751.568	1907.792	2065.203	2223.726	1262.792	1379.046	1495.682	1619.841	1743.341	1866.813	1990.72
60	1360.658	1525.559	1682.819	1839.737	1997.705	2156.972	2317.538	1409.921	1538.098	1664.18	1788.471	1911.724	2034.518	2157.293

	D							BB						
Qg\Ql	4000	6000	8000	10000	12000	14000	16000	4000	6000	8000	10000	12000	14000	16000
0.0	4769.772	4796.308	4830.128	4870.896	4918.474	4947.91	4969.833	4764.023	4776.737	4801.993	4831.015	4866.354	4915.565	4960.972
0.5	4550.384	4649.066	4708.406	4754.508	4798.932	4842.729	4888.259	4600.954	4601.871	4681.778	4734.155	4782.89	4845.891	4890.031
1.0	4224.466	4425.85	4566.856	4649.653	4716.237	4774.116	4831.024	4326.468	4326.698	4481.673	4584.199	4663.978	4743.789	4813.96
3.0	2975.698	3393.244	3729.144	3950.75	4114.438	4256.261	4350.009	2856.557	3234.852	3564.009	3837.484	4053.533	4224.693	4382.103
5.0	2327.737	2645.933	2972.689	3284.905	3562.002	3741.615	3872.282	2171.146	2568.8	2930.988	3207.089	3441.896	3682.032	3922.687
10	1470.635	1714.03	1961.302	2214.422	2476.666	2716.912	2955.817	1560.737	1904.533	2196.015	2445.185	2678.653	2913.244	3101.621
15	1139.12	1323.889	1518.203	1722.695	1933.436	2148.87	2380.394	1365.881	1663.165	1924.567	2159.272	2377.079	2583.855	2791.664
20	980.7591	1136.704	1305.032	1483.114	1668.813	1864.401	2064.447	1297.997	1575.414	1816.024	2044.062	2258.769	2459.931	2649.381
30	852.8502	988.8547	1135.073	1289.917	1455.95	1626.655	1803.607	1322.879	1565.237	1795.261	2013.329	2217.252	2411.754	2594.932
40	864.7425	959.618	1092.569	1240.599	1396.034	1561.2	1730.985	1440.97	1671.326	1885.907	2090.888	2289.857	2479.606	2660.164
50	976.5412	1000.743	1110.991	1244.26	1393.656	1553.812	1721.347	1593.087	1814.472	2023.278	2222.07	2411.836	2597.754	2778.519
60	1118.592	1069.963	1161.322	1282.328	1421.63	1573.465	1738.473	1761.693	1973.003	2178.343	2375.38	2562.398	2746.314	2921.334

FIGURE 130 – BASE CASE

	PC-S							PC						
Qg\Ql	4000	6000	8000	10000	12000	14000	16000	4000	6000	8000	10000	12000	14000	16000
0.0	5305.097	5301.657	5299.606	5298.206	5297.173	5296.37	5295.723	5312.773	5316.413	5321.48	5326.501	5331.108	5334.353	5338.152
0.5	4792.038	5021.106	5120.205	5172.356	5202.183	5223.457	5234.995	4800.81	5037.132	5143.178	5201.602	5236.997	5262.241	5278.102
1.0	3968.908	4527.224	4785.679	4928.167	5016.329	5074.828	5116.182	3980.679	4546.208	4810.957	4959.347	5052.8	5115.134	5160.602
3.0	1796.926	2572.776	3178.645	3624.181	3955.669	4201.194	4382.003	1834.882	2623.124	3230.433	3677.387	4010.84	4256.736	4438.763
5.0	1154.355	1607.464	2104.978	2561.064	2949.59	3272.633	3540.513	1221.965	1700.644	2199.28	2653.218	3039.467	3359.77	3624.173
10	831.481	932.224	1109.546	1333.142	1581.509	1837.659	2089.686	975.73	1112.917	1303.88	1527.919	1774.765	2028.13	2267.647
15	781.6108	791.0037	856.9771	960.2167	1090.203	1239.479	1404.544	975.5159	1030.797	1125.238	1238.58	1367.88	1519.259	1676.205
20	770.7622	745.7663	766.3582	816.6782	888.7078	977.5666	1086.614	1023.113	1041.251	1091.395	1160.368	1237.417	1325.283	1439.771
30	768.7085	720.9171	706.6521	714.2129	737.5001	778.4348	838.9415	1119.725	1121.623	1135.6	1153.252	1193.72	1232.71	1323.929
40	768.6474	716.4722	690.5253	682.069	686.2367	721.0613	762.1897	1205.253	1198.619	1200.743	1211.473	1216.631	1280.254	1353.335
50	765.6071	715.774	685.6588	670.0754	680.1363	709.8738	742.5488	1287.162	1278.298	1264.88	1268.868	1290.509	1360.371	1423.899
60	760.5044	715.4807	684.3594	669.0889	692.6112	719.0869	753.5277	1354.921	1336.008	1334.96	1320.771	1386.943	1451.101	1523.559

	BT							FB						
Qg\Ql	4000	6000	8000	10000	12000	14000	16000	4000	6000	8000	10000	12000	14000	16000
0.0	5312.133	5318.468	5332.234	5352	5375.625	5404.428	5437.177	5310.767	5321.383	5333.328	5345.612	5356.951	5368.165	5378.91
0.5	4800.122	5039.25	5154.625	5228.274	5282.997	5334.137	5379.386	4798.493	5042.416	5155.684	5221.487	5263.592	5296.727	5319.676
1.0	3979.7	4548.523	4823.361	4987.724	5100.971	5189.718	5265.105	3976.794	4552.071	4824.587	4980.557	5080.681	5150.819	5203.499
3.0	1832.26	2627.75	3252.6	3722.18	4079.516	4353.634	4567.691	1825.197	2635.951	3255.972	3712.35	4052.175	4303.901	4492.737
5.0	1217.417	1710.535	2240.113	2728.467	3147.568	3503.012	3804.502	1216.821	1724.51	2244.042	2712.143	3105.422	3430.793	3701.545
10	972.5759	1146.374	1403.978	1699.711	2011.521	2324.047	2626.994	856.1844	1030.501	1396.021	1652.041	1915.282	2174.056	2427.456
15	990.3072	1110.612	1289.118	1494.212	1718.872	1953.837	2200.157	634.0188	943.5821	1049.624	1180.068	1564.242	1728.468	1911.422
20	1055.888	1167.618	1322.689	1492.328	1681.361	1875.768	2087.77	629.5223	685.6429	1012.885	1096.323	1189.555	1583.274	1728.893
30	1221.832	1347.224	1490.007	1644.026	1805.79	1976.352	2159.433	662.9877	697.9186	741.3926	1095.964	1151.082	1216.236	1310.313
40	1412.453	1547.523	1689.927	1845.099	1999.952	2170.992	2344.844	705.4775	734.581	767.6507	805.5884	848.0598	1263.71	1345.018
50	1607.681	1749.369	1902.174	2055.354	2218.57	2389.251	2560.749	758.6255	782.4888	810.2238	841.8258	887.523	941.8264	1000.368
60	1804.323	1956.672	2114.383	2271.508	2443.381	2614.983	2788.955	805.3482	830.3448	854.6508	889.0351	941.382	995.0758	1052.889

	H							G						
Qg\Ql	4000	6000	8000	10000	12000	14000	16000	4000	6000	8000	10000	12000	14000	16000
0.0	4254.147	4303.993	4355.335	4385.664	4433.048	4459.469	4500.479	0	5474.699	5509.215	5573.167	5651.295	5740.863	5840.674
0.5	3126.982	3492.93	3655.621	3818.256	4062.72	4390.508	4727.554	4830.195	5070.959	5205.931	5307.444	5397.449	5488.774	5580.684
1.0	2768.215	2957.028	3172.857	3357.348	3471.821	3593.844	3732.475	4078.02	4601.326	4872.174	5047.868	5181.8	5297.233	5405.496
3.0	2063.897	2495.724	2864.667	3207.042	3534.848	3721.94	3761.922	2019.866	2783.496	3371.001	3815.624	4191.584	4476.043	4652.062
5.0	1830.28	2216.416	2553.142	2846.378	3128.805	3397.795	3659.089	1306.262	1845.878	2372.515	2840.742	3242.823	3586.619	3883.724
10	1581.734	1915.731	2216.718	2495.559	2735.958	2978.723	3214.207	896.2799	1154.291	1438.932	1740.874	2048.573	2352.332	2645.833
15	1476.127	1783.397	2066.517	2332.748	2576.243	2797.892	3024.99	855.937	1042.43	1240.135	1449.702	1669.45	1896.511	2127.759
20	1423.062	1713.418	1985.038	2243.26	2491.298	2701.98	2921.127	889.0538	1049.795	1214.221	1384.533	1561.382	1744.481	1933.013
30	1391.003	1660.173	1916.853	2164.486	2405.518	2628.874	2828.496	1013.086	1155.087	1295.35	1436.165	1578.888	1724.311	1874.634
40	1411.962	1666.593	1913.669	2154.65	2390.656	2622.638	2811.659	1157.418	1292.269	1423.893	1554.221	1686.315	1828.778	1975.427
50	1463.438	1706.55	1946.402	2182.362	2414.983	2644.703	2835.444	1305.245	1436.247	1564.353	1702.288	1842.199	1982.595	2123.999
60	1533.922	1768.414	2002.337	2234.525	2464.39	2692.532	2884.501	1452.481	1589.227	1730.913	1870.889	2010.087	2149.196	2288.736

	D							BB						
Qg\Ql	4000	6000	8000	10000	12000	14000	16000	4000	6000	8000	10000	12000	14000	16000
0.0	5546.379	5600.415	5690.131	5820.046	5990.087	6214.729	6590.296	5336.664	4776.737	4801.993	4831.015	4866.354	4915.565	4960.972
0.5	5004.26	5131.985	5267.182	5353.412	5436.762	5523.923	5617.446	5123.9	4601.871	4681.778	4734.155	4782.89	4845.891	4890.031
1.0	4672.74	4869.4	5004.729	5103.644	5175.778	5234.877	5287.443	4840.293	4326.698	4481.673	4584.199	4663.978	4743.789	4813.96
3.0	3713.944	4084.264	4340.074	4550.248	4657.771	4756.558	4855.473	3357.506	3234.852	3564.009	3837.484	4053.533	4224.693	4382.103
5.0	3018.175	3472.242	3790.921	4057.668	4285.221	4484.352	4658.665	2543.902	2568.8	2930.988	3207.089	3441.896	3682.032	3922.687
10	1988.397	2345.819	2736.698	3116.459	3418.105	3699.721	3952.457	1906.624	1904.533	2196.015	2445.185	2678.653	2913.244	3101.621
15	1555.752	1883.529	2141.106	2520.879	2769.968	3081.822	3395.245	1705.52	1663.165	1924.567	2159.272	2377.079	2583.855	2791.664
20	1303.735	1644.751	1877.33	2250.638	2483.488	2719.875	2955.572	1653.023	1575.414	1816.024	2044.062	2258.769	2459.931	2649.381
30	1065.418	1363.424	1643.68	1847.738	2209.471	2425.609	2643.632	1695.395	1565.237	1795.261	2013.329	2217.252	2411.754	2594.932
40	954.7069	1230.119	1486.142	1762.379	1957.311	2311.382	2522.371	1832.994	1671.326	1885.907	2090.888	2289.857	2479.606	2660.164
50	1064.784	1228.78	1465.056	1742.554	1933.416	2270.388	2475.308	1999.52	1814.472	2023.278	2222.07	2411.836	2597.754	2778.519
60	1227.512	1285.778	1427.707	1666.51	1941.321	2131.333	2468.248	2178.165	1973.003	2178.343	2375.38	2562.398	2746.314	2921.334

FIGURE 131 – OIL DENSITY SET TO API = 8

	PC-S							PC						
Qg\Ql	4000	6000	8000	10000	12000	14000	16000	4000	6000	8000	10000	12000	14000	16000
0.0	5064.584	5060.88	5058.672	5057.166	5056.054	5055.189	5054.493	5071.578	5075.966	5080.705	5085.617	5090.016	5092.997	5097.708
0.5	4622.506	4824.968	4910.32	4953.55	4979.565	4993.993	5005.177	4630.489	4840.927	4933.213	4982.889	5014.321	5032.548	5049.079
1.0	3861.667	4381.355	4615.776	4743.055	4819.867	4871.058	4906.009	3872.083	4399.598	4640.665	4774.156	4856.17	4910.898	4951.077
3.0	1717.28	2466.952	3069.583	3519.022	3847.752	4078.567	4246.689	1753.852	2514.686	3120.463	3572.607	3901.472	4132.695	4303.782
5.0	1118.319	1535.687	2009.264	2454.189	2839.582	3163.471	3433.895	1182.296	1625.184	2102.579	2547.265	2930.365	3250.366	3519.452
10	827.5905	911.9674	1070.897	1275.992	1507.694	1750.333	1991.94	965.2146	1089.582	1261.479	1471.482	1704.196	1942.292	2175.218
15	784.9897	785.4738	840.9277	932.5178	1050.22	1187.147	1337.937	978.7832	1025.418	1106.746	1206.961	1327.81	1468.88	1608.589
20	776.6261	745.9931	759.731	802.3234	865.939	945.8768	1042.215	1018.216	1036.138	1083.445	1143.65	1209.945	1297.053	1387.065
30	775.7947	725.3258	707.4267	710.7642	729.3807	759.7721	814.9774	1125.038	1120.172	1129.393	1148.767	1183.902	1209.495	1289.432
40	775.5705	722.0728	693.9346	682.7859	683.9137	708.1105	745.9562	1203.471	1197.334	1202.651	1206.403	1217.99	1254.615	1326.078
50	772.0513	721.6331	690.1378	672.7119	672.2331	699.5426	729.7062	1290.723	1279.044	1261.903	1270.629	1271.379	1337.726	1400.444
60	766.389	721.2451	689.2502	669.0527	685.5198	709.9357	737.026	1357.005	1342.548	1335.688	1320.297	1367.374	1430.447	1488.454

	BT							FB						
Qg\Ql	4000	6000	8000	10000	12000	14000	16000	4000	6000	8000	10000	12000	14000	16000
0.0	5070.862	5077.117	5089.402	5107.982	5130.755	5157.698	5189.282	5068.764	5079.528	5091.067	5103.583	5115.108	5126.509	5137.065
0.5	4629.657	4842.35	4942.608	5006.234	5056.325	5098.934	5142.691	4627.284	4844.935	4944.296	5001.512	5040.047	5066.753	5089.196
1.0	3870.879	4401.357	4650.901	4798.842	4900.045	4979.546	5047.384	3866.912	4404.503	4652.807	4793.847	4883.037	4946.177	4992.323
3.0	1750.535	2518.286	3138.868	3611.006	3962.252	4221.214	4421.541	1739.317	2527.223	3144.464	3604.806	3940.278	4179.124	4355.246
5.0	1179.089	1633.276	2137.285	2613.932	3028.731	3382.855	3684.526	1172.409	1647.671	2145.604	2603.419	2994.457	3321.017	3594.002
10	960.7334	1116.676	1351.088	1626.397	1920.058	2219.122	2509.083	843.4916	1002.711	1349.677	1589.277	1838.035	2085.896	2328.124
15	985.8949	1089.208	1252.087	1443.458	1652.236	1874.481	2103.041	626.1829	930.0671	1030.213	1148.041	1518.686	1670.943	1833.269
20	1046.459	1147.186	1291.454	1451.047	1626.376	1809.922	2005.178	626.2471	676.8995	996.8203	1075.794	1160.69	1545.342	1668.66
30	1211.428	1328.279	1462.305	1605.692	1759.599	1916.215	2089.188	660.8389	691.5476	731.7775	1084.242	1135.253	1185.964	1273.085
40	1399.662	1527.738	1660.204	1808.332	1954.398	2113.486	2278.434	702.1108	731.3044	761.5669	796.8904	835.6342	1237.935	1314.147
50	1594.512	1729.678	1872.414	2019.382	2169.94	2332.373	2495.454	756.6246	778.9323	804.7119	833.1261	871.6774	923.7663	978.03
60	1790.521	1933.901	2084.839	2232.402	2394.446	2557.95	2721.693	802.8095	826.176	850.4897	878.858	926.6295	976.5732	1029.213

	H							G						
Qg\Ql	4000	6000	8000	10000	12000	14000	16000	4000	6000	8000	10000	12000	14000	16000
0.0	4899.852	4949.041	4990.562	5033.339	5076.743	5109.647	5148.601	5078.598	5108.204	5145.522	5190.059	5241.487	5299.606	5364.275
0.5	4024.912	4331.479	4408.385	4444.427	4480.447	4513.578	4555.909	4648.884	4858.159	4968.034	5044.743	5111.322	5173.376	5238.512
1.0	2868.286	3660.834	4064.821	4193.673	4251.687	4282.925	4308.043	3955.556	4440.399	4681.836	4832.579	4942.931	5034.983	5118.356
3.0	1987.422	2427.323	2821.776	3208.562	3410.938	3454.591	3771.961	1917.157	2663.042	3246.998	3690.912	4024.011	4273.703	4471.258
5.0	1745.456	2112.085	2435.636	2730.116	3006.694	3275.482	3549.276	1242.305	1751.854	2258.824	2715.918	3111.058	3449.293	3740.584
10	1504.873	1796.24	2062.167	2307.111	2535.638	2751.565	2957.959	866.1421	1107.238	1373.323	1656.984	1948.031	2237.07	2517.425
15	1408.831	1664.081	1903.312	2127.871	2340.097	2542.304	2736.504	833.7248	1009.141	1194.431	1390.547	1596.301	1809.265	2026.547
20	1362.668	1596.142	1818.884	2031.044	2233.811	2428.66	2617.002	869.5614	1021.444	1176.275	1336.193	1501.936	1673.359	1849.761
30	1339.129	1548.361	1751.995	1949.658	2141.589	2328.412	2510.877	995.1333	1129.871	1262.696	1395.719	1530.208	1666.908	1807.521
40	1362.612	1560.38	1753.882	1943.648	2129.702	2312.326	2491.954	1139.598	1267.752	1392.708	1516.218	1641.285	1776.395	1914.601
50	1413.355	1604.948	1792.601	1977.662	2160.224	2340.792	2519.454	1286.944	1411.778	1534.017	1666.419	1799.133	1932.082	2065.757
60	1482.232	1670.612	1855.269	2037.994	2219.024	2398.473	2576.53	1432.318	1567.083	1701.979	1835.121	1967.359	2099.329	2231.512

	D							BB						
Qg\Ql	4000	6000	8000	10000	12000	14000	16000	4000	6000	8000	10000	12000	14000	16000
0.0	5102.322	5147.979	5205.026	5273.295	5353.018	5444.788	5495.098	5081.068	5105.075	5142.056	5185.184	5236.337	5301.766	5366.942
0.5	4795.024	4928.91	5008.212	5071.782	5131.093	5190.649	5253.791	4889.575	4874.854	4973.89	5046.87	5111.695	5184.139	5257.016
1.0	4489.177	4672.778	4789.238	4866.659	4923.347	4967.425	5050.699	4602.839	4547.491	4733.583	4859.168	4960.349	5053.459	5158.964
3.0	3428.529	3814.107	4107.98	4291.64	4410.883	4525.706	4613.23	3111.648	3397.571	3755.389	4022.163	4262.272	4481.595	4661.454
5.0	2725.167	3089.892	3433.167	3731.705	3978.071	4187.126	4307.855	2355.536	2779.269	3132.206	3444.177	3671.717	3900.278	4162.585
10	1768.956	2060.812	2337.209	2634.478	2933.024	3201.347	3454.591	1721.359	2108.69	2433.145	2708.48	2966.011	3223.761	3428.097
15	1373.385	1613.815	1849.677	2085.082	2320.309	2571.963	2843.923	1518.425	1862.485	2162.986	2430.758	2678.363	2911.84	3146.326
20	1180.001	1387.676	1596.987	1809.391	2023.518	2244.333	2463.747	1458.466	1774.875	2059.735	2319.24	2567.349	2798.804	3016.041
30	1017.667	1199.013	1379.679	1565.211	1759.684	1955.469	2155.339	1484.932	1779.089	2047.736	2304.073	2540.004	2767.01	2981.169
40	956.3341	1144.899	1314.547	1489.631	1669.158	1858.193	2049.997	1612.376	1885.391	2145.151	2391.458	2626.145	2846.794	3061.764
50	1057.88	1163.078	1312.666	1477.197	1650.881	1831.152	2019.594	1767.423	2037.082	2288.869	2524.682	2754.985	2975.093	3188.068
60	1177.222	1225.868	1347.176	1499.882	1665.708	1840.505	2023.11	1939.146	2205.14	2452.504	2686.946	2910.526	3126.864	3340.532

FIGURE 132 - OIL DENSITY SET TO API = 15

	PC-S							PC						
Qg\Ql	4000	6000	8000	10000	12000	14000	16000	4000	6000	8000	10000	12000	14000	16000
0.0	4363.431	4358.731	4355.93	4354.018	4352.607	4351.511	4350.627	4368.018	4372.783	4377.437	4381.482	4386.77	4391.176	4394.633
0.5	4134.697	4244.429	4286.028	4295.474	4301.724	4306.179	4309.525	4139.79	4259.302	4308.296	4323.595	4336.54	4346.557	4354.091
1.0	3634.665	3983.825	4126.656	4198.055	4238.149	4261.83	4280.647	3640.437	4000.492	4150.355	4227.179	4273.706	4302.954	4325.646
3.0	1560.901	2333.738	2986.902	3377.471	3619.376	3779.868	3892.001	1581.318	2380.506	3032.873	3422.438	3666.897	3830.645	3944.764
5.0	1040.112	1386.313	1840.509	2317.21	2752.328	3073.296	3307.823	1090.816	1470.572	1935.417	2409.867	2836.667	3152.736	3382.617
10	824.9308	868.3798	984.0571	1149.547	1351.204	1577.492	1817.555	932.2564	1021.345	1163.124	1343.834	1545.748	1773.292	2008.309
15	800.2785	777.6983	806.5588	869.7936	958.9804	1068.992	1196.027	976.8728	1002.393	1052.248	1136.787	1234.078	1345.647	1476.823
20	797.7858	752.5437	748.5178	771.4694	814.277	872.8603	944.6063	1023.987	1032.943	1055.293	1096.669	1155.154	1214.579	1294.591
30	799.1135	742.0303	714.6822	706.9818	713.4912	730.9864	757.4133	1131.921	1108.75	1119.336	1136.031	1147.878	1182.878	1207.619
40	797.6594	741.2553	707.5722	689.4035	682.558	684.4352	703.2817	1208.809	1203.846	1197.167	1197.641	1207.036	1216.094	1240.55
50	792.3663	740.9355	706.124	683.977	671.2299	671.8102	695.0246	1295.569	1278.659	1272.622	1263.809	1267.55	1267.842	1323.849
60	784.8621	739.8387	705.9042	682.4557	666.9786	684.8429	705.5206	1358.712	1353.266	1329.531	1332.14	1313.646	1363.008	1416.82

	BT							FB						
Qg\Ql	4000	6000	8000	10000	12000	14000	16000	4000	6000	8000	10000	12000	14000	16000
0.0	4366.982	4372.413	4381.299	4395.774	4415.49	4438.466	4464.894	4362.54	4373.878	4384.409	4396.73	4409.042	4420.437	4431.781
0.5	4138.773	4258.942	4312.425	4338.589	4366.284	4395.095	4426.111	4134.094	4260.537	4315.513	4339.38	4359.419	4376.405	4392.037
1.0	3639.344	4000.046	4154.762	4242.958	4304.522	4352.763	4399.297	3632.769	4001.7	4157.945	4243.636	4297.242	4333.41	4364.305
3.0	1581.093	2378.727	3038.731	3444.531	3706.891	3891.162	4031.489	1557.116	2381.255	3045.451	3445.985	3698.068	3868.031	3990.586
5.0	1085.31	1470.491	1948.242	2449.938	2899.985	3239.467	3497.49	1060.874	1479.419	1962.754	2452.776	2888.639	3209.065	3444.951
10	929.593	1036.21	1217.211	1445.889	1705.992	1983.922	2270.192	804.2925	930.9581	1233.506	1437.384	1665.529	1905.722	2149.305
15	972.5097	1035.053	1152.57	1305.839	1477.407	1664.304	1864.347	604.6478	893.7738	972.9953	1061.874	1399.543	1534.5	1675.382
20	1034.479	1093.716	1204.261	1332.483	1471.5	1625.019	1785.251	614.3186	654.542	968.2356	1019.97	1089.04	1444.264	1536.601
30	1187.781	1270.665	1379.529	1495.616	1619.831	1750.976	1883.572	652.4121	672.0959	708.2946	1054.804	1088.496	1133.922	1179.439
40	1362.258	1467.258	1579.091	1695.205	1820.178	1943.491	2076.963	697.5761	720.3137	743.027	769.9818	800.9747	1180.36	1223.816
50	1555.307	1667.887	1781.01	1906.791	2029.921	2157.378	2294.295	749.2644	766.4417	787.4838	811.5866	836.8278	869.8601	914.4208
60	1749.21	1866.91	1992.436	2118.435	2243.161	2380.957	2518.606	798.5783	817.6342	836.5871	856.2047	882.0904	924.5333	966.5029

	H							G						
Qg\Ql	4000	6000	8000	10000	12000	14000	16000	4000	6000	8000	10000	12000	14000	16000
0.0	3917.025	3944.528	3953.702	3958.997	3965.939	3977.322	3995.005	4354.342	4367.937	4385.355	4406.363	4430.825	4458.687	4489.906
0.5	3056.442	3531.974	3758.426	3898.157	3984.781	4056.225	4118.3	4133.834	4252.334	4310.282	4340.28	4369.919	4400.848	4433.872
1.0	1943.295	2893.881	3363.742	3625.063	3797.547	3930.379	4027.267	3674.538	4007.219	4157.37	4244.665	4305.157	4353.633	4400.144
3.0	1220.828	1461.296	1730.809	2165.619	2606.223	3018.572	3311.366	1692.623	2486.553	3107.588	3483.406	3727.771	3900.409	4032.79
5.0	1120.219	1301.466	1486.667	1678.786	1885.744	2148.807	2468.036	1079.575	1535.245	2037.772	2530.476	2957.182	3273.053	3512.75
10	1040.04	1182.757	1325.748	1470.603	1617.258	1765.79	1916.634	781.0752	979.4452	1201.975	1447.568	1711.245	1985.587	2262.643
15	1018.608	1152.725	1284.597	1418.147	1553.588	1690.698	1829.294	767.7839	912.9079	1065.695	1228.25	1401.191	1583.961	1775.11
20	1016.898	1150.588	1279.148	1408.899	1540.647	1674.296	1809.624	809.9291	936.5364	1064.852	1197.019	1334.241	1477.07	1625.568
30	1042.929	1183.777	1313.819	1443.551	1575.011	1708.53	1844.038	938.3122	1051.508	1162.66	1273.466	1385.062	1498.209	1614.186
40	1094.55	1245.142	1380.363	1513.704	1648.235	1784.713	1923.26	1082.093	1190.09	1295.166	1398.643	1507.477	1620.879	1735.184
50	1166.156	1325.629	1466.843	1604.89	1743.58	1884.019	2026.504	1227.942	1333.431	1445.197	1557.344	1668.598	1779.533	1890.591
60	1255.207	1421.45	1568.44	1711.389	1854.54	1999.248	2145.949	1380.438	1498.841	1613.068	1725.437	1836.602	1947.077	2057.267

	D							BB						
Qg\Ql	4000	6000	8000	10000	12000	14000	16000	4000	6000	8000	10000	12000	14000	16000
0.0	4361.696	4377.492	4398.34	4423.916	4454.059	4488.686	4527.766	4364.752	4366.757	4383.875	4402.72	4426.943	4468.277	4499.836
0.5	4180.171	4267.956	4317.598	4348.546	4379.869	4413.038	4448.786	4238.61	4253.228	4309.539	4335.156	4364.348	4422.49	4455.507
1.0	3875.363	4076.549	4192.979	4266.638	4321.51	4369.257	4415.684	4004.672	4052.161	4169.71	4239.851	4301.345	4369.68	4421.796
3.0	2588.112	3087.52	3420.903	3681.301	3856.18	3996.359	4106.697	2595.856	3081.621	3419.732	3661.983	3838.884	3972.821	4092.728
5.0	1939.729	2279.434	2636.028	2979.51	3210.776	3431.231	3691.357	1973.201	2356.744	2753.793	3034.51	3302.688	3519.868	3700.51
10	1183.284	1377.994	1598.693	1838.285	2101.999	2357.44	2612.988	1399.536	1704.03	1967.668	2197.104	2429.876	2639.357	2833.72
15	919.9678	1058.712	1218.677	1397.182	1589.528	1792.199	2011.063	1223.495	1477.374	1703.305	1908.909	2102.287	2286.404	2476.877
20	801.6383	919.2559	1056.536	1207.852	1370.6	1547.119	1731.519	1159.648	1395.033	1600.307	1792.339	1981.042	2154.846	2319.39
30	715.5376	821.0071	943.2461	1075.879	1220.846	1371.079	1529.926	1190.313	1387.789	1577.113	1760.954	1932.932	2094.787	2254.022
40	784.405	818.2025	926.0258	1054.607	1192.191	1339.124	1491.161	1308.434	1493.508	1669.45	1837.451	1999.783	2157.159	2308.905
50	924.5549	875.6581	961.5016	1072.883	1204.803	1349.422	1500.911	1462.883	1633.894	1802.719	1965.762	2120.513	2271.181	2418.293
60	1073.24	961.1835	1022.936	1122.803	1242.339	1378.203	1528.701	1627.792	1793.291	1954.955	2113.615	2267.103	2415.243	2560.203

FIGURE 133 - OIL DENSITY SET TO API = 40

	PC-S							PC						
Qg\Ql	4000	6000	8000	10000	12000	14000	16000	4000	6000	8000	10000	12000	14000	16000
0.0	4754.996	4750.902	4748.462	4746.796	4745.567	4744.612	4743.842	4760.549	4766.083	4770.812	4774.855	4779.42	4783.878	4787.372
0.5	4534.797	4636.415	4675.83	4686.636	4693.759	4698.818	4702.604	4541.493	4652.38	4698.923	4715.574	4728.42	4738.735	4746.909
1.0	4082.752	4393.879	4527.954	4596.623	4630.975	4656.953	4671.16	4091.176	4411.301	4552.187	4626.762	4666.53	4697.546	4716.145
3.0	2069.758	2971.78	3532.574	3861.259	4070.484	4211.105	4311.74	2103.324	3010.704	3572.998	3904.71	4116.392	4259.338	4363.861
5.0	1280.842	1842.052	2442.993	2960.664	3337.6	3606.314	3803.1	1345.836	1928.221	2526.855	3039.162	3409.802	3674.792	3872.464
10	872.7015	1016.894	1236.546	1510.356	1815.205	2127.089	2426.907	1016.868	1192.086	1425.966	1699.883	2003.286	2306.95	2593.969
15	787.481	836.8496	930.63	1059.555	1217.551	1398.898	1598.285	1004.404	1076.689	1190.235	1331.181	1489.26	1673.787	1861.326
20	752.2772	768.5515	815.2698	885.7771	976.2991	1084.239	1213.346	1024.028	1075.807	1136.974	1217.526	1317.679	1422.116	1558.408
30	717.6441	712.6165	725.4902	752.2634	790.5276	851.9271	919.6984	1103.294	1123.203	1145.021	1190.453	1224.407	1308.699	1398.456
40	697.4156	687.2351	689.121	703.8437	741.6333	783.2185	830.0323	1176.705	1177.203	1200.395	1214.151	1282.354	1350.418	1419.127
50	682.8389	671.6683	677.6811	705.3843	735.8577	772.519	819.208	1233.324	1242.443	1251.395	1315.003	1374.3	1438.968	1525.895
60	672.0608	675.4065	698.2565	723.4061	756.3603	796.7779	838.1865	1290.833	1307.14	1367.378	1422.564	1488.195	1570.263	1653.619

	BT							FB						
Qg\Ql	4000	6000	8000	10000	12000	14000	16000	4000	6000	8000	10000	12000	14000	16000
0.0	4759.91	4766.004	4776.546	4793.858	4815.256	4839.947	4869.901	4757.146	4768.467	4779.103	4791.537	4803.46	4814.831	4826.047
0.5	4540.788	4652.634	4705.368	4735.634	4765.75	4796.925	4831.804	4537.941	4655.198	4707.917	4732.839	4753.023	4770.459	4786.306
1.0	4090.346	4411.928	4559.544	4648.012	4705.448	4757.934	4803.318	4086.52	4414.63	4562.029	4644.812	4691.897	4730.216	4756.202
3.0	2100.056	3013.291	3586.559	3934.446	4167.101	4334.315	4466.396	2088.457	3020.805	3590.855	3930.102	4149.447	4299.771	4409.906
5.0	1340.668	1935	2555.347	3090.549	3486.076	3778.664	4004.015	1338.706	1948.746	2564.234	3084.124	3460.654	3731.666	3932.189
10	1022.734	1231.471	1518.83	1853.647	2208.329	2558.65	2886.663	915.455	1114.839	1513.597	1816.972	2132.26	2439.762	2730.805
15	1035.348	1179.606	1368.255	1584.591	1825.31	2079.263	2343.503	683.2381	1001.271	1121.321	1273.571	1680.158	1874.852	2083.753
20	1110.439	1243.936	1400.728	1574.125	1764.381	1964.47	2183.353	673.9662	744.6144	1070.263	1160.614	1272.046	1676.721	1840.308
30	1329.812	1457.343	1595.563	1743.485	1896.792	2067.27	2242.994	702.3378	745.1661	795.6768	1143.58	1200.504	1291.527	1388.506
40	1571.35	1702.53	1838.105	1978.89	2132.916	2290.161	2451.377	748.9193	782.7205	819.6225	864.7264	922.7773	1342.149	1417.109
50	1824.794	1956.879	2095.266	2243.483	2393.614	2547.385	2707.377	801.5316	830.8754	869.878	919.6161	971.8462	1027.873	1089.628
60	2078.757	2220.235	2366.829	2514.479	2665.771	2821.825	2980.645	856.6671	895.1915	941.1991	990.0455	1042.413	1098.815	1156.241

	H							G						
Qg\Ql	4000	6000	8000	10000	12000	14000	16000	4000	6000	8000	10000	12000	14000	16000
0.0	4652.247	4648.606	4610.805	4564.014	4524.114	4532.154	4512.194	4755.36	4775.044	4800.191	4830.457	4865.646	4905.646	4950.323
0.5	4086.55	4418.185	4553.048	4603.507	4638.686	4668.329	4697.367	4538.15	4653.852	4715.189	4753.531	4792.634	4834.218	4879.118
1.0	3134.105	3950.977	4269.702	4438.329	4540.027	4608.419	4666.545	4120.809	4423.016	4569.835	4661.735	4724.308	4784.012	4836.229
3.0	1668.503	2072.568	2675.215	3295.115	3743.79	4015.669	4224.527	2265.903	3122.966	3648.882	3973.061	4192.706	4355.111	4484.444
5.0	1487.562	1772.827	2058.768	2367.06	2777.583	3169.8	3559.034	1427.23	2060.793	2668.48	3171.108	3538.839	3813.291	4025.932
10	1345.895	1556.215	1763.03	1966.212	2166.895	2367.366	2571.73	970.2483	1243.28	1556.772	1898.031	2247.16	2585.84	2902.725
15	1313.05	1497.914	1680.761	1861.439	2039.799	2216.156	2391.131	937.5092	1121.296	1323.391	1544.218	1781.132	2029.034	2281.684
20	1317.804	1491.025	1662.39	1832.671	2001.614	2169.173	2335.517	986.1863	1136.963	1296.794	1467.113	1648.116	1838.843	2037.411
30	1382.829	1547.797	1709.65	1871.227	2032.647	2193.799	2354.652	1146.407	1271.471	1399.438	1531.385	1667.995	1809.726	1959.591
40	1493.027	1656.817	1816.023	1975.04	2134.444	2294.239	2454.389	1327.483	1441.892	1557.433	1677.084	1807.007	1940.527	2077.436
50	1634.655	1799.101	1958.062	2116.813	2276.269	2436.557	2597.669	1511.347	1630.221	1750.949	1873.08	1997.03	2123.104	2251.505
60	1800.934	1966.14	2125.667	2285.047	2445.389	2606.947	2769.768	1721.427	1840.623	1959.333	2079.017	2200.01	2322.577	2446.915

	D							BB						
Qg\Ql	4000	6000	8000	10000	12000	14000	16000	4000	6000	8000	10000	12000	14000	16000
0.0	4769.402	4796.002	4829.95	4870.888	4918.674	4973.296	5034.848	4764.879	4774.688	4800.004	4828.576	4863.945	4917.078	4962.736
0.5	4598.229	4677.67	4727.544	4766.95	4807.421	4850.679	4897.543	4626.915	4655.835	4716.24	4751.114	4790.356	4857.113	4902.884
1.0	4356.001	4527.403	4625.04	4694.58	4750.362	4804.236	4855.598	4396.659	4461.689	4580.513	4660.519	4725.757	4800.972	4860.084
3.0	3294.157	3700.05	3976.323	4216.29	4374.307	4493.389	4608.935	3168.222	3581.47	3903.979	4123.968	4295.619	4422.621	4550.439
5.0	2600.875	2998.735	3356.469	3600.193	3819.614	3984.499	4257.605	2472.71	2935.7	3291.107	3587.844	3837.555	4036.09	4200.503
10	1700.677	1992.006	2293.419	2582.893	2863.427	3132.136	3357.876	1799.971	2177.841	2486.841	2784.475	3021.812	3238.242	3462.293
15	1309.55	1525.729	1756.182	1998.11	2253.346	2512.709	2755.337	1573.28	1899.31	2180.941	2428.228	2661.528	2893.04	3090.433
20	1117.453	1294.536	1487.748	1694.123	1913.136	2138.834	2380.531	1507.269	1795.575	2057.308	2291.537	2513.974	2725.696	2927.615
30	956.5284	1099.777	1260.469	1436.415	1620.414	1816.001	2021.772	1548.417	1802.434	2036.762	2258.876	2464.624	2659.18	2847.85
40	962.4665	1053.547	1191.151	1353.001	1527.921	1709.042	1898.719	1694.533	1928.641	2148.893	2357.088	2557.215	2743.499	2922.421
50	1035.326	1090.509	1197.669	1336.814	1504.084	1683.011	1865.569	1882.441	2102.266	2310.033	2512.653	2701.424	2886.077	3062.097
60	1126.418	1158.868	1249.499	1369.995	1516.255	1687.795	1872.389	2082.384	2297.006	2498.859	2691.92	2878.503	3059.516	3235.646

FIGURE 134 - INJECTION GAS SET TO NITROGEN

	PC-S							PC						
Qg\Ql	4000	6000	8000	10000	12000	14000	16000	4000	6000	8000	10000	12000	14000	16000
0.0	4754.888	4750.794	4748.353	4746.688	4745.459	4744.503	4743.734	4760.441	4765.975	4770.704	4774.748	4779.312	4783.77	4787.265
0.5	4540.344	4639.62	4676.119	4686.858	4693.937	4698.964	4702.726	4547.067	4655.59	4699.22	4715.809	4728.608	4738.885	4747.039
1.0	4101.262	4404.842	4533.511	4600.758	4634.185	4660.448	4671.451	4109.678	4422.252	4557.743	4630.737	4669.748	4701.038	4716.453
3.0	2116.047	3020.157	3566.564	3886.541	4089.263	4226.985	4325.285	2149.483	3058.242	3606.64	3929.778	4134.503	4275.077	4377.327
5.0	1304.203	1884.094	2494.793	3009.4	3376.997	3638.319	3829.549	1370.339	1970.194	2577.595	3085.867	3447.908	3706.22	3897.616
10	879.8002	1031.756	1260.333	1543.862	1857.602	2175.895	2479.068	1023.232	1206.461	1449.964	1732.697	2044.345	2353.914	2643.314
15	790.22	844.5221	943.2174	1077.547	1241.569	1429.359	1635.37	1009.436	1085.72	1202.541	1349.223	1513.769	1703.529	1897.245
20	752.8626	773.074	823.3276	897.406	991.755	1103.882	1237.937	1024.583	1080.837	1146.091	1227.771	1333.113	1440.242	1583.895
30	716.0577	714.0945	729.5127	758.6007	800.7742	864.0594	933.8234	1102.001	1126.238	1149.75	1196.283	1235.049	1322.727	1413.462
40	694.799	687.2038	691.212	710.9385	749.7977	792.4807	842.2857	1175.589	1180.364	1201.327	1222.209	1293.36	1361.22	1435.387
50	679.766	670.7672	683.4413	711.9542	743.1894	782.9631	830.3531	1234.065	1239.278	1262.28	1325.398	1383.857	1454.702	1542.39
60	668.879	680.6284	704.1948	729.9647	766.355	807.1928	849.0838	1283.545	1319.048	1378.07	1431.981	1504.773	1587.244	1671.123

	BT							FB						
Qg\Ql	4000	6000	8000	10000	12000	14000	16000	4000	6000	8000	10000	12000	14000	16000
0.0	4759.802	4765.896	4776.438	4793.75	4815.149	4839.841	4869.795	4757.037	4768.359	4778.995	4791.429	4803.353	4814.724	4825.94
0.5	4546.36	4655.857	4705.691	4735.894	4765.971	4797.123	4831.983	4543.523	4658.421	4708.233	4733.084	4753.217	4770.622	4786.446
1.0	4108.84	4422.908	4565.153	4651.986	4708.729	4761.514	4803.725	4105.18	4425.612	4567.621	4648.747	4695.138	4733.737	4756.529
3.0	2146.285	3060.891	3620.365	3959.666	4185.137	4350.256	4480.041	2135.108	3068.226	3624.587	3955.174	4167.328	4315.534	4423.338
5.0	1364.316	1976.993	2606.064	3136.916	3523.642	3809.248	4028.971	1363.088	1990.667	2614.559	3130.228	3498.036	3762.232	3956.896
10	1031.1	1248.357	1544.077	1888.139	2249.977	2604.503	2934.166	925.33	1130.571	1538.591	1850.502	2173.206	2485.535	2778.6
15	1042.3	1192.144	1384.933	1606.111	1852.642	2111.653	2381.148	690.8723	1010.861	1135.552	1292.136	1704.37	1905.18	2120.552
20	1118.222	1255.857	1415.042	1591.824	1785.404	1989.721	2212.822	679.1833	752.7258	1079.608	1172.115	1288.278	1697.461	1866.626
30	1341.739	1470.216	1610.905	1759.735	1916.294	2088.722	2266.582	707.1813	751.4927	803.3092	1151.423	1213.289	1305.688	1404.574
40	1585.587	1719.354	1854.816	1998.693	2153.628	2312.033	2475.427	753.4117	788.2833	826.6832	874.5826	933.0517	1354.444	1433.354
50	1844.379	1975.645	2117.409	2265.964	2416.662	2572.231	2733.413	806.402	836.9824	879.5068	929.1911	982.5665	1040.303	1102.747
60	2101.379	2245.701	2392.231	2540.054	2692.961	2849.858	3009.711	862.3972	905.361	951.3918	1000.95	1055.032	1111.813	1169.704

	H							G						
Qg\Ql	4000	6000	8000	10000	12000	14000	16000	4000	6000	8000	10000	12000	14000	16000
0.0	4656.248	4653.965	4619.267	4575.989	4576.591	4546.714	4540.91	4755.261	4774.945	4800.093	4830.36	4865.551	4905.553	4950.232
0.5	4095.438	4423.383	4556.84	4608.667	4645.178	4676.092	4706.324	4543.449	4657.008	4715.643	4753.984	4793.123	4834.769	4879.753
1.0	3186.656	3964.151	4282.907	4451.549	4547.346	4620.395	4673.446	4137.667	4433.53	4575.352	4665.128	4727.738	4787.828	4837.02
3.0	1685.025	2099.648	2728.987	3350.937	3768.153	4043.492	4238.341	2312.781	3166.797	3679.891	3995.896	4210.345	4370.689	4497.012
5.0	1501.113	1789.673	2080.453	2400.531	2823.51	3235.563	3611.418	1455.808	2104.577	2718.107	3214.875	3574.548	3841.95	4050.48
10	1358.492	1570.371	1778.802	1983.706	2186.338	2389.276	2597.453	984.2914	1263.663	1585.268	1934.784	2290.375	2632.774	2950.803
15	1326.408	1512.441	1696.426	1878.209	2057.659	2235.117	2411.262	949.5483	1136.243	1342.374	1568.191	1810.601	2063.863	2321.123
20	1332.6	1506.799	1679.091	1850.245	2020.009	2188.348	2355.444	998.3746	1150.776	1312.957	1486.316	1670.926	1865.629	2068.257
30	1401.763	1567.436	1729.968	1892.174	2054.171	2215.851	2377.186	1160.402	1286.092	1415.118	1548.532	1686.98	1830.94	1983.358
40	1517.229	1681.449	1841.127	2000.598	2160.423	2320.606	2481.114	1343.728	1458.369	1574.472	1695.322	1826.486	1961.297	2099.709
50	1664.824	1829.408	1988.643	2147.694	2307.447	2468.022	2629.413	1530.427	1649.877	1770.792	1893.355	2017.964	2144.898	2274.342
60	1837.377	2002.449	2162.07	2321.619	2482.19	2644.026	2807.082	1743.923	1862.857	1981.592	2101.519	2222.954	2346.145	2471.27

	D							BB						
Qg\Ql	4000	6000	8000	10000	12000	14000	16000	4000	6000	8000	10000	12000	14000	16000
0.0	4769.412	4796.023	4829.989	4870.949	4918.76	4973.412	5034.995	4764.936	4774.629	4799.957	4828.498	4863.872	4917.108	4962.949
0.5	4601.12	4679.467	4728.169	4767.568	4808.07	4851.387	4898.333	4628.752	4658.933	4716.788	4751.605	4790.89	4857.925	4903.791
1.0	4363.407	4531.952	4628.469	4696.729	4752.52	4806.412	4856.571	4402.691	4469.827	4585.039	4663.612	4729.085	4813.448	4861.202
3.0	3325.029	3722.565	3992.985	4237.083	4384.45	4502.041	4616.174	3201.712	3608.295	3925.278	4140.834	4307.562	4445.151	4557.363
5.0	2636.096	3035.455	3382.933	3625.384	3840.731	4009.441	4272.634	2502.102	2974.902	3321.136	3617.229	3857.982	4067.201	4213.898
10	1726.428	2022.994	2330.45	2621.137	2902.621	3170.32	3369.627	1824.959	2205.999	2515.838	2813.523	3050.845	3269.009	3490.263
15	1328.514	1548.355	1783.172	2029.04	2290.364	2548.406	2792.799	1594.296	1923.742	2207.474	2455.766	2694.25	2921.024	3119.967
20	1132.358	1312.222	1508.15	1718.603	1940.959	2169.5	2413.541	1526.451	1817.631	2081.568	2317.108	2540.193	2755.188	2956.542
30	967.3578	1111.904	1274.693	1452.877	1639.214	1837.948	2046.669	1567.178	1824.654	2058.876	2282.363	2489.077	2684.273	2873.354
40	971.5298	1063.054	1201.986	1365.835	1542.938	1725.741	1918.425	1716.74	1950.104	2171.477	2381.972	2581.699	2768.58	2947.92
50	1044.203	1099.413	1206.722	1346.778	1516.329	1697.648	1881.785	1904.361	2125.279	2337.613	2537.511	2730.636	2913.077	3091.461
60	1129.273	1167.557	1257.902	1378.911	1526.884	1700.729	1887.55	2107.856	2323.765	2524.787	2720.752	2909.021	3088.117	3264.525

FIGURE 135 - INJECTION GAS SET TO AIR

	PC-S							PC						
Qg\Ql	4000	6000	8000	10000	12000	14000	16000	4000	6000	8000	10000	12000	14000	16000
0.0	4835.841	4831.851	4829.472	4827.849	4826.651	4825.72	4824.969	4841.789	4847.062	4851.79	4856.026	4860.507	4864.674	4868.439
0.5	4460.864	4637.507	4708.618	4744.779	4763.689	4777.882	4783.09	4467.696	4653.59	4731.755	4773.756	4798.283	4817.458	4827.203
1.0	3769.33	4244.955	4453.715	4565.481	4632.065	4676.472	4704.002	3777.978	4263.32	4478.777	4596.101	4667.943	4717.169	4749.132
3.0	1648.572	2380.709	2988.567	3445.008	3754.739	3968.564	4122.096	1681.912	2427.469	3040.008	3497.089	3806.718	4022.246	4178.721
5.0	1087.057	1473.129	1927.732	2366.816	2754.338	3083.847	3360.271	1149.454	1557.32	2019.969	2461.581	2844.636	3170.592	3445.246
10	825.2049	894.5756	1036.913	1225.63	1442.973	1674.53	1908.729	953.9927	1066.652	1222.506	1420.351	1640.402	1866.06	2096.79
15	789.1959	781.4237	827.1994	908.1904	1014.849	1140.815	1281.03	980.0684	1019.448	1087.938	1180.56	1294.946	1421.856	1557.884
20	783.0362	747.1844	754.5658	790.036	845.9627	917.8211	1002.513	1012.494	1032.009	1075.83	1126.392	1187.52	1269.237	1345.813
30	783.1659	730.2742	709.0069	708.417	722.7005	748.4323	792.963	1128.831	1117.366	1126.098	1146.877	1172.687	1203.066	1255.556
40	782.6539	728.0214	697.8791	684.2325	682.5302	696.086	730.8555	1205.028	1198.698	1202.757	1199.924	1216.899	1230.231	1298.598
50	778.5873	727.7292	695.0015	675.8808	666.7576	689.8615	717.6348	1293.319	1278.659	1263.377	1270.453	1260.954	1314.756	1376.366
60	772.3275	727.176	694.4285	673.046	678.8573	701.2868	725.9181	1358.347	1347.608	1335.075	1326.682	1347.541	1409.281	1465.543

	BT							FB						
Qg\Ql	4000	6000	8000	10000	12000	14000	16000	4000	6000	8000	10000	12000	14000	16000
0.0	4841.133	4847.251	4858.098	4875.766	4897.436	4922.652	4952.952	4838.497	4849.71	4860.535	4872.884	4884.613	4896.016	4907.176
0.5	4467.008	4653.98	4738.622	4794.289	4836.362	4877.04	4913.494	4463.907	4656.529	4741.044	4791.17	4823.023	4849.556	4866.539
1.0	3777.211	4263.904	4486.31	4617.698	4707.568	4778.826	4837.67	3772.052	4266.639	4488.911	4614.402	4693.679	4750.383	4789.341
3.0	1677.972	2430.293	3054.119	3528.685	3861.131	4101.305	4286.003	1663.044	2437.576	3059.904	3525.531	3843.839	4066.057	4227.937
5.0	1144.963	1563.914	2049.169	2518.139	2933.965	3290.906	3593.552	1131.922	1579.632	2059.821	2512.676	2906.921	3239.674	3515.508
10	948.3777	1089.452	1301.498	1559.34	1837.559	2124.393	2406.462	830.7416	977.871	1308.691	1533.177	1769.923	2009.56	2245.275
15	980.3268	1067.844	1218.754	1395.473	1589.825	1799.889	2014.445	618.7817	918.1744	1011.033	1117.358	1475.02	1619.534	1772.252
20	1038.068	1129.234	1261.4	1411.22	1573.459	1747.253	1926.766	622.6607	669.764	988.471	1057.801	1132.906	1508.003	1612.562
30	1200.711	1310.013	1435.201	1568.123	1714.062	1860.378	2020.735	658.3967	685.0237	722.3876	1075.058	1118.846	1170.473	1239.096
40	1386.77	1507.858	1633.994	1771.745	1911.323	2056.775	2212.989	699.3681	728.1357	755.8879	788.1686	823.3937	1212.211	1283.543
50	1581.283	1709.876	1842.916	1983.396	2122.49	2276.003	2430.71	754.4261	775.121	798.9165	824.8972	857.0928	906.0751	956.1752
60	1777.328	1911.171	2055.312	2194.882	2345.786	2501.208	2656.591	800.7822	822.5357	846.2457	871.8785	911.9938	958.5566	1008.496

	H							G						
Qg\Ql	4000	6000	8000	10000	12000	14000	16000	4000	6000	8000	10000	12000	14000	16000
0.0	3996.807	3880.151	3975.501	3877.456	3794.621	3723.241	3658.792	4838.258	4858.021	4883.144	4913.299	4948.298	4987.984	5032.252
0.5	3690.595	4290.945	4489.313	4561.652	4576.802	4588.485	4584.924	4481.815	4663.118	4752.799	4813.643	4862.508	4910.99	4954.642
1.0	2181.914	3293.755	3972.834	4277.294	4431	4522.102	4581.367	3854.088	4296.798	4510.212	4639.276	4730.798	4805.548	4868.333
3.0	1528.131	1856.455	2175.148	2506.529	2891.129	3230.895	3652.571	1838.157	2575.414	3164.326	3607.023	3916.746	4143.655	4318.417
5.0	1370.569	1630.921	1879.838	2119.779	2355.18	2592.45	2844.134	1194.253	1680.735	2175.16	2628.289	3023.026	3361.262	3646.62
10	1231.292	1430.853	1626.65	1817.731	2004.173	2186.626	2365.959	846.3991	1074.979	1327.491	1598.196	1878.133	2158.134	2430.952
15	1185.58	1362.012	1537.259	1710.824	1882.188	2051.305	2218.393	821.3976	989.2577	1166.077	1353.082	1549.501	1753.276	1961.69
20	1170.725	1336.327	1501.131	1665.741	1829.639	1992.556	2154.466	860.6262	1006.899	1155.66	1309.016	1467.782	1631.918	1800.809
30	1182.206	1340.776	1496.986	1653.912	1811.529	1969.564	2127.849	990.2844	1120.941	1249.661	1378.409	1508.383	1640.282	1774.465
40	1223.917	1383.304	1537.935	1693.095	1849.384	2006.709	2164.927	1138.16	1262.914	1384.607	1504.832	1624.678	1744.886	1866.72
50	1285.995	1448.87	1604.722	1760.562	1917.569	2075.97	2235.611	1289.017	1410.876	1529.214	1645.551	1764.496	1891.222	2018.473
60	1364.811	1532.249	1690.71	1848.588	2007.528	2167.849	2329.574	1438.137	1559.388	1679.628	1806.938	1933.274	2059.224	2185.234

	D							BB						
Qg\Ql	4000	6000	8000	10000	12000	14000	16000	4000	6000	8000	10000	12000	14000	16000
0.0	4824.45	4829.224	4835.455	4836.112	4838.891	4844.961	4848.894	4841.392	4854.623	4879.581	4908.433	4943.385	4991.222	5036.159
0.5	4602.569	4695.49	4741.851	4770.561	4791.483	4809.78	4824.375	4670.773	4667.477	4749.336	4806.135	4854.084	4919.532	4962.953
1.0	4257.34	4475.107	4589.727	4659.716	4706.426	4741.203	4768.816	4389.227	4377.605	4539.677	4644.627	4726.643	4808.592	4882.7
3.0	2967.881	3384.249	3740.379	3960.004	4135.857	4274.573	4373.7	2935.243	3278.65	3605.791	3872.036	4091.089	4274.421	4418.708
5.0	2333.697	2647.858	2970.766	3279.832	3554.184	3768.59	3896.944	2229.906	2629.253	2972.654	3257.948	3481.61	3703.771	3952.116
10	1483.662	1728.706	1977.444	2228.073	2486.719	2726.831	2963.489	1596.663	1943.412	2239.664	2491.851	2719.031	2957.723	3138.243
15	1150.18	1336.074	1532.536	1740.377	1954.365	2171.301	2398.214	1389.069	1690.393	1957.195	2195.719	2412.522	2614.05	2823.156
20	989.4955	1146.065	1317.624	1498.057	1689.404	1888.339	2092.346	1313.914	1595.155	1840.463	2070.079	2281.972	2485.283	2676.56
30	857.7522	995.1347	1143.816	1303.518	1474.02	1648.619	1832.657	1328.975	1575.555	1806.738	2026.467	2232.915	2429.733	2614.927
40	865.7828	964.7628	1100.148	1251.714	1413.106	1584.196	1757.775	1443.145	1676.398	1892.005	2099.307	2300.647	2492.619	2675.209
50	975.4965	1003.048	1117.544	1255.178	1410.078	1576.215	1751.28	1592.967	1816.087	2026.824	2227.603	2419.321	2607.286	2790.08
60	1115.85	1071.387	1168.053	1292.76	1436.319	1596.735	1768.092	1760.52	1973.061	2180.068	2378.913	2567.694	2753.493	2930.25

FIGURE 136 - WC SET TO 10%

	PC-S							PC						
Qg\Ql	4000	6000	8000	10000	12000	14000	16000	4000	6000	8000	10000	12000	14000	16000
0.0	4953.314	4949.469	4947.176	4945.612	4944.457	4943.559	4942.836	4959.782	4964.649	4969.377	4973.912	4978.264	4981.977	4986.164
0.5	4531.957	4727.121	4809.357	4849.853	4873.252	4887.262	4898.129	4539.364	4743.207	4832.428	4879.023	4907.779	4926.28	4942.124
1.0	3789.766	4298.092	4524.989	4647.723	4721.835	4770.507	4804.888	3799.322	4316.556	4550.046	4678.651	4757.857	4810.656	4850.034
3.0	1674.326	2405.715	3002.411	3450.545	3775.382	4002.005	4166.289	1709.455	2452.35	3053.583	3504.326	3828.616	4056.006	4223.541
5.0	1100.013	1497.5	1956.104	2392.347	2773.453	3095.473	3365.233	1163.52	1584.429	2048.599	2486.697	2864.411	3182.368	3451.553
10	826.0463	901.9332	1051.145	1246.162	1468.37	1702.826	1937.896	959.2747	1076.966	1238.941	1441.129	1665.741	1894.899	2124.15
15	787.1277	783.0362	833.0434	918.543	1029.731	1159.975	1303.946	979.7452	1022.404	1096.567	1191.831	1309.151	1441.761	1578.016
20	779.9909	746.4844	756.6958	795.29	854.5249	929.7775	1019.249	1015.331	1032.975	1079.572	1134.403	1196.623	1281.596	1362.826
30	779.7086	727.9055	708.1552	709.3252	725.5349	753.3171	802.7261	1127.312	1118.925	1127.935	1148.091	1178.117	1206.302	1271.19
40	779.3411	725.2151	695.9761	683.4561	683.026	701.5281	737.6761	1203.512	1197.506	1203.028	1203.229	1217.799	1241.044	1311.554
50	775.5101	724.8682	692.6938	674.3384	668.2391	694.2899	723.1524	1292.268	1279.069	1261.142	1270.889	1263.417	1325.681	1387.863
60	769.4957	724.3951	691.9877	671.1396	681.9273	705.2736	730.8374	1357.833	1345.504	1335.635	1324.117	1356.995	1419.418	1476.052

	BT							FB						
Qg\Ql	4000	6000	8000	10000	12000	14000	16000	4000	6000	8000	10000	12000	14000	16000
0.0	4959.1	4965.272	4976.751	4994.789	5016.927	5042.903	5073.737	4956.663	4967.706	4978.824	4991.246	5002.868	5014.255	5024.996
0.5	4538.615	4744.06	4840.42	4900.758	4947.66	4988.881	5031.581	4535.757	4746.602	4842.473	4896.965	4933.034	4959.338	4981.583
1.0	3798.313	4317.664	4558.808	4701.559	4799.506	4875.499	4942.016	3793.658	4320.488	4561.02	4697.582	4784.242	4844.887	4890.483
3.0	1705.798	2455.599	3070.104	3539.495	3886.246	4139.946	4335.963	1692.574	2464.463	3075.828	3534.977	3866.757	4101.651	4273.848
5.0	1159.615	1591.629	2080.32	2548.117	2958.301	3309.348	3609.6	1149.46	1606.493	2090.542	2540.273	2927.584	3252.964	3524.745
10	954.1677	1101.756	1323.356	1588.064	1871.193	2162.144	2445.222	836.6323	988.8485	1326.624	1556.823	1797.348	2037.984	2274.904
15	983.113	1077.826	1234.109	1417.037	1617.787	1832.785	2052.791	621.9964	923.7339	1019.722	1131.021	1494.295	1641.462	1796.309
20	1041.307	1136.942	1275.469	1429.739	1597.798	1775.95	1962.203	624.3715	673.085	992.4734	1066.104	1145.477	1524.896	1636.837
30	1205.848	1318.722	1447.795	1585.88	1735.552	1886.653	2052.834	659.5852	688.0994	726.6531	1079.547	1126.598	1177.784	1254.777
40	1392.904	1517.332	1646.224	1789.156	1931.856	2083.693	2244.058	700.6883	729.6838	758.6014	792.1893	829.1279	1224.317	1297.903
50	1587.573	1719.336	1856.869	2000.597	2144.7	2302.903	2461.643	755.4729	776.9584	801.6896	828.4467	863.3667	914.3538	966.3696
60	1783.59	1922	2069.416	2212.762	2369.042	2528.379	2687.742	801.376	823.9029	848.3089	875.2235	918.8732	966.8957	1018.11

	H							G						
Qg\Ql	4000	6000	8000	10000	12000	14000	16000	4000	6000	8000	10000	12000	14000	16000
0.0	4209.816	4321.677	3995.922	3934.793	3909.962	3940.939	4079.972	4959.271	4979.147	5004.213	5034.165	5068.833	5108.06	5151.779
0.5	3473.077	4252.261	4527.87	4639.838	4700.034	4719.791	4739.064	4562.718	4761.139	4861.49	4926.487	4979.082	5026.933	5075.679
1.0	2136.859	3002.553	3818.495	4216.535	4433.33	4566.808	4654.804	3893.237	4363.265	4592.992	4732.668	4831.383	4909.705	4978.881
3.0	1535.905	1860.418	2170.594	2478.139	2809.25	3089.797	3357.742	1890.989	2623.507	3200.213	3638.357	3960.895	4199.488	4384.662
5.0	1381.022	1640.414	1888.653	2126.958	2358.259	2586.369	2816.515	1235.137	1733.441	2231.421	2681.768	3070.72	3402.288	3685.886
10	1243.61	1443.046	1639.406	1831.622	2019.462	2203.303	2383.782	872.3834	1111.775	1375.199	1655.668	1943.243	2228.374	2503.938
15	1198.278	1375.124	1551.048	1725.83	1898.833	2069.853	2238.975	844.5584	1021.125	1207.137	1403.545	1609.151	1821.445	2037.338
20	1183.262	1349.823	1515.44	1681.259	1846.763	2011.585	2175.601	883.9696	1038.119	1195.067	1356.904	1524.303	1697.018	1874.192
30	1193.686	1354.213	1511.563	1669.747	1828.888	1988.695	2148.949	1016.716	1154.743	1290.917	1427.283	1565.042	1704.851	1846.995
40	1233.861	1396.029	1552.111	1708.608	1866.376	2025.355	2185.379	1168.991	1301.049	1430.045	1557.649	1684.978	1812.769	1941.493
50	1294.259	1460.567	1618.126	1775.382	1933.843	2093.704	2254.945	1324.861	1454.042	1579.713	1703.409	1826.102	1948.486	2071.049
60	1371.109	1542.487	1702.841	1862.145	2022.467	2184.226	2347.457	1479.287	1607.981	1731.829	1853.51	1973.861	2095.595	2225.623

	D							BB						
Qg\Ql	4000	6000	8000	10000	12000	14000	16000	4000	6000	8000	10000	12000	14000	16000
0.0	4939.317	4940.755	4942.583	4945.472	4947.178	4950.527	4954.268	4957.84	4971.672	4996.02	5024.413	5058.637	5104.333	5148.287
0.5	4687.564	4792.578	4843.69	4874.091	4894.551	4910.651	4924.967	4776.47	4762.64	4850.28	4910.307	4960.691	5017.95	5071.834
1.0	4300.615	4537.28	4665.506	4742.639	4793.312	4828.69	4858.222	4485.701	4448.704	4619.795	4731.299	4818.316	4906.301	4985.014
3.0	2983.214	3410.511	3752.42	4003.591	4165.621	4312.309	4419.787	3045.604	3344.512	3665.847	3916.763	4135.828	4334.173	4480.004
5.0	2356.25	2667.049	2991.622	3298.595	3567.699	3808.09	3983.602	2311.007	2714.839	3026.561	3329.969	3538.11	3748.568	3992.12
10	1505.393	1751.269	2001.438	2250.041	2510.018	2753.764	2990.396	1647.778	2006.318	2301.569	2557.395	2778.17	3025.456	3202.839
15	1166.068	1353.054	1552.011	1763.378	1980.65	2198.905	2423.217	1422.9	1729.447	2003.538	2247.445	2467.555	2669.016	2868.485
20	1001.318	1158.667	1333.304	1517.294	1714.115	1917.294	2124.959	1335.153	1623.127	1874.975	2109.954	2323.25	2523.024	2715.736
30	863.6815	1002.68	1154.406	1320.208	1495.072	1675.79	1866.799	1336.971	1591.886	1828.279	2046.155	2254.703	2454.819	2642.851
40	866.0059	970.1812	1109.032	1265.641	1433.996	1610.868	1790.683	1445.261	1683.105	1900.264	2110.071	2314.77	2509.887	2695.337
50	974.0607	1005.24	1123.913	1267.372	1429.969	1604.151	1784.98	1591.672	1817.956	2030.331	2233.828	2428.237	2619.063	2804.712
60	1112.97	1071.17	1174.787	1304.59	1454.497	1623.869	1805.354	1757.596	1971.6	2180.725	2381.998	2573.166	2759.142	2940.707

FIGURE 137 - WC SET TO 25%

	PC-S							PC						
Qg\Ql	4000	6000	8000	10000	12000	14000	16000	4000	6000	8000	10000	12000	14000	16000
0.0	5150.682	5147.058	5144.899	5143.425	5142.337	5141.492	5140.81	5157.828	5161.967	5166.683	5171.734	5176.158	5179.137	5183.673
0.5	4624.045	4859.286	4961.145	5014.802	5047.232	5067.272	5082.11	4632.28	4875.155	4983.945	5044.066	5081.906	5105.721	5125.627
1.0	3788.317	4352.23	4617.285	4763.62	4854.238	4914.417	4956.914	3799.475	4370.729	4642.487	4794.996	4890.713	4954.415	5001.792
3.0	1716.414	2445.139	3023.803	3453.148	3774.091	4019.389	4203.506	1753.635	2493.955	3075.679	3507.626	3830.179	4075.768	4261.847
5.0	1122.142	1537.66	2001.645	2432.572	2803.192	3113.367	3371.71	1186.231	1628.365	2095.585	2525.981	2894.849	3201.638	3458.398
10	827.9911	914.7776	1075.311	1280.443	1510.146	1748.747	1984.67	967.5269	1093.584	1267.226	1476.282	1706.407	1940.934	2167.055
15	784.1075	786.2258	843.3219	936.3131	1054.935	1192.08	1342.828	978.3524	1026.437	1110.28	1212.25	1331.955	1473.924	1613.726
20	775.2654	745.742	760.7206	804.5514	869.3014	950.1707	1048.007	1019.663	1037.592	1084.915	1147.077	1215.035	1301.25	1395.36
30	774.1963	724.2792	707.1066	711.2477	730.6974	762.9325	819.2687	1124.203	1120.943	1131.06	1149.082	1186.351	1213.7	1296.909
40	774.0048	720.7923	693.107	682.5012	684.2212	710.792	749.2519	1204.191	1198.075	1202.748	1208.094	1218.232	1260.912	1332.756
50	770.5219	720.3064	689.1002	672.056	673.9957	701.8235	732.5102	1290.172	1279.317	1262.555	1270.833	1275.311	1343.583	1406.592
60	764.904	719.9313	688.1339	668.2111	687.1635	712.043	740.8301	1356.717	1341.469	1336.048	1318.904	1372.519	1435.982	1497.376

	BT							FB						
Qg\Ql	4000	6000	8000	10000	12000	14000	16000	4000	6000	8000	10000	12000	14000	16000
0.0	5157.101	5163.352	5175.922	5194.679	5217.532	5244.755	5276.443	5155.196	5165.793	5177.46	5189.867	5201.273	5212.606	5223.154
0.5	4631.413	4876.83	4993.814	5068.031	5124.601	5173.078	5220.395	4629.146	4879.603	4995.391	5062.895	5107.699	5139.91	5165.847
1.0	3798.279	4372.655	4653.261	4820.498	4935.516	5024.378	5099.575	3794.41	4376.101	4655.136	4815.092	4917.826	4989.884	5043.304
3.0	1750.485	2497.878	3095.316	3548.411	3894.985	4168.419	4383.641	1740.283	2506.566	3100.434	3541.213	3871.021	4123.699	4314.809
5.0	1183.362	1636.973	2132.057	2595.639	2996.728	3338.883	3630.083	1178.364	1651.295	2139.418	2583.514	2960.138	3273.289	3534.981
10	963.3395	1121.829	1359.543	1635.394	1927.876	2223.496	2509.238	846.1513	1007.612	1356.079	1595.249	1842.082	2085.455	2321.622
15	987.1927	1094.179	1259.721	1453.614	1664.222	1887.214	2116.835	627.9013	932.5603	1033.856	1153.355	1525.586	1677.976	1841.715
20	1048.962	1152.169	1298.804	1460.521	1638.584	1823.66	2021.694	627.0287	678.3969	999.4392	1079.468	1166.026	1552.159	1679.15
30	1214.215	1333.03	1469.478	1615.414	1771.35	1931.047	2106.485	661.4111	693.076	733.9959	1086.364	1139.012	1191.938	1281.001
40	1403.015	1532.987	1668.022	1818.093	1966.351	2128.66	2295.98	702.7721	732.0608	762.9159	798.9869	838.4825	1244.257	1321.624
50	1597.968	1734.979	1880.373	2029.16	2183.029	2347.816	2513.307	757.1197	779.8782	806.1341	835.2924	875.48	928.0588	983.3259
60	1794.072	1939.974	2092.857	2242.716	2407.823	2573.714	2740.357	803.3613	827.2539	851.5575	880.9286	930.2536	981.0929	1034.945

	H							G						
Qg\Ql	4000	6000	8000	10000	12000	14000	16000	4000	6000	8000	10000	12000	14000	16000
0.0	4538.631	4657.036	4326.87	4490.772	4227.179	4117.53	4197.656	5162.588	5182.801	5207.771	5237.228	5271.053	5309.129	5351.393
0.5	2912.709	3961.415	4406.999	4616.74	4728.272	4800.291	4848.372	4673.645	4907.593	5026.604	5104.663	5166.045	5219.371	5270.73
1.0	2115.258	2725.459	3210.471	3815.575	4173.669	4401.86	4566.744	3923.988	4441.345	4706.096	4868.258	4982.744	5072.438	5148.557
3.0	1566.078	1889.136	2191.675	2478.491	2756.219	3033.597	3325.532	1973.998	2697.305	3255.118	3675.932	4000.807	4242.841	4461.365
5.0	1412.348	1674.114	1924.238	2162.729	2391.143	2611.525	2826.018	1300.978	1816.53	2318.347	2763.474	3143.621	3465.901	3740.996
10	1273.976	1476.678	1676.525	1872.591	2064.344	2251.852	2435.495	913.991	1170.612	1450.959	1745.986	2044.431	2336.517	2615.681
15	1227.1	1407.717	1587.089	1765.711	1942.899	2118.281	2291.785	881.036	1071.474	1271.982	1482.974	1702.53	1927.464	2154.221
20	1210.377	1381.276	1550.347	1719.851	1889.386	2058.505	2226.968	920.217	1086.83	1256.652	1431.701	1612.391	1798.126	1987.692
30	1217.141	1383.13	1544.087	1705.752	1868.588	2032.33	2196.705	1056.865	1206.398	1354.144	1502.268	1651.972	1803.838	1958.031
40	1253.48	1422.083	1581.954	1741.813	1903.009	2065.585	2229.36	1215.023	1358.341	1498.527	1637.381	1776.066	1915.317	2055.565
50	1309.659	1483.151	1644.642	1805.22	1966.957	2130.201	2294.899	1377.608	1517.931	1654.698	1789.479	1923.301	2056.875	2190.679
60	1382.53	1561.505	1725.787	1888.165	2051.414	2216.146	2382.435	1539.085	1678.931	1813.889	1946.63	2078.043	2208.777	2339.303

	D							BB						
Qg\Ql	4000	6000	8000	10000	12000	14000	16000	4000	6000	8000	10000	12000	14000	16000
0.0	5134.558	5135.417	5135.831	5137.013	5138.424	5140.045	5141.865	5152.911	5167.237	5190.104	5217.145	5249.454	5290.731	5332.219
0.5	4810.334	4938.356	5003.328	5041.355	5066.201	5083.873	5095.452	4952.238	4905.528	5002.705	5072.768	5128.606	5188.495	5250.866
1.0	4369.453	4621.049	4772.98	4866.695	4929.232	4972.508	5005.226	4667.293	4542.525	4730.98	4856.716	4953.487	5035.707	5125.013
3.0	3029.422	3448.766	3783.437	4053.894	4272.159	4386.766	4486.252	3224.077	3429.282	3765.581	3979.422	4185.467	4393.237	4571.367
5.0	2407.907	2725.832	3041.226	3333.974	3605.94	3836.693	4049.131	2437.653	2846.888	3135.421	3446.686	3634.976	3820.105	3999.981
10	1531.48	1775.197	2026.672	2276.297	2532.899	2790.375	3028.962	1728.653	2104.679	2407.777	2660.317	2881.791	3116.516	3304.946
15	1178.572	1363.698	1565.733	1780.988	2002.836	2224.692	2444.037	1475.751	1798.15	2076.189	2326.799	2551.929	2756.176	2948.591
20	1007.115	1163.569	1340.709	1529.88	1732.823	1942.818	2154.746	1368.083	1667.017	1926.883	2164.765	2389.052	2592.456	2783.185
30	862.5359	1001.944	1157.707	1330.347	1509.93	1699.839	1899.753	1346.618	1609.957	1854.362	2081.137	2289.548	2490.481	2681.373
40	858.902	966.8283	1110.842	1274.611	1452.071	1634.297	1824.321	1444.879	1685.754	1911.266	2123.265	2330.441	2530.064	2719.558
50	969.0248	1000.314	1124.121	1274.892	1446.916	1631.842	1818.602	1585.563	1813.26	2031.339	2236.468	2434.428	2626.756	2818.87
60	1108.135	1064.755	1174.203	1311.773	1472.081	1651.446	1843.419	1748.656	1963.669	2175.097	2376.641	2573.12	2762.309	2947.241

FIGURE 138 - WC SET TO 50%

	PC-S							PC						
Qg\Ql	4000	6000	8000	10000	12000	14000	16000	4000	6000	8000	10000	12000	14000	16000
0.0	5350.119	5346.699	5344.66	5343.269	5342.242	5341.444	5340.8	5357.723	5361.343	5366.361	5371.351	5375.919	5379.133	5382.923
0.5	4646.455	4940.923	5075.321	5149.284	5195.078	5225.491	5246.531	4655.438	4957.162	5098.416	5178.591	5229.865	5264.217	5289.54
1.0	3775.579	4335.671	4639.782	4820.513	4936.033	5014.858	5071.266	3787.872	4355.645	4665.97	4852.384	4973.126	5055.692	5116.031
3.0	1757.392	2481.949	3043.321	3455.316	3761.801	3995.96	4179.659	1795.643	2533.065	3096.503	3510.465	3819.346	4054.892	4239.977
5.0	1144.857	1577.152	2045.056	2470.104	2830.539	3129.619	3377.431	1212.624	1670.698	2140.066	2563.63	2922.395	3219.218	3463.966
10	830.5777	928.2967	1099.957	1314.698	1551.148	1793.093	2029.67	975.0682	1109.447	1294.761	1510.107	1745.067	1984.452	2208.904
15	781.5943	790.0094	854.2307	954.6697	1080.566	1224.312	1382.427	975.8541	1030.307	1123.123	1233.711	1358.835	1504.752	1654.736
20	770.957	745.5031	765.3067	814.4055	884.664	971.0878	1076.978	1023.493	1041.444	1091.01	1158.875	1234.128	1319.665	1430.903
30	768.9833	721.0359	706.4987	713.655	736.3787	776.4928	836.1302	1120.353	1122.218	1136.071	1153.451	1193.533	1231.598	1322.182
40	768.8851	716.6736	690.5982	681.9496	685.8547	720.2862	761.0751	1205.724	1199.281	1201.531	1212.137	1217.288	1280.437	1353.451
50	765.7129	715.992	685.8086	670.1174	679.9237	709.5383	742.06	1287.64	1279.011	1265.618	1269.774	1291.097	1361.097	1424.765
60	760.4621	715.6739	684.5372	669.0653	692.5409	718.9594	753.246	1355.242	1336.76	1335.8	1321.469	1387.751	1452.126	1524.586

	BT							FB						
Qg\Ql	4000	6000	8000	10000	12000	14000	16000	4000	6000	8000	10000	12000	14000	16000
0.0	5357.085	5363.364	5376.99	5396.582	5420.003	5448.54	5480.999	5355.713	5366.251	5378.096	5390.289	5401.544	5412.675	5423.333
0.5	4654.709	4959.247	5109.776	5205.098	5275.593	5335.674	5390.118	4652.88	4962.462	5110.911	5198.437	5256.391	5298.597	5330.918
1.0	3786.85	4358.013	4678.506	4880.923	5021.584	5130.534	5220.483	3783.831	4361.753	4679.921	4873.9	5001.376	5091.704	5159.082
3.0	1793.045	2537.881	3119.459	3557.017	3890.988	4157.245	4375.492	1786.093	2546.206	3122.855	3546.729	3862.446	4104.824	4297
5.0	1208.174	1680.801	2181.68	2640.48	3033.328	3367.034	3650.794	1207.636	1694.788	2185.487	2623.545	2989.865	3292.37	3544.04
10	971.8962	1142.955	1395.382	1682.691	1983.301	2282.956	2572.302	855.2868	1026.846	1387.246	1634.516	1886.124	2131.254	2370.032
15	990.5491	1110.167	1287.353	1490.085	1711.06	1941.077	2181.125	633.6557	942.8269	1047.364	1175.105	1555.775	1714.502	1890.671
20	1056.255	1167.861	1322.657	1491.533	1679.337	1871.798	2081.107	629.4402	685.1589	1012.212	1094.664	1186.227	1578.25	1720.756
30	1222.339	1347.956	1491.008	1645.192	1807.083	1977.495	2160.324	663.0418	697.8646	741.1669	1096.02	1150.775	1215.151	1308.548
40	1412.985	1548.474	1691.269	1846.945	2002.267	2173.756	2348.071	705.5237	734.6692	767.6555	805.5297	847.8147	1263.892	1345.073
50	1608.252	1750.469	1903.775	2057.591	2221.41	2392.838	2565.108	758.6428	782.6195	810.3555	841.9191	887.5091	941.7573	1000.239
60	1804.857	1957.858	2116.192	2273.948	2446.632	2619.117	2793.999	805.2619	830.4626	854.8023	889.1391	941.5277	995.2289	1053.019

	H							G						
Qg\Ql	4000	6000	8000	10000	12000	14000	16000	4000	6000	8000	10000	12000	14000	16000
0.0	4957.625	4751.245	4573.709	4427.5	4314.055	4213.531	4129.578	5367.891	5388.731	5413.833	5442.805	5475.497	5511.858	5551.809
0.5	2670.95	3144.43	3499.413	3930.752	4187.347	4350.035	4473.537	4715.672	5007.722	5157.118	5254.972	5329.624	5392.915	5450.449
1.0	2142.915	2641.769	3092.804	3528.851	3368.875	3487.381	3771.77	3941.138	4454.684	4742.297	4934.133	5087.931	5196.041	5286.131
3.0	1622.693	1949.535	2249.145	2525.115	2781.762	3023.015	3252.201	2052.695	2765.852	3306.319	3712.008	4025.473	4276.38	4484.025
5.0	1465.585	1735.195	1990.385	2231.289	2459.273	2676.095	2883.492	1365.126	1895.593	2399.509	2839.149	3211.348	3525.831	3794.258
10	1320.053	1531.468	1738.458	1940.806	2138.086	2330.354	2517.963	954.3749	1227.627	1523.827	1831.934	2139.7	2437.494	2719.543
15	1268.267	1457.603	1644.042	1829.121	2012.382	2193.483	2372.34	915.823	1119.702	1334.113	1558.86	1791.29	2027.626	2263.993
20	1247.641	1427.317	1603.254	1779.042	1954.59	2129.516	2303.581	954.2673	1132.895	1315.068	1502.687	1695.877	1893.691	2094.598
30	1247.946	1422.991	1590.49	1758.016	1926.486	2095.757	2265.575	1093.74	1254.248	1412.998	1572.266	1733.239	1896.418	2061.848
40	1278.662	1456.666	1622.845	1788.197	1954.641	2122.38	2291.273	1256.607	1410.572	1561.304	1710.732	1860.068	2010.039	2161.039
50	1329.525	1512.772	1680.424	1846.172	2012.802	2180.857	2350.336	1424.64	1575.405	1722.547	1867.671	2011.861	2155.847	2300.101
60	1396.596	1585.228	1755.366	1922.596	2090.451	2259.717	2430.526	1591.737	1742.024	1887.299	2030.293	2171.949	2312.945	2453.756

	D							BB						
Qg\Ql	4000	6000	8000	10000	12000	14000	16000	4000	6000	8000	10000	12000	14000	16000
0.0	5332.85	5332.955	5333.187	5333.515	5333.922	5334.401	5334.947	5348.901	5362.777	5382.975	5407.221	5435.956	5470.964	5507.867
0.5	4909.715	5057.763	5140.137	5190.343	5223.603	5246.598	5264.749	5147.782	5007.994	5124.987	5205.955	5269.483	5328.509	5395.504
1.0	4420.725	4690.943	4855.709	4961.339	5040.294	5097.41	5139.327	4818.839	4633.407	4798.24	4934.277	5042.234	5150.01	5236.491
3.0	3107.233	3495.155	3815.264	4080.479	4295.663	4483.097	4638.751	3405.008	3540.451	3869.167	4057.754	4225.798	4390.935	4592.079
5.0	2477.844	2782.006	3077.14	3371.184	3631.119	3865.373	4073.483	2559.244	2972.617	3253.999	3548.145	3733.215	3891.277	4054.914
10	1555.466	1790.581	2038.923	2287.948	2535.58	2794.29	3044.59	1805.245	2196.169	2506.336	2761.261	2977.494	3194.625	3395.372
15	1180.562	1358.59	1561.664	1780.023	2004.912	2230.764	2453.829	1523.631	1859.496	2146.582	2397.276	2624.414	2830.398	3018.632
20	999.2972	1151.81	1329.339	1523.841	1731.931	1946.741	2163.272	1395.018	1706.367	1970.027	2212.374	2441.741	2647.741	2840.045
30	848.9789	986.9007	1145.986	1323.284	1507.9	1705.121	1912.198	1349.001	1610.369	1867.795	2099.814	2311.746	2515.526	2705.84
40	846.5292	950.9015	1099.231	1269.252	1453.352	1641	1838.89	1436.781	1679.689	1908.193	2120.276	2329.699	2531.963	2722.707
50	963.8455	987.3937	1113.697	1270.268	1449.96	1641.857	1835.272	1571.684	1799.018	2015.877	2222.024	2422.053	2615.658	2804.219
60	1105.346	1053.295	1165.01	1306.984	1476.096	1664.115	1861.766	1731.895	1941.937	2153.484	2356.639	2553.373	2743.649	2930.018

FIGURE 139 - WC SET TO 75%

APPENDIX D

This appendix includes some flow charts for the UBD simulator. The finished MATLAB code is very complex and some of the processes include many additional steps. These are therefore included only as a guideline for understanding the main iteration process, and should not be through of as a true representation of the code itself.

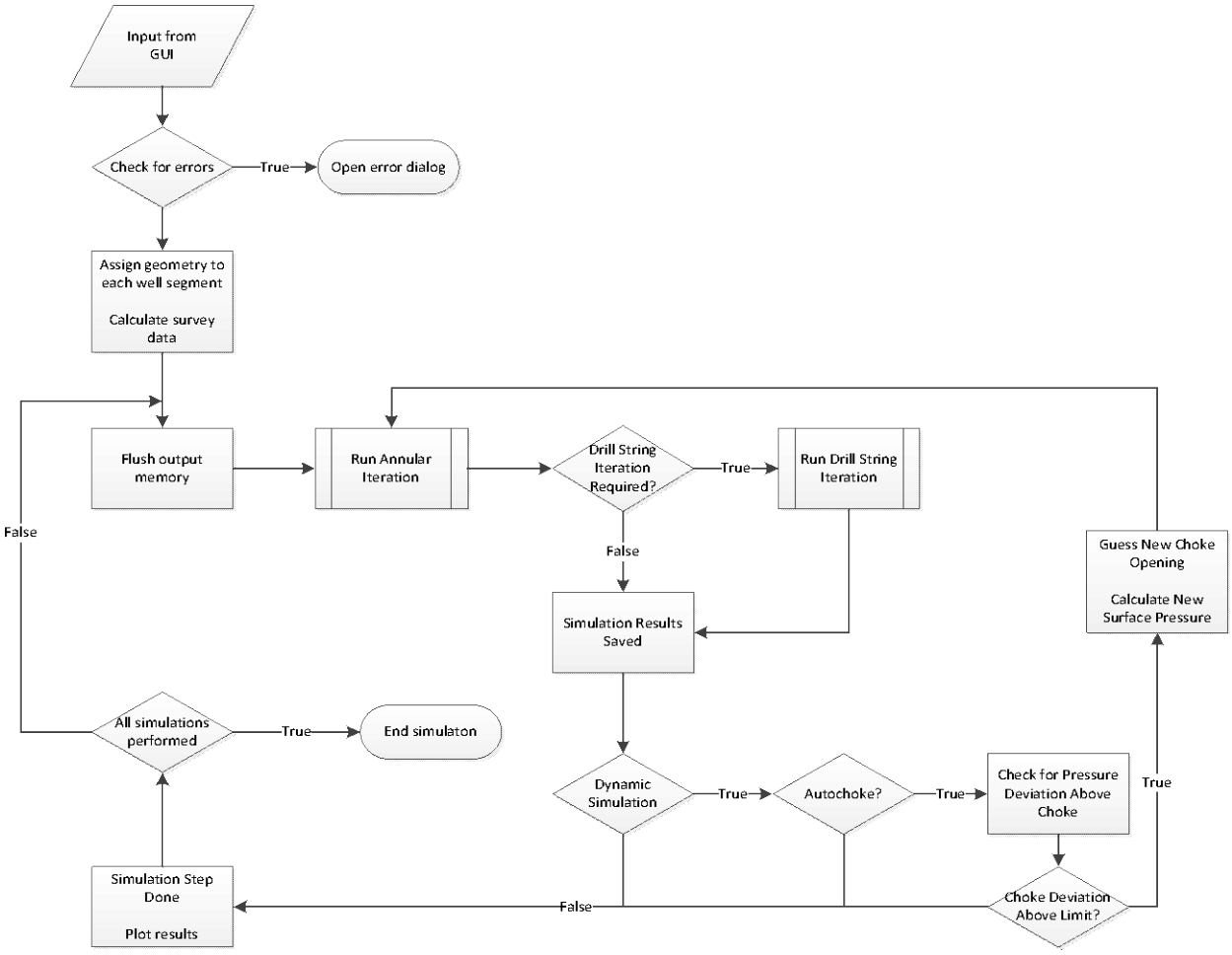

FIGURE 140 - GENERAL ITERATION PROCESS

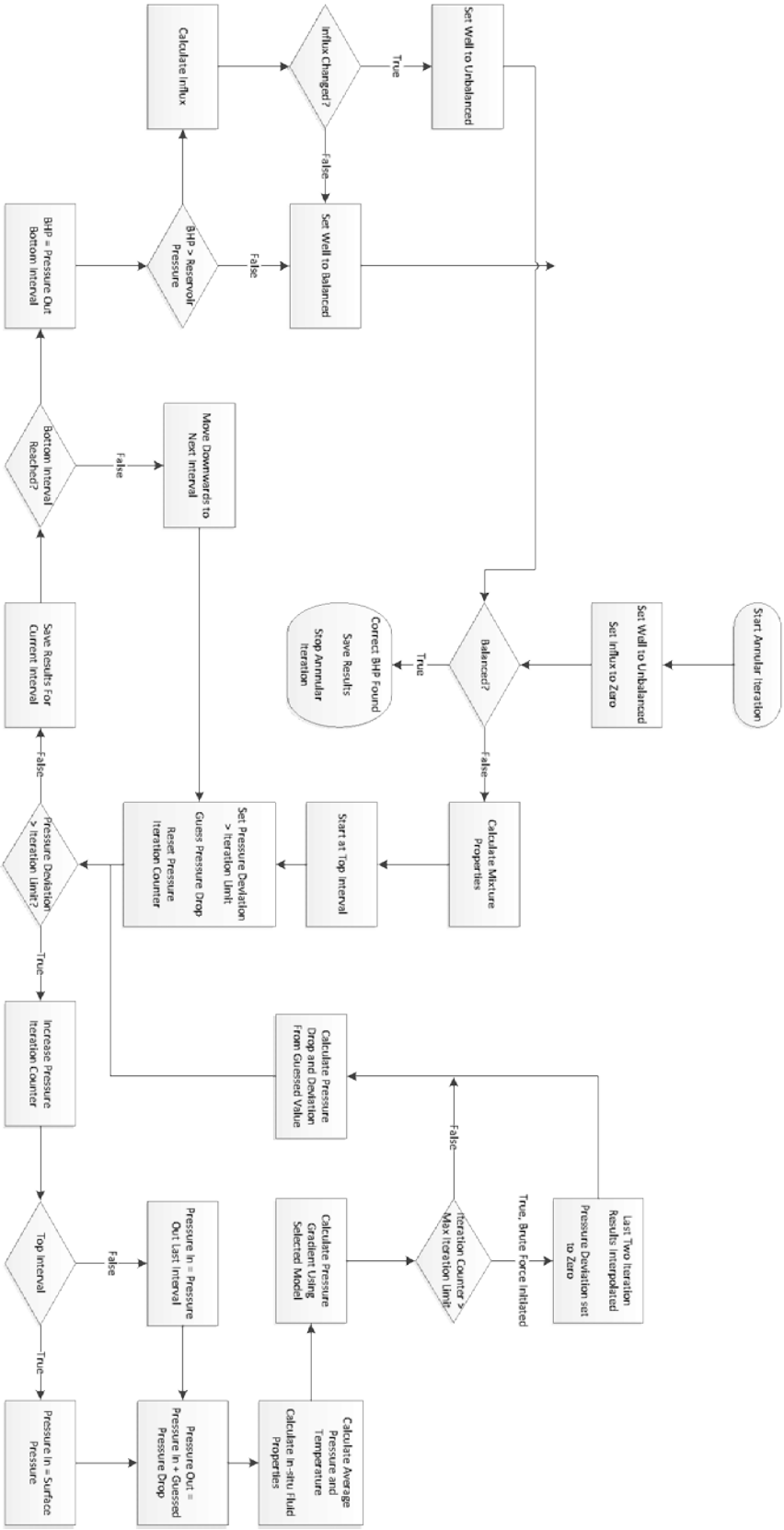

FIGURE 141 - ANNULAR ITERATION PROCESS

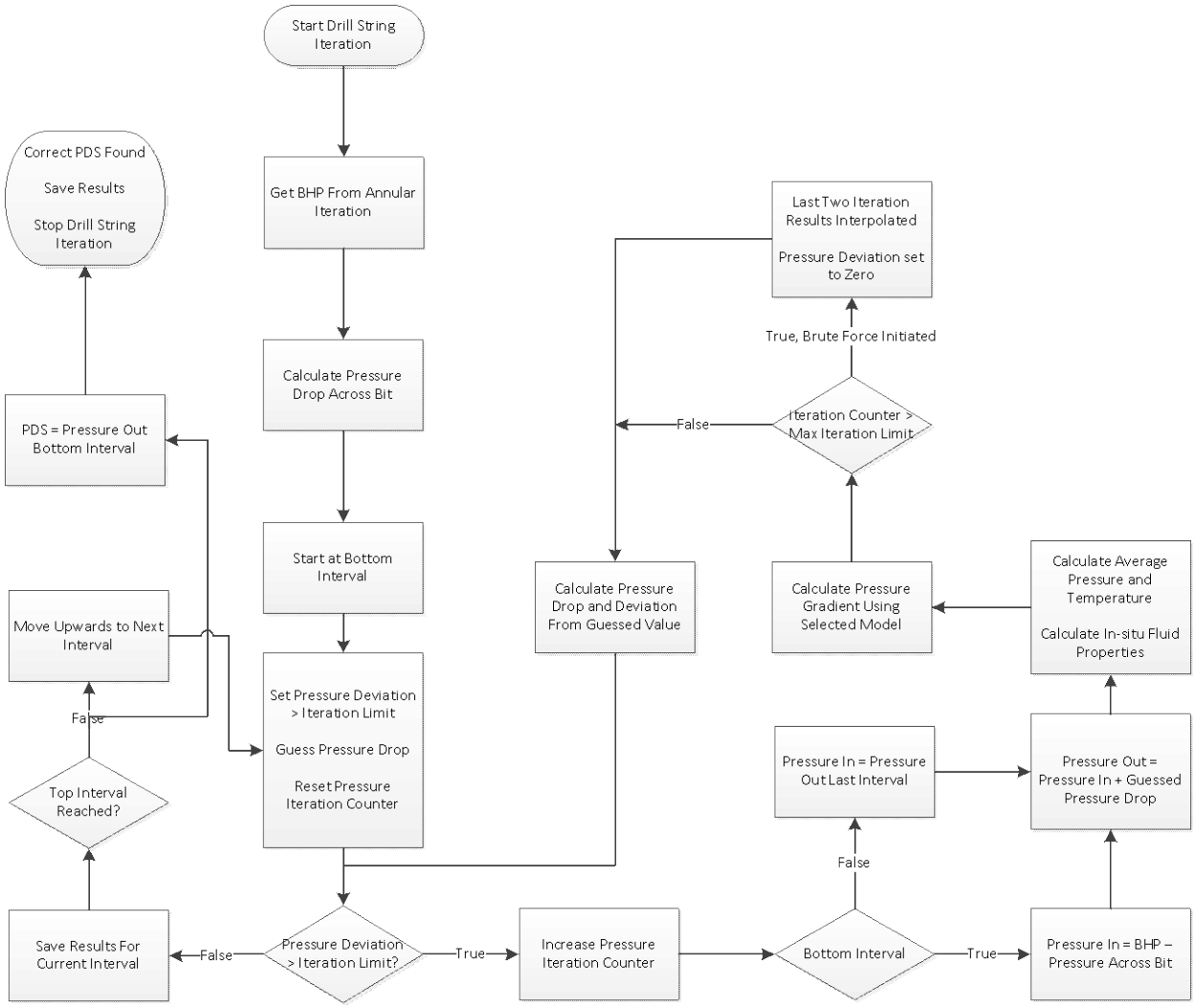

FIGURE 142 - DRILL STRING ITERATION PROCESS